THE DEVELOPMENT OF SINGLE-CHAIN VARIABLE FRAGMENT (ScFv) ANTIBODIES AGAINST *TOXOPLASMA GONDII* BY PHAGE-DISPLAY

SHERENE LIM SWEE YIN

THESIS SUBMITTED IN FULFILLMENT OF THE REQUIREMENTS FOR THE DEGREE OF DOCTOR OF PHILOSOPHY

INSTITUTE OF BIOLOGICAL SCIENCES
FACULTY OF SCIENCE
UNIVERSITY OF MALAYA
KUALA LUMPUR
2012

UNIVERSITI MALAYA

ORIGINAL LITERARY WORK DECLARATION

Name of Candidate: Sherene Lim Swee Yin (I.C/~~Passport~~ No: 811008-14-5722)
Registration/Matric No: SHC060035
Name of Degree: Doctor of Philosophy
Title of Project Paper/Research Report/Dissertation/Thesis ("this Work"):
The Development of Single-chain Variable Fragment (scFv) Antibodies against *Toxoplasma gondii* by Phage-display.

Field of Study: Biotechnology

I do solemnly and sincerely declare that:

(1) I am the sole author/writer of this Work;
(2) This Work is original;
(3) Any use of any work in which copyright exists was done by way of fair dealing and for permitted purposes and any excerpt or extract from, or reference to or reproduction of any copyright work has been disclosed expressly and sufficiently and the title of the Work and its authorship have been acknowledged in this Work;
(4) I do not have any actual knowledge nor do I ought reasonably to know that the making of this work constitutes an infringement of any copyright work;
(5) I hereby assign all and every rights in the copyright to this Work to the University of Malaya ("UM"), who henceforth shall be owner of the copyright in this Work and that any reproduction or use in any form by any means whatsoever is prohibited without the written consent of UM having first had and been obtained;
(6) I am fully aware that if in the course of making this Work I have infringed any copyright whether intentionally or otherwise, I may be subject to legal action or any other action as may be determined by UM.

…… ……
Candidate's Signature Date

Subscribed and solemnly declared before,

…… ……..
Witness's Signature Date
Name:
Designation:

ABSTRACT

The obligate intracellular protozoan parasite, *Toxoplasma gondii*, is the etiologic agent of an opportunistic infection affecting mainly immunocompromised patients, infants and neonates with immature immune system. There is a need for alternative anti-parasitic treatment for toxoplasmosis due to the associated toxicity and teratogenicity of the current drug treatment regime. To investigate a potential alternative strategy, we have used the phage-display system and developed a novel biopanning procedure to isolate single-chain Fv (scFv) antibodies probed against tachyzoites – the rapidly replicating form of *T. gondii* responsible for acute disease. The resulting scFv antibody library (complexity of 1.62 X 10^4 independent transformants) was co-incubated with the tachyzoites in a solution phase single-round biopanning procedure that was subtracted against a human cell line to minimize false positives. Phage-scFv output clones from the biopanning showed an average of at least 5.6-fold higher binding titer to *T. gondii* relative to unpanned clones. Here we show that despite well-acknowledged difficulties associated with biopanning with cells, this rapid biopanning approach was able to effectively generate specific scFv against *T. gondii*. ScFv TG130 which was isolated from this study demonstrated a 5-fold enrichment of binding to its' intended target *T. gondii* tachyzoites compared to the negative control cell line WRL68. Statistical assessment of the titer of bound recombinant scFv TG130 phage was found to be significantly higher with *T. gondii* than with WRL68 (Mann-Whitney test, P = 0.0303, n = 12).

In order to improve the binding properties of the anti- *T. gondii* scFv antibody, a second generation antibody library was generated based on the isolated scFv TG130 by using complementarity-determining region (CDR) mutagenesis for affecting an *in vitro*

antibody affinity maturation. Site-directed randomized mutations were introduced into specific DNA residues within the CDR known as hot spots – which are sequences that are prone to somatic hypermutations during the *in vivo* affinity maturation of antibodies. A screening strategy with increased stringency to select for antibodies with increased dissociation rate was employed to isolate improved scFv binders. Comparisons between the parental antibody and the affinity-matured antibody clone revealed that there was not a statistically significant difference in the binding titers of both antibodies to the target antigen *T. gondii*, although average titers for the affinity-matured TP60 was at least 1.8-fold higher than its parental counterpart. However, statistical analysis showed that the matured antibody fragment outperformed the parental antibody in terms of antibody specificity for *T. gondii* relative to negative control (t-test, $P = 0.018$, $n = 3$), indicating improved antibody selectivity for its target. These results demonstrate that scFv antibodies to *T. gondii* with improved properties can be generated through a combinatorial approach of phage-display and an *in vitro* antibody affinity maturation procedure. The potential implication of this study is for the enabling of the discovery and evolution of recombinant antibody fragments against *T. gondii* antigens in its native form and the development of bioimaging and cell-targeting ligands against this parasite.

ABSTRAK

Toxoplasma gondii adalah parasit protozoa intersel yang mengakibatkan jangkitan oportunis toksoplasmosis kepada individu-individu yang mempunyai sistem immuniti yang lemah, termasuk bayi dan fetus dalam kandungan. Disebabkan rawatan anti-parasitik terkini untuk gejala toksoplasmosis adalah toksik dan teratogenik – iaitu boleh mengakibatkan kecacatan dan kerencatan pertumbuhan normal kepada fetus dalam kandungan, rawatan alternatif untuk penyakit ini adalah diperlukan. Untuk mengkaji strategi-strategi alternatif, antibodi rantai tunggal Fv (scFv) telah dibangunkan melalui teknologi 'phage-display' dan 'biopanning' terhadap parasit peringkat akut jangkitan, iaitu takizoit. Perpustakaan antibodi scFv yang dibangunkan melalui teknologi tersebut (1.62×10^4 klon) telah diprobkan dengan takizoit dalam prosedur 'single-round biopanning' fasa cecair, dan penyaringan negatif terhadap titisan sel manusia untuk mengurangkan antibodi positif palsu. Klon-klon scFv yang terpilih melalui prosedur tersebut menunjukkan 'binding titers' 5.6-kali ganda lebih tinggi terhadap *T. gondii* berbanding output klon yang tidak disaringkan. Kajian ini menunjukkan bahawa walaupun terdapat kesukaran dalam keadaan mengoptimumkan biopanning sel, prosedur ini dapat membangunkan antibodi scFv yang spesifik terhadap parasit *T. gondii* dengan berkesan. Antibodi monoklon scFv TG130 yang terhasil daripada kajian ini menunjukkan 'binding titers' 5-kali ganda lebih tinggi terhadap *T. gondii* berbanding sel kawalan negatif WRL68. Penilaian statistik menunjukkan bahawa antibodi rekombinan scFv TG130 mempunyai kelebihan ketara dalam 'binding titers' terhadap *T. gondii* berbanding WRL68 (Mann-Whitney test, $P = 0.0303$, $n = 12$).

Bagi meningkatkan keberkesanan antibodi TG130 tersebut, perpustakaan antibodi generasi kedua telah dibangunkan melalui prosedur 'complementarity-

determining region (CDR) mutagenesis' untuk menghasilkan kematangan antibodi secara *in vitro*. Mutasi secara rawak pada lokasi spesifik di jujukan DNA antibodi tersebut yang dikenali sebagai 'hot spots' dijalankan. 'Hot spots' adalah jujukan DNA yang sering mengalami 'somatic hypermutations' dalam proses kematangan affiniti antibodi dalam sistem *in vivo*. Strategi penyaringan antibodi dengan kadar penceraian antibodi-antigen yang lebih tinggi dijalankan untuk mengasingkan antibodi generasi kedua dengan afiniti yang lebih baik. Walau bagaimanapun, perbandingan antara antibodi parental TG130 dengan antibodi generasi kedua tersebut menunjukkan bahawa scFv TP60 mempunyai titer yang 1.8-kali ganda lebih tinggi dalam reaksi terhadap antigen *T. gondii*. Analisis statistik menunjukkan bahawa antibodi generasi kedua tersebut mempunyai kelebihan ketara dalam kespesifikan terhadap antigen *T. gondii* berbanding dengan sel kawalan negatif (t-test, $P = 0.018$, $n = 3$), iaitu peningkatan keberkesanan antibodi tersebut untuk mendiskriminasikan di antara antigen dan sel kawalan negatif. Natijahnya, antibodi rekombinan dengan keberkesanan yang lebih tinggi boleh dikonstrukkan melalui kombinasi teknologi 'phage-display' dan prosedur kematangan afiniti antibodi *in vitro*. Implikasi kajian ini adalah dalam penemuan dan evolusi fragmen antibodi rekombinan terhadap *T. gondii*, serta potensi untuk membangunkan kaedah bioimaging, teknologi pensasaran sel serta kaedah 'immunotherapeutics' terhadap jangkitan toksoplasmosis.

ACKNOWLEDGEMENTS

I would like to thank Prof. Dr. Rofina Yasmin Othman (Ministry of Science, Technology & Innovation, and Department of Genetics, Institute of Biological Sciences, University of Malaya) and Associate Prof. Dr. Chua Kek-Heng (Department of Molecular Medicine, Faculty of Medicine, University of Malaya) for all their guidance, advice and constructive suggestions throughout the development of the present study and the completion of my thesis. My sincere gratitude also goes to Prof. Dr. Fong Mun-Yik (Department of Parasitology, Faculty of Medicine, University of Malaya) for all the helpful discussions given for this work and for kindly providing various resources in the Parasitology Department.

I would also like to gratefully acknowledge the assistance provided by Pn. Khatijah binti Othman in the *in vivo* passaging of *T. gondii* in mice, and Mr. Wong Yau-Hsiung for kindly providing the WRL68 cell cultures. My sincere gratitude also goes to Dr. Yusmin Yusuf for her support and facilitating the smooth-running as well as administration of the lab. My deepest appreciation is also extended to Ms. Ng Shearly who had been a very valuable help in the editing of graphs and figures to meet publication standards, as well as Dr. Teh Ser Huy for all her help in DNA sequencing. Special thanks also to friends from the Faculty of Medicine, University of Malaya, especially Ms. Ching Xiao Teng, Dr. Lau Yee Ling and Phyu Win Khaw for all their help and support. Thanks also to Genetics Lab BGM1 members Ms. Marina Mokhtar, Ms. Maria Ulfa, Ms. Nadiya Akmal Baharum, Ms. Akmar binti Mazlin, and Ms. Siti Nur Mariam binti Sulaiman.

Last but not least, I wish to extend my heartfelt gratitude to my very supportive parents Mr. Tommy Lim and Mrs. Mary Lim Swee Nyong for their unconditional love and unwavering faith in my work; to Ms. Tee Jin Ming, Rev. Kevin Loo & Esther Ku, Mr. Kevin Rimas Lee, Mr. & Mrs. Lee Kuan Meng, Ms. Anna Louis Tan, Ms. Jessica Yim and Ms. Debbie Teong for their encouragement and prayers throughout all stages in the preparation of this thesis.

Table of Contents

LIST OF FIGURES

LIST OF TABLES

LIST OF ABBREVIATIONS

%	:	percent
Å	:	angstrom
Ag	:	antigen
AMA1	:	apical membrane antigen 1
AP	:	alkaline phosphatase
≈	:	approximately
BCIP/NBT	:	5-bromo-4-chloro-3-indoll phosphate/nitro blue tetrazolium chloride
bp	:	base pair
°C	:	degrees Celsius
cDNA	:	complementary DNA
CDR	:	complementarity-determining region
cfu	:	colony forming unit
cm	:	centimetre
CMV	:	cucumber mosaic virus
DC	:	dendritic cells
DG	:	dense granule
DMSO	:	dimethyl sulfoxide
DNA	:	deoxyribonucleic acid
dATP	:	deoxyadenosine triphosphate
dNTP	:	deoxyribonucleoside triphosphate
DIG	:	digoxigenin
DTT	:	dithiothreitol
EDTA	:	ethylenediaminetetra-acetate acid
ELISA	:	enzyme-linked immunosorbent assay
ER	:	endoplasmic reticulum
Fc	:	fragment crystallizable
Fv	:	variable fragment
g	:	gram
Gus	:	β-D-glucuronidase
HRP	:	horseradish peroxidase
IFN-γ	:	interferon - gamma

IgG	:	immunoglobulin G
IgM	:	immunoglobulin M
IgE	:	immunoglobulin E
IgA	:	immunoglobulin A
IL	:	interleukin
i.p	:	intraperitoneal
IPTG	:	isopropyl-β-D-thiogalactopyranoside
i.v	:	intravenous
J cm^{-2}	:	joule per centimetre square
kb	:	kilobases
kbp	:	kilobase pair
kDa	:	kilodalton
l	:	litre
LB	:	Luria-Bertani
M	:	molar
µg	:	microgram
µl	:	microlitre
µM	:	micromolar
mAb	:	monoclonal antibody
mg	:	milligram
MIC	:	microneme protein
min	:	minute
MJ	:	moving junction
ml	:	millilitre
mM	:	millimolar
m.o.i	:	multiplicity of infection
mRNA	:	messenger ribonucleic acid
msec	:	millisecond
N	:	normality
ng	:	nanogram
nm	:	nanometer
PAGE	:	polyacrylamide gel electrophoresis
PBS	:	phosphate-buffered saline
PBS-T	:	phosphate-buffered saline-Tween 20

PCR	:	polymerase chain reaction
PEG	:	polyethylene glycol
pfu	:	plaque forming unit
PV	:	parasitophorous vacuole
PVM	:	parasitophorous vacuole membrane
r.c.f	:	relative centrifugal force
rmsd	:	root mean square deviation
RNA	:	ribonucleic acid
RON	:	rhoptry neck protein
ROP	:	rhoptry (bulbous) protein
RPAS	:	recombinant phage antibody system
r.p.m	:	revolutions per minute
RT-PCR	:	reverse-transcription polymerase chain reaction
SB	:	Super Broth
scFv	:	single-chain variable fragment
SDS	:	sodium dodecyl sulphate
sec	:	second(s)
SOC	:	Super Optimal Culture (media / broth)
TBE	:	Tris-borate-EDTA
TBS	:	Tris-buffered saline
TBS-T	:	Tris-buffered saline-Tween 20
TE	:	Tris-EDTA
TEMED	:	N,N,N',N',-tetramethyl-ethylenediamine
THB	:	Toxoplasma homogenization buffer
TNF-α	:	tumour necrosis factor - alpha
U	:	unit
UV	:	ultra-violet
V_H	:	variable heavy chain
V_L	:	variable light chain
v/v	:	volume per volume
w/v	:	weight per volume
X-Gal	:	5-bromo-4-chloro-3-indolyl-β-D-galactoside
YT	:	yeast-tryptone

1. General Introduction

1.1 – *Toxoplasma gondii* and the problem of the toxoplasmosis disease.

T. gondii is an obligate intracellular protozoan capable of invading and establishing productive infection in almost any nucleated cell where it produces a life-long chronic infection (Manger, Hehl, & Boothroyd, 1998). Consequently, up to one third of the world's population is infected (Montoya & Liesenfeld, 2004). It belongs to the phylum Apicomplexa which includes important human pathogens such as *Plasmodium* spp., the causative agent of malaria, and *Cryptosporodium* spp., the causative agent of Cryptosporidiosis. Toxoplasmosis infections in immunocompetent individuals are generally asymptomatic except for the minority of cases of mild, flu-like illness with low-grade fever, malaise, myalgia and headache (Dubey & Jones, 2008). These symptoms are usually self-limiting and are quickly resolved due to the hosts' immune system that puts the acute stage of infection in check. However, *T. gondii* can cause severe neurological birth defects when transmitted congenitally (Holliman, 1995) and is an opportunistic pathogen affecting immunocompromised individuals such as AIDS patients by causing the reactivation of latent infection into fulminant disease (Israelski, Chmiel, Poggensee, Phair, & Remington, 1993), with the most common clinical symptom and cause of morbidity being toxoplasmic encephalitis (B. J. Luft et al., 1993). Toxoplasmosis is a serious life-threatening complication in immunocompromised patients in the wake of emerging multi-drug resistant strains of the Human Immunodeficiency Virus (HIV) (Carruthers, 2002).

Current drug treatment for toxoplasmosis includes the administration of pyrimethamine and sulfonamides – both of which can cause toxic side-effects in

patients most commonly resulting in rashes, vomiting, nausea and leukopenia (Porter & Sande, 1992) with potential injury to the urinary tract (Simon, Brosius, & Rothstein, 1990). Toxoplasmosis treatment complications due to drug toxicity have been reported to range between 62 % to 71 % (Catherine et al., 1988; Porter & Sande, 1992). Although an effective anti-parasitic drug, pyrimethamine is known to be teratogenic and can cause developmental abnormalities to the developing foetus, especially during the first trimester of pregnancy (Sison & Sever, 1999). Therefore, an alternative treatment for toxoplasmosis which is safer for neonates and with lower propensity for inflammatory side-effects for immunocompromised individuals is needed to combat this opportunistic infection.

To resolve this, various studies have been conducted in search for a vaccine or immunotherapeutics to decrease the disease burden of toxoplasmosis. The various efforts at the development of antibody ligands against the protozoan parasite *T. gondii* have mainly focused on the isolation of binding antibodies against the parasites' known and soluble antigens which are strongly immunogenic. However, it has also been shown that antibody's binding to the immunogenic antigens does not necessarily correlate with effective disease inhibition (J. F. Dubremetz, Rodriguez, & Ferreira, 1985). This could be due to the parasite's sophisticated mechanism for immune evasion and subversion of infected leukocytes to cause widespread and rapid dissemination of the parasite throughout the host (Carruthers & Blackman, 2005; Laliberté & Carruthers, 2008).

1.2 – Development of recombinant antibodies by phage-display technology

Advances in the past two decades in recombinant antibody engineering has led to the development of phage-displayed antibody technology that circumvents the bottleneck problem of antibody design and production associated with hybridoma technology (McCafferty, Griffiths, Winter, & Chiswell, 1990). In the phage-display technology, viral phagemids harbouring polyclonal antibody genes are cloned into M13 bacteriophages, resulting in the production of phage particles expressing the antibody genes on the surface of filamentous bacteriophage as fusion proteins (Boel et al., 2000; C. Marks & Marks, 1996). Each phage particle displays one antibody, which effectively creates a convenient link between antibody phenotype and its' encoded genetic sequences (Clackson, Hoogenboom, Griffiths, & Winter, 1991). A polyclonal pool of these recombinant phages is referred to as a phage-displayed antibody library. Antibody genes engineered into being displayed on the bacteriophages are usually smaller fragments derived from immunoglobulins (Ig), such as Fab and scFv. The advantages of smaller antibody fragments are its ability to retain its' target specificity and affinity while being easier to produce in recombinant form, more amenable to mutational designs, higher tissue penetrability and also potentially avoids pathological immune effector responses. These antibodies have further potential as bioimaging and biotargetting tools for focused delivery of drugs to cells.

1.3 – Research objectives.

The aims of this study were:

i) To generate scFv antibodies against *T. gondii* tachyzoites using phage display technology.

ii) To develop an optimized suspension cell-based subtractive biopanning method for the selection scFv antibodies specific to *T. gondii* tachyzoites native antigens.

iii) To characterize the antigen-binding scFv clones by sequence, molecular structure and immunofluorescence analysis.

iv) To perform antibody affinity maturation using site-directed mutagenesis technique to increase the binding capacity of scFv antibodies against *T. gondii*.

1.4 – Outline of the thesis

This thesis is divided into 6 chapters:

Chapter 1	General Introduction
Chapter 2	Literature Review
Chapter 3	Materials & Methods
Chapter 4	Generation of anti-*Toxoplasma gondii* single chain variable fragment (scFv) antibodies by phage display.
Chapter 5	Development of anti-*Toxoplasma gondii* scFv antibody with improved affinity.
Chapter 6	Overall Conclusions.

2. Literature Review

2.1- The structure and life cycle of *Toxoplasma gondii*

T. gondii is an obligate intracellular apicomplexan protozoan, subclass coccidian; with a worldwide distribution and capable of infecting all endothermic vertebrates. The widespread expansion of Toxoplasma has been compounded by the acquisition of direct and enhanced oral transmission ability by the parasite through a seemingly recent evolutionary change (Su et al., 2003). *T. gondii* can take on several different forms at different life cycle stages, namely the oocyst, the tachyzoite, and the tissue cyst (zoitocyst) (Figure 2.1). The *T. gondii* genome is haploid, except during its sexual cycle in cats, and contains about 8 X 10^7 base pairs (Montoya & Liesenfeld, 2004).

The organism contains three types of specialized and morphologically distinct secretory organelles that are common to Apicomplexans – micronemes, rhoptries and dense granules (Hoppe, Ngo, Yang, & Joiner, 2000) (Figure 2.2). The molecular characterization and function of several proteins from these organelles have been reported (Brydges, Harper, Parussini, Coppens, & Carruthers, 2008; Cesbron-Delauw, 1994; Dlugonska, 2008; M-H Huynh & Carruthers, 2006; Tomley & Soldati, 2001) and is generally attributed to parasite's invasion and survival within its host. These organelles have a regulated function of deploying its protein content in a precisely orchestrated sequence throughout the invasion process and are major determinants to the parasitic pathogenesis, survival within its host and host interaction (Carruthers, 1999). The initiation of the invasion process begins with micronemal secretion of parasite adhesins responsible for the initial attachment and penetration into host cell

(Carruthers, 2002). The parasite promptly re-orientates itself so that the apical surface is closely positioned to the host cell membrane before the micronemes fuse to the tachyzoite cell membrane and deploys its' protein adhesins.

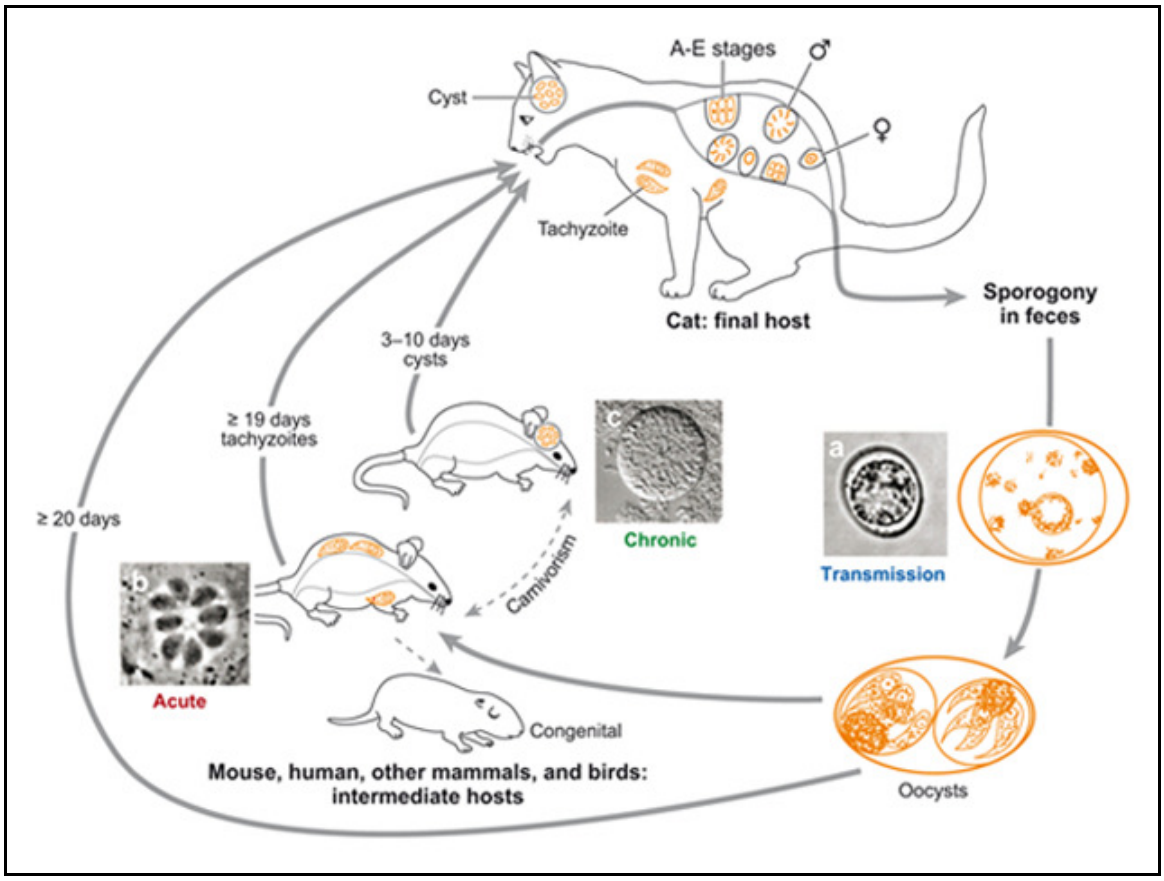

FIGURE 2.1 **Diagram depicting the life stages and modes of transmission of *Toxoplasma gondii*.** Members of the cat family serve as definitive hosts, where the sexual development of the parasite takes place within the small intestines. Haploid micro- and macrogametes forms within the enterocytes following a round of mitotic replication (A-E stages). Gametes fusion results in a diploid zygote that is shed as resistant oocysts (spore) in the feces. Transmission occurs when oocysts (a) contaminate food or water. Ingestion by a wide variety of warm-blooded hosts leads to an acute infection, characterized by fast-multiplying tachyzoites (b). Long-lasting chronic infection is typified by development of tissue cysts (c), which can also be transmitted by carnivourous feeding or scavenging. (Adapted from Sibley & Ajioka, 2008)

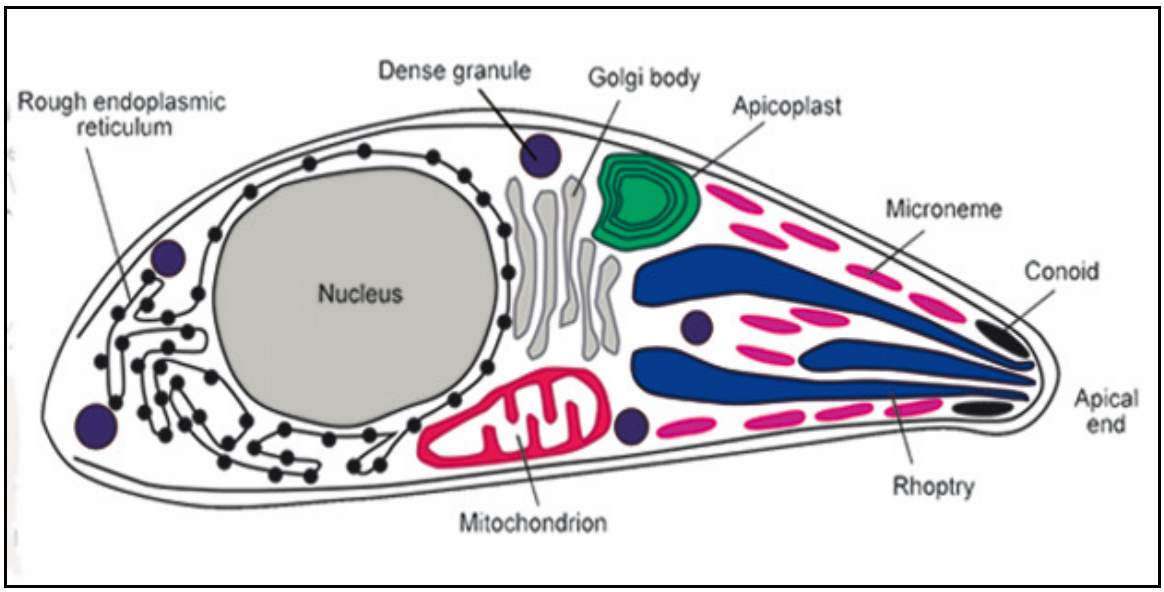

FIGURE 2.2 **The ultrastructure of a *Toxoplasma gondii* tachyzoite.** (Adapted from Coppens & Joiner, 2001)

Microneme secretion from *T. gondii* for initial attachment to host cell is followed by rhoptry secretion. Toxoplasma discharges its' rhoptry protein complexes in a timely manner to facilitate the establishment of infection and facilitating host organellar associations (Carruthers, 1999; Hoppe et al., 2000). Rhoptry secretions have been implicated to have a crucial function in the establishment of the parasitophorous vacuole membrane (PVM) that eventually encloses the intracellular parasite and delimits it from the host cell cytoplasm (Hoppe et al., 2000). As the tachyzoites invade, the host cell membrane invaginates and a tight junction is formed which is translocated backwards along the length of the parasite while host cell membrane proteins are shed off as the PVM envelopes the parasite (J. F. Dubremetz et al., 1985; Mordue, Desai, Dustin, & Sibley, 1999) and the rhoptries secrete its' protein content into the vacuolar space. The interesting feature of the PVM is the ability to resist acidification and fusion with host cells endocytic and lysosomal compartments which prevents the parasites destruction by the host lysosomes (Joiner, Fuhrman, Miettinen, Kasper, & Mellman,

1990; Mordue, Håkansson, Niesman, & David Sibley, 1999). This enables the parasite to multiply rapidly in this protected environment until the host cell ruptures and further dissemination can occur (Mordue, Desai et al., 1999).

It appears that the parasite's dense granules secretion is the final organellar discharge in *T. gondii*'s arsenal of secretory proteins. Soon after invasion, evidence indicates that the dense granule proteins function in structural modifications of the PV, immune protection and promoting intracellular replication through the transport and processing of nutrients from its host cells (Carruthers, 1999; Cesbron-Delauw, 1994; Zhou et al., 2005). Two of the most studied dense granule secretory proteins are GRA1 and GRA2 (Cesbron-Delauw et al., 1989; Sibley, Niesman, Parmley, & Cesbron-Delauw, 1995), which also happens to be among the most abundant Toxoplasma proteins at 2.0 % and 1.3 % of the total RH strain derived cDNA library ESTs (Ajioka et al., 1998b). Although the definite roles of these proteins are unknown and efforts to determine their respective functions are significantly hindered by the lack of homology with characterized proteins; GRA1 is potentially involved in the Ca^{2+} homeostasis within the PV (Cesbron-Delauw et al., 1989) while GRA2 may be responsible for acute virulence (Mercier, Howe, Mordue, Lingnau, & Sibley, 1998). Another well-defined dense granule protein is the nucleotide triphosphatase (NTPase) which is responsible for the supply of purines in this purine-auxotrophic parasite (Asai, Miura, Sibley, Okabayashi, & Takeuchi, 1995; Sibley, Niesman, Asai, & Takeuchi, 1994). In addition, *T. gondii* NTPase may function cooperatively with GRA1 in promoting parasite egress out of its host cell through the signals of elevated intracellular Ca^{2+} levels and depleted ATP (Silverman et al., 1998; Stommel, Ely, Schwartzman, & Kasper, 1997).

A critical parameter in the survival and persistence of parasitic infections is its different life cycle that allows the parasite to escape hosts' immune surveillance. The life cycle of *T. gondii* consists of two phases called the intestinal (or enteroepithelial) stage and extraintestinal stage. The intestinal phase occurs exclusively in members of the cat family (Felidae), which is the definitive host, and produces oocysts (Dubey, Miller, & Frenkel, 1970), while many mammals and birds serve as intermediate hosts harboring this parasite in the extraintestinal phase, including humans (Carruthers, 1999). The definitive hosts are not only restricted to domestic cats, but also other felids such as ocelots, margays, jaguarundi, Pallas cats, bobcats and Bengal tigers; although oocysts formation is greatest in domestic cats (Dubey, 1996). Throughout its life cycle, *T. gondii* has three morphological forms: the rapidly reproducing tachyzoites that causes parasite-directed host cell lytic destruction, the dormant bradyzoites that occupy tissue cysts and sporozoites that are contained within oocysts which are excreted in cats' feces (J. Jones, Lopez, & Wilson, 2003).

Cats become infected with toxoplasmosis by ingesting any of the three infectious stages of the organism; namely the actively multiplying tachyzoites, the quiescent bradyzoites that occupy cysts in infected tissues, and the oocysts shed in feces (Dubey et al., 1970). In the intestinal stage, when a cat ingests meat containing tissue cysts, the cyst wall is dissolved by the proteolytic enzymes in the stomach and small intestine, releasing bradyzoites enclosed within the cysts. The slowly-multiplying bradyzoites penetrates the epithelial cells of the small intestine and initiates the *T. gondii* asexual cycle which results in the rapidly proliferating tachyzoite form. Meanwhile, some of the parasites undergo the sexual cycle in which male and female gametes are formed and subsequently fuses to become a zygote. Oocysts (10 x 12 µm) are subsequently formed through the fertilization of the male and female gametes and

the development of two cell walls encircling the fertilized zygote (Dubey, Lindsay, & Speer, 1998). About 10 million uninfectious oocysts are excreted in the faeces daily for 7-21 days in an unsporulated stage and contaminate the surrounding environment. Sporulation occurs outside the body, and the oocysts become infectious 1 to 5 days after excretion depending on environmental conditions (Dubey et al., 1998). During acute infection, a 20 g cat stool can contain between 2 – 20 million oocysts, and when the fecal matter has decomposed, the local soil contamination can be as high as 100,000 oocysts/g (Webster, 2001).

During its maturation, the zygote undergoes differentiation to form sporozoites which is encased within mature oocysts – now known as sporulated oocysts and is the infective form (J. Jones et al., 2003). Sporulated oocysts are remarkably resistant in adverse environmental conditions and remain infectious for more than 1 year in a suitable environment (warm, moist soil). However, the infectious oocyst cannot survive well in arid, cool climates and can be destroyed by heating (Gagne, 2001). Due to this hardiness, *T. gondii* is a global zoonoses and is not restricted to any known geographical boundaries (Carruthers, 2002). This is a unique feature considering many other parasites that are mostly confined to tropical or subtropical regions.

The extraintestinal stage occurs in all infected animals, in both the definitive and intermediate hosts; and produces the rapidly multiplying form of the parasite-tachyzoites, and under immune pressure, eventually changes into the chronic infection form - bradyzoites. The causative agents for the extraintestinal stage infection are mostly the consumption of oocysts or bradyzoites-contaminated food and water. Other modes of transmission include congenital infection through transplacental transmission

in infected pregnant females, blood transfusion and organ transplant from infected donors (Hill & Dubey, 2002).

In humans, ingestion of tissue cysts in uncooked, infected meat or contaminated water results in the rupture of the cysts, releasing bradyzoites that are either phagocytosed or infects epithelial cells, differentiates into tachyzoites and disseminates throughout the host via the blood and lymph. Tachyzoites measure approximately 6 X 2 µm and are generally crescentic (Dubey et al., 1998). It is the acute stage form of the disease and is the actively replicating form that invades all organs, rapidly proliferating until a threshold limit where the parasite egresses and ruptures the host cell. In immune dysfunction, the tachyzoites' repeated replication and host cell lytic destruction causes widespread necrotic lesions that are the hallmark tissue pathology of a toxoplasmosis infection. The tachyzoites also invades immune-privileged sites such as the central nervous system (CNS), the brain, eye and muscles (including the heart) (Elsheikha & Khan, 2010). The widespread dissemination and persistence in its host can be attributed to one of the parasite's striking ability to subvert infected host cells and to breach the blood-brain barrier. *T. gondii* is known to employ the 'Trojan horse' mechanism in hijacking migratory leukocytes to transport the tachyzoites to distant tissues (Tardieux & Ménard, 2008); as well as to disseminate by paracellular transmigration across biological barriers (Barragan & Sibley, 2002). Contrary to oocyst, tachyzoites are very sensitive to extreme temperatures and can penetrate the buccal mucosa. Tachyzoite is the virulent form of *T. gondii* and causes a strong inflammatory response and tissue destruction, and therefore is responsible for the clinical manifestations of this disease (Montoya & Liesenfeld, 2004).

The host usually can arrest this phase of infection by mounting an immune response, and the parasite is then pressured into differentiating into the quiescent bradyzoite form which is eventually isolated in tissue cysts enclosed in a thin membrane. Studies have well established that a reduction in growth rate of the parasite results in a switch from tachyzoite to bradyzoite, and hence the promotion of cytogenesis (Ellis, Sinclair, & Morrison, 2004). The infected individual then acquires a lifelong immunity against toxoplasmosis provided the host remains immunocompetent. Bradyzoites are morphologically identical to tachyzoites but multiply slowly, express stage-specific molecules, and are functionally different. Bradyzoites are also more resistant to proteolytic degradation than tachyzoites (Jacobs, Remington, & Melton, 1960). Tissue cysts (about 60 µm in diameter) can contain hundreds of bradyzoites and are typically sequestered in the brain, liver, and muscles (Dubey et al., 1998). One of the most distinguishing features of its life cycle is that Toxoplasma tissue cysts are generally undetected and inaccessible by the immune system, and because of this the parasite remains dormant for the lifetime of the host as long as the person remains immunocompetent (He, Grigg, Boothroyd, & Garcia, 2002; Zhang, Halonen, Ma, Wittner, & Weiss, 2001). However, once the immune system is impaired, reactivation of latent infection can cause widespread tissue damage and severe pathology such as cerebral encephalitis due to the rupture of the tissue cysts releasing active infection.

2.2- Epidemiology

T. gondii is a major cause for food- and water-borne protozoal infection (Tenter, Heckeroth, & Weiss, 2000) with the status of being the third highest cause of food-borne mortality in the United States (Mead et al., 1999). Due to the remarkably broad

tissue-range and host-range of *T. gondii*, toxoplasmosis infection is widespread globally with an estimated 500 million humans being seropositive for the parasite (Dubey, 1996). However, the prevalence of infection in both humans and animals may differ in different parts of the world due to varying environmental conditions, culture and healthcare awareness (Dubey, 1996).

In the United States, approximately 20-25% of adolescents and adults have laboratory evidence of infection. That means at least 1 out of every 4 individuals in the American population is infected. Toxoplasmosis is one of the diseases comprising the 'TORCH' infections (*T. gondii*, Others [if done, e.g. syphilis, varicella zoster virus, human immunodeficiency virus, parvovirus, herpes virus 6 and 8, enterovirus and Epstein-Barr virus], rubella, cytomegalovirus [CMV] and herpes simplex viruses [HSVs]). TORCH refers to a group of infections that can pose a serious threat to the developing foetus or neonate by causing congenital illness or death (Abu-Madi, Behnke, & Dabritz, 2010). *T. gondii* infection has been known to cause perinatal death if the organism is acquired during pregnancy (Nissapatorn & Abdullah, 2004), or blindness (retinochoroiditis), fetal mental and psychomotor retardation, encephalitis, hepatitis, intracranial calcifications, and hydrocephaly (Abu-Madi et al., 2010).

The current prevalence of chronic toxoplasmosis among the Malaysian population is estimated to vary between 10-50% (Nissapatorn, Lee, & Cho, 2003). There is an upward trend of an increase in toxoplasmosis seroprevalence in the general healthy Malaysian population from 20% to 30% from 1985 to 2004 (Nissapatorn & Abdullah, 2004). There is also a significant percentage of latent toxoplasmosis seroprevalence in Malaysian pregnant women of 49% (Azmi et al., 2003), a surprisingly high rate compared to previous studies conducted. This implies that the rate of disease

transmission may be on the increase with a particular risk for mothers who are infected for the first time during pregnancy (J. Jones et al., 2003). In a study conducted in the U.S. the rate of congenital transmission of toxoplasmosis is approximately 1 in every 1000 live births (Roberts, Murrell, & Marks, 1994), while the rate of congenital transmission in Malaysia is currently unknown. However, the increasing trend of seroprevalence in the general Malaysian population should warrant intensified research efforts and diagnostic vigilance for pregnant women. Mothers infected for the first time during pregnancy lack the secondary immune response necessary to prevent disease transmission to their unborn foetus during gestation and this may result in severe congenital disease or spontaneous abortions. In Europe, toxoplasmosis has been identified as a serious disease and compulsory screening for pregnant women is being practiced in many countries (Fishback; & Frenkel, 1991). However, in Malaysia, the 'TORCH' infections testing protocol is not yet a rule of practice. Studies done in different parts of the world showed a wide range of varying seroprevalence for toxoplasmosis, from 17.2% in Singapore (Wong, Tan, Tee, & Yeo, 2000) to 67% in Brazil (Reiche et al., 2000).

Specific treatment for immunocompetent non-pregnant adults and adolescents is usually not necessary because infection of definitive and intermediate immunocompetent hosts is generally asymptomatic (Newton, 1999; Piper & Wen, 1999). In rare instances symptoms in otherwise healthy humans may include mild malaise, lethargy, and lymphadenopathy (Gagne, 2001). These symptoms are self-limited, and would normally spontaneously resolve in weeks to months. Seroconversion occurs primarily between the ages of 15 and 35 (Gagne, 2001). Most cases of toxoplasmosis in humans are acquired by the inadvertent ingestion of either tissue cysts in infected inadequately cooked meat, or oocysts in food or water contaminated with the

definitive host's (Felids) feces, through handling of litter boxes or outdoors in the soil through gardening and through handling of unwashed fruits and vegetables. *T. gondii* can also be transmitted through organ transplantation from an infected donor causing recrudescence of infection due to the immunosuppressed state of the organ recipients on corticosteroids (Brooks & Remington, 1986). In rare instances, infection can also occur through blood or leukocytes transfusions (S. E. Siegel et al., 1971) and also laboratory mishaps by contact with contaminated needles, glassware and animals (Jack S. Remington & Gentry, 1970).

Following oral ingestion, the cysts releases sporozoites from oocysts or bradyzoites from tissue cysts which rapidly penetrates the intestinal epithelium and differentiates into tachyzoites (Sumyuen, Garin, & Derouin, 1995). Tachyzoites have the proficient ability to disseminate throughout the host through the hijacking of migratory leukocytes, particularly dendritic cells (DC) and macrophages (Lambert & Barragan, 2010) to transmit to the developing fetus through the placenta and to gain access to immunologically pristine sites such as the central nervous system (CNS). The parasite's invasion across the blood-brain barrier results in severe neurodegeneration and toxoplasmic encephalitis.

The most significant morbidity and mortality associated with reactivated *T. gondii* infection in AIDS patients is caused by toxoplasmic encephalitis (Elsheikha & Khan, 2010). Congenital infections are largely subclinical, but infants that do develop disease may be aborted or may suffer severe and irreversible cognitive impairments and retinochorditis blindness. Toxoplasmosis is touted as a significant health care burden due to the parasite's ability to survive and persist within its host. Congenital disease manifestations often require life-long healthcare and institutionalization for children

suffering from the irreversible cognitive dysfunctions arising from the disease. Although 50% of cases of toxoplasmosis are caused by contaminated food and water, the economic burden is primarily related to congenital toxoplasmosis, at a cost of approximately USD 5.2 billion per year in 1994 (Roberts et al., 1994), and an escalating cost of USD 7.7 billion per year in 1996 in the United States alone (Buzby & Roberts, 1996). Findings by the New England Screening Program in year 2000 indicates that screening for IgM positive neonates in the American population costs USD 220,000 to screen 100,000 infants per year and is translated to USD 30,000 per infant identified (Lopez, Dietz, Wilson, Navin, & Jones, 2000). In view of the potential lifelong monetary and social costs for raising a visually impaired or intellectually compromised child, this is quite a reasonable cost-to-benefit ratio (Roberts & Frenkel, 1990). These findings provide a strong basis for intensified research to be done on therapeutic intervention and vaccines against toxoplasmosis. Therefore, a recombinant scFv against toxoplasmosis would be beneficial as an alternative non-teratogenic management of this silent disease, which is a safer option for pregnant mothers.

2.3- Toxoplasmic Pathogenesis

Unlike many pathogenic bacteria, *T. gondii* does not produce any cytolytic toxins; tissue necrosis is caused by intracellular multiplication of tachyzoites, followed by localized inflammation. In adults, the incubation period for toxoplasmosis infection ranges from 10 to 23 days if contaminated, undercooked meat is ingested; and from 5 to 20 days after ingestion of oocysts from cat's feces (J. Jones et al., 2003). The acute infection phase generally occurs in the initial 8-12 days where tachyzoites actively replicate and disseminate in host tissues (Carruthers, 2002). After the parasite's invasion

into enterocytes, *T. gondii* infects antigen-presenting cells (APCs) in the intestinal lamina propria, and stimulates a strong and persistent T-helper-1 (Th1) response characterized by production of proinflammatory cytokines including interleukin 12, interferon-γ (IFN-γ), and tumour necrosis factor α (TNFα) (Gigley, Fox, & Bzik, 2009). The synergistic action of these cytokines and other immunological mechanisms protects the host against rapid multiplication of tachyzoites and the resulting pathological implications, therefore striking a delicate balance in ensuring the survival of the host and the parasites' persistence (Yap & Sher, 1999). Within 2-weeks after infection, IgG, IgM, IgA, and IgE antibodies against many *T. gondii* proteins can be detected (Montoya & Liesenfeld, 2004). Production of IgA antibodies on mucosal surfaces can protect the host against the sequelae of reinfection. In this case, reinfection can occur, but the host seems to be free from the clinical pathology of the disease and congenital transmission of the parasite (Montoya & Liesenfeld, 2004).

The cytokine IFN-γ secreted from antigen-specific T-cells is the major mediator of resistance in acute toxoplasmosis. As the host's proinflammatory responses gains momentum over several weeks, IFN-γ progressively inhibits tachyzoite replication, leading to differentiation to bradyzoites and encystation (Bohne, Heesemann, & Gross, 1994; Suzuki, Conley, & Remington, 1989). The formation of the slower-replicating bradyzoites marks the beginning of the chronic infection phase. As a parasite adaptation strategy, the chronic infection phase effectively promotes the parasite's survival by changing its morphological form and encapsulating itself within tissue cysts which are immunologically inert (Ferguson & Hutchison, 1987). The parasite persists within the host as a life-long chronic infection in this semi-dormant bradyzoite-containing tissue cysts stage. These tissue cysts are mostly sequestered within the brain, and to a lesser extent, in muscle tissues and other organs (Bohne et al., 1994). Within the brain,

bradyzoites were detected in astrocytyes, neurons and microglial cells (Fischer, Nitzgen, Reichmann, Groß, & Hadding, 1997). This latent form of infection remains silent throughout the lifetime of the host as long as the immune system is fully functional. However, in the wake of an impaired immune system, excystation takes place releasing bradyzoites from the ruptured tissue cysts which differentiates back into tachyzoites and rapidly begins its lytic cycle. This toxoplasmic disease reactivation causes widespread tissue destruction and severe pathology.

The severity of disease closely correlates with the immune status of the infected person. Severe disease is typically observed in congenitally infected children by transplacental transmission and also in immunocompromised individuals. This opportunistic infection is among the most major cause of mortality in AIDS patients, which is a situation that is exacerbated in underdeveloped countries with limited financial resources and infrastructure to acquire and distribute the anti-retroviral drugs (Brindle, Holliman, Gilks, & Waiyaki, 1991). Thirty percent to 50% of HIV-positive patients with latent *T. gondii* infection will develop toxoplasmic encephalitis (TE) when afflicted with severe immune dysfunction (Benjamin J. Luft & Remington, 1992).

Patients with moderate to severe immune impairment are significantly more prone to reactivation of latent infection. Reactivated infection causes the most severe clinical manifestation to the CNS, which is toxoplasmic encephalitis (TE) - an important and severe pathology of opportunistic toxoplasmosis in immunocompromised patients. TE results in multiple large necrotic abscesses in the brain, some as large as over 4.0 cm in diameter (Figure 2.3) (Carruthers, 2002). Initiation of TE occurs through localized parasite growth from the initial site of tissue cysts, which rapidly expands into spherical plaques of tissue necrotic lesions. These multiple lesions are most often observed in the

cerebral hemisphere and basal ganglia through magnetic resonance imaging (MRI) and computed tomography (CT) scans (Carruthers, 2002). Due to the tachyzoites' aggressive lytic cycle, the necrotic lesions in TE shows complete obliteration of host cells in the center of the plaques, with infected cells only being seen at the periphery of the expanding necrotic plaques (Strittmatter, Lang, Wiestler, & Kleihues, 1992).

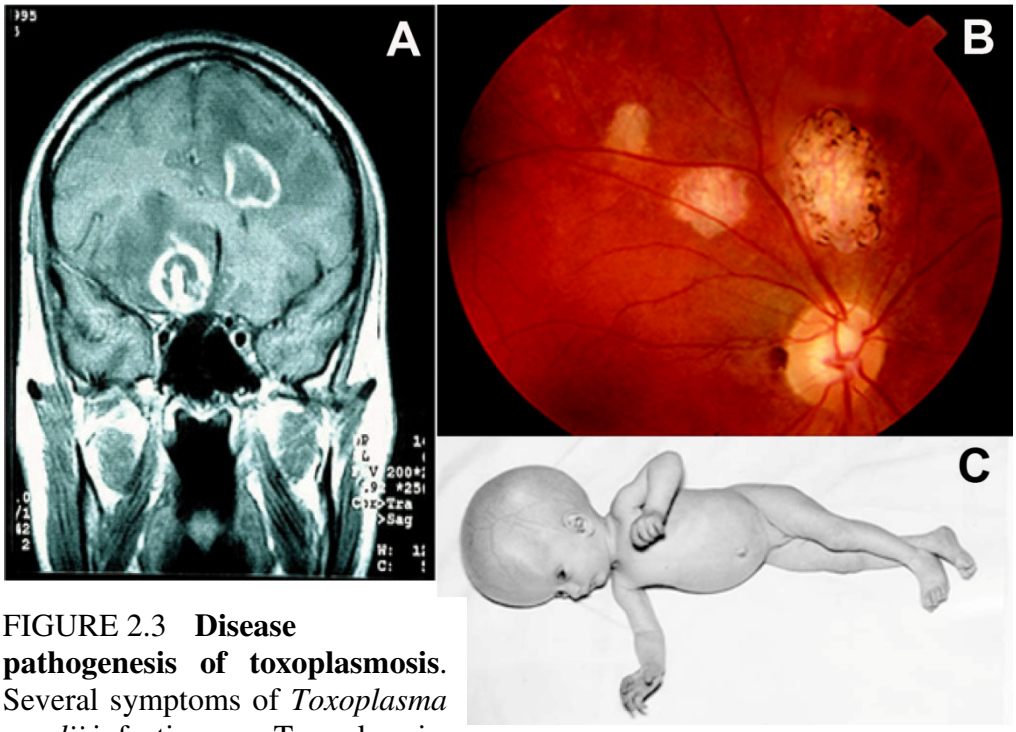

FIGURE 2.3 **Disease pathogenesis of toxoplasmosis**. Several symptoms of *Toxoplasma gondii* infections are Toxoplasmic Encephalitis (TE) which can be seen in this cerebral MRI scan of an AIDS patient showing two ring-enhancing lesions (A); retinochoroiditis which can be seen as retina scarring (B); and hydrocephalus in a congenitally-infected infant (C). (Adapted from Dubey & Beattie, 1988 for (C); and Miro & Alvarez-Martinez, 2011 for (A); Stanford, Tomlin, Comyn, Holland, & Pavesio, 2005 for (B))

Clinical presentation of TE consists of either focal or non-focal neurological dysfunction. Focal neurological deficits arising from TE includes hemiplegia, hemisensory loss, cerebellar tremor, hemiparesis, visual field defects, cranial nerve

palsies, aphasia, severe localized headache, and convulsions (Benjamin J. Luft & Remington, 1992). On the other hand, non-focal TE manifestations include weakness, disorientation, frank psychosis, lethargy and confusion (Benjamin J. Luft & Remington, 1992). Progression of the infection can also lead to coma and death. Reactivation of latent infection leading to TE is significantly correlated to CD4 levels that drop below 100 cells per cubic millimeter in patients with simultaneously existing human immunodeficiency virus (HIV) and *T. gondii* infection (Nissapatorn et al., 2004). In the weakened immune state, the bradyzoites differentiates back into tachyzoites and rapidly proliferates in microglia and astrocytes (Lüder, Giraldo-Velásquez, Sendtner, & Gross, 1999). Other accompanying severe manifestations of the disease may include splenomegaly, polymyositis, dermatomyositis, myocarditis, hepatitis, chorioretinitis, pneumonitis, and multisystem organ failure (Gagne, 2001). Experimental reactivation of chronic latent *T. gondii* infection in laboratory animals can be initiated by administration of corticosteroids, anti-lymphocyte serum and other immunosuppressants (Dubey, 1996). Disease reactivation can also occur in other immunosuppressed states, such as systemic lupus and transplant recipients.

T. gondii disease transmission can also occur from pregnant women to their unborn fetus via the placenta. The disease transmission rarely occurs to women who were infected at least 4 to 6 months or earlier prior to conception as the protective immunity gained from the previous infection protects the developing fetus from vertical transmission upon subsequent exposures (Tenter et al., 2000). However, acute infection and reactivation of latent infection due to immunosuppression can transmit the parasite transplacentally and cause severe sequelae to the fetus. The propensity for congenital disease is lowest in the first trimester of maternal infection (10 to 25 percent) and highest in the third trimester of maternal infection (60 to 90 percent) (J. S. Remington,

McLeod, Thulliez, & Desmonts, 2001). Clinical disease is often more severe in congenital infections acquired during the first two trimester of pregnancy (Dunn et al., 1999). Congenital *T. gondii* infection often involves the brain and retina and may result in a wide spectrum of clinical disease. Mild infection may lead to slightly impaired vision, whereas severely diseased infants may exhibit a classic tetrad of signs: retinochoroiditis, hydrocephalus, convulsions, and intracerebral calcifications. Hydrocephalus is the rarest but most dramatic lesion of congenital toxoplasmosis whereas visual impairment is the most common sequelae (Figure 2.3). Congenitally-infected premature infants may develop CNS and ocular disease in the first 3 months of life, while full-term infants usually present milder symptoms such as lymphadenopathy and splenomegaly in the first 2 months of life (J. Jones et al., 2003; Montoya & Remington, 2000). Most congenitally-infected infants are born without any obvious clinical presentation of toxoplasmosis upon routine newborn examination. But up to 80 percent of infants infected *in utero* will develop learning or visual impairments later in life (C. B. Wilson, Remington, Stagno, & Reynolds, 1980), with ocular disease (focal chorioretinitis) potentially occurring even at the third decade of life or later. Long-term sequelae resulting from congenital toxoplasmosis include seizures, spasticity, visual impairment, deafness and mental retardation (J. Jones et al., 2003).

Due to its highly promiscuous ability to infect virtually all warm-blooded organism, *T. gondii* is capable of causing severe pathology in animals other than humans. Cats, dogs, and many other warm-blooded pets can die of pneumonia, hepatitis, and encephalitis due to toxoplasmosis. It is one of the leading causes of abortion in pigs, sheep and goats in many countries, including Australia and the United States (Dubey, Miller, Desmonts, Thulliez, & Anderson, 1986; J.-H. Kim et al., 2009; Pereira-Bueno et al., 2004). Among meat-producing animals, tissue cysts are frequently

found in infected pigs, sheep and goats; and less frequently found in infected poultry, rabbits, dogs and horses (Tenter et al., 2000). Sheep and goats show the highest titer of seroprevalence in many areas of the world, at 92 and 75 percent respectively. Pork is generally considered a major source of *T. gondii* infection in Europe and the U.S. with tissue cysts being found in most commercial cuts of pork (Dubey, Murrell, Fayer, & Schad, 1986). However, in 1992, a current management practice of raising pigs for unprocessed pork consumption in well-managed indoor facilities has led to a dramatic decline of *T. gondii* infection prevalence from 14.0 % to 0.9 % in Austria (Edelhofer, 1994). The difference in seroprevalence in different animals may be affected by several factors such as animal containment, hygiene of stables, type of feed and regulatory enforcement of farm management (Tenter et al., 2000).

2.4- Diagnosis of toxoplasmosis

Diagnosis of toxoplasmosis is largely dependent on serological tests. Parasites are normally scarce in body fluids and tissues and thus difficult to isolate for histologic examination, except for cases of extremely high parasite tissue burden. Clinical signs alone are too ambiguous for the definite diagnosis of this parasite infection as symptoms of toxoplasmosis appears similar to several other infectious diseases. Definitive diagnosis is especially vital in pregnant patients because administration of early treatment can protect the fetus against the sequelae of acute toxoplasmosis.

In initial diagnosis screenings, the IgG and IgM antibody levels against *T. gondii* is tested in pregnant women. IgM antibody level is used to aid in determining the approximate time of infection and to rule out acute infection. Normally, a positive IgG

result and a negative IgM result is interpreted as an infection that was acquired at least 6 months prior to testing. Recommendation for best practice is to collect a second blood serum sample from IgM-positive subjects at 2-4 weeks after the first sample. A 4 to 16-fold rise in antibody titer in the second sample is indicative of an acute infection (Hill & Dubey, 2002). However, the persistently elevated levels of IgM antibodies even after 18 months of *T. gondii* infection has made this routine diagnosis complicated (M. Wilson & McAuley, 1999). This diagnostic complication is further compounded by occurrences of false-positives in commercial tests (M. Wilson et al., 1997). Determining the recency of infection is especially crucial in pregnant women due to the risk of transplacental disease transmission and the need for medical intervention to minimize damage to the developing fetus (Hill & Dubey, 2002). Therefore, a positive IgM test result should be followed up by a referral to a Toxoplasma Reference Laboratory where the possibility of acute infection is confirmed and the time-frame of infection is narrowed through the use of specific tests or serological profiles such as the IgG avidity test, IgM immunofluorescent (IFA) test, IgM enzyme-linked immunosorbent assay (ELISA), IgA ELISA, IgE ELISA and differential agglutination (Jenum, Stray-Pedersen, & Gundersen, 1997; Liesenfeld et al., 2001; M. Wilson et al., 1997). However, at the present time, Malaysia does not have an official Toxoplasma Reference Laboratory to date, although the Institute of Medical Research and a few private pathology centers can provide serological testing for *T. gondii* infection.

The most reliable, sensitive and specific serologic tests for toxoplasmosis available presently are the Sabin-Feldman or Methylene Blue dye (MBD) test (Sabin & H.A., 1948) and the IgM Indirect Fluorescent Antibody (IFA) tests (J. S. Remington & Miller, 1966). The MBD test is useful in the diagnosis of toxoplasmosis in patients with ocular disease as these patients normally have low titers of *T. gondii* antibodies. Despite

the advantages of specificity and sensitivity conferred by the MBD test, it has some significant drawbacks that render the test less suited to large volumes of infection analysis. The MBD test is expensive and requires the use of viable, virulent tachyzoites as antigen to be screened against the test serum, and thus poses a potential health hazard to pathology lab personnel (Dubey & Beattie, 1988).

The IgM indirect fluorescent antibody (IFA) test overcomes some of the drawbacks of the MBD test. The IFA test does away with the health hazard associated with the use of live, virulent *T. gondii* and instead uses commercial preparations of killed tachyzoites as antigen with a test sensitivity comparable to the MBD method (Dubey & Beattie, 1988). However, the IFA test also has its disadvantages as it requires the use of microscopes with UV light, and specific fluorescent anti-species globulin for each species to be tested – making this an expensive assay. In addition, false positives may also occur in the IFA test for hosts with anti-nuclear antibodies (Dubey, 1996). Although the IFA test is not perfect, it is useful for diagnosis of acquired acute toxoplasmosis in humans (Dubey, 1996), but is not an economically-viable option for animal diagnostics. Other serologic tests that offer several different advantages are the indirect hemagglutination test, the latex agglutination test (LAT), modified agglutination test (MAT), and the enzyme-linked immunoabsorbent assay (ELISA). The agglutination tests presents low health hazard risks as soluble *T. gondii* antigen commercial preparations are used, requires no special equipments or conjugates and are easy to carry out. The MAT is widely used in animal diagnosis of toxoplasmosis (Dubey, 2007). The shortcoming of the agglutination tests is its' low sensitivity as it lacks the ability to detect acute infection (Dubey, 1996). ELISA tests perform better in terms of sensitivity compared to the agglutination tests.

Once it has been confirmed that a pregnant mother is infected with toxoplasmosis, the next step is to determine whether her fetus *in utero* is also infected. Monoplex and multiplex Polymerase Chain Reaction testing of amniotic fluid (PCR-AF) is useful for the identification or exclusion of fetal *T. gondii* infection using the B1 gene as a target sequence (Burg, Grover, Pouletty, & Boothroyd, 1989) . The PCR-AF method is also a safer and more sensitive test option compared to fetal blood sampling while allowing earlier detection of fetal infection (Foulon et al., 1999; Hohlfeld et al., 1994).

In clinical cases of HIV-positive or immunocompromised patients with impaired immune function, histologic examination or PCR screening can be used to diagnose *T. gondii* infection using cerebrospinal fluid, tissue biopsies, and vitreous body from patients with suspected ocular toxoplasmosis (uveitis) (Costa et al., 2001; Dabil, Boley, Schmitz, & Van Gelder, 2001; Vidal, Colombo, Penalva de Oliveira, Focaccia, & Pereira-Chioccola, 2004). Rapid diagnosis can be made by making simple impression smears of lesions on glass slides, fixation with methanol and staining with one of the Romanowsky stains such as the Giemsa stain. Other methods in aiding diagnosis includes the identification of *T. gondii* bradyzoites using periodic acid Schiff (PAS) staining, immunohistochemical staining of the parasite with fluorescent or other forms of anti-*T. gondii* antisera conjugates and electron microscopy (Hill & Dubey, 2002). When staining fails to result in definite diagnosis, for example in tissue samples with degenerating parasites common in lesions; inoculation of biopsy materials into laboratory mice or cell cultures can aid diagnosis (Hill & Dubey, 2002).

2.5- Treatment and management of Toxoplasmosis

Toxoplasmosis in humans is widely treated with a combination of sulphadiazine and pyrimethamine (Daraprim) (Guerina et al., 1994). The commonly used sulfonamides: sulfadiazine, sulfamethazine and sulfamerazine, are all effective against toxoplasmosis. The pyrimethamine and sulfonamide treatment need to be administered in combination with folinic acid (Leucovorin) to alleviate the suppressive side effects on the bone marrow caused by the folic acid inhibitory reaction of the drugs. Pyrimethamine and sulfonamide works synergistically in interfering with folic acid synthesis by inhibiting the enzymes dihydrofolate reductase from the folic-folinic acid cycle; and dihydropteroate synthetase from the p-aminobenzoic acid (PABA) pathway respectively. These drugs are effective against tachyzoites, but not against bradyzoite or the encysted form of the parasite, and thus cannot fully eradicate the infection (Hill & Dubey, 2002; Hokelek, 2009). Sulfa drugs must be administered in daily divided doses because sulfa compounds are excreted within a few hours of administration.

Pregnant women with a positive serologic profile for acute toxoplasmosis is treated with Spiramycin (Rovamycin) to prevent vertical transmission of the parasite to the fetus (J. Jones et al., 2003). Spiramycin achieves high tissue concentration in the placenta and inhibits parasite transmission across the placenta (Gagne, 2001). Generally, pyrimethamine (pregnancy category C drug) is not prescribed to pregnant women before confirmation of fetal infection due to the bone marrow suppressive and teratogenic effect of the drug. However, once amniocentesis diagnosis by PCR-AF confirms that the developing fetus is already infected *in utero*, pyrimethamine (Daraprim), sulphadiazine and Leucovorin (folinic acid) treatment regime is prescribed for the affected mother. However, it is a general rule of practice that pyrimethamine is

never administered before the 12th week gestation period (Pastorek, 1994). Evidence shows that the pyrimethamine-sulphadiazine treatment regime reduces the risk of congenital toxoplasmosis by 70% and effectively crosses the placental barrier (Gagne, 2001). Postnatally, congenitally-infected infants are continued on the standard treatment regime of sulphadiazine and pyrimethamine in conjunction with antibiotics and leucovorin (folinic acid) for 1-2 years (J. Jones et al., 2003) to prevent late sequelae and relapse of toxoplasmosis, especially the occurrence of chorioretinitis.

In HIV-positive patients with clinical presentation of TE, the standard treatment regime consists of pyrimethamine with sulphadiazine or clindamycin (Dannemann et al., 1992; Benjamin J. Luft & Remington, 1992). However, this treatment frequently causes severe allergic and hematotoxicity side effects that forces the discontinuation of therapy (Dannemann et al., 1992). An alternative treatment with less toxic side effects is the drug Atovaquone which blocks the parasite's respiratory chain, and is effective against both the tachyzoite and cystic form of *T. gondii* (Baggish & Hill, 2002; Chirgwin et al., 2002; Shubar et al., 2009). Other drugs that have been used to treat more difficult cases of toxoplasmosis in sulfa-drugs hypersensitive adult patients includes rifabutin, doxycyclin, the macrolide antibiotic azithromycin, and clarithromycin (Araujo, Suzuki, & Remington, 1996; Rothova, Bosch-Driessen, van Loon, & Treffers, 1998). However, alternative treatments with these macrolides have proven to be less efficacious (Fernandez-Martin et al., 1991; Hagberg, Palmertz, & Lindberg, 1993; Saba et al., 1993).

2.6- Invasion of host cells

T. gondii invasion is by parasite-directed active penetration into host cells. This process is dependent on parasite motility powered by the parasite's actin-myosin motor (Dobrowolski, Carruthers, & Sibley, 1997; Dobrowolski & Sibley, 1996). Initiation of Toxoplasma invasion begins by the orientation of the parasite's apical end towards the host cell surface (Chiappino, Nichols, & O'Connor, 1984; T. C. Jones, Yeh, & Hirsch, 1972). Invasion is an active process that not only depends on the apical-polarized attachment of the parasite onto host cell surface, but also the gliding motility locomotion of *T. gondii* whereby the parasite adhesin - host receptor complex linkage is translocated towards the posterior end of the parasite along a tight apposition structure known as the moving junction (MJ) during parasite penetration. As the parasite enters, it progressively slides into a parasitophorous vacuole (PV) which resists acidification and fusion with lysosomes (Joiner et al., 1990; Mordue, Håkansson et al., 1999), forming a safe haven for Toxoplasma to replicate within the confines of the PV (Figure 2.4). The invasion event is rapid with complete penetration of the parasite into the host cell by 15 to 30 s. During invasion, there is a peculiar constriction of the parasite as it squeezes through the MJ into the host cell (reviewed in Black & Boothroyd, 2000) (Figure 2.5). This active parasite-directed invasion process is distinct from Toxoplasma phagocytosis observed with professional phagocytes such as macrophages. Phagocytosis is a comparatively slow process (2 to 4 min), with no apical orientation of the parasite, no obvious MJ constriction deformity, and also a more spacious endocytic vacuole compared to the tight confines of a PV in active invasion.

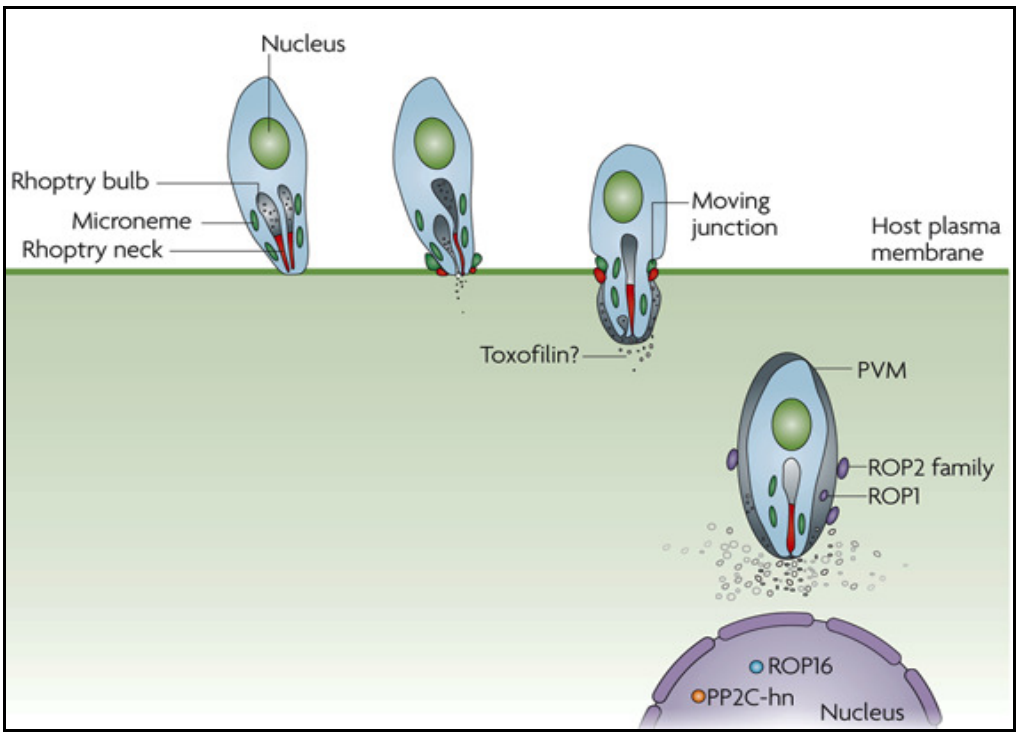

FIGURE 2.4 **Schematic model of *Toxoplasma gondii* invasion.** The rhoptry bulbs (grey), rhoptry necks (red) and microneme simultaneously release their contents during the invasion process and collaborate to form the moving junction (MJ). The MJ migrates down the length of the parasite forming a ring of contact with the host plasma membrane which effectively excludes host integral membrane proteins to form the parasitophorous vacuole membrane (PVM). (Adapted from Alexander, Mital, Ward, Bradley, & Boothroyd, 2005; and John C. Boothroyd & Dubremetz, 2008)

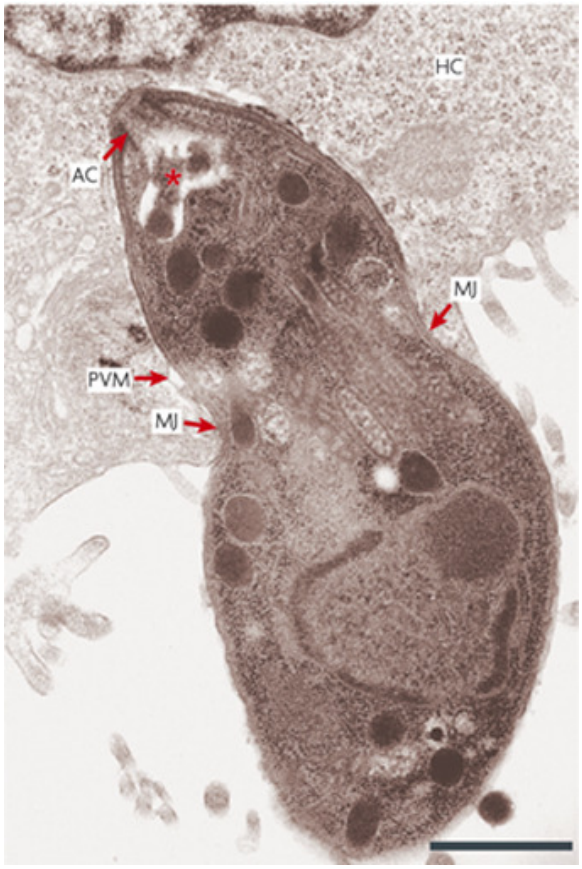

FIGURE 2.5 ***Toxoplasma gondii*** **tachyzoite constriction at the moving junction during invasion.** A TEM image of a *T. gondii* tachyzoite invading a HeLa cell (HC). Rhoptry exocytosis yields an irregularly shaped organelle (asterisk) near the apical cytoskeleton (AC). The host cell membrane-derived parasitophorous vacuole membrane (PVM) is seen closely enveloping the parasite portion that has invaded the host cell. Invasion is thought to be driven by parasite actin-myosin motors acting at the moving junction (MJ). Scale bar represents 0.5 µm. (Adapted from John C. Boothroyd & Dubremetz, 2008; and Jean Francois Dubremetz, 1998)

There are 3 distinct secretory organelles in *T. gondii* that plays crucial roles in the invasion and establishment of infection within its host and whose function critically depends on the precisely orchestrated sequence of secretory discharge in the invasion process. The first two organelles – the micronemes and rhoptries, are located at the apical end of the parasite, whereas the third organelle – the dense granules (DG) are dispersed in the parasite's cytoplasm. It is speculated that *T. gondii* compartmentalizes its secretory proteins in separate organelles according to common function, thereby promoting its regulated order of secretion during invasion (Carruthers, 2002).

Upon initial contact of the apical pole of Toxoplasma on a host cell surface, micronemes would be the first to discharge its secretory contents that functions in

parasite attachment and penetration into host cells. There are approximately 100 micronemes that are localized to the apical end of *T. gondii*, which can dynamically shuttle along the parasite's microtubules or microfilaments to the extreme apical tip where it fuses with the plasma membrane and deploys its protein content at the initiation of invasion (Carruthers, Giddings, & Sibley, 1999). Following microneme secretion, the rhoptries immediately begin to inject its protein contents into the host cell cytoplasm at the invasion loci (Barbara A. Nichols, Mary Louise Chiappino, & G. Richard O'Connor, 1983). Usually, there are 8-16 rhoptries per parasite. During invasion, the club-shaped rhoptries fuse with the parasite's cell membrane at the apical tip and discharge their protein content into the nascent PV via the fused channel formed at the conoid (B.A. Nichols, M. L. Chiappino, & G. R. O'Connor, 1983). Besides this, ROP proteins from the rhoptry bulb are also deployed into the host cell via small vesicles known as evacuoles. Subsequently, the ROP-containing-evacuoles fuse with the developing PV and disperses the ROPs onto the cytosolic face of the PVM (Hakansson, Charron, & Sibley, 2001). The rhoptry proteins functions in PV biogenesis and host organellar (mitochondria and ER) attachment to the PV as well as parasite virulence (Beckers, Dubremetz, Mercereau-Puijalon, & Joiner, 1994; Nakaar et al., 2003; Qiu et al., 2009). A study to discover the composition of the PV showed that approximately 20% of the PV membrane is generated by the parasite rhoptries during penetration, while the majority of the membrane is derived from the host cell (Suss-Toby, Zimmerberg, & Ward, 1996). Early invasion events captured on electron micrographs shows membranous whirls being secreted from rhoptries lumen and which is possibly responsible for the extension of the PV encapsulating *T. gondii* (Barbara A. Nichols et al., 1983).

Finally, the parasite's DG secretes its protein into the PV lumen once invasion is complete with the PV budding off from the host cell membrane and *T. gondii* is fully enveloped within the PVM. The DG proteins play crucial roles in the structural modification of the PV, nutrient acquisition from its host cell and also promoting the parasites' replication by endodyogeny within the PV confines (Cesbron-Delauw, 1994).

Among the three organelles, the micronemes have the most significant conservation among all apicomplexan parasites (Carruthers, 2002). Therefore, it is speculated that micronemes may be essential in apicomplexan parasite invasion and has generated a growing interest and intensified research efforts at discovering and characterizing its' proteins. There are several characteristics of microneme proteins (MICs) that have been elucidated through several studies. The first is that nearly half of it is predicted to be Type 1 membrane proteins with a single membrane-spanning domain located near the C-terminus. This is a divergence from other previously characterized Toxoplasma surface proteins (SAGs) that are tethered on the cell membrane surface by linkage to glycosylphosphatidylinositol (GPI) anchors (J. C. Boothroyd, Hehl, Knoll, & Manger, 1998). This is an important distinction from the SAG family surface proteins because the membrane-tethered MICs allows it to be the bridge proteins between host cell receptors and the parasite's internal actin-myosin (or actomyosin) motor that powers the gliding translocation essential for parasite invasion. This is because GPI-bound proteins are only linked to the cell membranes' lipid moiety and do not interact with the underlying parasite actomyosin. In particular, the TgMIC2-TgM2AP microneme-secreted protein complex is found to be co-localized to the MJ during Toxoplasma invasion, implicating these proteins to be directly involved in the motility-dependent host cell invasion (Rabenau et al., 2001). However, the MIC2 protein is only transiently detectable on the parasite surface when there is contact with

the host cell and is proteolytically released from the cell surface once invasion is complete (Vern B. Carruthers et al., 1999).

The membrane-spanning domain of several MICs characterized thus far contains recognition sequences for rhomboid proteases, which is essential for intramembrane proteolytic cleavage of the MIC adhesins in order to disengage receptors for the completion of its' invasion (Brossier, Jewett, Sibley, & Urban, 2005; reviewed in Dowse & Soldati, 2004; Reiss et al., 2001). Interestingly, this membrane-spanning domain of surface MICs is a site that is conserved for all Apicomplexan microneme proteins (Opitz et al., 2002), implying the essential nature of the intramembrane proteolysis event for effective release of the PV from host cell membrane. Another adaptation of the MIC proteins is that it consists of domain structures homologous to vertebrate adhesive proteins such as integrins, thrombospondin and epidermal growth factor (EGF) (reviewed in Tomley & Soldati, 2001), which is a feature that potentially resolves the reason for the parasite's remarkable ability at establishing infection in a wide range of host and nucleated cells. The MICs also appear to require being in the form of adhesive complexes in order for it to be functional (Carruthers, 2002). To date, there are three MIC complexes discovered – they are the TgMIC1-TgMIC4-TgMIC6 (Reiss et al., 2001), TgMIC3-TgMIC8 (Meissner et al., 2002), and TgMIC2-TgMIC2-associated-protein (or TgMIC2-TgM2AP) (Rabenau et al., 2001).

There are several postulates as to the reason why it is the general rule that MICs function in complexes, the first is that some heterologous members of the protein complex function as 'quality control' chaperons that is needed to allow the complex to exit the Golgi apparatus on its way to the micronemes (reviewed in Carruthers, 2002; Reiss et al., 2001). Targeted genetic disruptions of TgMIC1 and knockout mutation of

TgM2AP caused its respective complex partner MIC proteins to be retained in the Golgi and endoplasmic reticulum (ER) instead of reaching its intended destination in the microneme (My-Hang Huynh et al., 2003; Reiss et al., 2001). The second postulate is that MIC proteins function in the form of complexes because each complex consists of one membrane-spanning protein required for correct microneme targeting, membrane anchoring, and intramembrane proteolytic cleavage to disengage host receptor attachments upon successful completion of invasion; while at least another one of the MIC proteins would be responsible for binding to host cell receptors. The Toxoplasma parasite's broad host and target cell range may be attributed to the MIC proteins' homologous vertebrate adhesive protein domains which confers the ability of pervasive lectin-like binding to extracellular matrix proteins commonly expressed among vertebrate cells such as laminin and heparan sulfate proteoglycans (HSPG) (Carruthers, Hakansson, Giddings, & Sibley, 2000; Furtado, Slowik, Kleinman, & Joiner, 1992). Therefore, the MIC proteins achieve its' multifaceted role in the invasion of target cells by forming multimeric complexes of MICs with distinct functions – some for membrane anchoring, some for receptor binding and some as 'quality control' chaperons.

Ca^{2+} signalling seems to play a crucial role in *T. gondii* invasion processes. Microneme discharge is triggered by a Ca^{2+}-dependent signaling pathway. This condition can be simulated by the addition of calcium ionophores or short chain alcohols to elevate Ca^{2+} levels and specifically trigger microneme release (Carruthers, Moreno, & Sibley, 1999; Carruthers & Sibley, 1999). On the other hand, addition of a Ca^{2+} chelator, such as BAPTA-AM, not only blocked microneme secretion, but also abrogated parasite's attachment to host cells (V. B. Carruthers et al., 1999), inhibited gliding motility and invasion into host cells by > 90% compared to controls

(Mondragon & Frixione, 1996; Mondragon, Meza, & Frixione, 1994). Although the *T. gondii* Ca^{2+}-dependent signaling pathway has not been fully elucidated, there are evidence of two calcium-dependent protein kinases – which is TgCDPK1 and TgCDPK2, that have been shown to function in the regulation of motility and host cell attachment (Billker, Lourido, & Sibley, 2009; Kieschnick, Wakefield, Narducci, & Beckers, 2001). These kinases may directly or indirectly influence micronemal discharge. Another invasion protein which may be dependent on Ca^{2+} signaling is the secretion of a phospholipase from rhoptries that was formerly termed as a penetration enhancement factor (PEF) (Lycke & Norrby, 1966; Saffer & Schwartzman, 1991) for its role in causing morphological degeneration of host cell membranes and thus facilitating host cell entry. These discoveries imply that Ca^{2+} signaling may be an important pathway to target for therapeutic inhibition of *T. gondii* invasion into host cells.

2.7- Toxoplasma Replication and Egress

The lytic cycle of *T. gondii* consists of parasite invasion, replication and egress. Following invasion, the parasite commences replication within the confines of the PV in a process known as endodyogeny (Zypen & Piekarski, 1967). However, for replication to effectively take place, *T. gondii* seems to modify its PVM to allow for nutrient acquisition in order to support parasitic growth. Toxoplasma is auxotrophic for purine biosynthesis and therefore needs purine salvage in order to persist and proliferate within its host (Schwartzman & Pfefferkorn, 1982). There are two features of *T. gondii* to facilitate this; firstly, the porous structure of the PVM (size exclusion limit ~ 1.3 kDa) which is presumably formed by DG protein secretions, allows the acquisition of purines in the form of ATP from the host cytosol. Secondly, the parasitic enzyme NTP

hydrolase (NTPase) that was discovered in the PV lumen (Asai et al., 1995; Asai, O'Sullivan, & Tatibana, 1983) may be responsible in the purine salvage process by hydrolyzing host ATP into adenosine for *T. gondii* utilization in nucleic acid synthesis (Schwartzman & Pfefferkorn, 1982). The NTPase may possibly not be the only enzyme involved in the purine salvage process and like many other parasitic invasion and metabolic processes - it may be a redundant pathway. However, this remains to be elucidated in greater details. Other than purines, the parasite is also auxotrophic for tryptophan, arginine, polyamines, cholesterol, iron and other essential nutrients (reviewed in Laliberté & Carruthers, 2008). To circumvent this, *T. gondii* acquires its nutrients from host cells via both passive and active transport at the PVM which consists of elaborate pores that allows the passage of small, soluble metabolites within the range of 1.3 – 1.9 kDa, such as glucose, amino acids, nucleotides and ions (Schwab, Beckers, & Joiner, 1994).

Immediately following invasion, *T. gondii* also modifies the PVM to support its rapid growth and replication. Within 4 hours post-infection, the PVM recruits host mitochondria and ER to be intimately joined to its surface (Sinai, Webster, & Joiner, 1997), presumably for lipid trafficking into the parasite; and also recruits host endo-lysosomal vesicles selectively for scavenging host cholesterol (Coppens et al., 2006). The remodeling of the PVM during Toxoplasma parasitism is caused by the sequestration of DG proteins. In particular, GRA3 was found to be involved in ER attachment to the PVM (J. Y. Kim, Ahn, Ryu, & Nam, 2008), and GRA7 was found to be intimately associated with host endolysosomes for cholesterol salvage (Coppens et al., 2006). The association between the PVM and the host mitochondria and ER remains stable throughout the evolution of the PV.

T. gondii endodyogeny replication begins with the formation of a pair of nascent pellicular membranes from the middle of the cell. This membranous structure extends itself from its tip that resembles a rudimentary conoid and microtubule-organizing center to delineate each daughter cells. This is followed by the formation of nascent micronemes and rhoptries at the apical tip of each daughter cell while the mother cell grows more spherical to accommodate the growing daughter cells. The mitochondria, apicoplast and nucleus would then begin to divide between the daughters. As the progenies continue to grow, the cytoplasm and all of its other contents would divide between the 2 daughters until eventually the mother's inner membrane complex (IMC) disintegrates and the original plasmalemma envelopes the two daughter cells. Finally, the two new cells begin to separate extending from the anterior pole throughout most of the cell but maintains a residual linkage at the posterior end. This posterior pole attachment results in the 'rosette' formation as the parasite continues to replicate within the PV (Figure 2.6) (reviewed in Carruthers, 2002; Zypen & Piekarski, 1967).

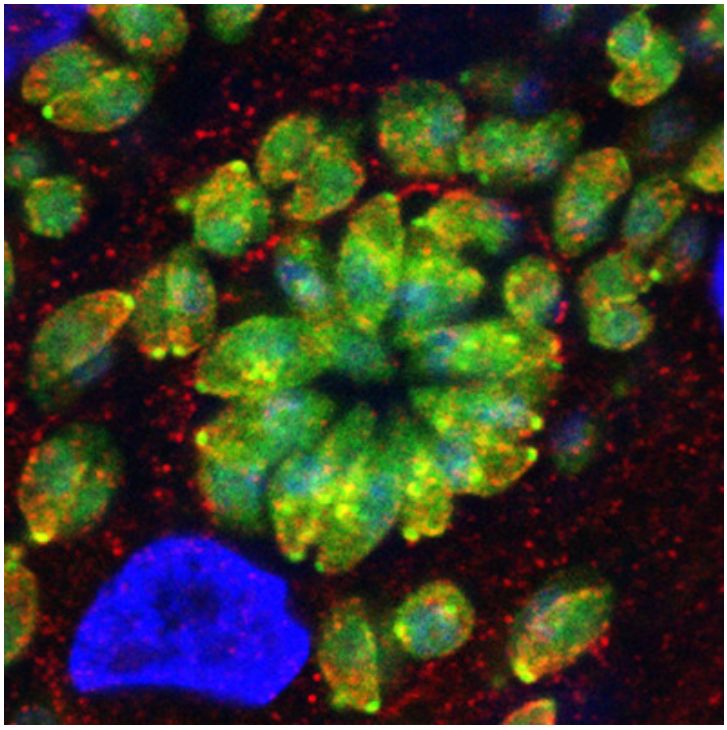

FIGURE 2.6 **Intracellular *Toxoplasma gondii* rosette formation.** A confocal fluorescent microscopy image of a *T. gondii* rosette (green). (Image courtesy of Kamal, from the Albert Einstein College of Medicine, New York)

When *T. gondii* replication reaches a critical threshold within host cells, the parasites will rupture the PV and release highly motile tachyzoites out of the host to rapidly invade neighbouring cells in a process known as egress. Parasite egress causes cell lysis and necrotic foci that is responsible for the pathogenesis of the disease. The egress of even a single Toxoplasma parasite out of the host cell is enough to cause the lytic destruction of the cell.

Parasitic egress is triggered by Ca^{2+} signaling, and can be induced by addition of calcium ionophores such as the A23187 drug to cell cultures infected with *T. gondii* (Endo, Sethi, & Piekarski, 1982; Pressman, 1976). This drug increases the permeability of cell membranes for the passive diffusion of Ca^{2+} and results in an increase of Ca^{2+} levels within the PV. This is followed by parasite movement within the PV, the rupture of the PV, rapid migration of the parasites through the host cytosol and puncturing out from the host plasmalemma and cell membrane (Endo et al., 1982). The reducing agent dithiothreitol (DTT) is also capable of inducing parasite egress (Stommel et al., 1997). DTT stimulates parasite egress by activating the parasite's vacuolar NTPase, which degrades the host ATP and ADP for purine salvage, followed by elevated levels of cytoplasmic Ca^{2+} and parasite egress (Silverman et al., 1998). Activation of NTPase from just a single parasite is sufficient to exhaust the entire pool of host ATP within minutes, triggering egress (Silverman et al., 1998); which explains why cell destruction can occur even in infections with just a single tachyzoite. Although the link between NTPase activation and the parasite's elevated vacuolar Ca^{2+} level is uncertain, these observations implies that NTPase influences the intracellular Ca^{2+} flux and parasite egress (Stommel et al., 1997).

2.8- Immune Evasion and Host Cell Subversion

T. gondii has the remarkable ability to invade and establish infection in nearly all nucleated cells. This ability has led to many fascinating discoveries on the strategies utilized by the parasite to manipulate host cellular responses in order to establish infection and to cause widespread dissemination. *T. gondii* has an obligate intracellular existence, and is adapted to rapidly invade host cells to avoid the host's cellular and humoral immunity capable of killing extracellular pathogens. Therefore, an immunotherapy strategy to circumvent the infection is to inhibit the parasite's cellular invasion.

Parasite dissemination occurs through several routes – the paracellular pathway, the transcellular traversal, and the leukocyte-assisted transfer which is also known as the Trojan Horse mechanism (Figure 2.7) (reviewed in Lambert & Barragan, 2010; reviewed in Tardieux & Ménard, 2008). Both the paracellular and transcellular systemic dissemination involves extracellular *T. gondii*, whereas the Trojan Horse mechanism involves intracellular *T. gondii*. The parasites' competent ability at systemic dissemination results in unhampered Toxoplasma invasion into immunologically-privileged sites such as the blood-brain barrier, the blood-retina barrier, the blood-testis barrier and the placenta where it causes the most severe pathology (reviewed in Lambert & Barragan, 2010).

In the paracellular route, *T. gondii* tachyzoites uses its gliding motility locomotion to breach intercellular junctions and traverse between the host cell linings without disrupting the integrity of the epithelial layer. In a study conducted by Barragan and co-workers, it was shown that the parasite's micronemal adhesin MIC2 interacts

with host cell ICAM-1 in the paracellular transmigration of *T. gondii* across cellular barriers (Barragan, Brossier, & Sibley, 2005). As for the transcellular pathway, active invasion by the parasite may result in the breaching of the apical surface of an endothelial cell and exit through the basolateral side. It is still a theoretical pathway as there has been no documented evidence to prove (or disprove) it. However, it is a characteristic translocation observed in the dissemination of highly motile *Plasmodium* sporozoites (Mota et al., 2001) and may possibly be a yet unobserved pathway utilized by *T. gondii*.

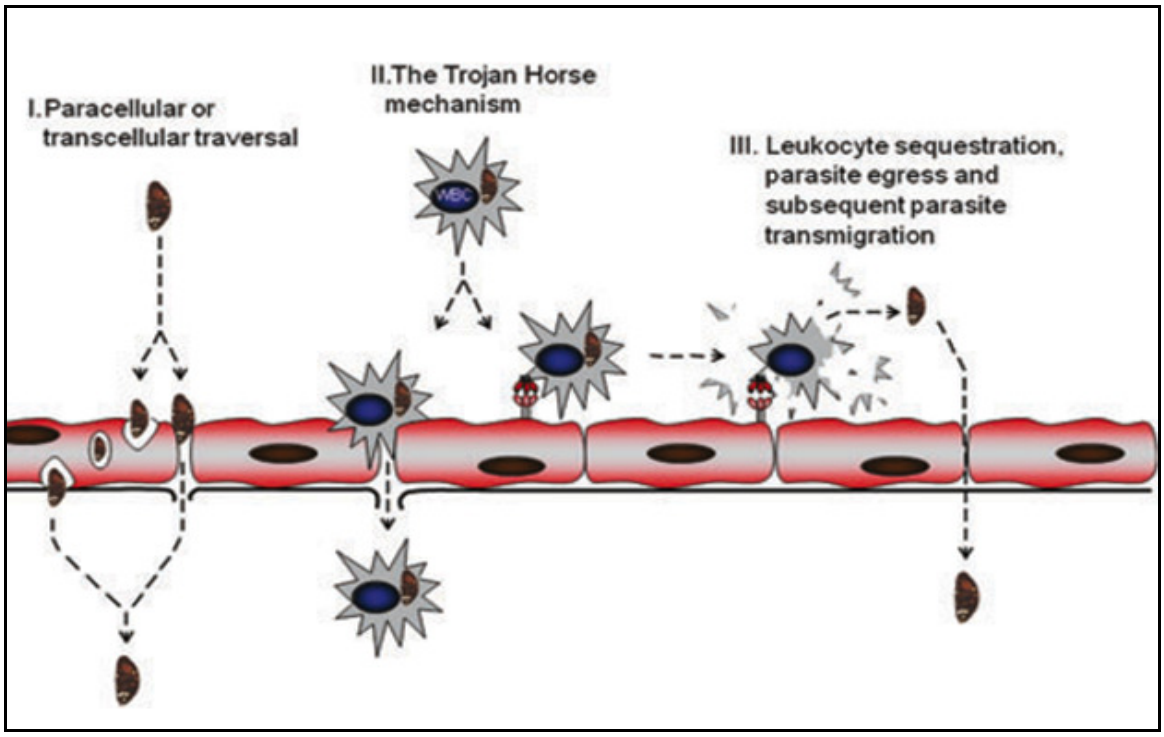

FIGURE 2.7 **Strategies for *Toxoplasma gondii* dissemination across cellular barriers.** (I) Parasites may transmigrate via its gliding motility through the intercellular junctions without disruption of the integrity of the cellular barrier (paracellular traversal); or may actively invade the apical part of the cell and exit through the basolateral side (transcellular traversal). (II) The parasites can also disseminate through infected leukocytes (WBC) by the Trojan Horse mechanism, or (III) binding to apoptosis-inducing ligands on the endothelial barrier which may induce parasite egress from the infected WBC, with subsequent parasite traversal. (Adapted from Lambert & Barragan, 2010)

In the Trojan Horse mechanism, *T. gondii* is known to hijack migratory leukocytes (WBC) to breach cellular barriers. When a host ingest oocysts or tissue cysts through contaminated food or water, the zoites infects enterocytes within the gut lumen to initiate its' parasitic lytic cycle. Infected enterocytes secrete chemokines such as monocyte chemotactic protein 1 (MCP-1 / CCL-2), macrophage inflammatory proteins 1α and β (MIP-1α and β / CCL-3 and CCL-4), and MIP-2 / CXCL2, which is responsible for the recruitment of leukocytes to the inflammatory site of the lamina propria, followed by the hijacking of the migratory leukocytes by the zoites (Buzoni-Gatel et al., 2001; Luangsay et al., 2003). Within 3 hours post-invasion, infected human and murine dendritic cells (DCs) and macrophages adopts a hypermotility phenotype and disseminates the parasite to distant organs and immunoprivileged sites such as the brain (Courret et al., 2006; Lambert, Hitziger, Dellacasa, Svensson, & Barragan, 2006). In an alternative mechanism, leukocytes infected with tachyzoites may cross the placenta to cause congenital infection through the paracellular route. The maternal-fetal interface consists of layers of protective fetal trophoblast cells to prevent maternal transmission of cytotoxic adaptive immune response, as well as cytolytic mediators such as perforin and Fas/Fas ligand (FasL) which normally restricts leukocytes passage and provide host defense against infection (Crncic et al., 2005). However, *T. gondii*-infected leukocytes may still circumvent this epithelial barrier by active egress out of infected leukocytes upon binding of the apoptosis-inducing Fas ligand or perforin-mediated cytotoxicity, followed by paracellular traversal into neighboring cells, including the specific targeting immune cells itself which triggered the parasite egress (E. K. Persson et al., 2007), thereby promoting its dissemination.

Extracellular tachyzoites are resistant to non-immune human serum but sensitive to antibody-mediated lysis (Couper, Roberts, Brombacher, Alexander, & Johnson, 2005). Therefore, its dissemination strategy is to allow parasite translocation away from the inflammatory site and into the circulation where it can be sequestered into immunologically-restricted tissues for protection. Toxoplasma translocation occurs either through the extracellular route which involves direct tissue penetration by motile parasites via the paracellular pathway or through leukocyte-mediated transfer (Trojan Horse mechanism). The preference and kinetics of the pathways utilized by the parasite to assure its propagation is strain-specific and differs between each genotype. *T. gondii* is mainly divided into three distinct genotypes which differ genetically by not more than 1 % (Sibley & Boothroyd, 1992; Su et al., 2003). The murine-virulent Type 1 parasite exhibits superior transmigratory capacity via the extracellular route and higher growth rates resulting in rapid dissemination and higher parasite tissue burden (Barragan & Sibley, 2002). In contrast, Type II and Type III parasites have a significantly less potent transmigratory capacity and demonstrates lower virulence in mice (Jeroen P. J. Saeij, Boyle, Grigg, Arrizabalaga, & Boothroyd, 2005). Despite this reduced virulence, it is the Type II genotype that is most prevalent in human infections globally (Darde, 2004). The Type II and Type III genotype preferentially disseminates through the leukocyte-mediated transfer route and achieves significantly higher parasite loads in the circulation, while Type I tachyzoites are substantially less efficient in exploiting host leukocytes for dissemination (Lambert, Vutova, Adams, Lore, & Barragan, 2009). In acute infection, Type II and Type III parasites are found intracellularly in the circulation soon after infection whereas the Type I parasite preferentially invades the mesenteric circulation as extracellular parasites (Courret et al., 2006). In terms of disease pathogenesis, severe human toxoplasmosis is usually associated with Type I and rare, atypical strains; while the more prevalent Type II strain causes varied disease severity

(Darde, 2004). Mice are hypersensitive to Type I infection, and the lethal dose is a single viable parasite; whatever the genetic background of the mice may be. Type II and Type III strains cause less aggressive infections with a 50% Lethal Dose (LD_{50}s) in mice of $> 10^3$, with variations between different host genotype backgrounds (Jeroen P. J. Saeij et al., 2005). Taken together, this indicates that the efficiency of the tachyzoites' exploitation of the host leukocytes-mediated transfer pathway or the direct tissue penetration pathway is strain-specific; with Type I strain being most proficient at direct tissue penetration via extracellular parasites, while Type II strain is superior at leukocyte-mediated transfer for its tachyzoite-shuttling function and dissemination.

Following active invasion, *T. gondii* induces a hypermotility phenotype in human and murine macrophages and DCs. This phenotype is characterized by random directional amoeboid-like motion, increase in speed, distance and transmigratory capacity across epithelial cells (Lambert et al., 2006) which may be a post-transcriptionally regulated event (reviewed in Lambert & Barragan, 2010). To gauge the impact of infected DCs on murine host parasitic burden and pathogenesis, a study was conducted by adoptive-transfer of *T. gondii*-infected DCs into immunologically-compatible mice. The findings showed that infected DCs caused a substantially more rapid dissemination of *T. gondii* to distant organs and a more severe pathogenesis compared to intraperitoneal inoculation with extracellular parasites (Lambert et al., 2006). Interestingly, this hypermotility phenotype exhibited by infected DCs can be abrogated by inhibiting leukocyte motility (Lambert et al., 2006). Presumably, the hypermotility phenotype of infected DCs is controlled by G*i*-protein coupled receptors (G*i*-PCR) signaling which mediates leukocyte chemotaxis through binding of chemokines to the G protein receptors (reviewed in Lambert & Barragan, 2010; Rot & von Andrian, 2004).

The *T. gondii* parasite is not only capable of hijacking immune cells as a conduit for its dissemination, but the parasite is also capable of evading the host immune defenses to ensure its propagation. Cell-mediated cytotoxicity is an important immune defense mechanism of the host to protect against pathogen infections. Cytotoxicity can be induced by two mechanisms: the first is via the induction of apoptosis upon death receptor ligation by effector T cells (both $CD4^+$ and $CD8^+$) and NK cells, and the second is via the secretion of perforin and granzymes by cytotoxic lymphocytes. However, Toxoplasma infection not only renders both of these cytotoxic mechanisms ineffective in eradicating the parasite but is instead redirected for its disseminative advantage. When effector T cells engages the death receptors on infected target cells, it does not show characteristic signs of apoptotic degradation, but instead triggers rapid parasite egress which releases highly infectious parasites that infects other surrounding cells, including the specific effector T cell themselves (Figure 2.7) (E. K. Persson et al., 2007). This death receptor-induced egress pathway is stimulated by caspase activation and a concomitant release of intracellular calcium (E. K. Persson et al., 2007). The perforin or granzyme-cytotoxicity pathway also triggers the same signature rapid parasite egress that leaves necrotic cell and tissue abscesses in its wake with transmission of infectious tachyzoites to its surrounding cells, although this process does not depend on the caspase activation of the apoptotic mechanism. *T. gondii* has also been shown to be able to infect cells of the innate immune system. In particular, perforin-dependent NK cells targeting infected DC for cytotoxic destruction has been shown to trigger parasite egress and became infected themselves along with other surrounding cells (C. M. Persson et al., 2009). In addition, these infected NK cells are themselves not efficiently targeted by non-infected NK cells for perforin-dependent

killing (C. M. Persson et al., 2009), which may be another novel mechanism for parasite sequestration and immune evasion.

Toxoplasma infection of the Type I strain induces a vigorous Th1 immune response and extremely elevated levels of pro-inflammatory cytokines such as interferon-γ (IFN-γ), tumor necrosis factor-α (TNF-α), interleukin-12 (IL-12), and IL-18, whereas infection with Type II and Type III strains produce a more modest Th1 response (Gavrilescu & Denkers, 2001; Mordue, Monroy, La Regina, Dinarello, & Sibley, 2001). The moderated Th1 immune response seen in the less virulent Type II infections leads to controlled infection and minimal tissue damage with latent infection of bradyzoites sequestered within immune-privileged tissues (Lang, Groß, & Lüder, 2007). It has been proposed that the inflammatory Th1 immune response to *T. gondii* infection may be necessary to prevent intermediate host mortality and thereby promote the parasite's life-long quiescent persistence within its host (Lambert & Barragan, 2010). Despite elevated levels of the principal Th1 cytokine IFN-γ in *T. gondii* infected cells, the increased cytokine level seems ineffective in the stimulation of inducible nitric oxide synthase (iNOS) and MHC class II within macrophages (Lüder, Algner, Lang, Bleicher, & Gro, 2003). Zhao and co-workers have also shown that IFN-γ-primed macrophages infected with *T. gondii* are also capable of resisting the microbicidal effects of the immunity-related GTPase (IRG) protein family (Y. Zhao et al., 2009). However, this immune-evasion mechanism is only observed within the virulent Type I Toxoplasma infection in which fully armed macrophages resist IRG-mediated disruption of its PVM and escape autophagic destruction (Y. Zhao et al., 2009). This IRG-mediated resistant phenotype was also observed in infected murine fibroblasts (reviewed in Y. O. Zhao et al., 2009). Genome-wide transcriptional profiling lends support to these observations as it was elucidated that there is a globally repressive

effect of *T. gondii* infection on IFN-γ activated cells that causes silencing of the cytokines' default modulation of host immune response to eliminate infection (S.-K. Kim, Fouts, & Boothroyd, 2007). Toxoplasma infection inhibits STAT1 function in the nucleus and subsequently blocks the STAT1-induced expression of IFN regulatory factor 1 (IRF1), which is a transcription factor for many of the IFN-γ responsive genes (S.-K. Kim et al., 2007). This immune-silencing effect in the midst of strong IFN-γ activity is possibly a contributing factor to the parasite's persistence within the host.

Toxoplasma infection also induces the production of immune-regulatory and anti-inflammatory cytokines such as IL-10, transforming growth factor-β (TGF-β) and lipoxin which dampens the Th1 immune response, deactivates macrophages and lessens immune-associated pathology (reviewed in Lang et al., 2007; Machado & Aliberti, 2006). Collectively, this indicates that *T. gondii* maintains a delicate balance between stimulation and suppression of host immune responses in order to persist and survive within its host and to allow propagation to subsequent intermediate hosts.

Another host immune response to limit infections caused by viruses, bacteria, and eukaryotic pathogens is by the induction of apoptosis or programmed cell death. Apoptotic cells emit signals for macrophages activation and phagocytic engulfment of the infected cells. In addition to the ability of the parasite to subvert host cells to its advantage for dissemination across cellular barriers and nutrient acquisition, *T. gondii* has also evolved mechanisms to impede the apoptotic immune response and avoid rapid clearance by macrophages. The apoptosis pathways involve the activation cascade of a class of cysteine proteases known as caspases. It has been observed that Toxoplasma normally manages to silence the apoptotic immune response by impairing the host' caspase activation at multiple points in the pathway. The apoptotic process for the

elimination of pathogen-infected cells can be induced via several pathways: the mitochondrial apoptotic pathway (Williams, 1994), the death receptors (Fas/CD95 or TNF-R) ligation pathway (Dockrell, 2003; Krammer, 2000), and the perforin and granzymes-mediated killings by NK cells or T cells (reviewed in Lieberman, 2003). *T. gondii* has been shown to inhibit apoptosis in the first two pathways, and to redirect perforin and granzymes-mediated cytotoxicity to cause rapid parasite egress for its dissemination to adjacent cells, including the immune cells that triggered the egress itself (Denkers et al., 1997; C. M. Persson et al., 2009; E. K. Persson et al., 2007).

In the death receptor pathway, ligation of the TNF-R or Fas death receptors on the target cell plasma membrane will trigger the assembly of a complex known as the death-inducing signaling complex (DISC). The DISC complex then activates caspase 8, which in turn induces the suicide spiral of the caspase cascade of apoptosis. In *T. gondii* infection, activation of caspase 8 is antagonized by aberrant proteolytic cleavage and degradation, leading to inhibition of apoptosis in infected cells (Vutova et al., 2007). In the mitochondrial apoptotic pathway, the suicide spiral is normally induced by stress or DNA damage to the cell, and is initiated by the mitochondrial release of cytochrome c into the cytosol. Cytochrome c then induces the caspase cascade beginning with the activation of caspase 9 and followed by the proteolytic cleavage of caspase 3, which leads to the cell undergoing self-catabolism (Lemasters et al., 1999). However, this apoptotic process is also inhibited in *T. gondii*-infected cells by the substantially lowered cytochrome c release and consequently the muted activation of caspase 9 and caspase 3 activity (Carmen, Hardi, & Sinai, 2006; Keller et al., 2006).

In addition to the ability of *T. gondii* infection to impair or evade elimination by the three apoptotic pathways, the parasite also modulates the host cell signaling factors

to enhance anti-apoptotic mechanisms. Toxoplasma infection has been shown to be able to restrain apoptosis via interference of the NF-κB pathway. The NF-κB proteins are transcription factors that promotes the transcription of anti-apoptotic factors such as the cellular inhibitors of apoptosis proteins (c-IAPs) and Bcl2-family proteins (Stehlik et al., 1998). It is maintained in an unactivated state by the inhibitor κBα (IκBα) protein within the cytosol. When the IκBα protein is phosphorylated by the IκB kinase (IKK) complex, this leads to the degradation of IκBα and the subsequent activation of NF-κB which is translocated to the nucleus. At the nucleus, the NF-κB proteins upregulates the transcription of anti-apoptotic genes (reviewed in Ghosh & Karin, 2002). In *T. gondii*-infected cells, phosphorylated IκBα (p-IκBα) protein is found not only in elevated levels (Molestina, Payne, Coppens, & Sinai, 2003), but in sustained increase and concentrated on the *T. gondii* PVM (Molestina et al., 2003), implying a parasite-directed event and resulting in the upregulation of the NF-κB target genes (Molestina & Sinai, 2005). A study conducted by Molestina and co-workers showed that this sustained NF-κB target genes upregulation is a result of a two-step process in which the host's IKK is responsible for the initial NF-κB activation, and the parasite's IKK (TgIKK) sustains the activation when the host IKK activity wanes; resulting in effective maintenance of the host cell in an anti-apoptotic state (Molestina & Sinai, 2005). However, this pattern of NF-κB activation does not happen for all cell types infected with *T. gondii*, particularly in macrophages whereby the translocation of NF-κB to the nucleus is blocked (Butcher, Kim, Johnson, & Denkers, 2001). Another factor that complicates the disease intervention endeavours of this highly complex parasite is that there are also some differences in the modulation of host immune responses between immune cells of monocytic origins (such as macrophages and dendritic cells) and other non-immune cells in a *T. gondii* infection.

Other than the inhibition of NF-κB to the nucleus, Toxoplasma infection in macrophages induces the phosphorylation of the transcription factors STAT3 and STAT6 from the Janus kinase (JAK)/STAT pathway. The parasitic protein responsible for this is the rhoptry protein ROP16, which is implicated to be involved in parasite replication and virulence (J. P. J. Saeij et al., 2007). However, the ROP16-induced phosphorylation of STAT3/6 differs between different parasite strains. Infection with Type II parasites results in a transient increase in phosphorylated STAT3/6, but it is not sustained; unlike infection with Type I and Type III parasites with sustained phosphorylation of STAT3/6 even after 18 hours post infection (J. P. J. Saeij et al., 2007). The lack of STAT3/6 suppression in Type II parasites may explain the reason why it is a less virulent infection. The inability to sustain STAT3/6 phosphorylation in Type II infection leads to overproduction of proinflammatory cytokine IL-12 (Robben et al., 2004; J. P. J. Saeij et al., 2006), which stimulates specific T-cells to produce IFN-γ, resulting in the activation of NK cells to limit the infection and suppress parasite replication (reviewed in Laliberté & Carruthers, 2008). By contrast, the dampening of the production of IL-12 in Type I-infected macrophages leads to unhampered parasite replication and febrile disease. Although there is effective sustenance of STAT3/6 phosphorylation in Type III strain infection, it still lacks the aggressive virulence observed in Type I infection, suggesting that there are more virulence factors at play other than ROP16. It has been speculated that the absence of ROP18 expression within Type III *T. gondii* may be the explanation for its suppressed virulence (reviewed in Laliberté & Carruthers, 2008).

Another anti-apoptotic mechanism within mammalian host cells is the phosphoinositol 3 kinase (PI3K) pathway, which stimulates a phosphorylation cascade

that ultimately activates a key kinase known as Akt/PKB. *T. gondii*-infected cells shows elevated levels of phosphorylated Akt/PKB (L. Kim & Denkers, 2006). The activated Akt/PKB kinase seems to be like a pivotal point where it influences several pro- and anti-apoptotic factors, such as causing the inactivation of pro-apoptotic proteins caspase 9 and Bad, suppressing several pro-apoptotic factors like Bim and FasL, and also inducing the NF-κB pathway to trigger the transcription of anti-apoptotic genes (reviewed in Laliberté & Carruthers, 2008). Although the molecular mechanism of the parasite's interaction with the NFκB and PI3K signaling pathways are not fully elucidated, what is clear is that *T. gondii* possesses the ability to manipulate these pathways for the maintenance of infected cells in an antiapoptotic state, and thereby promoting its survival and propagation within the host.

2.9- Antibody-mediated resistance to Toxoplasmosis

While T cells and IFN-γ are important mediators of the host immune responses to resist *T. gondii* infection, B cells are essential for long-term resistance to the disease by the production of specific antibodies (Kang, Remington, & Suzuki, 2000). Kang and co-workers demonstrated that although mice deficient in B cells production are capable of surviving the acute stage of *T. gondii* infection, they were susceptible to mortality in the chronic stage of infection – mainly due to unrestricted parasite proliferation in the brain and lungs causing widespread tissue necrosis (Kang et al., 2000). It was also discovered that the absence of specific antibodies is correlated with an increased prevalence of tachyzoites and parasitic tissue cysts in the brain and lungs of B-cell deficient mice (Kang et al., 2000). This implies that even with unimpaired T lymphocytes response and undisrupted expression of IFN-γ, TNF-α, and iNOS, the

absence of antibody production in the host results in reduced resistance to *T. gondii* and chronic stage mortality.

In an experiment where unimmunized mice were repeatedly administered with *T. gondii*-immune serum, the mice still seemed to lack effective disease resistance; suggesting that both humoral and cellular immunity of the host needs to act in synergy for effective resistance to toxoplasmosis (unpublished observation in Sayles, Gibson, & Johnson, 2000). In addition, B cells-deficient mice immunized against *T. gondii* also showed substantially prolonged survival to challenge infection with the virulent RH strain compared to unimmunized B cell sufficient mice (Sayles et al., 2000). This again lends support to the point that even when humoral immunity is impaired, some host resistance from cellular immunity is still developed but is unable to completely stave off infection, especially in the chronic stage. However, it is also worth noting that at present time, there is no effective and safe human vaccine against the disease of toxoplasmosis.

Although $CD8^+$ T cells and IFN-γ has been established to be critical in host resistance to *T. gondii*, the knockdown of $CD4^+$ helper T cells and the resulting deficient antibody responses has been shown to significantly reduce host resistance and impairs the host's successful response to *T. gondii* vaccination (Johnson & Sayles, 2002; Sayles et al., 2000). It was also shown that adoptive transfer of immune serum to syngeneic mice with deficient antibody response substantially improved resistance and prolonged survival to infection (Johnson & Sayles, 2002), lending further support to the notion that antibodies play critical roles in limiting toxoplasmosis pathogenesis. Antibody-mediated resistance to *T. gondii* was previously believed to limit infection in two ways: antibody-dependent activation of the host's complement system to rapidly lyse tachyzoites (Fuhrman & Joiner, 1989; Schreiber & Feldman, 1980), and phagocytic killing of

antibody-coated tachyzoites by activated macrophages (Anderson, Bautista, & Remington, 1976). However, a relatively more recent study showed that direct antibody inhibition of tachyzoites' host cell invasion may be the critical factor for resistance rather than macrophage and complement-mediated effector mechanisms (Sayles et al., 2000). Therefore, the protective role of B cells in toxoplasmosis is via the production of specific anti-*T. gondii* antibodies. For complete disease resistance, specific and neutralizing antibodies targeted to the parasite are needed.

2.10- Engineered antibody fragments

Engineered antibodies have emerged as a strong frontrunner in the arsenal of biopharmaceuticals. The global market for monoclonal antibodies (mAb) has been increasing since 2009 and achieved the highest combined sales in 2011 worth USD 65 billion, which included sales of therapeutic, diagnostic and research reagent mAbs (Maggon, 2012). Table 2.1 shows this increasing market for mAbs by listing the revenues generated by the top ten therapeutic mAbs for the past 3 years. As of year 2010, there are 30 IgGs and their mAb derivatives on the market (17 mAbs marketed, and 1 withdrawn) and at least 130 more in clinical trials (Beck, Wurch, Bailly, & Corvaia, 2012). Using recombinant DNA technologies, humanized murine mAbs have been developed with enhanced clinical efficiency and have led to regulatory approvals for immunoglobulins (Ig) and Fab molecules as immunotherapeutic agents for cancer, infectious and inflammatory diseases. Since the advent of mouse, chimeric and humanized IgG1 antibodies in the market during the late 1990s, the diversity of engineered antibody structures have greatly expanded (Table 2.2). Currently, the majority of recombinant protein pharmaceuticals in use in the clinic comprise of mAbs,

with a significantly higher success rate (29% for chimeric antibodies, 25% for humanized antibodies) (Reichert, Rosensweig, Faden, & Dewitz, 2005) compared to small-molecule drugs (11%) (Kola & Landis, 2004).

Recombinant antibodies come in various forms, either as smaller fragments such as Fab and single-chain variable fragment (scFv), which are the classic monovalent forms; or as engineered variants such as diabodies, triabodies, minibodies and single-domain antibodies (reviewed in Holliger & Hudson, 2005). Much interest has been generated in the area of antibody engineering because of the potential to form potent therapeutic and diagnostic agents, particularly for targeting inflammatory, cancer, autoimmune and viral diseases (Holliger & Hudson, 2005). This is accompanied by many advances in scaffold design, repertoire construction and selection methodologies.

Engineered antibody fragments have the added advantage of being less immunogenic with receptors mediating unwanted, inflammatory effector functions omitted. The bivalent, Y-shaped IgG is the main serum antibody that is most frequently used in nearly all approved antibody drugs (Reichert et al., 2005). In its intact form, IgG is a multidomain protein and carries its antigen-binding sites on its two Fab tips while the recruitment of effector functions is mediated by the stem Fc domain. There are many immunotherapeutic applications however, whereby the Fc-mediated effects are undesirable because of the immunogenic response it illicits as well as its cytotoxic effects resulting from massive cytokine release. To circumvent this, the Fc domains of the IgGs are removed, and genetically engineered into monovalent (Fab, scFv, single variable V_H and V_L domains) or bivalent fragments (Fab'_2, $scFv_2$ diabodies, minibodies) (Figure 2.8). As only the conserved Fc domains are removed from the final antibody

fragment, this exercise does not compromise on the antibody's specificity or affinity on its targets (Holliger & Hudson, 2005).

TABLE 2.1 **Top ten monoclonal antibodies in 2011 and revenue generated.**

Generic Name	Brands ®	Companies	Indications*	Sales $ Billion (USD)		
				2009	2010	2011
Infliximab	Remicade	J&J, Merck, Mitsubishi Tanabe	RA, UC, CD, Ps, PsA, AS	6.91	8.0	9.0
Adalimumab	Humira	Abbott	RA, Ps, JIA, PsA, AS, CD	5.49	6.5	7.9
Rituximab	Rituxan	Roche	NHL, RA	5.8	6.7	6.6
Bevacizumab	Avastin	Roche	Colon Cancer	5.92	6.8	5.8
Trastuzumab	Herceptin	Roche	Breast Cancer	5.02	5.5	5.7
Rarubizumab	Lucentis	Roche, Novartis	Wet Macular Degeneration	2.43	3.1	3.6
Cetuximab	Erbitux	BMS, Merck Serono	Colon, Head and Neck Cancer	2.57	3.2	3.4
Natalizumab	Tysabri	Biogen Idec, Elan	Multiple sclerosis	1.06	1.75	2.6
Omalizumab	Zolair	Roche, Novartis	Allergic Asthma	0.91	1.1	1.3
Palivizumab	Synagis	Astra Zeneca	RSV	1.1	1.0	0.975

Source: Maggon K., Monoclonal Antibodies Market 2008 – 2011, Top Ten Monoclonal Antibodies 2011. URL: http://monoclonalantibodies.wordpress.com/2012/03/18/top-ten-mabs-2011/

*NHL Non Hodgkin's Lymphoma, RA Rheumatoid Arthritis, JRA Juvenile Rheumatoid Arthritis, JIA Juvenile Idiopathic Arthritis, Ps Psoriasis, PsA Psoriatic arthritis, CD Crohn's Disease; UC Ulcerative Colitis, AS Ankylosing Spondylitis, RSV Respiratory syncitial virus

Engineered antibody fragments are also more economical to produce (compared to intact IgG molecules) and more tractable to mutational designs for improvements in *in vivo* pharmacokinetics, stability, affinity, and specificity (Holliger & Hudson, 2005). Engineered antibodies have been constructed into multivalent and multispecific reagents, conjugated to therapeutic payloads (such as toxins, liposomes, enzymes, radionuclides and viruses), mutated for enhanced therapeutic effects on immunosilent or refractory targets in enzymes, cell receptors, haptens and other infectious agents. It has also been shown that antibody fragments can be designed as robust diagnostic reagents, or as non-immunogenic *in vivo* biopharmaceuticals with better biodistribution and blood clearance properties (reviewed in Holliger & Hudson, 2005). Additional benefits include amenability to mutational designs which increase the potency of antibody fragments and increasing its plasma half-life, therefore allowing for its reduced dosage and frequency of administration. This leads to cost reduction for the immunotherapeutic drugs, better convenience and improved quality of life for patients (Carter, 2006).

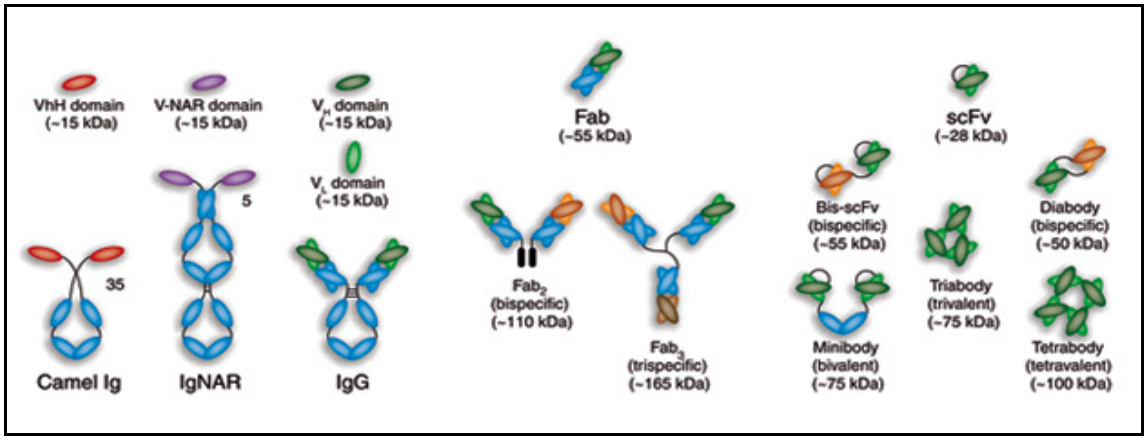

FIGURE 2.8 **Diagram of different antibody formats.** An intact classic IgG molecule is shown alongside the unusual immunoglobulin-like structures of camelid VhH-Ig and shark Ig-NAR. The different formats of antibody fragments shown here include the Fab, scFv, single-domain V_H, VhH and V-NAR. A variety of multimeric formats depicted here are the minibodies, bis-scFv, diabodies, triabodies, tetrabodies and chemically conjugated Fab multimers. Approximate size of each antibody format is given in kilodaltons. (Adapted from Holliger & Hudson, 2005)

TABLE 2.2 **Therapeutic antibodies with alternative protein and antibody scaffolds.**

Name	Scaffold or format	Developer or licensee	Parent protein structure	Clinical trial phase	Disease	Target
Ecallantide (Kalbitor/ DX88)	Kunitz domain	Dyax	Human lipoprotein-associated coagulation inhibitor (LACI)	FDA approved (December 2009)	Hereditary angioedema	Kallikrein inhibitor
TRU-015	SMIP	Trubion/Pfizer	Various origin and length	Phase IIb	NHL	CD20
Dom-0200/ART621	Domain antibody	Domantis (now GlaxoSmithKline)/ Cephalon	V_H or V_L antibody domain; 100–130 amino acids	Phase II	Rheumatoid arthritis and psoriasis	TNF
MT103	BiTE	Micromet	scFv–scFv; 200–260 amino acids	Phase II	ALL	CD19 and CD3
				Phase I	NHL	
Angiocept (BMS-844203/ CT-322)	Adnectin	Adnexus (owned by Bristol-Myers Squibb)	10th FN3 domain of fibronectin; 94 amino acids	Phase II	Colorectal cancer, NSCLC and glioblastoma	VEGFR2
ALX-0081	Nanobody	Ablynx	VHH; ~100 amino acids	Phase II	ACS and TTP	vWF
ESBA105	Stable scFv	ESBATech/Alcon	scFv with hyperstable properties	Phase II	Uveitis	TNF
AMG-220 (C326)	Avimer	Avidia (owned by Amgen)	Domain A of LDL receptor; a repeating motif of ~35 amino acids	Phase I	Crohn's disease	IL-6
MT110	BiTE	Micromet	scFv–scFv; ~500 amino acids	Phase I	Lung and gastric cancers	EPCAM and CD3
ABY-002	Affibody	Affibody	Z domain of protein A from *Staphylococcus aureus*; 58 amino acids	Phase I	Breast cancer imaging	HER2
MP0112	DARPin	Molecular Partners	Ankyrin repeat proteins; 67 amino acids plus a repeating motif of 33 amino acids	Phase I	Ophthalmological diseases	VEGF
PRS-050 (Angiocal)	Anticalin	Pieris	Lipocalin; 160–180 amino acids	Phase I starts early 2010	Solid tumours	VEGF

ACS, acute coronary syndrome; ALL, acute lymphoblastic lymphoma; BiTE, bispecific T cell engager; DARPin, designed ankyrin repeat protein; EPCAM, epithelial cell adhesion molecule; FDA, United States Food and Drug Administration; HER2, human epidermal growth factor receptor 2; IL, interleukin; LDL, low-density lipoprotein; NHL, non Hodgkin's lymphoma; NSCLC, non-small-cell lung carcinoma; R, receptor; scFv: single-chain variable domain antibody fragment; SMIP, small modular immunopharmaceutical; TNF, tumour necrosis factor; TTP, thrombotic thrombocytopenic purpura; VEGF, vascular endothelial growth factor; V_H, heavy chain variable domain; VHH, heavy chain variable domain (in camelids); V_L, light chain variable domain; vWF, von Willebrand factor.

Source: (Beck et al., 2012. Strategies and challenges for the next generation of therapeutic antibodies. Nat Rev Immunol 10(5), 345-352)

2.11- Phage-displayed scFv antibody libraries

Library phage display has overtaken hybridoma technology through the creation of large natural and synthetic *in vitro* repertoires of antibody fragments with affinities comparable to those generated from hybridoma technology, and the ability to design greater antibody affinity to levels that were previously out of reach of the natural immune system (Bradbury & Marks, 2004). Phage display enables the presentation of large protein or antibody libraries on the surface of filamentous phage, which leads to the selection of binding ligands with high affinity and specificity to almost any target.

ScFv antibody libaries displayed on phage was first described in 1990, and demonstrated how antigen-binding phages can be recovered from selective screening, with the added advantage of having the displayed antibody phenotype being encoded within the phagemid sequence (McCafferty et al., 1990). Figure 2.9 shows the basic overview of a phage-display technology workflow. Additional key strengths of phage-displayed antibody libraries are that it is a platform that enables direct selection of rare binding properties, such as specific species or strain crossreactivity (Popkov et al., 2004); and also enables the generation of very large panels of polyclonal antibodies against a particular antigen (Edwards et al., 2003). At this time of writing, one human antibody derived from phage-display technology has been approved and is widely used for the treatment of rheumatoid and psoriatic arthritis (Humira, adalimumab; Abbott Laboratories) (Carter, 2006), and at least 8 more are in clinical development phase (Lowe & Jermutus, 2004).

The intense interest in engineered antibodies development has much to do with designing new binding specificities, especially to refractory and immune-evasive targets that are inaccessible to the natural immune response (Holliger & Hudson, 2005). Single-chain variable fragment (scFv) antibodies consist of the antigen-binding domains of Ig heavy (V_H) and light (V_L) chain regions connected by a flexible peptide linker, all encoded by a single gene cassette. This popular engineered antibody format retains the specificity and antigen-binding affinity of its parent IgG while providing improved pharmacokinetics of tissue penetration. ScFv antibodies are preferred over Fab antibody formats due to their superior expression levels in bacteria – which leads to cost-effectiveness, although its yield varies according to the monoclonals to be expressed (reviewed in Holliger & Hudson, 2005). In a relatively recent development, the smallest known engineered antibody fragment known as domain antibodies (dAbs) (11-15 kDa),

whereby the antigen-binding site is concentrated over a smaller area, was developed against HIV-1 envelope glycoprotein gp120. This dAb antibody format was derived from an initial scFv antibody format and has proved to be potently neutralizing against HIV-1 (W. Chen & Dimitrov, 2009). Together with the slew of anti-cancer and anti-inflammatory scFv-based immunotherapeutics currently developed, this suggests that scFv antibodies are being widely established as stable recombinant protein biopharmaceuticals.

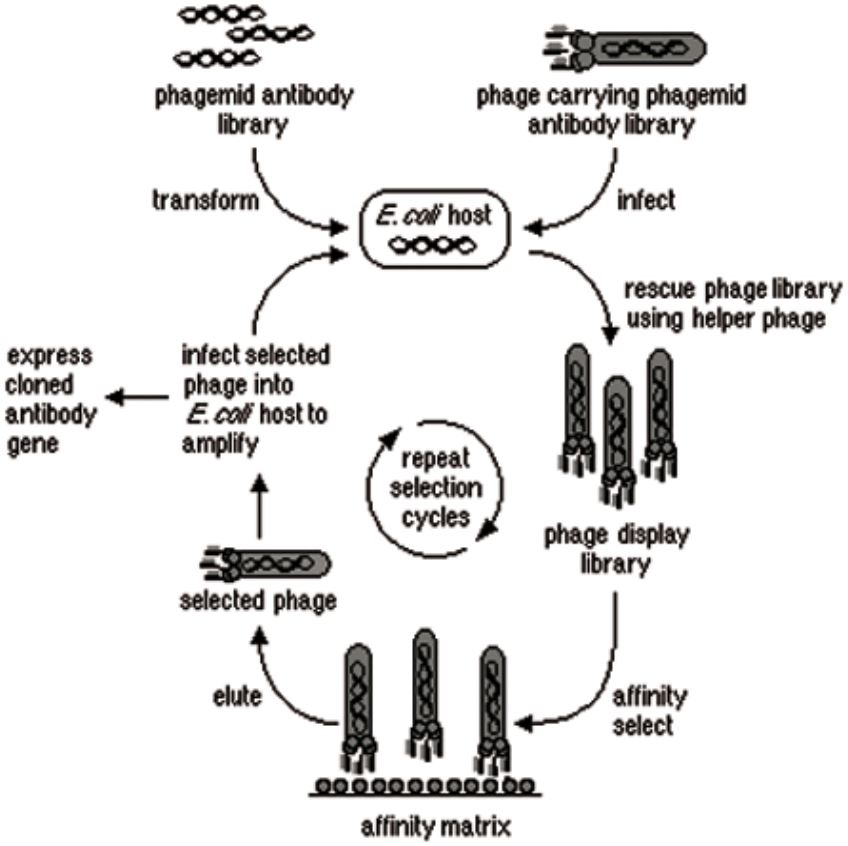

FIGURE 2.9 **Schematic representation of the phage display technology.** A phage-displayed antibody library has its genotype (phagemid) linked to its phenotype. The phage-displayed antibody library is used to infect *E. coli* and subsequently rescued by helper phage to produce functional recombinant phage particles. The phage display library is then processed through affinity selection (biopanning), and selected phages are amplified, characterized and expressed. (Adapted from Galanis, Irving, & Hudson, 2001)

A scFv antibody library is constructed with V_H and V_L gene pool derived from source B-cells (from diverse lymphoid sources such as spleen, bone marrow, peripheral blood or tonsils) by PCR-based or similar cloning techniques and subsequently cloned into a suitable vector for expression as a combinatorial antibody library. The single gene design of scFv simplifies the construction of fusion proteins such as cancer immunotoxins and facilitates intracellular expression in eukaryotic cells to suppress or neutralize antigen functions. Besides improved tissue penetration, the smaller size of the scFv antibodies also means that it is potentially useful for targeting cryptic epitopes that reside within immunosilent crevices in many pathogenic agents (especially viruses) (Holliger & Hudson, 2005). These cryptic epitopes may be part of the pathogens adaptation to allow binding to target receptor but evade host immunosurveillance. Due to the limited complementarity-determining region (CDR) diversity in the natural immune system, antigen-binding sites of antibodies produced are mainly constrained to flat or concave topologies, and rarely penetrate into the cavities of cryptic epitopes (Cardoso et al., 2005; Hudson & Souriau, 2003).

An alternative antibody development to target immune-evasive cryptic epitopes is the discovery of single V-like domains in camelids (camels and llamas) and cartilaginous fish (wobbegong and nurse sharks) (De Genst et al., 2004; Dooley & Flajnik, 2005). The distinct characteristic of these high affinity V-like domains from these two organisms is that they express long cavity-penetrating loops that are often longer than conventional murine and human antibodies which are effective at accessing deep cavities and canyons in enzyme active sites and disease biomarkers (De Genst et al., 2005; Streltsov & Nuttall, 2005). However, these V-like domains are unsuitable for *in vivo* applications due to its high immunogenicity (reviewed in Holliger & Hudson, 2005).

Generation of scFv using antibody phage display library is now an established procedure for the rapid production of panels of high-affinity monoclonal antibodies (mAbs) to a wide variety of protein antigens. The advent of the antibody phage display system also overcame the limitations associated with the slow and laborious processes involved in hybridoma technology. Basically, the scFv gene repertoires are constructed by cloning the antigen-binding V_H and V_L fragments fused to a minor coat protein of bacteriophage (PIII). The resulting phage has a functional antibody protein on its surface and contains the gene encoding the antibody incorporated into the phage genome. The number and affinity of the antibodies generated against a particular antigen is a function of library size and diversity, with larger libraries yielding a greater number of high-affinity antibodies.

However, it should be noted that most scFvs are a mixture of monomer and homodimer (Viti, Tarli, Giovannoni, Zardi, & Neri, 1999). It is essential that when the role of binding affinity in targeting antigens is being studied that purified antibodies of defined oligomeric state be used for the research. This is because that although the affinity of these molecular species towards a monomeric antigen is identical when measured in solution, the avidity (or functional affinity) may be higher for a dimerized scFv binding to an immobilized antigen due to rebinding effects and by the simultaneous binding of two antigens (Crothers & Metzger, 1972; Neri, Montigiani, & Kirkham, 1996). Monomeric and dimeric scFvs also have different sizes and pharmacokinetics (Adams et al., 1993). It is worth noting that in a study done by Viti and co-workers, it was demonstrated that the bivalence and slower clearance of antibodies seem to drive the antigen targeting process, despite the increased antibody size (Viti et al., 1999). Bivalent antibodies may also present some therapeutic

advantages as was demonstrated in a work by Adams and his co-workers, whereby divalent antibody-binding has improved tumor retention compared to its monovalent counterpart (Adams et al., 1993).

A previous study elucidated that synthetic V_H diversity alone may be sufficient for the generation of high-affinity antibodies from phage-display; thus, it may be possible to do without the V_L light chain altogether, significantly simplifying the design of scFv libraries (Sidhu et al., 2004). However, although V_H domain does play a dominant role in antigen binding, several other studies indicate that the V_L and non-hypervariable domains of engineered antibodies do play a significant role in increasing antigen binding affinity and overall stability; and thus cannot be ignored in affinity maturation refinement endeavours (Boder, Midelfort, & Wittrup, 2000; Lu et al., 2003). In general, there are two kinds of library which can be generated: naïve or immune antibody libraries. Generally, antibodies isolated from immunized libraries tend to have much higher affinities for the immunizing antigen used compared to a naïve library of an equivalent size (Bradbury & Marks, 2004; Schoenberger & Crotty, 2008).

Construction of a recombinant scFv targeted against *T. gondii* could be an alternative source of antibodies for diagnostics and perhaps treatment of opportunistic and congenital toxoplasmosis. The production of recombinant scFv antibody library could potentially be a more cost-effective and easier approach in the development of diagnostic reagents for *T. gondii* and as an alternative anti-toxoplasmosis immunotherapy without the risk of teratogenicity associated with some present treatment regimen.

2.12- The design of phage-displayed antibody libraries

Antibody's V-regions differ in various pharmacokinetics properties which affect the expression of the antibody fragments - such as stability, solubility and folding kinetics (Carter, 2006). A key strength of using the phage-display platform to express antibody libraries is that it directly selects for favorable antibody properties such as optimized binding affinity, robust expression, high stability and solubility during the selective screening stage; while disadvantaging weaker and less favorable clones from selection (Holliger & Hudson, 2005). Incorporation of rational antibody design into the phage-displayed library could also enhance the selection of improved biophysical properties, for example, a high-affinity specific antibody could have its' CDR grafted into a more stable antibody framework and subsequently include point mutagenesis at framework region residues for increased thermodynamic stability (Ewert, Honegger, & Plückthun, 2004; Ewert, Huber, Honegger, & Plückthun, 2003). There are numerous qualities that define a prime candidate engineered antibody fragment for clinical evaluation as an immunotherapeutic agent. The desirable properties of an antibody molecule are subnanomolar affinities, low dissociation constant, potent receptor-mediated killing of target cells, absence of extracellular toxicity, low immunogenic potential and ease of production. As for a high-quality phage-display library, it is one that provides high diversity, good expression, stability and solubility; which are properties often observed to be co-selected with binding activity (Holliger & Hudson, 2005).

Generally, the affinity of the antibodies isolated is proportional to the initial size of the library used for selection (Vaughan et al., 1996). Therefore, the creation of large antibody libraries has become an important goal for the selection of antibodies against

any antigen and giving rise to new specificities. Commonly, such libraries are made by performing a large number of ligations and transfections. To generate a large repertoire of antibody fragments it is certainly necessary to have a large amount of good quality DNA and to have good transformation efficiency of competent cells (at least 10^9 CFU transformation efficiency). It is possible to construct libraries of a great size by increasing the number of electroporations, from which relatively high affinity antibodies can be directly rescued without any further modifications. The number of electroporations depends on the amount of DNA- as a general guideline: 500 ng of DNA in 4-5 µL of ligation mix with 50 µL of *E.coli* cells should be used per electroporation (Pini, Giuliani, Ricci, Runci, & Bracci, 2004).

However, these libraries are limited resources as reamplification cannot be carried out without potential loss of diversity (Rader, Steinberger, & Barbas, 2001). An elegant strategy to circumvent this and to create large antibody libraries has taken advantage of the Cre recombinase bacteria expression system to drive recombination of a primary phage scFv library in a phagemid vector containing two nonhomologous lox sites, and infecting the bacteria at a high multiplicity of infection (MOI- 200:1) to cause many different phagemids to enter a single bacterium (Sblattero & Bradbury, 2000). The primary library can be amplified without a reduction in diversity because diversity is regenerated each time recombination comes into play to create each new secondary library. Using this approach, a high library diversity of 3×10^{11} has been reported although a relatively small primary library was used as starting material (7×10^7 was used) (Sblattero & Bradbury, 2000). The *in vivo* shuffling of the V_H and V_L genes between the lox sites of the polyclonal phagemid vectors creates many new V_H/V_L combinations, all of which are functional (Sblattero & Bradbury, 2000). Recombination to create a large library can only be effective when there are many phagemids interred

within each single cell for gene shuffling to take place. But p3 expression from the phagemids inhibits this multiple infection from occurring by retarding pilus synthesis. However, this inhibition can be lifted by inhibiting p3 synthesis with glucose.

Another effective method of boosting antibody library size involves the use of a new generation helper phage, known as hyperphage; integrated into any compatible phage display system used. The use of hyperphage may increase the number of scFvs presented on filamentous phage particles generated with antibody display phagemids by more than two orders of magnitude and significantly blocks the generation of 'blank' phages (Rondot, Koch, Breitling, & Dubel, 2001). As a result of this considerable increase in the fraction of phage particles carrying an antibody fragment on their surface, there is a concurrent increase of antigen-binding activity of up to 400-fold, and about 17-fold increase in the percentage of positive scFv-phage particles in a selective screening using an initial naïve human scFv antibody repertoire (Rondot et al., 2001).

Natural human and mammalian antibody response is restricted by the limited diversity of complementarity-determining region (CDR) loop lengths, which constrains the displayed antigen-binding surface to mostly flat or concave topologies (Hudson & Souriau, 2003). This phenomenon bars the immune system from recognizing and accessing cryptic epitopes in the form of narrow cavities (canyons) on antigenic surfaces that have evolved within many pathogenic microorganisms to escape immunosurveillance.

Further refinements to generate better performing antibodies can include point mutations (either random or justified) or combinatorial mutagenesis to improve affinity, antigen localization, yield and stability, resistance to aggregation and protease resistance

of phage-displayed proteins. The process of creating targeted mutations in the antibodies is known as affinity maturation (which will be dealt with in a following section). For example, it has been shown in recent structural studies that specific targeted mutations in the V_H region (such as Gly35) brings dramatic effect to the stability of antibody scaffolds and may therefore be the preferred choice in engineering more stable antibody variants (Jespers, Schon, James, Veprintsev, & Winter, 2004). However, it is worth noting that these mutations to improve stability may only apply to some, and not all V_H-like domains; and the significant contribution of VL domain to stability and overall binding affinity cannot be disregarded as documented in a study done by Boder E.T. and coworkers (Boder et al., 2000). The development of recombinant antibodies for diagnostic and therapeutic applications demands that the designed antibody provides efficient targeting while retaining its' high-affinity and high-specificity. In lieu of this, studies have shown encouraging results that increased binding affinity and valence of recombinant antibody fragment could potentially lead to improved targeting of antigenic epitopes of up to 760-fold (Viti et al., 1999), and even up to the femtomolar range by increased affinity of 1800-fold (Midelfort et al., 2004).

Another aspect in antibody engineering that needs to be considered is the expression system used to drive the production of stable, high-affinity mAb in high yield. Among the diverse range of expression systems available today (bacteria, yeasts, plants, insects, mammalian cell lines and transgenic animals), bacteria expression systems are favored for their high expression levels of small, nonglycosylated Fab and scFv fragments, diabodies and V domains, with low-cost associated with it (Carter, 2006); whereas mammalian or plant cells are preferred hosts for high-yield expression of larger intact antibodies and minibodies.

Efforts to improve recombinant antibody expression have led to the development of several strategies. Quite frequently, recombinant antibodies are engineered to carry terminal polypeptides such as c-Myc, histidine, GST and the 'Flag' epitope for the purpose of affinity purification after expression into the periplasm of *E. coli.* Simple and inexpensive large scale recombinant expression is also made possible by using a heat-inducible system that minimizes the risk of immunogenicity related to using terminal polypeptides (Power et al., 2001).

2.12.1 - Antibody multivalent designs

For the purpose of immunotherapeutic applications, the nonequilibrium environment of the vasculature and tissues demands that engineered antibodies provide slower dissociation rates and higher retention times while maintaining high affinity; basically properties that are lacking with even high-affinity monovalent interactions (Holliger P. *et al*, 2005). Therefore, for therapeutic applications it may be favourable to fuse monovalent Fab, scFv or V-domain molecules into multivalent formats which are capable of engaging two homologous or heterologous targets simultaneously, thereby increasing avidity and lowering dissociation rates for cell surface or multimeric antigens. The antibody multimers remain smaller than intact immunoglobulin molecules (55-110 kDa) and still provide improved antigenic site penetration and faster blood clearance (Holliger P. *et al*., 2005).

In addition, a multivalent antibody fragment can be designed to bind to cell surface receptors or effector molecules leading to a desired macrophage activation and/or apoptosis through transmembrane signaling pathways, which may result in the

neutralization of the target antigen (Linsley, 2005; Teeling et al., 2004). The multivalent antibody format is also pliable to conversion to multispecific molecules which allow the direct association of 2 differing targets for the engagement of cytotoxic cells or gene delivery capsules and immunodiagnostics. It is also now possible to target intracellular antigens either through intracellular monoclonal antibody (mAb) fragments (intrabodies) by joining the intrabody to a membrane translocator sequence, or through a naturally internalizing mAb or direct selection for internalization properties (Milroy, 2006).

Engineered dimeric, trimeric or tetrameric conjugates of scFv and Fab fragments using chemical or genetic cross-links have shown improved avidity, retention and internalization properties as compared with the parent IgG (Adams et al., 1993; Holliger & Hudson, 2005). It is also interesting to note that the avidity of an antibody seems to be more important than affinity, with diabodies formed from lower-affinity scFv antibodies consistently achieving increased tumor uptake and retention despite innate difficulties for antibodies penetration to the tumor mass due to its surrounding vasculature network (Nielsen, Adams, Weiner, & Marks, 2000). Thus, it is now possible that antibody fragments with relatively enhanced potency can be engineered by forging into multivalent formats to target hitherto immunoevasive epitopes such as those present on *T. gondii* invasion proteins.

The pharmacokinetic properties of engineered mAb fragments can also be biochemically altered by several strategies. For instance, polyethylene glycol (PEG) linkage (PEGylation) has been very efficient for increasing half-life and scFv stability, as well as reducing immunogenicity (Knight et al., 2004). Antibody fragments have significantly shorter half-lives (few hours) than its intact antibody counterparts (few

weeks) (Carter, 2006). Fusion or noncovalent interaction with long-lived serum proteins such as albumin (Huhalov & K.A., 2004) or serum immunoglobulin (Holliger, Wing, Pound, Bohlen, & Winter, 1997) is also another effective strategy to extend the serum half-life of mAb fragments. Increasing the terminal half-life of antibodies may be desirable for improved efficacy, target localization, and reduced dosage and administration frequency. However, it may not always be such a good option to extend the antibody terminal half-life in applications where it would be more advantageous to decrease whole-body exposure or to increase the ratio of target to non-target binding – especially in immunodiagnostics imaging settings (Carter, 2006). Therefore, in antibody fragment design, the final application in clinical settings needs to be carefully kept in mind before embarking on antibody enhancements and modifications.

Antibody fragments have been conjugated or genetically fused to a wide range of molecules that confer auxiliary function following target binding for enhanced immunotherapeutics applications; such as cytotoxic drugs, toxins (Bang, Nagata, Onda, Kreitman, & Pastan, 2005; Vallera et al., 2005), peptides, proteins (Halin et al., 2002), enzymes (Krauss, Arndt, Vu, Newton, & Rybak, 2005; Sharma et al., 2005), liposomes for improved drug delivery (Schnyder & Huwyler, 2005) and even viruses for targeted gene therapy (Nakamura et al., 2004). However, the problem of immunogenicity associated with these bifunctional antibodies will still need to be resolved in order to pass clinical testings. A highly promising concept that is of relevant interest to this project of generating recombinant antibodies targeted to *T. gondii,* is the advent of immunoliposomes; which are mAb fragments that can potentially deliver drugs to the brain as they are able to cross the blood-brain barrier.

Although the use of engineered antibody fragments gives the advantage of reduced immunogenicity in target recipients, in some applications the mediation of immune effector functions such as antibody-dependent cell-mediated cytotoxicity (ADCC) and complement-dependent cytotoxicity (CDC) are desirable in contributing to the immunotherapeutic efficacy of target cell destruction (Carter, 2006). Therefore, there are antibody fragments that are grafted with engineered Fc regions to stimulate effector functions while ameliorating disease pathogenesis. The most convincing example of the designed synergy of engineered antibody fragments and the immune effectors it stimulates is the drug rituximab (Genentech Inc., and Biogen Idec Inc.) which contains a Fc region that interacts with the recipients' FcγRn and may trigger ADCC for antitumor activities in non-Hodgkin's lymphoma (Weng & Levy, 2003). Other examples of engineered antibody fragments with designed mutations for enhanced Fc-mediated effector responses include the drugs alemtuzumab (Genzyme Corporation and Schering AG; for treatment of B-cell chronic lymphocytic leukaemia), trastuzumab (Genentech Inc. and F.Hoffman-LaRoche Ltd., for treatment of metastatic breast cancer) (Lazar et al., 2006) and ocrelizumab (Genentech Inc., F.Hoffman-LaRoche Ltd., and Biogen Idec Inc., for treatment of rheumatoid athritis) (Vugmeyster et al., 2005). Due to the immune-evasive nature of *T. gondii* bradyzoites-filled tissue cysts and to a lesser degree – the rapidly proliferating tachyzoites, an Fc-mediated, precisely-targeted effector function coupled to scFv antibodies targeted to *T. gondii* may prove to be therapeutically beneficial in future developments.

2.12.2- Selection and Screening Strategies

The creation of the antibody phage display library provides a rapid selection platform for isolating antibodies based on its antigen-binding behaviour from a combinatorial pool of millions of clones; thereby bypassing hybridoma technology, which was the traditional means of manufacturing mAbs. The connection between phenotype and genotype in phage libraries allows for the selection of clones binding to desirable antigens and many different selection methods have been developed that separate clones that bind from clones that do not (Figure 2.10).

For phage display libraries, selection involves the exposure of the antibody library to the antigen of interest to allow for antigen-specific phage antibodies to bind to their targets during biopanning. This is followed by recovery of antigen-bound phage and reinfection in bacteria. Iterative rounds of biopanning are carried out to enrich for the best binders from the library (Figure 2.9). Tailoring the selection procedure of an antibody library can lead to the selection of antibody fragments with improved binding affinity and kinetics. For instance, by using limited and decreasing amounts of antigen, the selection favors clones with lower K_d; by increasing and lengthening the washing steps after the incubation of target antigen, clones with improved off-rate are selected; and by using very short incubation times, the selective pressure favors clones with improved on-rates. Generally, low density target coating and extensive washing of the tube enrich high-affinity binders. When selecting from a secondary phage antibody library to improve affinities, the antigen concentration is typically decreased below the K_d of the parent clone to allow preferential selection of higher affinity mutants.

The antibody phage display platform also allows another effective system of selection, which is selection by competition. Briefly, in this system specific phage binders can be detached from the target antigen by exposure to a competitor molecule, which binds the antigen naturally and causes the elution of the reactive phages (Mourez et al., 2001).

In the future, protein microarrays may also become important for high-throughput analysis of antibody specificity and affinity. Apart from enabling the discovery of mAb with high-affinity bindings to specific targets, selection strategies can also be applied to improve other properties, such as enhanced stability, resistance to proteases, aggregation behaviour, expression level in heterologous systems, intracellularly-expressed antibodies (or intrabodies) and even antibody-mediated catalysis (reviewed in Hoogenboom, 2005). Rising to the attractive prospects of creating intrabodies, Desiderio, A. and co-workers described a library which enables the isolation of intracellularly stable new binding specificities to be exploited as immunochemical reagents (Desiderio et al., 2001). Basically, synthetic phage antibody libraries can be constructed on the scaffold of a scFv previously proven to be endowed with high intrinsic thermodynamic stability and functionally expressed in the reducing environment of bacterial and plant cytoplasm.

Current antibody libraries commonly display synthetic or natural diversity in multiple CDRs and routinely produce single-digit nanomolar or subnanomolar affinity antibodies, which are affinities equal to the affinities of antibodies regularly isolated from immunized mice or recombinant immune libraries. In general antibody affinities from libraries are proportional to the size of the library- a library of 10^7 to 10^8 clones can yield up to 10 nM affinity, and the best libraries of over 10^{10} members can yield up

to 0.1 nM in antibody affinity (Hoogenboom, 2005). These libraries used in conjunction with high-throughput screening can facilitating the identification of antibody leads with the highest potencies (Edwards et al., 2003). Table 2.2 shows examples of antibodies that have been obtained by *in vitro* selection and / or optimization.

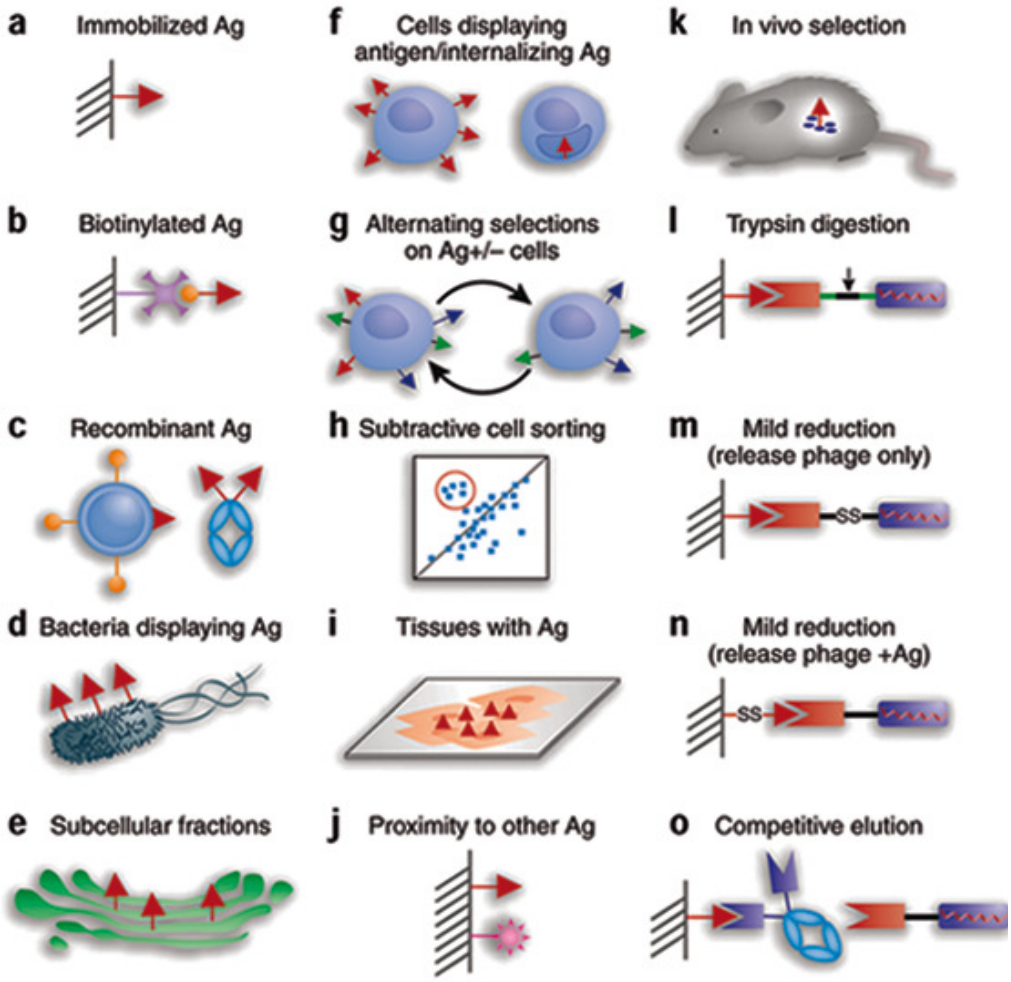

FIGURE 2.10 **Methods for *in vitro* selection screening of antibody library displays.** (a) Antigen (Ag) immobilization on solid supports or BIAcore sensorchips; (b) Biotinylated Ag (red) captured by streptavidin-coated beads (gray); (c) diverse recombinant antigens such as incorporation into paramagnetic liposomes (left) and immunoadhesins (right); (d) fixed prokaryotic cells-Ag display; (e) enriched subcellular or membrane fracions; (f) binding selection on transfected or tumor cells; (g) alternating selection on Ag+ cells and quenching on Ag- cells; (h) subtractive selection using flow cytometry; (i) selective enrichment on tissues; (j) proximity to another bound ligand; (k) injection into living animals; Selection via modulation of elution conditions, such as via (l) trypsin digestion; (m) and (n) mild disulfide-bridge reduction; and (o) competitive elution to displace the relevant binding phage antibody. (Adapted from Hoogenboom, 2005)

TABLE 2.3 **Examples of engineered antibodies generated by *in vitro* selection and / or optimization.** (Adapted from Hoogenboom, 2005)

Antibody/developer	Target	Mutagenesis	Strategy	Increase in affinity/ result[a]
Vitaxin (MEDI-522)/Medarex, Gaithersburg, MD, USA	αvβ3	Focused on CDR	Screening	×80
Synagis (palivizumab)/MedImmune, Gaithersburg, MD, USA	Respiratory syncytial virus	Focused on CDR	Screening	×100 off-rate; ×5 on-rate
RFB4/National Cancer Institute, Bethesda, MD, USA	CD22	Hot-spot mutagenesis	Screening	×15
b4/12/Scripps Research Institute/ La Jolla, CA, USA	gp120	CDR walking	Selection on phage	×420 to 15 pM
C6.5/University of California, San Francisco	c-erbB2	CDR3 mutagenesis	Selection on phage	×1,230 to 13 pM
L19/University of Siena, Italy	Fibronectin	CDR3 mutagenesis	Selection on phage	×1,317 to 54 pM
G8/University of Maastricht, The Netherlands	MHC peptide	Chain shuffling and CDR3 mutagenesis	Selection on phage	×18 to 14 nM
Fab-12/Genentech, S. San Francisco, CA, USA	VEGF	CDR3 mutagenesis	Selection on phage	×100 potency
1121/ImClone System/New York	VEGF receptor	Chain shuffling	Selection on phage	>×30 to 0.1 nM
Humira (adalimumab)/ Abbott Laboratories, Deerfield, IL, USA	TNFα	Guided selection	Selection on phage	0.3 nM
A4.6.1[b]/Genentech/ S. San Francisco, CA, USA	VEGF	Framework-region library of mAb	Selection on phage	×125
H6/University of Zurich/Switzerland	GCN4	Error-prone PCR and DNA shuffling	Selection on ribosomes	×500 to 5 pM
C11L34/University of Zurich/Switzerland	GCN4	Immune library and error-prone PCR	Selection on ribosomes	×65 to 40 pM
4M5.3/University of Illinois, Urbana, IL, USA	FITC	Error-prone PCR and DNA shuffling	Sorting using yeast	×1,800 to 48 fM
smE3/Massachusetts Institute of Technology (MIT), Cambridge	CEA	Error-prone PCR and DNA shuffling	Sorting using yeast	×285 to 30 pM/expression increases
VL-12.3/MIT	Huntington (htt) protein	Error-prone PCR/homologous recombination	Sorting using yeast	×10
14B7/University of Texas, Austin, Texas	Anthrax toxin	Error-prone PCR	Sorting using bacteria	×200-fold improvement to 21 pM

MHC, major histocompatibility complex; VEGF, vascular endothelial growth factor; GCN4, general control protein 4; FITC, fluoroisothiocyanate; CEA, carcinoembryonic antigen.

2.13- Antibody affinity maturation

An antibody's potency is frequently associated with its affinity for its target antigen (Carter, 2006), with higher affinities leading to increased pharmacokinetics and safety profiles while reducing dosing, toxicity and cost of therapy. Although initial antibody leads from display libraries shows many promising characteristics, their potency is sometimes insufficient for therapeutic or sensitive diagnoses applications. Therefore, a popular strategy for successful increment of antibody potency is via the

affinity maturation of existing antibodies with subsequent functional screenings (Carter, 2006).

Antibodies are affinity matured in the natural immune system in a stepwise fashion by incorporating mutations and selecting variants under increasing selective pressures. However, there are inherent limitations to this *in vivo* somatic hypermutation mechanism. An *in vitro* antibody directed evolution approach developed by Boder, E.T. and co-workers demonstrated that *in vitro* affinity maturations are generally able to sample areas of antibody sequence space infrequently accessed by the *in vivo* process (Boder et al., 2000). It was shown in this study that 9 out of 10 consensus mutant substitutions introduced by *in vitro* evolution into murine scFvs occurred in fewer than 10% of known mouse antibody sequences (Boder et al., 2000).

Diversity in the antibody genes may be introduced *ex vi*vo via a variety of methods, which are either random or localized; as reviewed by Bradbury, A.R.M. and Marks, J.D. (Bradbury & Marks, 2004). The first and simplest form of *ex vi*vo library affinity maturation basically focuses diversity at a small number of residues that are most likely to interact with the antigen, namely the CDRs, using oligonucleotides and PCR. For example, residues that modulate affinity may be randomized, ideally four to six residues at a time to allow efficient sampling of the sequence space (Bradbury & Marks, 2004). Screening is then carried out to isolate variants with improved affinity, and mutations conferring the highest affinities are combined in a single clone. Randomization may also be focused at various positions identified with sequence motifs frequently targeted for somatic hypermutation *in vivo*, known as 'Hot spots', which are most likely to result in improved affinity or influence affinity based on structural analysis. It was demonstrated that affinity maturation focused on germline hot spots

mutagenesis results in substantially improved antibody binding affinity as compared to non-germline hot spots mutagenesis (Ho, Kreitman, Onda, & Pastan, 2005).

In general, mutations introduced into the CDR loops leads to affinity gain as a result of providing new contacts with the antigen, influence of positioning the side chains contacting the antigen or the replacement of low-affinity contact residues with those of more favorable binding kinetics (Hoogenboom, 2005). Examples of successful affinity maturations of phage-displayed mAb fragments by point mutagenesis are the improved mAb affinity for HIV-1 envelope glycoprotein gp120 (W.-P. Yang et al., 1995); and HER-2 (or ERBB2) antigen associated with metastatic breast cancer (Schier et al., 1996).

There is also substantive evidence that the fine-tuning of antibody interactions from nanomolar to femtomolar affinity levels involves affinity maturation mutations at the residues outside of the antigen contact cavities or CDR loops. Observations indicate that ultra high affinity antibodies in the femtomolar range may be also effectively developed via changes in 'vernier' or second sphere residues (residues with one or more atoms directly contacting any residues in the first sphere of antigen contact) rather than contact residues, such as mutations in the V_H-V_L interfacial sites which improves stability and / or orientation of the V domains pairing (Boder et al., 2000; Midelfort et al., 2004). Interestingly, while it is a normal assumption that large binding improvements should be attributed to dramatic changes in either structure, hydrogen bonds or salt bridges; a previous study showed that improved engineered antibody binding affinity to the femtomolar range is formed through the interaction of a variety of interactions and the sum of many small changes, with a lack of visible structural

changes – whereby the structural comparisons of both the parent scFv and affinity-matured variant showed very small rmsd deviations (Midelfort et al., 2004).

While the many contributing factors to the affinity gains of antibodies subjected to affinity maturation is complex and not fully understood at present time, it remains that any recombinant antibody should be empirically tested to determine the extent of enhancement of a produced antibody's efficacy, if any.

2.14- Phage display applications

The advantage of the phage display technology is its ability to isolate bio-interactive proteins and other molecules without pre-existing knowledge about the interactions (M. A. Arap, 2005). This versatile technology has benefited studies and discoveries done in the fields of cell biology, immunology, and pharmacology. Applications of phage display can be grouped into three main categories, they are: *in vitro* identification of receptor-ligands, selection of receptor-ligands in complex biological systems, and *in vivo* selection of receptor-ligands.

For the *in vitro* identification of receptor-ligands, phage display peptide libraries have been used for the isolation of antigenic mimotopes of the human hepatitis B viral envelope (HBsAg), with potential diagnostics application (Folgori et al., 1994). The phage display platform had also enabled the determination of peptide structures recognized by major histocompatibility (MHC) molecules, which has important implications for the development of MHC-specific antagonists in the control and treatment of MHC-associated autoimmune conditions in humans (Hammer, Takacs, &

Sinigaglia, 1992). Besides selection for interacting proteins, the phage display technology also proved to be a useful tool in the identification of peptides affecting protein-DNA interactions, peptides binding to carbohydrates, and even peptides binding to small chemical compounds such as taxol (reviewed in M. A. Arap, 2005). One of the unique applications of this phage display technique is for the isolation of allergens by expression of a cDNA library on phage particles (Rhyner et al., 2004). Another powerful approach in utilizing the phage display technology is for the *in vitro* directed evolution of enzymes and antibodies For instance, a mechanistic-based study described by Pedersen and co-workers enables the *in vitro* isolation of enzymes based on its ability for reaction catalysis, rather than merely its structure or substrate binding (Pedersen et al., 1998). The rapid and high-throughput directed evolution of antibodies with improved stability and antigen-binding properties have also been made possible by using phage display libraries (O'Neil & Hoess, 1995).

Conventional methods of biopanning entail antigen purification and immobilization on an inert substrate, followed by probing with binding ligands, such as an antibody library. This is a relatively straightforward and reliable protocol for certain specific, soluble protein antigens. However, the conventional biopanning method has its limitations and is not amenable for screening of binding ligands for native conformational states of cell surface receptors or functional cell membrane epitopes (Eisenhardt, Schwarz, Bassler, & Peter, 2007) or in instances where the antigen is yet unknown or has not been fully characterized. Common methods of antigen immobilization normally involves either extended time incubations or desiccation (Sorokulova et al., 2005) or even the use of poly-L-lysine coated surfaces (Yavin & Yavin, 1974), each of which can cause the loss of native protein structure, conformation and functionality.

In the second category of phage display applications, which is the selction of receptor-ligands in complex biological systems, a phage display library can be directly screened against molecules expressed on living cells and tissues. This allows for the binding receptors on viable cells to be selected in its native conformation and doesn't require production of purified epitopes. However, optimization for specific phage binders is usually necessary for such complex targets as unspecific background phage adherence is a common problem with this method (M. A. Arap, 2005). This method is most frequently applied for studies related to cancer cells; such as the discovery of antibodies against melanoma cells (Kupsch et al., 1999) and a tumor target known as the Glucose-regulated protein-78 (GRP78) (Mintz et al., 2003), and also the isolation of binding peptides to urothelial carcinoma cells (Ardelt et al., 2003). In fact, the vast number of applications of phage display for the isolation of tumor-targetting peptides includes the development of targeted cytotoxic chemotherapy, pro-apoptotic peptides, cytokines-targeting to angiogenic vasculatures and tumor-imaging ligands (reviewed in M. A. Arap, 2005). Besides cancer cells, the application of phage display has also been extended for use in the discovery of binding ligands as antagonist to thrombin receptor (Doorbar & Winter, 1994) and antibody clones against parasitic diseases (Hoe, Wan, & Nathan, 2005; Wajanarogana, Prasomrothanakul, Udomsangpetch, & Tungpradabkul, 2006).

A common difficulty in all types of biopanning is the tendency of non-specific phage binding to its target of interest. This effect is more pronounced in cell-based biopanning because cell surfaces are complex and contains many non-specific carbohydrate, lipids and protein-conjugated antigens (D. L. Siegel, 2001). Therefore, although the cell-based biopanning approach offers several important advantages such

as facilitating the screening of antibodies on target antigens in its' native environment, the challenge of minimizing the false positives must be addressed. Several strategies of optimizing cell-based biopannings have been documented, including tweaking the input phage titers, incubation duration and temperature, and number of washing steps (Watters, Telleman, & Junghans, 1997); doing a negative and positive cell selection rounds to quench non-specific phages (Cai & Garen, 1995; Eisenhardt et al., 2007; J. D. Marks et al., 1993); differential centrifugation of phage-probed cells through a non-miscible organic phase (Giordano, Cardo-Vila, Lahdenranta, Pasqualini, & Arap, 2001); using fluorescent activated cell sorting system (de Kruif, Terstappen, Boel, & Logtenberg, 1995); and using magnetically-activated cell sorting (MACS) system (Chang & Siegel, 2001). This is not an exhaustive list of the strategies that has been employed in optimizing cell-based biopanning approaches; but what is clear from each is that there are advantages and disadvantages associated with each strategy, and this caveat needs to be noted in its application of cell-based biopannings in other experimental conditions with its own unique settings. For instance, application of the (Giordano et al., 2001) strategy of biopanning with differential centrifugation through a non-miscible organic phase was found to be not ideal for biopanning against *T. gondii* as the high shear force and the toxic organic phase employed in this method results in tachyzoite cell disruption (unpublished observations).

In the application of phage display for the *in vivo* selection of receptor-ligands, phage libraries are injected into animals and organs or tissues are subsequently harvested for the recovery of binding phages. The advantages of this method is the ability of selection based on ligand functionality, stability in *in vivo* systems, and the depletion of low-affinity unspecific binders from the circulation (M. A. Arap, 2005). The in *vivo* phage display system has been successfully applied in studies to reduce

prostate cancer risks (W. Arap et al., 2002), targeting of adipose tissues to reduce high-calorie related obesity in live animals (Kolonin, Saha, Chan, Pasqualini, & Arap, 2004), and also to elucidate the molecular heterogeneity of organ-specific vasculature – with potential implications for the development of these molecular targets for diagnostics or targeted therapeutics (Rajotte et al., 1998). The vast number of applications of phage display for both basic and clinical research highlights the versatility of this technology in facilitating the diagnosis and treatment of human diseases.

2.15- Phage display strategies for enhanced specificity

While phage display is a powerful tool for discovering ligands to various protein and even non-protein targets, false positives in the form of binding phages with no actual affinity to the intended target may be recovered. As reviewed by Vodnik and co-workers recently, there are several consensus peptides recovered from different laboratories targeting commercial phage display libraries to different targets, causing these binding peptides to be highly suspect as target-unrelated peptides (Vodnik, Zager, Strukelj, & Lunder, 2011). Thus, strategies to avoid their isolation need to be studied and implemented as an important step towards phage display selections of greater integrity. A successful biopanning experiment of a phage display library entails the screening of the peptide or antibody library against a target, followed by the removal of a vast majority of non-binders during washing steps and the final elution of only a few clones capable of high-affinity binding to the target. False positive phages with no actual affinity to their target can be recovered due to binding to other components of the screening system, such as contaminants in the target sample, solid phase (immobilizing plastic plates, beads), capturing reagents (streptavidin, protein A/G, biotin, secondary

antibodies), blocking reagents (BSA, milk) (Vodnik et al., 2011). Another contributing factor to the occurrence of false positive phages is due to propagation advantages. In this case, selection is driven by faster propagation of some phage clones. Therefore, these phages are recovered not because of their target affinity, but because their intrinsic replication advantage enables them to predominate in the phage pool (Brammer et al., 2008; Thomas, Golomb, & Smith, 2010).

In order for a phage display selection system to distinguish between true binders and false positives, careful design of experimental conditions can reduce the possibility of recovering target-unrelated peptides or antibodies. Binding to immobilizing solid phase, such as plastics, can be circumvented by blocking the surface or using higher density of target immobilization on the surface (Adey, Mataragnon, Rider, Carter, & Kay, 1995). However, a higher target density will inadvertently reduce the stringency of selection and may cause the isolation of more abundant low affinity binders (Vodnik et al., 2011). Another strategy to reduce background phage binding is through subtractive biopanning. In this strategy, the input phage pool is incubated with a negative capturing agent or blocking reagent in the subtractive biopanning round to adsorb non-specific binders, prior to selection against target (de Kruif et al., 1995). For instance, in the application of a phage display antibody library to select for tumor targeting antibodies, the phage display library can be subtracted against a normal human cell line prior to screening on the intended cancer cell line (Kupsch et al., 1999).

A recurrent problem in phage display systems is the propagation advantage of some phage clones. Phage clones with normal propagation rates may be outnumbered in the library by clones with propagation advantage, and are therefore likely to be eliminated in affinity-driven selections by abundant clones that are target-unrelated

binders (Thomas et al., 2010). In this situation, a clone population bottleneck can cause even rare target-unrelated clones with propagation advantage to have an opportunity to predominate, especially if many amplification steps are performed. Therefore, in general, serial amplifications of a phage display library is to be avoided. In addition, reamplification of the input phage after the subtractive biopanning round is also not recommended (Vodnik et al., 2011). Another option to overcome propagation-related false positive clones is to use the T7 lytic phage-displayed peptide libraries. The T7 phage display library system is less prone to sequence bias in comparison to M13 phage display libraries, and is less likely to carry radically faster propagating phage clones due to its lytic nature – as host cell membrane transport cannot affect phage particles assembly (Krumpe et al., 2006).

While many precautions can be taken to minimize false positives, it is impossible to completely avoid recovery of background phage binders. Traditional approaches in identifying phage clones with true binding affinity to its target often involved ELISA assays and surface plasmon resonance (SPR) experiments. Testing selected clones to each component of the selection system separately is also recommended to discriminate target-unrelated peptides from specific binders (Vodnik et al., 2011). Recent advances now allows the bioinformatics analysis of phage display selection outputs through a web server known as SAROTUP, an acronym for 'Scanner And Reporter Of Target Unrelated Peptides' (Huang, Ru, Li, Lin, & Guo, 2010). SAROTUP (http://immunet.cn/sarotup/) is a freely accessible web tool for scanning, reporting and excluding possible target-unrelated peptides from phage-displayed antibody libraries. Phage display investigators need to only input the peptide sequences of their clones in FASTA format, and the server compares each sequence with its database and potential false positives are reported in a table. Although a highly useful

tool, this approach has its limitations as the SAROTUP database is rather limited with only 23 target-unrelated motifs recognized. Complementary analysis of the phage display library output can also be done by performing a search on the MimoDB (Ru et al., 2010) and PepBank (Shtatland, Guettler, Kossodo, Pivovarov, & Weissleder, 2007) databases. Both are free web-accessed databases with a large depository of peptides obtained by phage display on different targets. Comparing phage clones from an experimental output to other phage clones selected to various targets within these databases can provide some clues to distinguish true binders from target-unrelated peptides.

Despite the many advantages of the phage display technology in the high-throughout selection for antibodies or peptides against any target, the integrity of the phage output clones can be further strengthened by careful examination for non-specific binding, comparisons to known target-unrelated peptide motifs and bioinformatics analysis via web tools. Thus, it is important incorporate these strategies to facilitate the discovery of binding ligands with true affinity to its target.

CHAPTER 3. METHODOLOGY

3.1. Key Research Questions

There are three primary aims of this study: The first is to develop an optimized procedure for *T. gondii* cell-based biopanning to screen for scFv antibody binders against tachyzoite cells. The second is to isolate and characterize the anti-*T. gondii* scFv antibodies obtained through the optimized biopanning, and the third is to improve the binding affinity of the isolated antibodies through a combinatorial molecular biology and computational design approach. This study is focused on addressing the main research questions of whether or not a recombinant scFv antibody with rationally-designed mutations could lead to enhanced binding affinity or selectivity to its antigenic target parasite.

3.2. Research design

This study was exploratory and interpretative in nature as it did not begin with a screening of the scFv antibodies against defined antigens, but rather the immunized-scFv antibody polyclonal repertoire was subjected to solution-phase binding with the native antigenic landscape of viable *T. gondii* tachyzoites to mimic *in vivo* conditions. To date, various methods have been employed for cell-based biopannings, each with its own advantages and drawbacks. The most persistent and common problem in cell-based biopannings is the issue of false positives or also known as the problem of ‘noise’. The key in optimizing for the best method is to strike a balance between significantly lowering false positives or ‘noise’, while preventing the loss of specific binders by

stringent conditions. This study's approach in optimizing the cell-based biopanning of the scFv library against *T. gondii* is by incorporating a multiple round subtractive biopanning step against a normal human hepatocyte cell line WRL68, followed by a single-round antigen biopanning against *T. gondii*.

To date, various methods have been developed incorporating a single subtractive biopanning round followed by multiple rounds of library selection against the antigen of interest. However, it was decided that the inverse method of selection (i.e. multiple rounds of negative selection followed by a single-round of positive selection) was the best method to adopt for this investigation due to several factors: First, recombinant phages displaying scFv antibodies on its g3 protein will not all be carrying full-length antibody fusions. In fact, it is a common problem for truncated sequences to be displayed along with the full-length functional scFvs due to stop codons and frame shift mutations (Kramer et al., 2003); second, the complex native landscape of cells means that smaller truncated protein fragments are easily 'trapped' on the cell surface even though there is no real specificity for the antigens of interest, leading to false positives (D. L. Siegel, 2001); third, there may be an aberrant enrichment of non-functional and non-full-length fragments above the truly functional full-length scFvs due to the innate enhanced growth rates of bacteria not expressing the full-length protein.

Through the optimized cell-based biopanning method developed for this study, scFv antibodies that were isolated were verified to be full-length, functional genes before proceeding with antibody characterizations and homology modeling. Analysis of antigen-binders and *in silico* homology modelling of selected scFv antibody enables the rational design of point mutations at antibody hot spot residues, with the aim of

increasing antibody binding affinity or selectivity against *T. gondii* tachyzoites. The overview of the research design is illustrated in Figure 3.1.

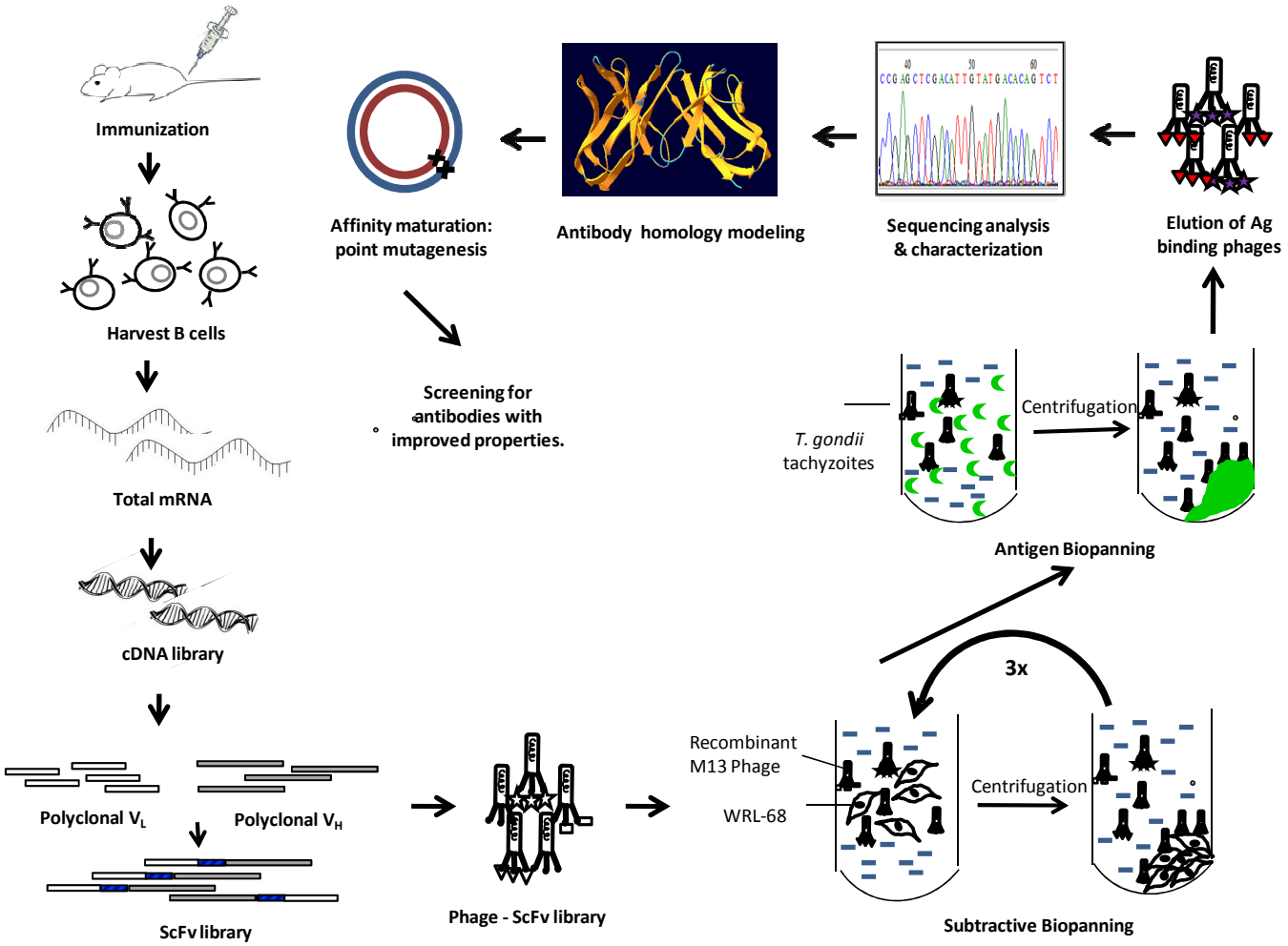

FIGURE 3.1 Isolation and development of phage-displayed scFv antibodies against *T. gondii*. Immunized mice are euthanized to harvest its splenic B cells, from which the scFv library was generated. Library biopanning was done in 2 steps, with a negative selection round against WRL-68 cells preceding the Ag biopanning. Molecular structure of isolated scFv is modelled *in silico*, before antibody affinity maturation was performed. Finally, the recombinant scFv antibodies are tested for binding to target cells by immunofluorescence assay.

3.3 Research procedures

3.3.a. Mouse immunization against *Toxoplasma gondii*

3.3.a – i Parasites and *in vivo* passaging in mice

Tachyzoites of the *T. gondii* RH strain (Pfefferkorn & Pfefferkorn, 1976) was maintained by serial passage in either 6 – 8 weeks old ICR albino or BALB/c mice. Mice were inoculated intraperitoneally with 10^4 to 10^5 tachyzoites each. Three to 7 days post-inoculation, the peritoneal exudate containing extracellular *T. gondii* parasites was aspirated from anesthetized mice, and this parasite suspension was then added with 15% DMSO in a 1:1 ratio, incubated at 37°C for 15 min, and followed by rapid cooling in a pre-chilled -80°C bath of ethanol before storage in a -80°C freezer. The frozen antigen was thawed and aliquot for use as and when it was needed within a time frame of 4 months from the date of exudate collection.

Parasites were purified for use as antigen in the biopanning experiments as previously described (Dempster, 1984) with some modifications. Thawed parasite suspensions were washed 3 times in PBS (0.15 M NaCl, 5 mM NaH_2PO_4, pH 7.2) by centrifuging at 1000x*g* for 5 min to pellet the cells in 10-ml polypropylene tubes. In the final centrifugation step, the tachyzoites cell pellet was resuspended in Toxoplasma Homogenization Buffer (THB) (20 mM HEPES/KOH pH 7.0; 50 mM potassium acetate; 10% (w/v) sucrose, 1 mM EDTA) (M. Yang et al., 2004) and the washed peritoneal exudate was then homogenized by passaging through a 27-gauge needle 3 times. The homogenized parasite suspension was then filtered through a 3.0 µm Nucleopore polycarbonate filter (Whatman, 1980-002 and 110612) to remove

contaminating mouse leukocytes and other cell debris. The filtered parasites were then quantified with a haemocytometer and trypan blue cell viability staining according to standard procedures (Sambrook & Russell, 2001). A 0.2 ml aliquot of filtered cell suspensions were mixed with an equal volume of a solution of Trypan Blue (0.4% w/v). The cells were incubated with the dye for approximately 3 minutes before loading 9.0 µl of the mixture unto each chamber of a coverslipped-haemocytometer by capillary action. The trypan blue viability staining method works on the premise that normal, viable cells are able to exclude the dye, but unviable cells would have the dye diffused into it due to lost membrane integrity. The number of viable cells in 5 out of the 9 squares in each chamber was scored to obtain the total number of cells in 10 squares. The total number of cells was then multiplied by the cell suspension's dilution factor and by 1000 to result in the number of tachyzoite cells per ml in the filtered cell suspensions.

3.3.a – ii Mice immunization

Immunization was carried out with BALB/c mice, 6-8 weeks old; with a subcutaneous injection interval of 2 weeks (Day 0 and Day 14). Each mice were given the first immunization with 2.02 x 10^6 – 4.04 x 10^6 *T. gondii* RH tachyzoites emulsified in Freund's Complete Adjuvant (FCA) (Sigma, F-5881) (ratio of 1:1), followed by a 1st and 2nd booster injection on Day 14 and Day 21 respectively with approximately the same amount of tachyzoites as the prior inoculations. The booster antigen was not mixed with any adjuvant because the use of cells as immunogens obviates the need for further use of adjuvants (Andris-Widhopf, Rader, & Barbas, 2001). The immunized mouse was bled 4 days after the final booster and its serum was tested for the presence

of IgG antibodies to *T. gondii* by Western Blotting according to standard procedures (Towbin, Staehelin, & Gordon, 1979). All procedures were performed in accordance with the Faculty of Medicine's guidelines of the Animal Care and Use Ethical Committee (ACUC) with approved applicable number PAR/18/06/2007/FMY(R). Briefly, *T. gondii* crude tachyzoite proteins was separated on a 10% (w/v) discontinuous SDS-polyacrylamide gel (Laemmli, 1970) and was subsequently transferred to a hydrophobic PVDF membrane (Hybond-P, Amersham Biosciences, RPN303F). The membrane was blocked in 5% skim milk in PBS (PBS-M) for 1 hour at room temperature and followed by 3 cycles of 5 min washes with 0.1% (v/v) Tween-20 in PBS (PBS-T). In the following steps, membrane was sequentially probed with immunized mouse sera diluted in 2% PBS-M (1:500) for 30 min at room temperature, washed in alternating cycles of PBS and PBS-T (1 X 5 min with PBS, 3 X 15 min with PBS-T, and final rinse with PBS), and finally incubated in alkaline-phosphatase conjugated goat anti-mouse IgG (whole molecule) (Sigma, A-3562) (1:30 000) for 1 hour at room temperature. After a final washing cycle similar to that described previously in this section to thoroughly remove any excess secondary antibody; *T. gondii* – positive IgG was detected by adding the corresponding substrate (Western Blue® stabilized substrate, Promega, S3841) to the membranes. An unimmunized mouse serum was incorporated in these steps as a negative control. Following the positive demonstration of IgG antibodies to *T. gondii* on Western Blots, the mouse spleens were harvested, snap-frozen in liquid N_2 and stored in a -80°C freezer until needed.

3.3.b. Construction and biopanning screening of a phage-displayed scFv antibody library

3.3.b – i ScFv phage-display library construction

Total RNA was prepared from homogenized mouse spleen using the RNeasy Mini Kit (QIAGEN GmbH, Hilden, 74104) according to the manufacturer's instructions. This was followed by mRNA purification using the MicroPoly(A) Purist™ small scale mRNA purification kit (Ambion, 1919). Following a spectrophotometric check on mRNA concentration and purity, the resultant mRNA (7.8 µg) was used as template for cDNA synthesis using the Superscript™ III Reverse Transcriptase (Invitrogen, 18080-093) according to the manufacturer's protocol. Typically, 0.2 µg of mRNA was utilized as template for first-strand reaction and primed by Oligo-$(dT)_{20}$ primer (Invitrogen, 18418-020). The resulting first-strand cDNA was used as a template for the amplification of the murine IgG variable heavy (V_H) and variable light (V_L) chain gene regions. V-region PCR amplifications were performed using a protocol modified from Nathan, S. *et al.* (Nathan, Li, Mohamed, & Embi, 2002) to incorporate *Sfi* I and *Not* I restriction sites flanking the assembled scFv fragments at the V_L 5' and V_H 3' domains respectively. All primer sequences are listed in Appendix III. These primers were adapted for the pCANTAB5E phagemid vector (Amersham Biosciences) (Appendix IV) and the primer combinations were designed to amplify most of the known mouse antibody sequences.

A total of 23 Vκ region PCR reactions in 50 µl volumes were carried out for amplification of κ light chain variable region as follows: 0.4 µM of MSCVκ (Vκ 5' sense / *Sfi* I) primer mix, 0.4 µM of MSCJκ (Vκ 3' antisense / short linker) primer mix,

2 µl of the first-strand reaction, 0.3 mM dNTP mix (Promega, U1515), 1X PCR Buffer and 2.0 U DyNAzyme™ II DNA Polymerase (Finnzymes, F-501L). Meanwhile, Vλ gene region amplifications were prepared using one set of forward and reverse primers only. The Vλ amplifications were set up as above except that the primer mixes were substituted with the MSCVL-1 (Vλ 5' sense / *Sfi* I) and MSCJKL-B (Vλ 3' antisense / short linker) primers. A total of 4 Vλ PCR reactions were prepared.

For the V_H gene regions, PCR amplifications were done using a combination of 19 forward primers and 3 reverse primers, making up a total of 30 V_H region PCR reactions prepared as described above. The VH regions PCR reactions utilized the MSCVH (V_H 5' sense) and MSCG (V_H 3' antisense / *Not* I) primer mixes for the amplification of V_H regions IgG1, IgG2a, IgG2b, IgG3 and IgM. All amplifications were performed in a thermal cycler (Mastercycler Gradient 96, Eppendorf, Germany) (94°C for 3 min, 30 cycles of 94°C for 30 s, 56°C for 30 s, 72°C for 90 S; 72°C for 2 min). The PCR products were analysed on 1% (w/v) agarose gel electrophoresis and purified by QIAquick Gel Extraction Kit (QIAGEN GmbH, Hilden, 28704). Multiple PCR reactions were set up to obtain a more diverse V-gene library by avoiding possible bias likely to occur in a single reaction.

Subsequently, the V_H and V_L coding sequences were fused using the flanking primers MSCF (5-GCGGGGCCCAGCCGGCCGAGCTCG-3) and RSCB (5-GCCTGCGGCCGCACTAGTGACAGA-3) through splice-overlap extension PCR (SOE-PCR) to produce the single-chain variable fragment (ScFv) with an 8-amino acid flexible linker in between (Figure 3.2). The scFv assembly reaction was carried out as follows: 1 µM of MSCF primer, 1 µM of RSCB primer, approximately 50 ng of each of V_H and V_L coding sequences, 1 mM dNTP mix, 2X Amplification Buffer, 1 mM

$MgSO_4$, 2X PCR_X Enhancer solution, 1 U of Platinum *Pfx* DNA Polymerase (Invitrogen, 11708-013). The cycling conditions for the assembly reaction is: 7 cycles of 92°C for 1 min, 63°C for 30 s, 58°C for 50 s, and 72°C for 1 min; followed by 23 cycles of pull-through reactions of 92°C for 1 min, 63°C for 30 s, 72°C for 1 min; with final extension at 72°C for 10 min.

The resulting polyclonal pool of scFv fragments library was approximately 0.75 kb in size and was gel purified. This was followed by a sequential restriction digestion of the scFv fragments with *Sfi*I (NEB, R0123S) and *Not*I (NEB, R0189) according to manufacturer's instructions. The restriction digested and purified scFv DNA was cloned into the *Sfi*I and *Not*I pre-digested pCANTAB5E phagemid vector (GE Life Sciences – formerly Amersham Biosciences, RPAS Expression Module, 27-9401-01). Cloning of the generated scFv antibody fragment pool into the *Sfi*I - *Not*I polyclonal cloning site within the pCANTAB5E phagemid vector results in a COOH-terminal E-tag and a UAG-amber stop codon between the E-tag and a g3p gene encoding the phage minor coat protein (Appendix IV). Transformation of the scFv-pCANTAB5E vector into the *E. coli* suppressor strain TG1 makes it possible to produce phage-displayed scFv when co-infected with M13 helper phage that provides the gene apparatus for the assembly of recombinant phage particles. Sub-cloning of the recombinant phagemid vector into the non-suppressor *E.coli* strain HB2151 would lift the UAG stop codon suppression present in TG1 and result in the expression of soluble scFv antibodies.

To prepare the DNA for electroporation, the ligation reactions were cleaned up using the StrataClean Resin (Stratagene, 400714) according to the manufacturer's protocol. The purified ligation products (10 – 20 µl) were transformed into *E. coli* TG1 electroporation - competent cells (Stratagene, 200123) by electroporation (2.5 KV, 200

ohms, 25 μF; time constant > 3.6 msec). Five sets of library electroporation transformations were done resulting in a complexity of 1.62 X 10^4 independent transformants.

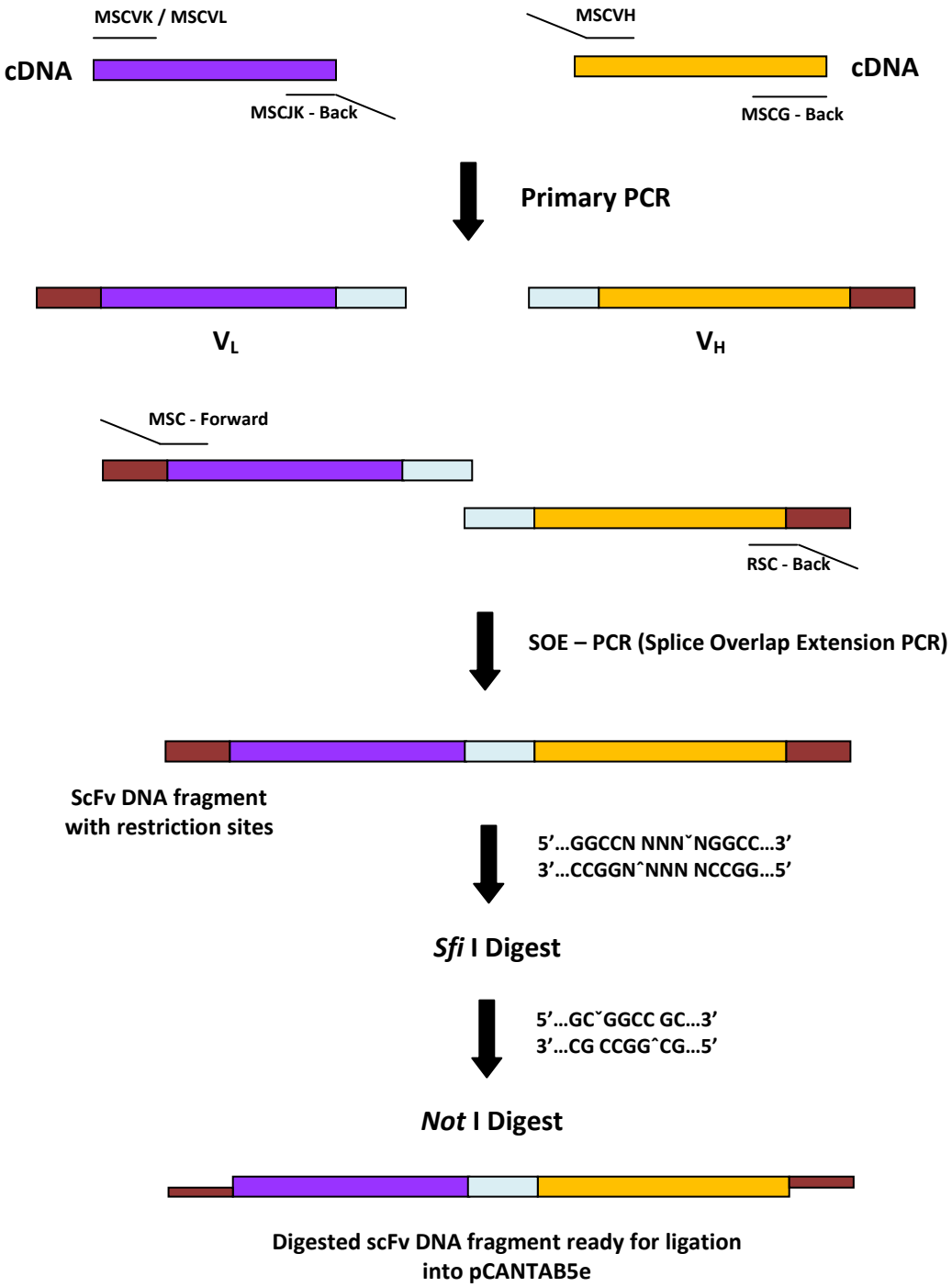

FIGURE 3.2 **Strategy of scFv fragment assembly.** A short peptide linker (SSRSSGG) was incorporated into V_H and V_L and fused into scFv fragments by splice overlap extension PCR. Restriction sites for both *Sfi* I and *Not* I are incorporated at both ends of the scFv for subcloning into phagemid vector pCANTAB5E.

3.3.b – ii Recombinant phage-scFv rescue

All subsequent steps from the library construction which involves the recombinant phage-scFv antibody rescue, biopannings and phage titering procedures were carried out with tubes and lab consumables treated against phage contamination as described in Phage Display – A Laboratory Manual (Burton, 2001) and in Appendix II. All recycled tubes and lab consumable were autoclaved (121°C, 15 p.s.i., 15 minutes) followed by baking at 105°C for at least 4 hours in a dry oven. This extra dry heat-treatment of autoclaved lab wares is necessary as phages are known to survive standard autoclaving conditions. The rescue of the recombinant phage-scFv antibody library from the electro-transformed TG1 cells was carried out according to standard pCANTAB5E phagemid (Amersham Biosciences, 27-9401-01) manufacturer's protocol using VCSM13 interference-resistant helper phage (Stratagene, 200251). The recombinant phage suspension was precipitated with Polyethylene glycol 8000 (PEG) as previously described (Rader et al., 2001). The recombinant scFv-phage supernatant was precipitated by the addition of 2.0 ml PEG/NaCl (20.0 % PEG, and 14.6 % NaCl) to 10.0 ml of supernatant. The mixture was then allowed to stand for 1 hour on ice, before centrifugation at 13,000x*g* in a pre-chilled Beckman JA-20 rotor for 20 min at 4°C. The supernatant was carefully decanted and all traces of buffer were drained by blotting on a clean paper towel. The resulting scFv-phage pellet was aseptically resuspended in 3.0 ml of 2x YT medium (1.7 % (w/v) Bacto-tryptone, 1.0 % (w/v) Bacto-yeast extract, and 0.5 % (w/v) NaCl). The PEG-precipitated phage suspension was subsequently blocked with BSA Blocking Buffer (1% BSA in PBS) in a 1:1 ratio in preparation for the biopanning procedure. Biopanning procedures are carried out immediately following phage rescue and PEG precipitation to avoid proteolysis of scFv fragments as some recombinant phage preparations may be unstable.

3.3.b – iii Subtractive Biopanning

Subtractive biopanning was performed on normal hepatocyte human cell line WRL68 to remove phages that binds non-specifically to cells. The WRL68 cell line was kindly provided by Wong Yau-Hsiung and Dr. Habsah A. Kadir (Department of Biochemistry, Institute of Biological Sciences, University of Malaya, Kuala Lumpur). Prior experiments were carried out to determine the amount of absorber WRL68 cells and panning rounds required to sufficiently reduce non-specific binding phages. Each successive panning rounds for this phage-quenching study was monitored for the average phage-binding titers to the absorber cells. A plateau in the binding titer is taken to indicate as a sufficient threshold for the subtractive biopanning rounds. Through this study, it was determined that at least 3 rounds of subtractive biopanning would be required (Appendix V).

For phage absorption, WRL68 cells (1.27×10^4) were transferred to a pre-blocked microcentrifuge tube. The cells were pelleted by centrifuging at 1000x*g*, 4°C, for 5 minutes, and the supernatant removed. The pre-blocked and precipitated recombinant phage-scFv suspension (1.10×10^{11} cfu/ml) was then added in and the cell-phage mixture was rotated at 8°C for 30 min. The cells were then pelleted as before, and the supernatant with unbound phages was transferred to another aliquot of WRL68 cells (1.27×10^4) for another round of phage absorption. A total of 3 rounds were carried out before proceeding with the selective biopanning on *T. gondii.*

3.3.b – iv Selective Biopanning on Cells

The subtracted recombinant phage fraction was added to a filtered *T. gondii* tachyzoites cell suspension (2.88 x 10^4) in a pre-blocked microcentrifuge tube, and the mixture was incubated at 8°C for 2 hours on rotation. At the end of the incubation, tachyzoite cells were pelleted by centrifugation at 1000x*g*, 4°C, for 5 minutes; and the supernatant was discarded. The cells were then washed 5 times with THB-T (THB with 0.05% Tween-20) with vigorous vortexing at each rounds and similar spin conditions. Bound phage was eluted by resuspending cells in 200 µl Glycine-HCL (pH 2.2) elution buffer at 4°C for 10 min and subsequently neutralized by addition of 26.7 µl Tris-Cl (pH 8.0). The phage eluate was then re-infected with 1.0 ml of log-phase *E. coli* TG1 and plated on SOBAG media (2.0% (w/v) Bacto-tryptone, 0.5% (w/v) Bacto-yeast extract, 0.05% (w/v) NaCl, 1.5% (w/v) Bacto-agar, 10 mM $MgCl_2$, 100 mM Glucose, and 100 µg/ml ampicillin) overnight at 30°C, at 100x and 10x dilutions for phage output tittering of transformed clones with ampicillin resistance. Phage output titer was calculated from the mean of triplicate sets of each dilution to determine the number of phage captured on the cells. The remaining phage-infected *E. coli* TG1 suspension was plated on large SOBAG plates (145 x 20 mm) (Greiner Bio-One, 639102) and also incubated at 30°C overnight to obtain single colonies of *T. gondii*-binding scFv clones.

3.3.b – v Polyclonal phage-scFv output binding screening

To verify the polyclonal phage-scFv output derived from the single-round selective biopanning procedure is specific for the target antigen – *T. gondii* tachyzoites, and quenched from unspecific binding to WRL68; an output binding screening was

performed. Because the single-round selective biopanning phage-scFv recovery tends to be low, it needs to be re-amplified prior to the binding screening.

For phage-scFv re-amplification, 1.0 ml of the biopanned polyclonal phage output fraction was transferred aseptically to a 50 ml centrifuge tube and subsequently diluted to an O.D. at A_{600} of 0.3 with 2x YT medium. The diluted culture is then incubated at 37°C at 250 rpm for 30 min. Following this incubation, sterile ampicillin and glucose was aseptically added into the culture at a final concentration of 100 µg/ml and 2.0 % respectively; and the culture was further incubated for another 1 hour at 37°C and 250 rpm. At the end of this, the turbid culture was inoculated with the VCSM13 helper phage to a multiplicity-of-infection (m.o.i) to the *E. coli* cells of 5:1, with the assumption that the O.D. at A600 by then is 0.5 and which is equivalent to an amount of 2.5 x 10^8 cells in the sampled volume. The estimated amount of cells in the sampled volume is multiplied by the total volume of the *E. coli* culture to obtain the total number of cells in culture. The VCSM13-infected *E. coli* culture was incubated again at 37°C, first without shaking for 15 min to allow for phage infection, and next with shaking at 250 rpm for 45 min. Next, the culture was centrifuged at 1000x*g* for 10 min and the supernatant was discarded. The pellet was gently resuspended in 10.0 ml of 2x YT-AK medium (2 x YT medium with 100 µg/ml ampicillin and 50 µg/ml kanamycin) and incubated for 16 hours or overnight at 37°C and 250 rpm. On the next day, the overnight culture was centrifuged at 1000x*g* for 20 min. The supernatant which contained the amplified recombinant phage-scFv was carefully transferred to a 50.0 ml Beckman centrifuge tube and was PEG-precipitated as described previously. After allowing the PEG-precipitation mixture to stand on ice for 60 min, the mixture was centrifuged in a Beckman Avanti™ Centrifuge J-25 I machine at 13,000x*g*, 4°C for 20 min. The supernatant was discarded and the resulting phage pellet was resuspended in

2.0 ml of 2x YT medium and blocked for at least 15 min with 2.0 ml of BSA Blocking Buffer containing 0.01 % sodium azide as preservative.

Four sets of experimental conditions and one negative control were designed to compare the binding between the biopanned-output phage repertoire and unpanned original phage library with the tachyzoites and the WRL68 absorber cells (Table 3.1). The procedure carried out was similar to the methods in subtractive biopanning (for WRL68 cells) and selective biopanning (for *T. gondii* tachyzoites) with the exception that only 1 round of negative selection biopanning was done for the binding study sets with WRL68 cells. Each experimental condition sets were performed in triplicates and the mean average titers from each set was calculated and normalized against the background phage-binding negative control reading (Set 5, Table 3.1).

Table 3.1. Experimental condition sets for polyclonal phage-scFv output antigen binding screening.

Experimental Sets	Binding conditions
1	Biopanned-output phage-scFv with *T. gondii* tachyzoites
2	Unpanned -phage-scFv library with *T. gondii* tachyzoites
3	Biopanned-output phage-scFv with WRL68 cells
4	Unpanned -phage-scFv library with WRL68 cells
5	Biopanned-output phage-scFv without cells (Negative control)

3.3.c. Analysis of putative anti-*Toxoplasma gondii* scFv antibodies

3.3.c – i Sequencing Analysis

Each scFv clone was further screened by PCR to verify for the presence of full-length scFv genes. The colony PCR screening was carried out with the primer pairs pCANTAB5 S1 (Forward) (5-CAACGTGAAAAAATTATTATTCGC-3) and pCANTAB5 S6 (Reverse) (5-GTAAATGAATTTTCTGTATGAGG-3) (Amersham Biosciences, 27-1585-01) with the following conditions: 0.2 µM of S1 primer, 0.2 µM of S6 primer, 0.2 mM dNTP mix, 1X Amplification Buffer, 4.0% DMSO, 1 U of DyNAzyme™ II DNA Polymerase (Finnzymes, F-501L). The screening PCR was carried out in a thermal cycler (Mastercycler Gradient 96, Eppendorf, Germany) programmed at 94°C for 3 min, 30 cycles of 94°C for 20 s, 56°C for 20 s, 72°C for 20 S; 72°C for 2 min. Short-listed full-length scFv genes were then fingerprinted with the DNA restriction enzyme *Mva*I (Fermentas, FD0554) in conditions according to manufacturer's instructions. Full-length scFv genes with unique fingerprint patterns was selected and the clones were sequenced using the dideoxy method with the pCANTAB5 sequencing primer pairs – S1 and S6 (Amersham Biosciences, 27-1585-01). DNA Sequencing was performed using ABI PRISM BigDye™ or Amersham Pharmacia Biotech DYEnamic ET Terminator kit (AIT Biotech, Singapore).

The ScFv sequences were analysed with BioEdit v 7.0.5.3 (Hall, 1999) for full-length coding sequences without any internal stop codon and truncation mutations. Out of this analysis, 4 full-length scFv clones were selected. The full-length V_H and V_L chain region sequences were numbered according to the IMGT unique numbering scheme (Lefranc et al., 2003), and analysed using the online software V-Quest provided

by the International ImMunoGeneTics (IMGT) database (imgt.cines.fr/textes/vquest) for the determination of the CDR regions and the germline origins of V regions of the scFv clones.

3.3.c – ii Monoclonal ScFv Binding Titer Assay

Phage rescue of the monoclonal full-length scFv clones was performed as outlined in the manufacturer's protocol (RPAS Expression Module, Amersham Biosciences, 27-9401-01) using VCSM13 interference-resistant helper phage (Stratagene, 200251). The recombinant phage suspensions (mean titer of 2.03 x 10^{11} cfu / ml) were each blocked with 1% BSA blocking buffer before incubation with *T. gondii* tachyzoites (1.0 x 10^5 cells / reaction). Each verified functional full-length scFv clone was also tested for binding with negative control WRL68 cells (1.0 x 10^5 cells /reaction) in parallel with the *T. gondii* binding study to analyse for the binding titer comparison. A second negative control was also incorporated into the experimental set-up, which was the testing of the binding titer of non-scFv fusion-VCSM13 or 'blank' phages with *T. gondii*. All of these reactions were incubated at 8°C for 2 hours with rotation. The centrifugation, washing and phage-elution steps from the cells were carried out as described before; except that 4 rounds (instead of 5 rounds) of washing were conducted with THB-T wash buffer. The phage eluate recovered was reinfected with log-phase TG1 and titered to determine phage capture from the mean of replicates. Comparison of means between both the samples and negative controls were done by using the one-tailed Wilcoxon-Mann-Whitney statistical test ($H_0 < H_A$, $\alpha = 0.05$), on the Analyze-It v.2.2 platform.

3.3.c – iii Structural Modelling of V Regions

The structural modelling of the V-regions of the scFv clones and its' germline counterparts were accomplished by using the web-based antibody modelling software – Rosetta Antibody: Structure Prediction Server (Sircar, Kim, & Gray, 2009) provided by the Department of Chemical and Biomolecular Engineering, Johns Hopkins University (http://antibody.graylab.jhu.edu/). The modelling protocol incorporates an *ab initio* loop modeling of CDR H3, simultaneous optimizing of the CDR backbone dihedral angles and the relative orientation of the light (V_L) & heavy (V_H) chains (Sivasubramanian, Sircar, Chaudhury, & Gray, 2009). Only 1st rank predictions were used for each scFv model.

The resulting molecular models were viewed and analysed using the software VMD version 1.8.7 (2009) (www.ks.uiuc.edu/). The analysis and superimposition of the recombinant and germline scFv molecular models was generated with the SwissPdb-Viewer (DeepView) version 4.0.1 (2008) (http://spdbv.vital-it.ch/) and also PyMOL for windows.

3.3.d. Affinity maturation of anti-*Toxoplasma gondii* scFv antibodies and its' analysis

3.3.d – i Construction of Hotspots Affinity-Matured Phage-display Libraries

Hot spots are regions within an antibody's CDRs that are naturally prone to somatic hypermutations during the *in vivo* affinity maturation of an antibody (Neuberger & Milstein, 1995). Based on the identification of hot spots residues within the scFv antibodies' CDR using the V-Quest software (imgt.cines.fr/textes/vquest), the hot spot motif RGYW (R = A or G, Y = C or T, W = T or A) was chosen as the loci for introducing randomized mutations to produce a 2nd generation scFv antibody library for the purpose of affinity maturation against *T. gondii*. A RGYW-hot spot region on the V_L fragment, CDR1 of TG130 scFv was targetted for the affinity maturation procedure.

Completely overlapping sense and antisense DNA oligomers were designed to generate a library randomizing 4 nucleotides (2 consecutive amino acids) at the targeted hot spot region, while preventing the introduction of stop codons through the randomized mutations. The following degenerate oligomers were used: pCANTAB5 E – RGYW Fwd (Sense), 5'- G GCC AGT CAG GAT GTG **VNS NCT** GCT GTA GCC -3'; pCANTAB5 E – RGYW Rev (Antisense), 5'- GGC TAC AGC AG**N SNB** CAC ATC CTG ACT GGC C 3', (V = A or C or G, S = C or G, B = C or G or T). The 4-nucleotide-point mutation was carried out on scFv TG130 as the parental template and using the QuickChange Lightning Site-Directed Mutagenesis Kit (Stratagene, La Jolla, CA, Cat. No. 210518).

Usage of degenerate DNA oligomers in PCR is normally a less efficient process; therefore before commencing the site-directed mutagenesis PCR reaction, oligonucleotide adaptors were generated from the degenerate oligomers to improve the mutagenesis PCR run. Equimolar amounts of point mutagenesis degenerate oligonucleotides (pCANTAB5 E – RGYW Fwd and pCANTAB5 E – RGYW Rev) were resuspended in Annealing Buffer (10 mM Tris-HCl pH 7.5 / 60 mM NaCl), and

subsequently heated to 95°C for 10 min before allowing to cool to room temperature overnight to form an oligonucleotide duplex.

Following the generation of the degenerate oligonucleotide adaptors, the mutagenesis PCR reaction was carried out using 10.6 ng of the phagemid pCANTAB5E-TG130 which contains the scFv TG130 as template; with 30.0 pmol of the degenerate DNA adaptors (15.0 pmol or 153.4 ng each of the degenerate DNA oligomers pCANTAB5 E – RGYW Fwd and pCANTAB5 E – RGYW Rev). The scFv template and DNA adaptors were mixed with the QuikChange Lightning enzyme and its component reagents according to manufacturer's protocol in a total of 50.0 µl volume and cycled according to this condition: 1 cycle at 95°C for 2 min, followed by 18 cycles at 95°C for 20 s, 60°C for 10 s, and 68°C for 2.5 min, and 1 final extension cycle at 68°C for 5 min. The mutagenesis PCR product from this described reaction was *Dpn*1-digested to remove all parental phagemid dsDNA, ethanol precipitated, and subsequently cloned into XL-10 Gold® ultracompetent cells according to manufacturer's protocol provided in the kit. Transformed clones were verified by colony PCR using the S1 and S6 primers (similar protocol to section 3.3.c-i) and sequenced to check for successful sequence diversification at the targeted mutation loci.

Once sequence verification has confirmed the presence of the targeted mutations, the point-mutated phagemids were isolated from the XL-10 Gold cells using the conventional alkaline lysis minipreparation procedure (Sambrook & Russell, 2001), and transformed into chemically-competent *E. coli* TG1 using an optimized protocol published by Tu Zhiming and co-workers (Tu et al., 2005). The point-mutated scFv library was rescued from the transformed TG1 *E.coli*, titered and immediately used for the 2nd generation biopanning procedure.

3.3.d – ii Biopanning screening of 2nd generation clones (RGYW-point mutants)

The resulting recombinant phage derived from the phage rescue in section 2.3l was PEG-precipitated, and blocked in 2% BSA (1:1 ratio) before biopanning. The panning antigen, *T. gondii* tachyzoites was purified and prepared as previously described in section 3.3a. The phage mixture (~2.7 x 10^{12} cfu) from the RGYW-point mutated library was added to the purified tachyzoite cells suspension (~ 4.0 x 10^5 cells) in pre-blocked microcentrifuge tubes, and the mixture was rotated at 4 rpm at 8°C for 1 hr. This biopanning reaction was run in triplicate sets in parallel with double negative controls: *T. gondii* tachyzoites incubated with the parental strain scFv TG130 as the first control; and *T. gondii* tachyzoites (~2.0 x 10^5 cells) incubated with non-recombinant VCSM13 helper phages as the second control. All experimental conditions for the controls were similar to those applied for the samples unless otherwise stated.

As the purpose for this biopanning screening of the 2nd generation scFv clones is for the isolation of antibody fragments with improved affinity; a shorter co-incubation time and a longer and more stringent wash conditions was employed compared to the protocol described in section 3.3f. Antibody fragments with faster on-rates (k_{on}) and longer off-rates (k_{off}), would result in a lowered affinity constant (K_D) and therefore an improved binding affinity. Following the 1h incubation, cells were pelleted by centrifugation at 1000x*g*, 4°C for 5 min and the supernatant was discarded. The cells were washed by resuspension in cold THB-T (0.05%), vortexed and subjected to a further washing incubation for 5 min at 4 rpm, 8°C. This washing step was repeated for 10 consecutive rounds, and bound phage were eluted by resuspending the washed cells in 200 µl of ice-cold Glycine-HCL (pH 2.2) Elution Buffer (EB) and incubated on ice

for 10 min. The eluted mixture was then neutralized by addition of 26.7 µl Tris-HCL (pH 8.0) and reinfected with 1.5 ml of log-phase *E. coli* TG1 cells. The eluted phages from each experimental sets and controls were titered to determine the amount of captured phages on the antigens, and glycerol stocks of the eluate were prepared and stored at -80°C.

3.3.d – iii Immunofluorescence Assay

Extracellular live tachyzoites were prepared for the surface indirect immunofluorescence assay according to the procedure described in section 3.3a. Filtered tachyzoites were blocked with 2% BSA in PBS-T (Blocking Buffer) prior to antibody co-incubations. Blocked tachyzoites were probed with the candidate recombinant phage-displayed scFv antibodies suspension in Blocking Buffer for 1 hour at 4°C. This was followed by a double washing round in 2 ml of Toxoplasma Homogenization Buffer (THB) by centrifuging the mixture at 1000x*g* for 4 min at 4°C.

Anti-M13 g8p phage coat protein monoclonal antibody (Pierce Biotechnology, MA1-06603) was conjugated to Alexa Fluor® 488 chromogen using the Alexa Fluor® 488 Monoclonal Antibody Labelling Kit (Molecular Probes, A20181); and was subsequently used as the secondary antibody for the detection of scFv binding to the target. The secondary antibody (1:50 dilution) was incubated with the washed tachyzoites for 30 min at 4°C in the dark, followed by a similar double washing round with THB as mentioned previously. Labelled parasites were subsequently fixed in 1 ml of cold 2.5% formaldehyde in PBS, pH 7.4, for 20 min on ice. After 20 min, the fixed tachyzoite cells were immediately washed in double rounds of ice-cold THB. The fixed

and labelled tachyzoite cells were then embedded with ProLong Gold mounting medium with DAPI (Molecular Probes, P36935) for microscopy. Slides were allowed to cure for at least 24 hours before microscopy. A magnification of × 63 was used to view the cells on a Leica TCS SP2 AOBS Confocal microscope.

CHAPTER 4. RESULTS & DISCUSSION (PART 1): GENERATION OF ANTI-*TOXOPLASMA GONDII* ScFv ANTIBODIES BY PHAGE-DISPLAY.

4.1 Strategy

The purpose of this study was to construct a scFv phage display library targeted against *T. gondii* tachyzoites from an immunized mouse B-cell repertoire. The resulting antibody library was then screened against the whole tachyzoite cells to isolate and further characterize the binding scFv antibodies. The antibody screening procedure was optimized to reduce false positive binding to the target cell surface as well as to minimize loss of functional full-length scFvs and diversity of clones captured. The binding specificity of the candidate scFv antibody that was developed in this study was verified through determination of target binding titers and immunofluorescence localization. The strategy for the generation of anti-*Toxoplasma gondii* scFv by phage-display is shown in Figure 4.1.

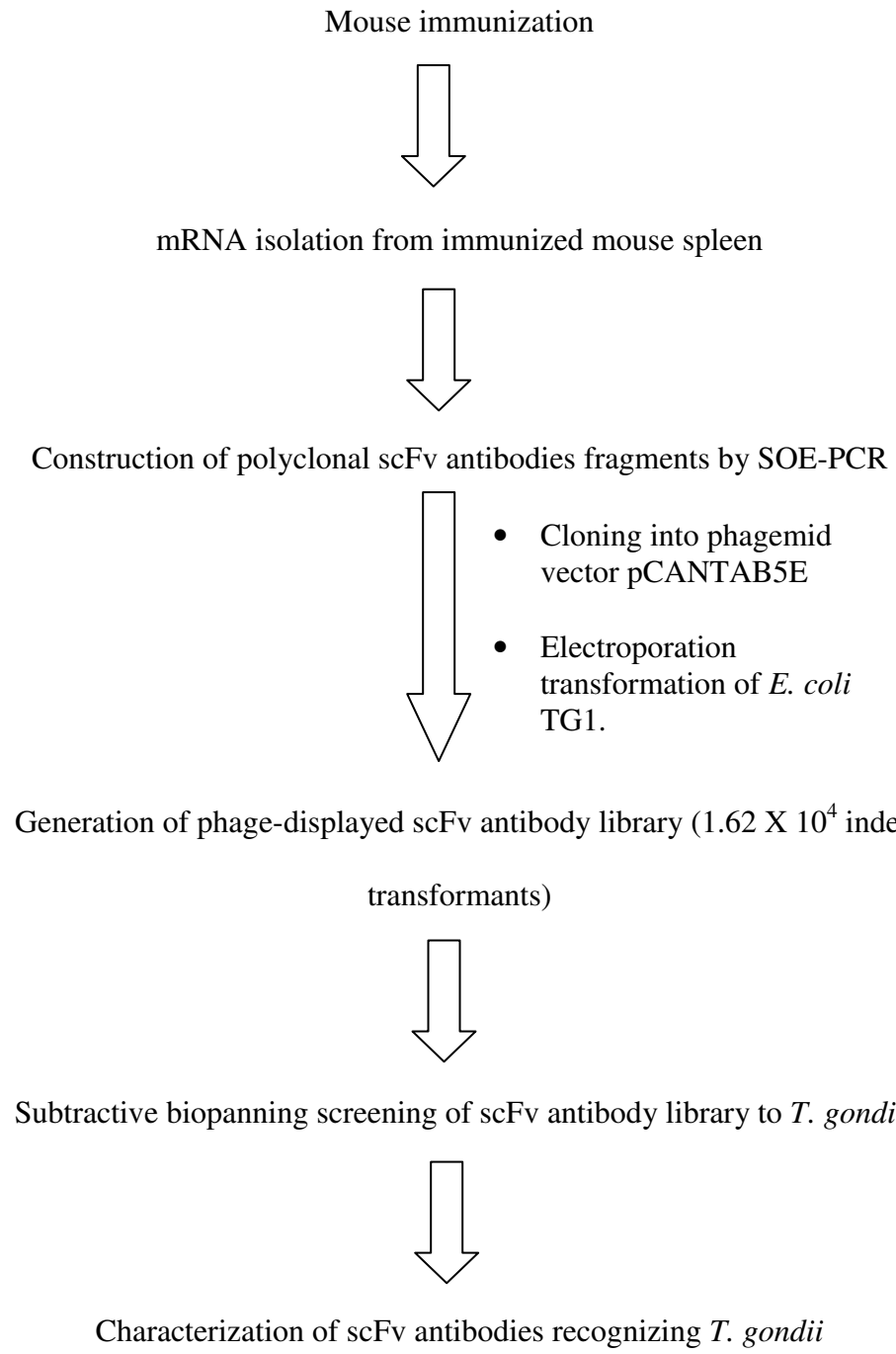

FIGURE 4.1 The workflow of procedures for the generation of anti-*T. gondii* scFv antibodies by phage-display is summarized in this schematic diagram.

4.2 Results

4.2.1 - Mouse immunization with *T. gondii*

BALB/c mice that were immunized with *T. gondii* tachyzoites according to standard procedures as detailed in Methodology section 3.3a were bled on the 4th day after the final 2nd booster. A total of 3 mice were immunized and its serum tested for the presence of IgG antibodies to *T. gondii* antigens by an immunoblot assay. Results of the immunoblot analysis showed seropositivity of all 3 mice to *T. gondii* with serum IgG that was reactive to a wide range of *T. gondii* antigens separated on the blots (Figure 4.2). This provides the verification needed to proceed with the splenic harvest of the immunized mice.

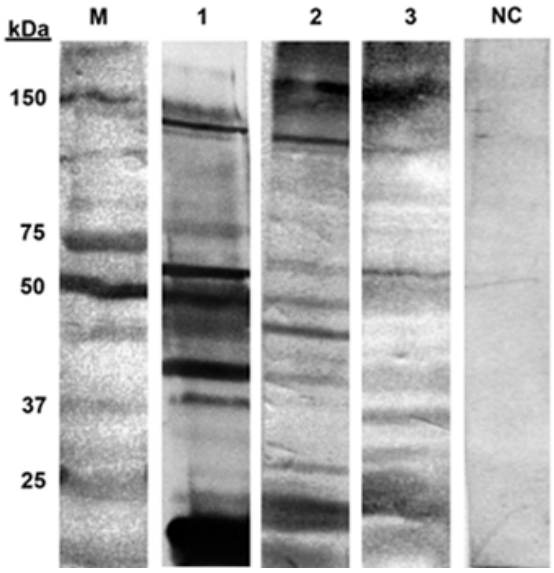

FIGURE 4.2 **Immunoblot verification of mouse serum immunized against *T. gondii*.** Western blot strips of *T. gondii* parasite separated on SDS-PAGE were probed with immunized mouse serum individually. The immune mice serum (*lanes 1 – 3*) showed IgG reactivity with the parasite antigens. Uninfected mouse serum was used as negative control (*lane NC*). The migration of size markers is indicated in kilodaltons (Prestained protein ladder, Fermentas, SM0671).

4.2.2 - Assembly of *T. gondii*-immunized scFv phage-displayed library

Total RNA isolated from splenic cells of *T. gondii* immunized mice (Figure 4.3) was evaluated for integrity and purity. As shown in the gel electrophoresis of Figure 4.3, total RNA isolation samples showed sharp bandings of 18S and 28S ribosomal RNA at approximately 1.9 kbp and 4.7 kbp respectively; indicating intact total RNA. There was a total of 8 batches of total RNA isolated from a single mouse spleen organ. Although sectioning the spleen tissues to 8 batches may slightly lower the isolated RNA concentration, this was necessary to avoid the clogging of the RNA spin columns due to the inherent viscosity of homogenized animal tissues. The purity and the concentration of the total RNA isolated were assessed by spectrophotometric readings (Table 4.1). These RNA samples were then pooled together into 3 batches and used for mRNA isolation by Poly(A) selection. Messenger RNA samples isolated were spectrophotometrically assessed for purity, and only mRNA samples with an A_{260} / A_{280} absorbance value ratio of 1.45 – 1.80 were used for downstream cDNA synthesis and primary PCR amplification (Table 4.2).

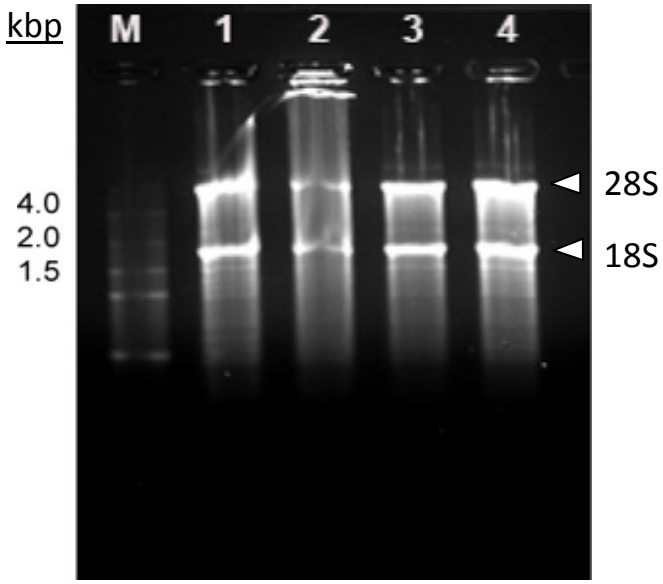

FIGURE 4.3 **Quality of RNA isolated from immunized mouse spleen tissues.** A fraction of approximately 5 – 10 µg of total RNA prepared from approximately 30 mg tissue samples were loaded into each well (lanes 1-4). The 18S and 28S rRNA bands are indicated (arrowheads). The size of the RNA ladder marker (Fermentas RNA Ladder, High Range, SM1821) is indicated at the left in kbp.

TABLE 4.1. **Total RNA isolation and quantitation.**

Immunized mouse spleen was harvested and its tissue sectioned into 30 mg cubes for total RNA isolation and purification. Results of the 8 batches of samples showed good RNA recovery, but with lowered purity. However, these RNA samples were of satisfactory quality for mRNA isolation.

Total RNA Sample	Dilution Factor	A_{260}	Concentration (µg/ml)	A_{260} / A_{280}
1	100	0.093	372.0	1.34
2	100	0.071	284.0	1.32
3	100	0.093	372.0	1.40
4	100	0.138	552.0	1.32
5	100	0.160	640.0	1.35
6	100	0.122	488.0	1.35
7	100	0.157	628.0	1.33
8	100	0.073	292.0	1.30

TABLE 4.2. **mRNA purification and quantitation.**

Total RNA isolated from immunized mice were pooled and purified for mRNA fraction. mRNA samples 1 and 3 were used for further downstream work, while sample 2 was discarded due to poor purity. A total of approximately 240 mg of splenic tissues were used to derive a combined mRNA total yield of 7.8 µg.

mRNA Sample	Dilution Factor	A_{260}	Concentration (µg/µl)	A_{260} / A_{280}
mRNA 1	50	0.020	0.04	1.62
mRNA 2	20	0.331	0.26	1.03
mRNA 3	50	0.019	0.04	1.51

Primary PCR amplification of V_H and V_L gene fragments using primer mixes of MSCVκ and MSCJκ (for V_L); and MSCVH and MSCG (for V_H) (Appendix III) from the immunized mouse splenic mRNA resulted in gene fragments of approximately 340 bp and 325 bp in size respectively. This was followed by the assembly of the scFv constructs by Splice-Overlap Extension (SOE) PCR of V_H and V_L gene repertoires with an intervening 8-amino acid flexible linker sequence, resulting in a 750 – 800 bp polyclonal gene fragment pool (Figure 4.4). At least 10 separate PCR rounds for the construction of the scFv fragments were carried out to increase library size and diversity. The peptide linker sequence bridging the 2 gene fragments was necessary to provide a degree of flexibility and hydrophilicity to the recombinant antibody fragment in binding to its' target parasitic antigen.

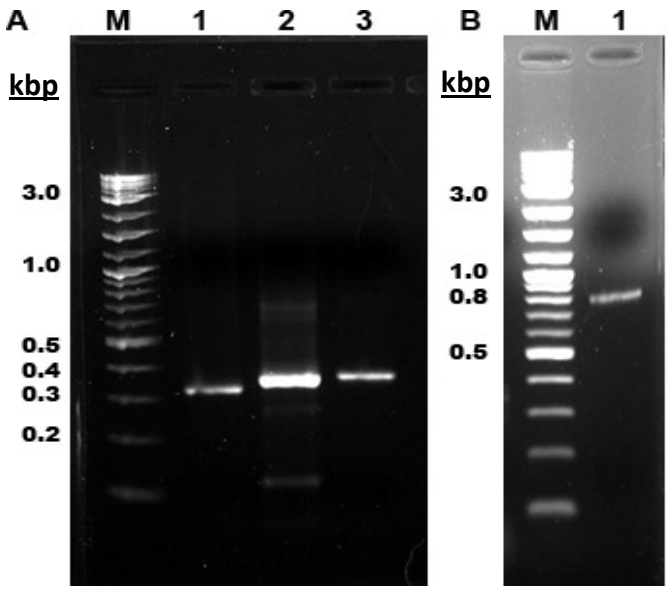

FIGURE 4.4 **Primary PCR amplification of V-region genes and scFv assembly.** A, Amplified V_H and V_L fragments. Lane 1, V_L fragment; lane 2, V_H fragment; lane 3, V_H size-marker (GE Life Sciences, formerly Amersham Pharmacia). B, lane 1, SOE-PCR-assembled scFv antibody fragment. The size of the DNA ladder marker is indicated on the left in kbp.

4.2.3 - Rapid selective screening for scFv antibodies binding to *T. gondii* tachyzoites.

The recombinant phage-display library generated through 5 rounds of electroporations contained at least 1.62×10^4 independent transformants of scFv antibodies and was used to screen for binding to *T. gondii* tachyzoites in a single-round solution-phase biopanning. Transformants that were generated through the electroporations were verified by colony PCR for full length scFv antibody inserts (Figure 4.5). After 3-rounds of subtractive biopanning followed by a single-round of antigen biopanning screening, 3.13×10^3 cfu/ml phages were recovered.

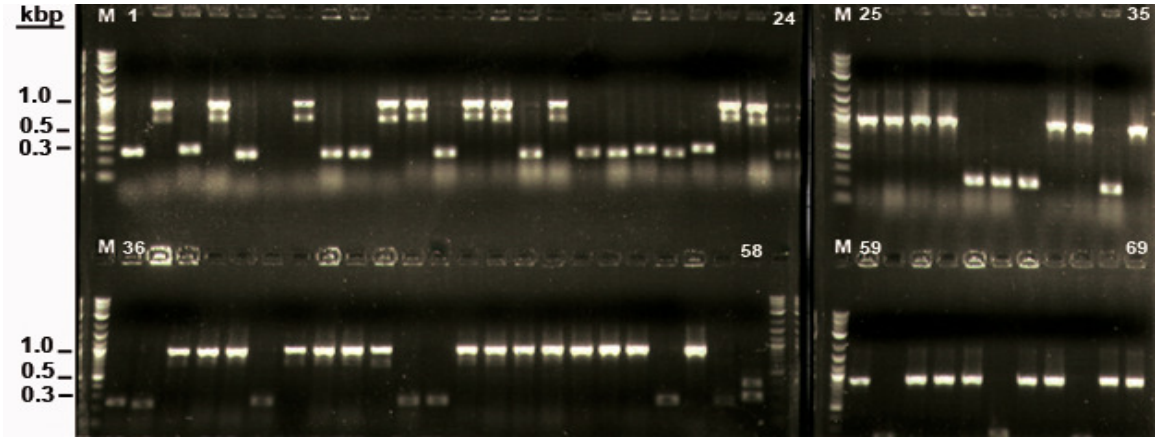

FIGURE 4.5 **Colony PCR results of the scFv genes cloning into *E. coli* TG1 by electroporation.** A recombinant phage display library was generated by electroporations of pCANTAB5e phagemid vector carrying scFv antibody fragments into electrocompetent *E. coli*, resulting in a scFv-phage display library size of 1.62×10^4 transformants. Transformants were verified by colony PCR to check for full length scFv inserts (~750 – 800 bp). A total of 180 single colony clones were amplified by PCR. A representative of 69 clones that was amplified is shown here. M, 2-Log DNA ladder marker (NEB, N3200).

In order to ascertain whether the phages recovered from the antigen biopanning output had selective binding advantage to *T. gondii*; we subjected the pool of recovered phages to another round of selective screening against the binding target in parallel to negative control absorber cells WRL68 and the un-panned scFv library fraction. The WRL68 cell line is a normal human hepatocyte cell line used as a sink to absorb unspecific binding phages from the scFv library. The study found that the single-round biopanned output phage fraction had a binding titer of at least 5.6 fold higher than the un-panned phage fraction from the primary library (Figure 4.6), indicating moderate enrichment for *T. gondii*-binding phage scFv. To further investigate the antibody's specificity against the tachyzoites, we compared the phage scFv binding titers between *T. gondii* and absorber cells WRL68. The results showed that the single-round

biopanned phage scFv had at least a 2.3 fold higher binding titer to *T. gondii* relative to WRL68 (Figure 4.6), indicating a binding advantage to the target antigen.

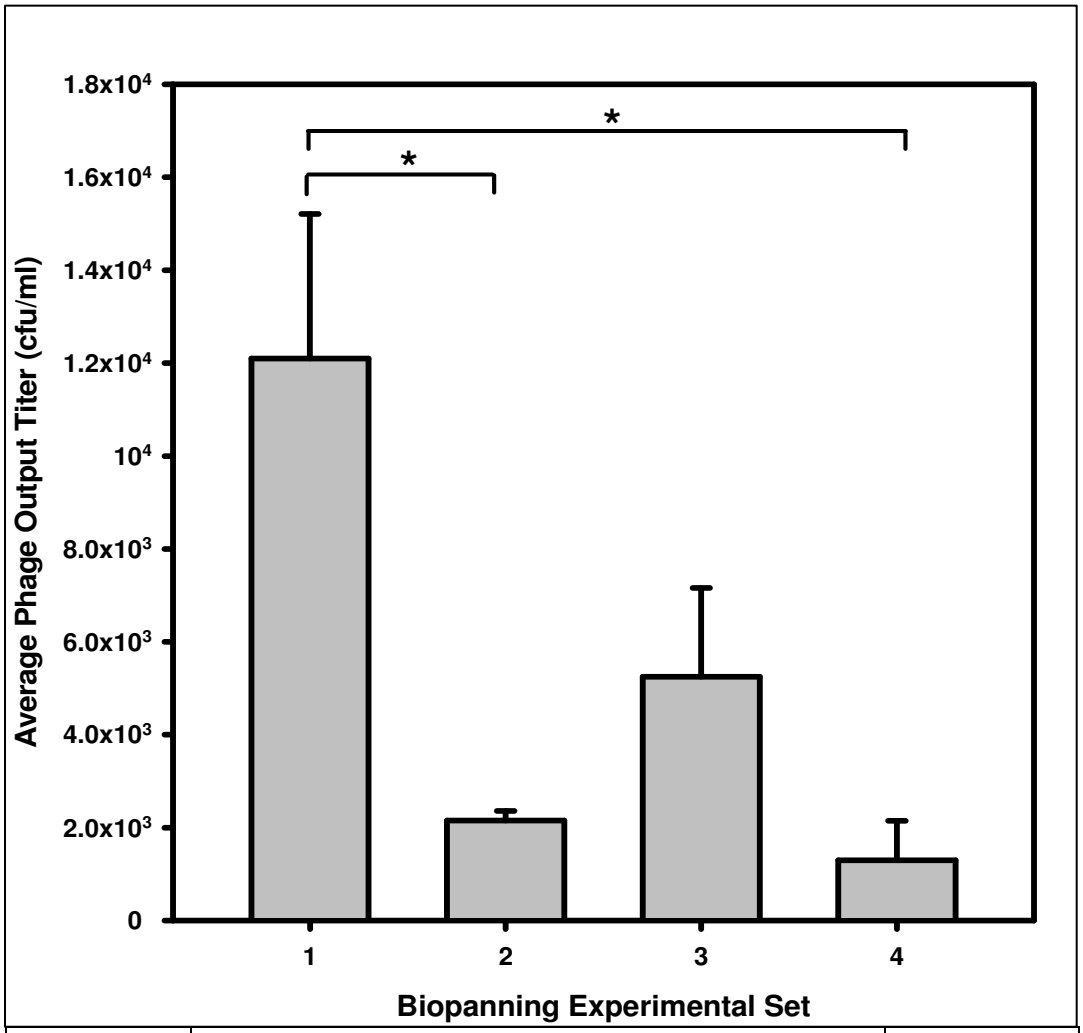

Experiment Set	Antigen-binding screening		Average Output Titer (10^3)
	ScFv-Phage	Antigen cells	
1	Single-round Output Phage	*T. gondii* tachyzoites	12.10
2	Unpanned Phage Library	*T. gondii* tachyzoites	2.15
3	Single-round Output Phage	WRL68	5.25
4	Unpanned Phage Library	WRL68	1.30

FIGURE 4.6 **Pooled scFv-phage binding titers on *T. gondii* and the WRL68 human cell line.** ScFv-phages were co-incubated with either *T. gondii* or WRL68 for 1 hour with conditions described under Methodology section 3.3b. The binding titers of the pooled scFv - phage population through a rapid single round biopanning procedure with preceding subtractive biopanning rounds is shown here in the bar graph, with a tabled description of each binding experiment set-up. ScFv-Phages incubated in BSA Blocking Buffer without any cells were used as background controls. Binding titers from triplicate experiments of these background controls was consistently non-detectable. Single-round biopanned phage-scFvs pool were at least least 2.3-fold higher in its binding affinity for *T. gondii* compared to binding with the normal human liver cell line – WRL68. *Error bars*, ± S.D. from the means of duplicate experiments. Asterisks (*) denotes a statistically significant difference between experiment set [t-test, Power of performed test with alpha = 0.05; 0.630 (Experiment set 1-2) and 0.666 (Experiment set 1-4)]

From the single-round of selective biopanning followed by 5 rounds of stringent washes, up to 131 clones were selected and PCR screening was carried out for full length clones from the eluted phage binders (Figure 4.7). Out of these clones, 9 full length scFv gene sequences were selected (Figure 4.8) and fingerprinted with the restriction enzyme *Mva*1 with each showing a unique DNA fingerprinting pattern (Figure 4.9), indicating the recovery satisfactory diversity in the scFv gene sequences captured. Through analysis of the unique scFv clone sequences, the candidate scFv list was further shortlisted to 4 translational full-length clones that were free from any frameshift mutations and intervening stop codons – scFvs TG64 (GenBank accession no. JN104603), TG69 (GenBank accession no. JN104604), TG116 (GenBank accession no. JN104605) and TG130 (GenBank accession no. JN104602) (Appendix VI). Sequencing results and protein translation of the remaining 5 truncated scFv sequences with intervening stop codons are also provided in Appendix VII.

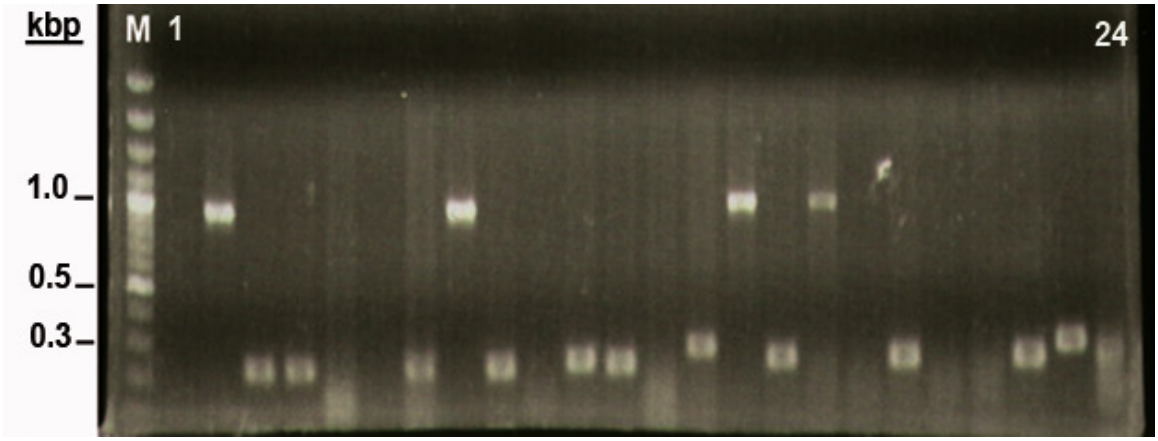

FIGURE 4.7 **Colony PCR screening of eluted scFv-phage displayed clones from antigen biopanning.** ScFv antibody clones binding to *T. gondii* cells were recovered from biopanning and amplified to select for full-length antibodies (~ 900 bp). A total of 131 clones were screened by PCR. This figure shows a representative of 24 clones from the PCR screening. M, GeneRuler 100 bp Plus DNA Ladder (Fermentas, SM0323).

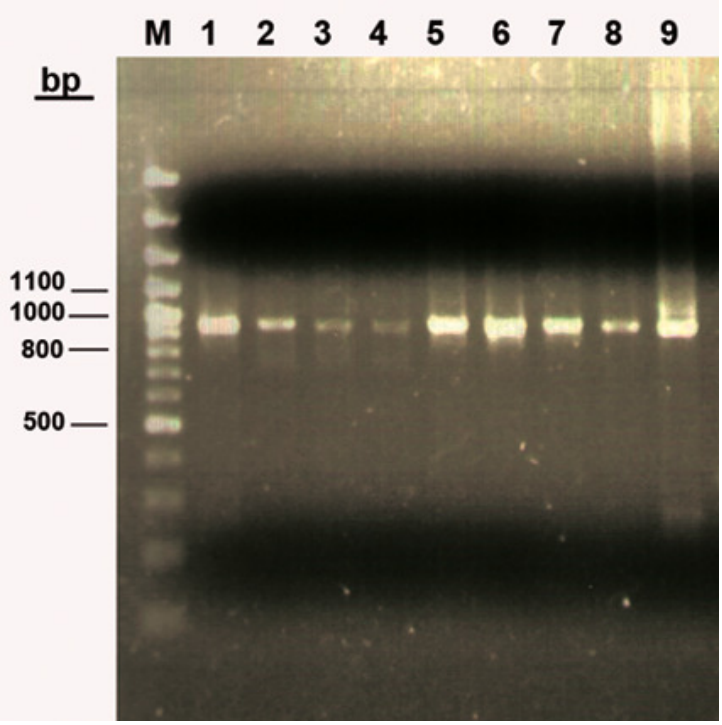

FIGURE 4.8 **PCR amplification of full-length scFv clones from antigen biopanning.** Amplification of 9 full-length scFv antibodies eluted from *T. gondii* biopanning using the S1 and S6 primers show the expected DNA fragment sizes of approximately 900 bp.

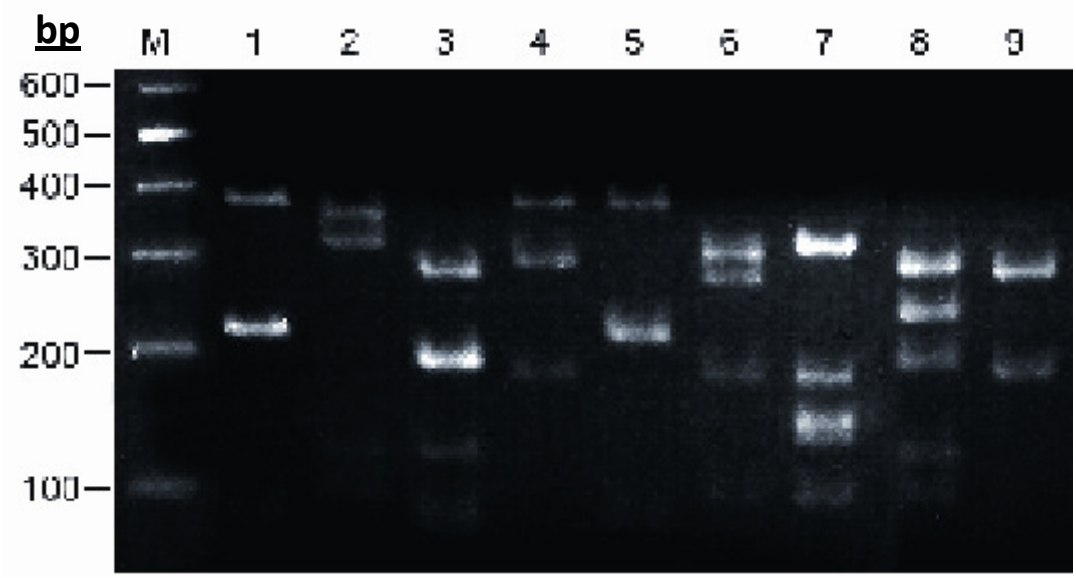

FIGURE 4.9 **Unique fingerprint profiles of full-length scFv gene fragments**. Monoclonal scFv antibody clones obtained after elution from the biopanning reactions with tachyzoites were fingerprinted, showing diversity in captured scFv clones (*lane 1-9*). Fingerprint profiles were generated by digestion with the restriction enzyme – *Mva* I.

4.2.4 - ScFv antibodies with specific binding advantage to *T. gondii* tachyzoites isolated through the rapid selective screening procedure.

To assess whether the functional scFv antibody clones that were recovered through our optimized cell-based biopanning procedure possesses true binding advantage to the intended target – *T. gondii* tachyzoites, monoclonal scFvs binding titers were determined against both the target cell and the negative absorber cell WRL68 in independent experiments (Figure 4.10). As shown in figure 4.10, among the four scFv clones that were assessed in its binding capacity, clone TG116 showed the highest mean binding titer to *T. gondii* at 5.62 x 10^5 cfu/ml, while TG130 showed the lowest mean binding titer to *T. gondii* at 2.05 x 10^5 cfu/ml. The one-tailed Wilcoxon-Mann-Whitney statistical analysis test was applied to test the hypothesis that the recombinant scFv clones has a higher binding capacity to *T. gondii* tachyzoite cells compared to negative control WRL68 normal hepatocyte cell line for each clone, with an alpha value of 0.05 with n = 12. As the data set did not fit a normality curve, the non-parametric Wilcoxon-Mann-Whitney test was chosen for the statistical analysis (Wilcoxon, 1945). This two group comparison was carried out to investigate the specificity of the scFv antibodies for *T. gondii*, based on whether there is a statistically significant preference for the parasite cells compared to normal cells. It was found that there was no statistically significant difference in the binding capacity of the 3 scFv antibodies isolated – scFvs TG64, TG69 and TG116 in its interaction between *T. gondii* tachyzoite cells and WRL68 (exact P value = 0.44; 0.11; and 0.50 respectively), despite moderately high binding titers of up to 5.62 x 10^5 cfu/ml (scFv TG116) (Figure 4.10). In other words, these antibodies were not significantly able to distinguish for specific binding to the target parasite antigen.

However, further analysis elucidated a statistically significant difference in the binding capacity of scFv TG130 to *T. gondii* compared to WRL68 at the $p = 0.05$ level (exact P value = 0.0303, n = 12) and a 97% exact confidence interval of 5.0×10^3 cfu/ml (Appendix X and XI). Despite demonstrating the lowest binding titer to *T. gondii* (1.74×10^5 cfu/ml) compared to our other 3 candidate antibodies, the scFv TG130 displayed at least a 5-fold higher binding titer relative to absorber WRL68 (Figure 4.10). It's also shown through this study in figure 4.10 that the scFv binding advantage to tachyzoites was not a result of phage background binding as the untransformed VCSM13 controls showed either negligible binding titers with *T. gondii* (mean = 1.0×10^3 cfu/ml), or no detectable binding at all with WRL68. Viewing these preliminary findings from the premise that antibody binding specificity should take precedence over mere binding titer values as indication of a bona fide ligand targeted against *T. gondii*, the TG130 clone is selected as superior in its selectivity in binding to *T. gondii* in comparison to the other isolated scFv clones; and thus this antibody fragment was chosen for further characterization.

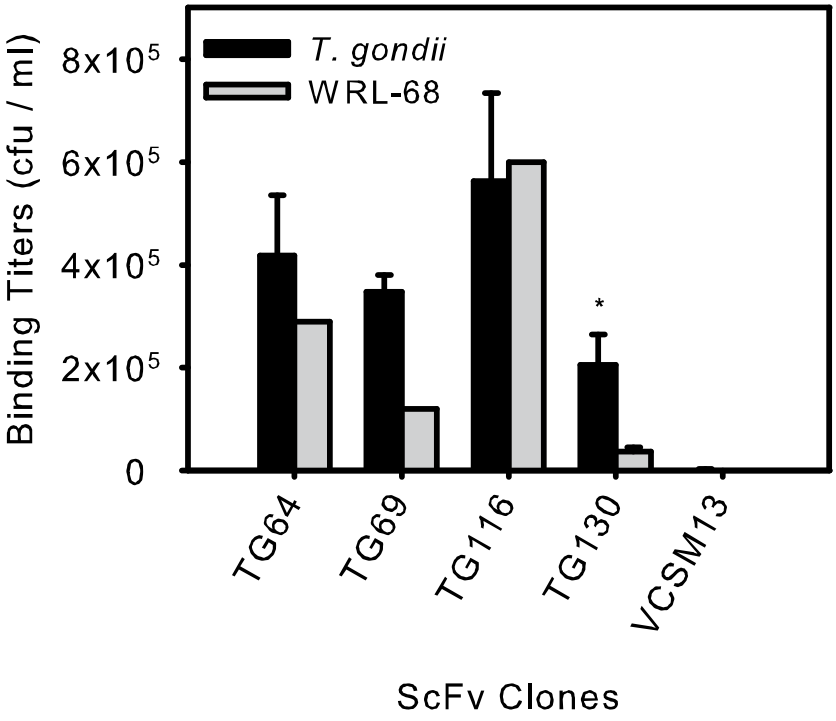

FIGURE 4.10 **Monoclonal functional scFv binding titers to *T. gondii* tachyzoites and WRL68 human cell line.** Candidate scFv antibody clones recovered from the biopanning procedure were tested to compare its binding capacity between *T. gondii* and WRL68. An asterisk (*) denotes a statistically significant difference in scFv binding advantage to *T. gondii*. The titers of phage captured from co-incubation with the cells shown are average values of duplicate or triplicate experiments, and untransformed VCSM13 binding titers are shown as equivalent negative controls to rule out background binding. Determination of negative control VCSM13 binding titers were done with Kanamycin-resistance selection instead of Ampicillin as the untransformed phage does not contain the pCANTAB5E phagemid which carries the Amp resistance gene. *Error bars*, ± S.E.M. from the means of duplicate or triplicate experiments.

4.2.5 - Sequence analysis of putative anti-*T. gondii* scFv antibodies

The sequence assessment of the short-listed 4 translational full-length scFv clones – TG64, TG69, TG116 and TG130, was done through the V-Quest at IMGT program (imgt.cines.fr/textes/vquest) (Lefranc, 2001). The V-Quest analysis carried out includes the identification of IgG antibody framework and CDR regions, and a homology search for germline sequences of origin (Table 4.3). The closest homology germline gene sequences of the V and J regions for each of the scFv clones were manually assembled and translated into amino acid sequences for both the V_H and V_L chain fragments; which was subsequently aligned with the nucleotide and amino acids sequence of its respective scFv V_H and V_L chains. As the focus for the antibody characterization was on TG130 due to its binding selectivity to *T. gondii*, the alignment for scFv TG130 is shown in figure 4.11 while the alignments for scFvs TG64, TG69 and TG116 are provided in the Appendix VIII. The aligned scFv sequences were compared for sequences which differs from its' germline counterpart; and amino acid sequence changes within the hypervariable CDRs were identified (Figure 4.11). The findings of our investigation on the sequence divergences of the scFv genes from its germline counterparts are summarized in Table 4.4. This is pertinent to our antibody characterization because deviations of the scFv DNA and amino acid sequences imply the occurence of somatic hypermutational events of B cells through antigenic exposure (reviewed in Li, Woo, Iglesias-Ussel, Ronai, & Scharff, 2004; and MacLennan, 1994).

The CDR regions are hypervariable sites that are juxtaposed to form the antigen-binding site of an antibody, with the V_H chain CDR3 usually presenting the greatest length and sequence variability, especially following an *in vivo* immune response (Burton, 2001). As can be seen in Figure 4.11, the comparison of the candidate scFv

sequences shows that scFv TG130 has the highest number of amino acid point mutations in the CDR regions accumulated, which is 6 residues within the V_H and V_L chains combined (Table 4.4). These somatic mutations are mostly localized to the CDR3 regions for both the V_H and V_L chains, which is the antibody region that is known to contribute the most significant contacts in antigen interactions. Comparatively, the non-specific scFv clones (scFvs TG64, TG69 and TG116) were found to have an overall lesser deviation from germline sequences and therefore exhibit less somatic mutations in *in vivo* affinity maturations resulting from an immune response. ScFv TG69 and TG116 had only 2 residue mutations within the V_H CDR3 and V_L CDR1 regions respectively, while scFv TG64 had no mutation at all found within its CDR regions. It was therefore hypothesized that scFv TG130 could be the most affinity-matured antibody fragment for specific binding to *T. gondii* amongst the clones which merited further examination and study.

Through a V-region sequence analysis using the V-Quest program (Appendix IX), it was found that the light chain variable region of scFv TG130 originates from the Vκ6 class, and has the highest sequence homology with the germline light chain gene IGKV6-17*01 (GenBank™ accession number Y15978) at 96% identity at the nucleotide level. It was also found that the V_L chain region of TG130 was possibly formed through the recombination of the Vκ6 gene IGKV6-17*01 with the Jκ5 gene IGKJ5*01 (GenBank™ accession number V00777) which has the highest homology with TG130 sequence at a 94.6% identity at the nucleotide level. Overall, the V_L region showed multiple somatic mutations and had a 91% amino acid identity with its' closest germline sequences.

A similar V-Quest sequence assessment was done for the heavy chain variable sequence of TG130 to identify the germline origin of the fragment (Appendix IX). The analysis showed that the heavy chain variable sequence is of the V_H germline gene IGHV1S29*02 (GenBank™ accession number J00488) origin which displayed the highest sequence homology at 97.6% identity at the nucleotide level. The C-terminal region of the scFv TG130 fragment possibly arose through the somatic recombination of the V_H germline gene IGHV1S29*02 with the closest homology germline J gene IGHJ3*01 (GenBank™ accession number V00770) (93.8% identity at the nucleotide level). The overall homology of the V_H region to its' closest germline sequences stands at 94.8% at the amino acid level.

Non-synonymous somatic mutations in the genes of the V regions as compared to its' germline counterparts leads to 15 amino acid changes (Figure 4.11). In the V_L chain: Phe → Leu-L70 (FR-L3), Ser → Asn-L74 (FR-L3), Ala → Ser-L77 (FR-L3), Val → Glu-L82 (FR-L3), Tyr → Phe-L84 (FR-L3), His → Tyr-L88 (CDR-L3), Tyr → Asn-L89 (CDR-L3), Thr → Tyr-L91 (CDR-L3), and Pro → Tyr-L93 (CDR-L3). For the V_H chain, the mutations are: Gln → His-H3 (FR-H1), Gln → Val-H5 (FR-H1), Gln → Glu-H6 (FR-H1), Ser → Arg-H84 (FR-H3), Ala → Asp-H100 (CDR-H3), Trp → Gly-H101 (CDR-H3). Out of these 15 amino acid changes, 6 of these mutations are found within the CDR and are all concentrated to the CDR-H3 and CDR-L3.

The sequence analysis of scFv TG130 via V-Quest also generated an IMGT Colliers de Perles diagram of the antibody's V domains (Figure 4.12). The Colliers de Perles diagrams (Ruiz & Lefranc, 2002) are standardized two-dimensional graphical representations of antibody V domains annotated according to IMGT unique numbering rules (Lefranc et al., 2003), which allowed for the visualization of the framework and

CDR residues. Due to the parity of resolved antibody three-dimensional structures available, Collier de Perles diagrams are particularly useful in antibody engineering studies to help identify the connection between linear amino acid sequences and its' structural features within an antibody such as turns, loops, and strands; as well as positions likely to be involved in antigen contacts.

TABLE 4.3. **Anti-Toxo ScFv IGHV and IGKV subgroup usage and H / κL-CDR3 motifs**

Candidate scFv clones binding to *T. gondii* were analysed to determine its CDRs and origin of murine germline V-regions using the online V-Quest software provided by the International ImMunoGeneTics data base (IMGT, imgt.cines.fr/textes/vquest/).

Clone ID	IGHV	H chain CDR3	H chain CDR3 length (bp)	IMGT - H [CDR1.CDR2.CDR3] length	GenBank accession no.	IGKV	L chain CDR3	L chain CDR3 length (bp)	IMGT - L [CDR1.CDR2.CDR3] length	GenBank accession no.
TG64	1-4*01	CAREAWFAYW	8	[8.8.8]	AC073561	4-70*01	CHQRSSYPYTF	9	[5.3.9]	AJ235943
TG69	14-3*02	CARLPYW	5	[8.8.5]	AJ851868	6-23*01	CQQYSSYHTF	8	[6.3.8]	AJ235961
TG116	14-3*02	CASSHGYEDYFDYW	12	[8.8.12]	AJ851868	6-13*01	CQQYSSYPYTF	9	[6.3.9]	J00569
TG130	1S29*02	CARGDGFAYW	8	[8.8.8]	J0048	6-17*01	CQQYNSYPYTF	9	[6.3.9]	Y15978

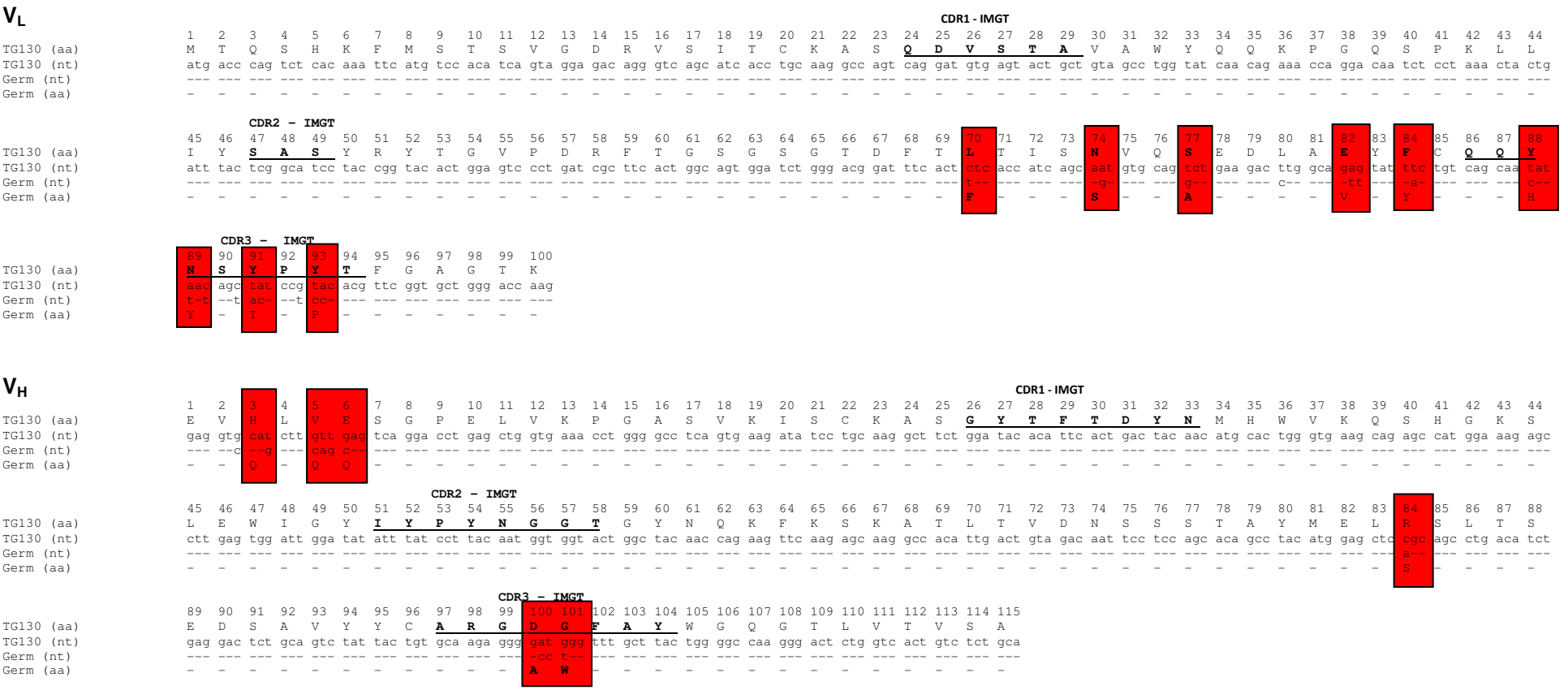

FIGURE 4.11 **Alignment of the V_H and V_L regions sequences of TG130 with its germline counterparts.** The CDR domains are defined according to the IMGT numbering scheme (Lefranc et al., 2003). For germline genes, V gene IGKV6-17*01 and J gene IGKJ5*01 fragments were manually assembled for V_L region; while V gene IGHV1S29*02 and J gene IGHJ3*01 fragments were manually assembled for V_H region. An exact residue match is indicated by a dash; and a sequence gap is indicated by a dot. Somatic mutational divergences from germline sequences identified in the scFv are shown in red-highlighted boxes.

TABLE 4.4. **Anti-Toxo ScFv IGHV and IGKV percentage identity and somatic mutations at the nucleotide and amino acid level**

DNA (nt) and amino acid (a.a) sequences of recombinant scFv-phages isolated after biopanning with *T. gondii* tachyzoites were aligned and comparatively analysed against its' closest homology V-region germline counterparts. V-regions' and J-regions' identity levels were determined through the V-Quest program analysis; while CDR mutational events were manually identified and calculated.

Clone ID	IGHV						IGKV					
	V-region identity (%)	V-region identity (nt/nt)	J-region identity (%)	J-region identity (nt/nt)	CDR a.a. mutations[a] (%)	CDR a.a. mutations[b] (nt)	V-region identity (%)	V-region identity (nt/nt)	J-region identity (%)	J-region identity (nt/nt)	CDR a.a. mutations[a] (%)	CDR a.a. mutations[b] (nt)
TG64	96.5	278 / 288	100.0	48 / 48	0.0	0	97.8	261 / 267	97.3	36 / 37	0.0	0
TG69	99.0	285 / 288	90.7	39 / 43	9.5	2[c]	99.6	269 / 270	100.0	35 / 35	0.0	0
TG116	100.0	288 / 288	100.0	48 / 48	0.0	0	98.2	265 / 270	97.3	36 / 37	11.1	2[d]
TG130	97.6	281 / 288	93.8	45 / 48	8.3	2[c]	95.9	259 / 270	94.6	35 / 37	22.2	4[c]

[a] Percentage of total number of CDR1 – CDR3 a.a residues that differs from its germline a.a sequence of origin, presumably produced during the somatic hypermutation of B cells on exposure to antigens.
[b] Total number of a.a residues mutated from the germline sequence of origin in CDR1 – CDR3.
[c] Amino acid residue mutations present in CDR3.
[d] Amino acid residue mutations present in CDR1.

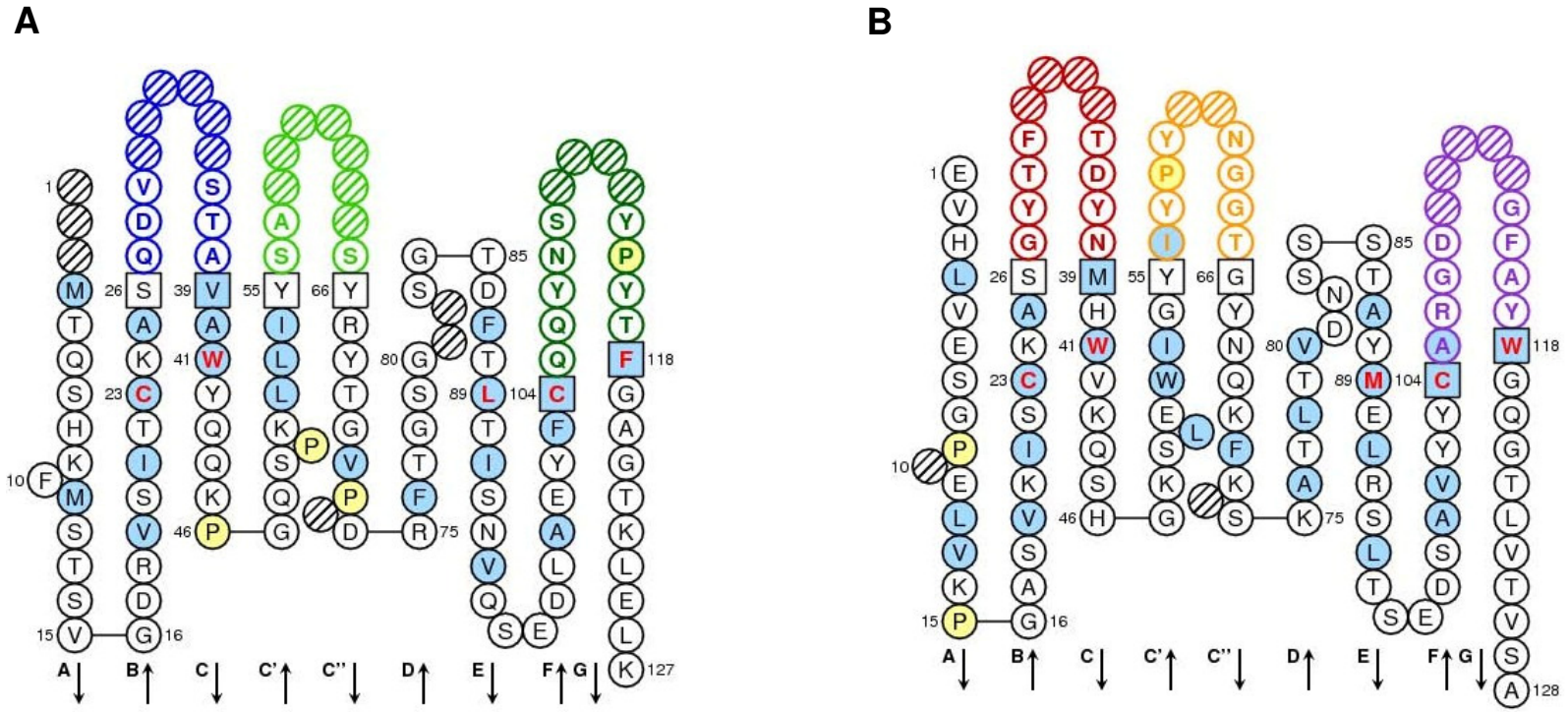

FIGURE 4.12 **IMGT Collier de Perles of scFv antibody TG130 V domains.** These standardized graphical representations of the antibody V domains here show the 2-D structure of TG130 V_L chain (A) and V_H chain (B) with one-letter amino acid codes. The standardized delimitation of the strands of the framework regions (FR) and loops of the CDRs (CDR) are based on IMGT nomenclature. CDR loops are highlighted in colours, positions where hydrophobic amino acids are found at more than 50% of analyzed sequences are coloured in blue, all proline residues are in yellow and hatched circles represents missing positions. The antibody CDR loops are delineated by 'squared' sequences which are anchor residues. Arrows show the direction of the beta strands. The CDR-IMGT loop lengths are [6.3.9] for V_L (A) and [8.8.8] for V_H (B), corresponding to [CDR1. CDR2. CDR3].

4.2.6 – Molecular modelling of a putative anti-*T. gondii* scFv antibody.

In this study, the Rosetta Antibody Structure Prediction Server program was used to generate the 3-dimensional antibody molecular model for this work. The PDB files of both scFv TG130 fragment and the assembled V_H and V_L germline counterpart sequences generated through this program was viewed using the SwissPdb Viewer (DeepView). The structural divergence of TG130 scFv from its germline counterparts was subsequently investigated by performing a molecular superimposition of the 2 structures via the DeepView program. The structural alignment output of the superimposed ribbon diagrams of the germline and scFv TG130 V-regions is shown in Figure 4.13a, which displays a slight displacement at the V_L chain CDR L3 region, but a significant displacement at the V_H chain CDR H3 region from its' germline molecular structure – implying of a somatic hypermutational event and that the CDR H3 loop may be directly involved in antigen binding interactions. The structural alignment of the antibody models revealed the highest displacement point for the V_L chain is at the L3 Thr^{94} germline residue which had been mutated to Tyr^{94} in scFv TG130, showing a root mean square deviation (rmsd) value of 2.523 Å. Whereas in the V_H chain CDR H3 region, the highest displacement point was found to be at the Ala^{96} germline residue which was mutated to Asp^{96} in the scFv TG130 fragment, with the average distance between the atoms computed to be rmsd value of 4.729 Å.

A space-filled model of the antibody scFv TG130 (Figure 4.13b) was generated by molecular modelling using the web-based antibody modelling software WAM (antibody.bath.ac.uk/index.html) which uses a modified form of the algorithm used in the AbM antibody modelling software of Oxford Molecular (Accelrys, San Diego, CA). The atom coordinates was viewed and analyzed using the VMD program (www.ks.uiuc.edu/). The accessibility screen and the CONGEN iterative algorithm was

chosen (Bruccoleri & Karplus, 1987) for the antibody modelling side-chain building. The amino acid residues of CDR H3 and CDR L3 that are most significantly displaced from its germline counterparts based on its structural rmsd value are highlighted as red and blue molecules for V_H Asp^{96} and V_L Tyr^{94} respectively in this model (Figure 4.13b). A view of the antigen-binding surface of the TG130 antibody demonstrates that these residues are strategically positioned to be exposed on the surface and extends from the antibody's groove pocket, suggesting that they may form the antibody-antigen interface.

Taken together, the antibody's V-region sequence and structural divergence from its germline counterparts is characteristic of an *in vivo* affinity maturation from antigenic exposure. This may correlate with its' binding specificity, although not necessarily with its' binding affinity to the target antigen.

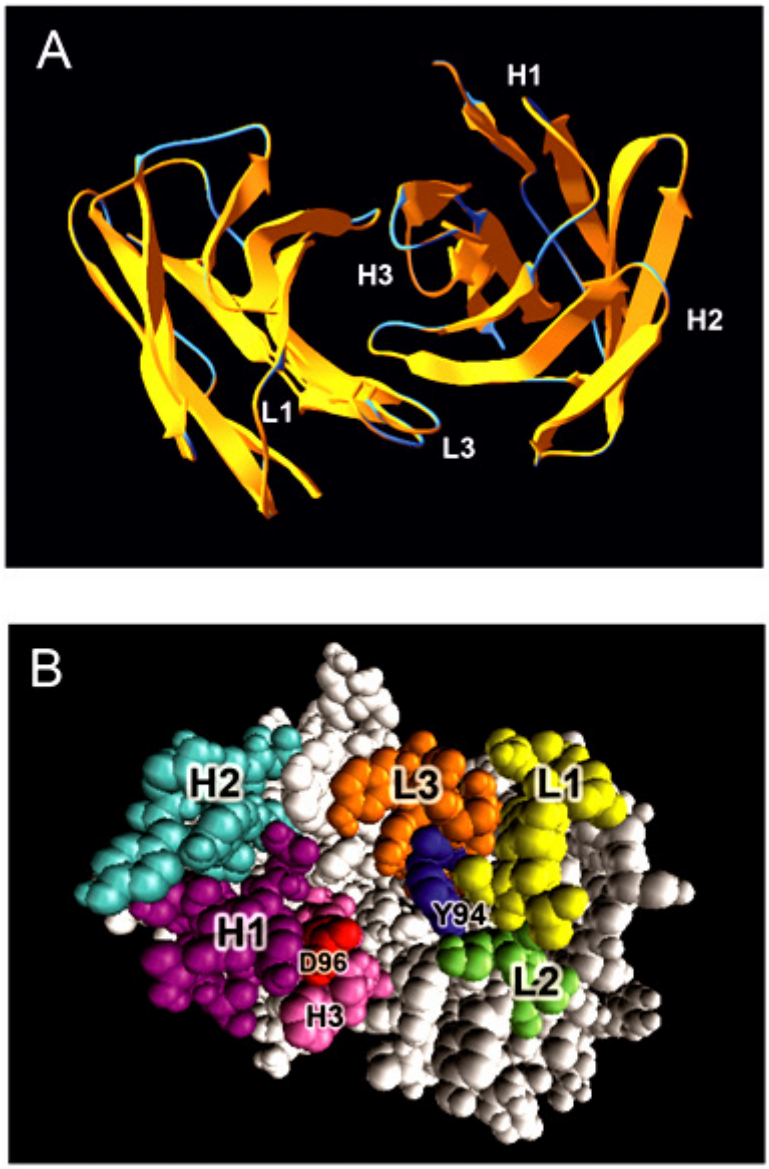

FIGURE 4.13 **Structural divergences of CDR loop regions of scFv specific for *T. gondii*.** A, ribbon diagram of scFv TG130 variable regions (*orange*) is superimposed with that of its germline counterpart (*cyan*). H1, -2, and -3, heavy chain CDR1, -2, and -3; L1, and -3, light chain CDR1, and -3. L2, or light chain CDR2 is located on the upper right loop directly above the L1 loop. Heavy chain CDR3 for TG130 shows significant displacement from that of its closest germline counterpart, suggesting that heavy chain CDR3 is directly involved in antigen binding. B, a space-filled model of scFv TG130. The view is looking down on the antigen-binding surface pocket groove. CDR1, -2, and -3 for light chain of TG130 are coloured (*yellow, lime,* and *orange* respectively). CDR1, -2, and -3 for the molecule's heavy chain are coloured (*purple, cyan,* and *pink* respectively). The amino acid residues of CDR H3 and CDR L3 that are most significantly displaced from its germline counterpart (up to rms: 4.7) and most likely to be involved in antigen binding – V_H Asp 96 (D96), and V_L Tyr 94 (Y94) are labelled and shown as *red* and *blue* molecules respectively. Residues are numbered according to the IMGT unique numbering scheme (Lefranc et al., 2003).

4.2.7 – Detection of *T. gondii* – binding scFv antibody by immunoflouorescence.

To further test whether scFv antibody TG130 specifically recognized *T. gondii* tachyzoites, confocal microscopy was used to localize the antibody's antigen recognition. Negative control immunofluorescence staining using untransformed VCSM13 filamentous phages did not show specific staining on the cells (Figure 4.14), while the entire surface of extracellular tachyzoite cells were stained when tested with scFv TG130 (Figure 4.15). From these experiments, we can conclude that the scFv TG130 binding antibody fluorescence was not a result of background false positives, but that the phage-displayed antibody is specifically reactive to *T. gondii* tachyzoites.

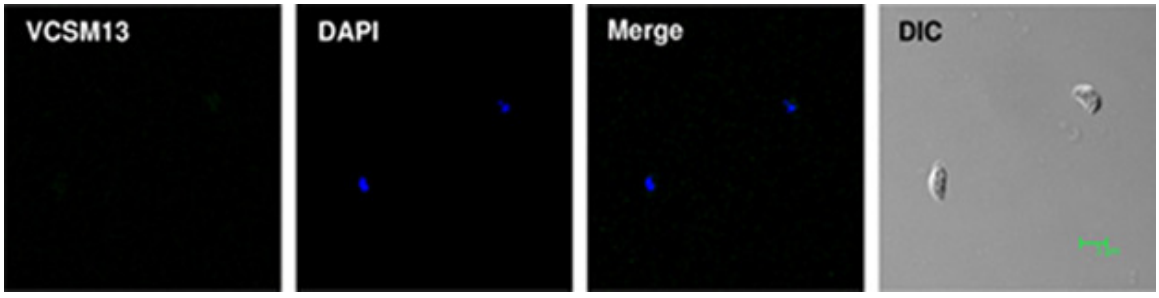

FIGURE 4.14 **Negative control untransformed phage immunofluorescence probing with *T. gondii* tachyzoites.** Confocal laser-scanning microscopy of negative control VCSM13 filamentous phage reacted against tachyzoite cells showed weak background staining and negligible signals. Images are a representative of duplicate experiments with similar results. DAPI, 4',6-diamidino-2-phenylindole; DIC, differential interference contrast. Scale bar represents 3 μm.

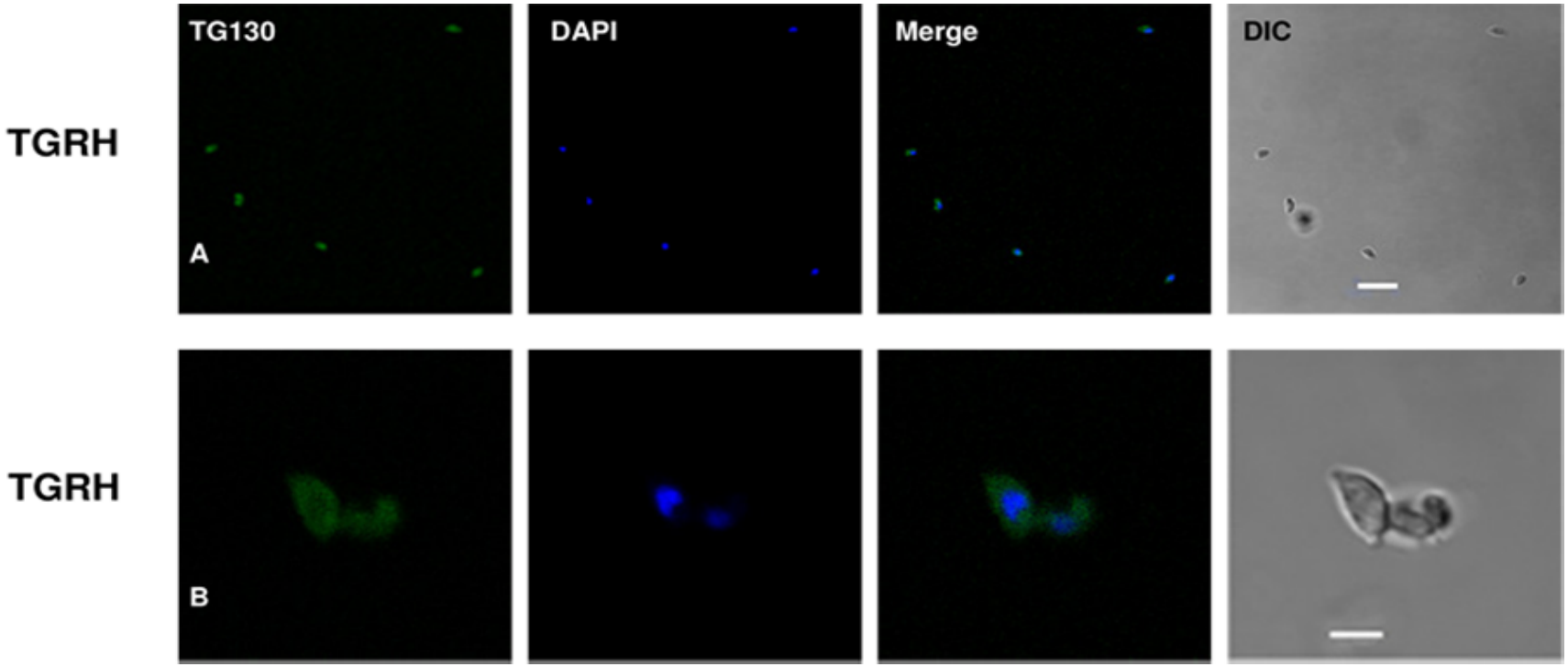

FIGURE 4.15 **Confocal laser-scanning microscopy of extracellular *T. gondii* tachyzoites surface recognition by scFv antibody TG130.** These cells were incubated with phage-displayed TG130 scFv and then with Alexa Fluor 488-labelled monoclonal antibody to bacteriophage coat protein g8p (green). Nuclei were counterstained with DAPI (blue). A magnified view of tachyzoites showing surface staining with the scFv antibody is shown in panel B. DAPI, 4',6-diamidino-2-phenylindole; DIC, differential interference contrast. Scale bars represent 10 µm and 3 µm respectively in panels A and B.

4.3 Discussion

4.3.1- Isolation of anti-*T. gondii* scFv antibodies with specific target binding advantage through an optimized selective screening procedure.

In the current study, a scFv antibody fragment to *T. gondii* tachyzoites was generated from a polyclonal filamentous phage display scFv library derived from immunized mouse B cells. We employed a procedure using an intact cell surface for the biopanning screen to select for phage particles bearing scFv antibodies with the ability to bind to native antigen on the tachyzoite cell surface. However, biopanning on intact cell surfaces poses a challenge of capturing false positive ligands due to the innate complexity of cell surfaces with multimeric and non-specific antigens (D. L. Siegel, 2001).

To address this challenge, a subtractive biopanning round was incorporated into an optimized biopanning procedure to quench for false positive binders by using WRL68 hepatocytes cell line. The WRL68 cell line was used as absorber cells in the subtractive biopanning steps, which is also referred to as negative selection. Several subtractive biopanning procedures documented thus far (Eisenhardt et al., 2007; Hof, Cheung, Roossien, Pruijn, & Raats, 2006) involves several cycles of positive and negative selection rounds, without empirical analysis of the number of negative selection rounds that is required for adequate quenching. In the present study, the quenching ratio of the negative selection rounds was first monitored in a mock biopanning test prior to running the procedure against the target cells. It was found that the quenching ratio drops and plateaus after 3 negative selection rounds against the absorber cells WRL68 (Appendix V). Therefore, 3 subtractive biopanning rounds

followed by a single antigen biopanning round were carried out to recover for *T. gondii* – binding scFv antibodies.

Analysis of the scFv antibodies captured through the biopanning procedure by PCR showed the recovery of 9 functional full-length scFv clones. These 9 scFv clones were selected and fingerprinted with the restriction enzyme *Mva*I, with results demonstrating diversity in the scFv gene sequences captured. In various procedures for the standard analysis of antibodies, fingerprinting with either of the restriction enzymes *Mva*I, *Bst*N1 or *Bst*OI is a useful approach commonly employed to analyze antibody fragment clones for diversity relatively quickly and inexpensively (Barbas, Burton, Scott, & Silverman, 2001). The restriction enzymes *Mva*I, *Bst*N1 and *Bst*OI are isoschizomers of each other and can be used interchangeably for this purpose. However, upon further analysis, stop codon mutations was discovered in 5 out of the 9 clones, which led to a truncated scFv display on the phage g3p protein (Appendix VII). Due to the complexity of cell membrane surfaces, biopanning procedures had the propensity to enrich for truncated, non full-length scFv antibodies due to the 'trapping' of smaller ligands on cell surfaces and the enhanced growth rates of bacteria harbouring aberrant phage particles with smaller protein expression (Kramer et al., 2003). To avoid enriching for these aberrant phages displaying truncated scFvs and the loss of clonal diversity, antigen biopanning was limited to a single round. A single biopanning round is also favourable to obtain scFv antibodies with maximal diversity, as another study has also shown that performing additional rounds of panning does not increase the chances of recovering binders already detected in the first round (Pansri, Jaruseranee, Rangnoi, Kristensen, & Yamabhai, 2009). Through the optimized biopanning selection procedure carried out in this study, 4 functional full-length scFv clones were recovered and each antibody fragment showed diversity in its unique fingerprint profile.

The recovery of 4 functional full-length scFv antibodies against the parasite target in this study is comparable to several other phage display experiments with the final isolation of 1 – 4 candidate antibody clones specific against a target of interest (Kabir, Krishnaswamy, Miyamoto, Furuichi, & Komiyama, 2009; Kupsch et al., 1999; Muraoka et al., 2009; Pansri et al., 2009). This is because the basic aim of a phage display study is to leverage the high-throughput screening of an antibody or peptide library to narrow down the leads to a few specific target binders. However, the specificity of scFv antibodies against a target can also be further improved with the construction of a large phage displayed-antibody library in the range of 10^9 – 10^{11} cfu (Vaughan et al., 1996). In another effort to circumvent the well known problem of truncated scFv-pIII fusion in phage display libraries due to stop codons and frameshift mutations introduced during library construction, Kramer and co-workers have developed a mutant helper phage system that partially ameliorates this by enriching for functional scFvs by 3-fold (Kramer et al., 2003). However, at present time this mutant helper phage is not available commercially and is therefore beyond the reach of most laboratories.

Considering the high artefact background obtained despite the optimized biopanning procedure and stringent washing rounds, the scFvs that were eluted from the *T. gondii* tachyzoites may either have demonstrated false positive binding due to aggregation or miscellaneous influence by the background aberrant Fv fragment displays, or the eluted scFvs may in fact be true antigenic binders to *T. gondii* tachyzoites. In order to distinguish between these two possibilities, each isolated monoclonal antibody was compared in their mean binding titers to Toxoplasma and WRL68. Determination of the binding titers against *T. gondii* for the shortlisted scFv

clones – scFv TG64, TG69, TG116 and TG130, showed that among the 4 scFv antibodies, only one scFv antibody - TG130 displayed statistically significant binding specificity to *T. gondii* tachyzoites with up to 5-fold binding advantage over negative absorber cells. Therefore, results of this study showed that the optimized selective screening procedure with empirically determined-subtractive biopanning rounds was effective in the development of a specific scFv antibody capable of distinguishing between negative absorber cells and its' antigenic target – *T. gondii*.

4.3.2- ScFv antibody TG130 displays sequence diversity and structural divergence from homologous germline antibody structures.

The closest murine antibody germline to the V_H gene of scFv TG130 is IgHV1S29*02 of the VH1 family and JH3 for the V and J segments respectively (Table 4.3). A survey of literatures revealed several mouse antibody genes inducing protective immunity in parasitic infections that belonged mainly to either the VH1 or VH5 family. An inhibitory monoclonal antibody against *T. gondii* heat shock protein-70 (TgHSP70) also consisted of a heavy chain fragment of the VH1 family, but the closest J segment was from JH1 (M. Chen, Aosai, Norose, Mun, & Yano, 2003). In another study, protective antibody repertoire to parasitic enteric helminth infections displayed a preference for both the VH1 and VH5 gene families (McCoy et al., 2008). Similarly, protective murine antibody specific against the Apical Membrane Antigen 1 of *Plasmodium vivax* (PvAMA1), which is involved in erythrocyte invasion; had a heavy chain fragment of the VH5 family, but had JH3 as its' closest germline sequence for the J segment (Igonet et al., 2007) – similar to the scFv in this study, scFv TG130.

The closest V germline to the V_L chain is IgKV6-17*01 of the Vκ6 family and Jκ5 for the J segment of the antibody's light chain (Table 4.3). Unlike the predominance of VH1 and VH5 gene family preference in the heavy chain repertoire of antibodies involved in parasitic infections immune responses, there is a parity of studies done on mouse antibody light chain preference for parasitic diseases. In two examples, it was found that a monoclonal anti-PvAMA1 antibody displayed Vκ4 and Jκ4 in its V and J segments respectively, and another antibody against the Merozoite Surface Protein 1 of *Plasmodium falciparum* (PfMSP1) also displayed its closest germline light chain gene homology to the Vκ4 family (Igonet et al., 2007; Lazarou et al., 2009). Interestingly, another protective antibody against falciparum malaria, specific for the PfMSP1 antigen, showed the exact same V gene family usage to scFv TG130, in both the V_H and V_L chains (Lazarou et al., 2009). Both antibodies had a heavy chain fragment from the VH1 family, although anti-PfMSP1 carried a different VH1 classification, which was IgVH1S81*02; while scFv TG130 was of the IgVH1S29*02 classification. The light chain fragment of both anti-PfMSP1 and scFv TG130 antibodies are of the Vκ6 family and even shares an identical classification – IgKV6-17*01.

The V_H region shows numerous mutations with a homology to its' closest germline sequences at 94.8% at the amino acid level, typical of an affinity-matured antigen-driven immune response. This finding is in good agreement with several other studies on the characterization of antigen-binding scFv and IgG antibody phage-displays that showed comparable levels of somatic hypermutation levels with our candidate scFv against *T. gondii*. For instance, the V_H region homology percentage of antibody fragments characterized thus far ranges from 93% to 94% for several cancer-targeting antibodies (Hansen, Nielsen, & Ditzel, 2002; Ho et al., 2005), and from 92.8% to 99.0% for several other virus-targeting antibodies (David, Goossens, Desgranges, Thèze, &

Zouali, 1995; Ray, Embleton, Jailkhani, Bhan, & Kumar, 2001). A similar trend can also be observed for the V_L regions somatic mutations in these antibodies.

It is also interesting to note that although the CDR-L3 region of the antibody light chain had twice as many mutations (4 amino acid substitutions) compared to the CDR-H3 region (2 amino acid substitutions), molecular superimposition of the scFv structure to its closest germline homology structure revealed that the greatest structural deviation to be located at the heavy chain CDR-H3 loop, and not the CDR-L3 (Figure 4.16). Viewing the molecular structure of TG130 indicates that 6 out of the 15 somatic mutations relative to its germline counterpart [His → Tyr-L88 (CDR-L3), Tyr → Asn-L89 (CDR-L3), Thr → Tyr-L91 (CDR-L3), and Pro → Tyr-L93 (CDR-L3), Ala → Asp-H100 (CDR-H3), Trp → Gly-H101 (CDR-H3)], which are fixed within the CDR3 loops, forms the antigen binding site (Figure 4.16). Nine other mutated residues are located in vernier positions that are not directly contacting the antigen. Calculation of the mutation ratios within the antibody's CDRs and framework regions of the variable domains revealed a higher percentage of amino acid residue changes within the CDRs compared to the framework regions; with 14.3% mutations within the CDRs and 5.1% mutations within the framework regions. This is also in close agreement with observed trends in the process of somatic hypermutation of the humoral response, whereby average mutational probabilities for core and antigen-combining site residues are ~4% and ~12% respectively (Clark, Ganesan, Papp, & van Vlijmen, 2006).

As shown in Figure 4.16, the 6 amino acids mutations concentrated at the CDR3 loops forms a dramatically different antigen combining site compared to the antibody's germline structure (Figure 4.16-A and B). Somatic mutations of an antibody repertoire's variable regions provides increased ligand diversity and is also an established hallmark

of its' affinity maturation for a more effective immune response (French, Laskov, & Scharff, 1989; Tonegawa, 1983). As such, the structural changes found within scFv TG130 is taken to be indicative of an antigen-driven selective process in the maturation of the antibody from its germline precursors.

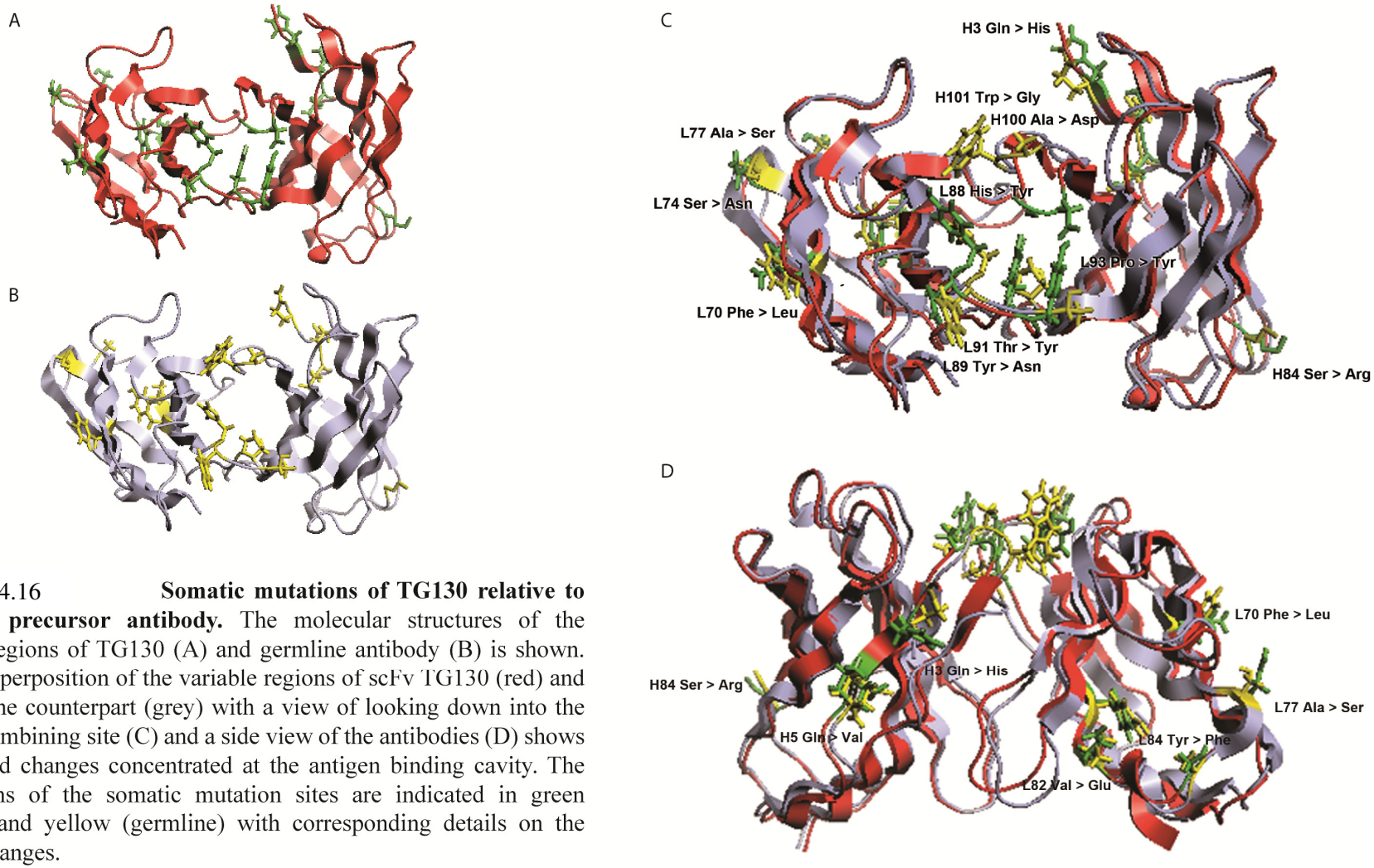

FIGURE 4.16 **Somatic mutations of TG130 relative to germline precursor antibody.** The molecular structures of the variable regions of TG130 (A) and germline antibody (B) is shown. Ribbon superposition of the variable regions of scFv TG130 (red) and its germline counterpart (grey) with a view of looking down into the antigen combining site (C) and a side view of the antibodies (D) shows amino acid changes concentrated at the antigen binding cavity. The side chains of the somatic mutation sites are indicated in green (TG130) and yellow (germline) with corresponding details on the residue changes.

4.3.3- ScFv antibody TG130 shows binding to *T. gondii* tachyzoites membrane surface.

The surface adhesins of *T. gondii* have been implicated to be connected to the adherence and invasion of host cells. Several experiments employing the use of antibodies targeted against proteins expressed on the parasite surface have shown evidence of inhibition of cellular invasion to varying degrees (Vern B. Carruthers et al., 1999; Fu et al., 2011; Hehl et al., 2000), although a subset of these antibodies had no effect on blocking invasion, indicating that there are functional epitopes within these parasite surface adhesins (Grimwood & Smith, 1996). Inhibitory antibodies against parasite surface proteins have ranged from constitutive to transiently-expressed proteins. The parasite surface is primarily coated with the immunogenic and closely-related antigens from the surface antigen 1 (SAG1)-related sequences (SRS) superfamily which consists of at least 160 members, with some members being developmentally expressed (Jung, Lee, & Grigg, 2004; Manger et al., 1998). In addition to the abundant SRS antigens on the surface of *T. gondii*, several other surface adhesins involved in the host cell attachment and penetration process includes the microneme-secreted proteins, which are also known as MICs; and includes the apical membrane antigen 1 (AMA1) protein which bears interesting homology to the AMA1 of *Plasmodium* spp. (Carruthers, 2002; Hehl et al., 2000).

In lieu of the present evidences of the favourable ability of antibodies targeted to the membrane surface of *T. gondii* in blocking host cell adherence and invasion, this study was formed to develop scFv antibodies based on its ability to bind to native antigens on intact extracellular tachyzoite surface with higher affinity. A limitation with the shaping of the humoral response *in vivo* is the inability to select for antigen-reactive

antibodies with affinities higher than the ceiling dissociation rate constant (k_{off}) of 12 minutes, which is the approximate time needed for B cell receptors (BCR) internalization of antigens (Batista & Neuberger, 1998; Foote & Eisen, 1995). Therefore, to mitigate the intrinsic affinity ceiling for antibodies selected *in vivo*, through this study, antibody biopanning selection on intact tachyzoite cell surface was carried out with 5 rounds of washing and a corresponding off-rate selection of at least 30 min, which is nearly double of the 12 minutes BCR internalization rate window period. Currently, it is unclear on which parasite surface ligands the scFv TG130 antibody is binding to on the parasite surface; however, confocal microscopy in the present study demonstrates that scFv TG130 recognizes an antigen distributed over the entire surface of extracellular tachyzoites (Figure 4.15). Studies to identify these parasitic ligands on *T. gondii* that reacts to the recombinant antibody is needed, and further experiments on refining the binding properties of TG130 could potentially see this developed as a diagnostic tool or a blocking antibody against parasite invasion.

4.4 General Conclusion

In conclusion, through the subtractive cell suspension-based biopanning strategy developed for *T. gondii* in this study, a scFv antibody with evidence of a 5-fold binding advantage to tachyzoites was successfully isolated and characterized. The present study shows results of the scFv TG130's specific recognition of *T. gondii* tachyzoites by binding titers testing and immunofluorescence assays. Further affinity maturation designs may improve the current levels of binding selectivity and affinity of the TG130 scFv against *T. gondii* tachyzoites. Development of the second generation antibody is being undertaken, and further investigations are needed to elucidate the affinity of the antibody once the antigenic target has been identified. From the early reports on the genome constitution of this organism (Ajioka et al., 1998a), knowledge of the genes controlling biological traits of this evolutionarily-divergent parasite is growing (Adomako-Ankomah, Wier, & Boyle, 2011). The present study was designed to facilitate the rapid discovery of new binding ligands to complement genetic and genomic information on potential antigenic targets that could be used to further understand this pathogen and its interaction with the host cells. Overall, the biopanning strategy outlined in this study has potentially useful applications in the biopanning of phage-displayed antibody fragment libraries and other formats of ligands such as random peptides, haptens and immunotoxins against the complex, mutimeric, and native landscape of *T. gondii* cell surface. The current findings on the scFv antibody TG130 recognizing *T. gondii* antigens could also form the base of further investigations on improving antibody affinity and selectivity to the target parasite cell.

CHAPTER 5. RESULTS & DISCUSSION (PART 2): DEVELOPMENT OF AN ANTI-*TOXOPLASMA GONDII* ScFv ANTIBODY WITH IMPROVED BINDING PROPERTIES

5.1 - Strategy

The aim of this study was to improve the binding properties of the scFv antibody TG130 against *T. gondii* tachyzoites by affinity maturation. This necessitated the identification of antibody CDR hotspot regions as targets for affinity maturation through analysis by the V-Quest (IMGT) (Lefranc, 2001) software. Hotspots, which are DNA sequences within the antibody's variable regions that are naturally prone to somatic hypermutations during the *in vivo* affinity maturation of the humoral immune response to pathogens; are most often located in the CDRs, particularly CDR1 (Neuberger et al., 1998). One of the hot-spots nucleotide sequence motifs that is often favoured for affinity maturation is the (A/G)G(C/T)(A/T) sequences or also known as the RGYW motifs. The frequency of somatic mutations introduced at or very near these RGYW motifs is a total of 50 – 60% (Neuberger et al., 1998). Therefore, it can be surmised that targeting the RGYW motifs for the *in vitro* affinity maturation of the antibody scFv TG130 could lead to improvements in its' antigenic binding properties (Chowdhury & Pastan, 1999).

Identification of hot-spots within the antibody V-regions was followed by an optimized rapid *in vitro* antibody affinity maturation procedure by site-directed point mutagenesis using degenerate primers. The point-mutated second generation TG130 scFv library was assessed to determine for successfully randomized point mutated amino acids; and subsequently screened again with more stringent conditions than

employed in the previous study with the parental antibody (TG130) to isolate improved binders. The putatively affinity-matured scFv isolated was characterized for its target binding titers and molecular structure divergence relative to the originating parental antibody; as well as scFv immunofluorescence localizations on tachyzoites. The strategy of this section of study is shown in Figure 5.1.

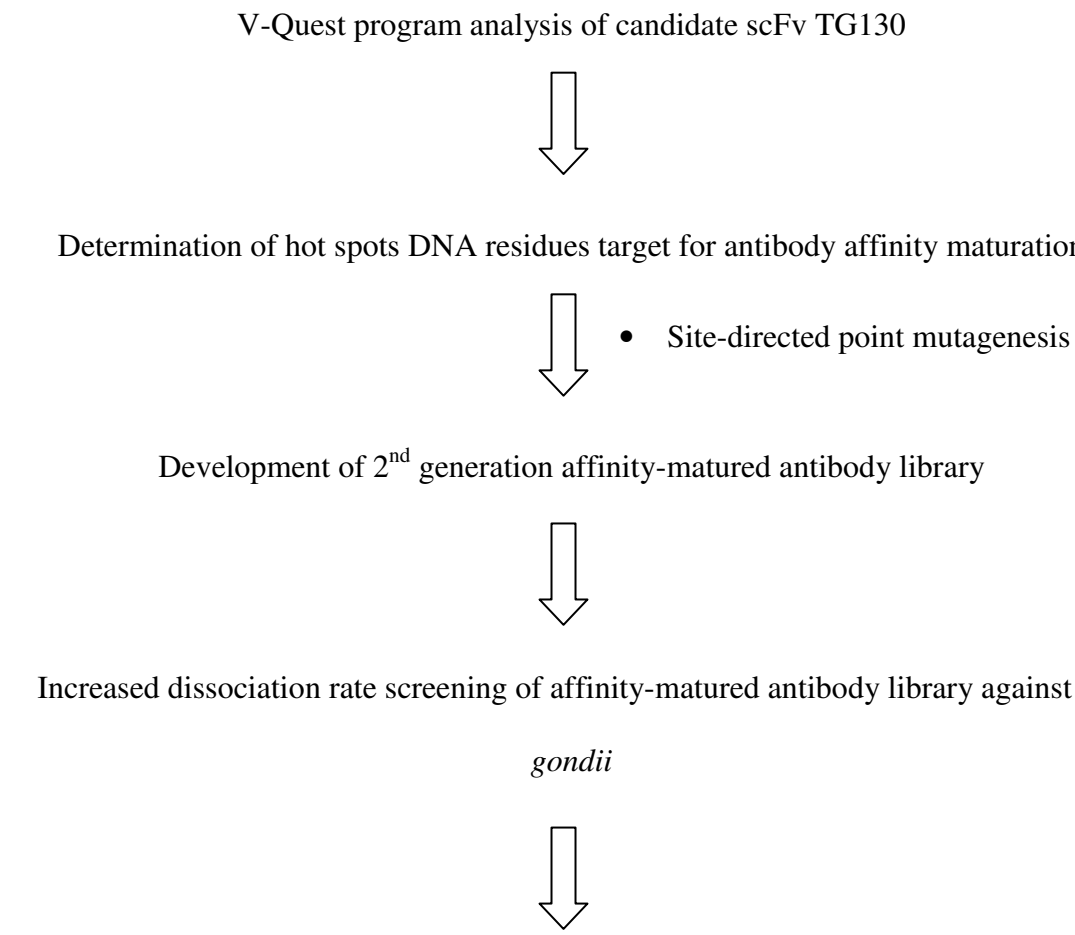

FIGURE 5.1 The workflow of procedures for the development of an anti-*T. gondii* scFv antibody with improved binding properties is summarized in this schematic diagram.

5.2 - Results

5.2.1- Identification and selection of antibody hotspot residues for site-directed affinity maturation.

In the strategy to develop an antibody with improved affinity against *T. gondii*, an *in vitro* site-directed hot-spot point-mutagenesis procedure was employed with the phage-display platform. For the selection of a RGYW motif hot-spot for the affinity maturation procedure, an analysis of scFv TG130 sequence through V-Quest at IMGT (imgt.cines.fr/texts/vquest/) (Lefranc, 2001) revealed a total of 5 hot-spots within the variable regions, which are all located within its' CDRs (Figure 5.2). The results are summarized in Table 5.1. These RGYW hot-spots within the antibody are located either at germline genes or close to non-germline residues – which are presumably mutated during the somatic hypermutation of B cells. For this study, the selection for a site-directed mutagenesis target was focused on germline hot-spots. Both of the hot-spots clusters within V_L CDR3 (Positions 314-317 and Positions 325-328) are considered to be non-germline residues hot-spots and are therefore not considered as mutagenesis candidates.

A check of the distance measurements of the three-dimensional molecular model of TG130 generated through PyMOL (Figure 5.3) shows that the V_L CDR1 and V_H CDR2 loops are located closer to the V_H CDR3 loop (16.15 Å and 13.95 Å respectively), compared to V_L CDR2 (16.85 Å); suggesting a higher likelihood that both of the closer loops may be involved in key antibody-antigen interactions. As there seems to be a correlation between a lower number of germline hot-spots with higher affinity and matured antibodies (Ho et al., 2005), the V_L chain was deemed to be less-

matured and therefore a preferred target for affinity maturation due to its higher number of hotspot clusters (Table 5.1). In the present study, the germline-type RGYW hotspot sequence motif within V_L CDR1 was chosen as the target residues for the antibody affinity maturation (Figure 5.3).

TABLE 5.1 **DNA sequence hot-spots with RGYW motifs within the variable regions of antibody scFv TG130.** The sequence cluster selected for affinity maturation of the antibody is highlighted in yellow. All residues are numbered according to the IMGT numbering scheme.

	Motif	Positions	Hot-spots Type
V_H	ggta	190-193 (CDR2)	Germline
V_L	agta	106-109 (CDR1)	Germline
	ggca	168-171 (CDR2)	Germline
	agca	314-317 (CDR3)	Non-germline
	agct	325-328 (CDR3)	Non-germline

ScFv TG130

V_L

```
          1   2   3   4   5   6   7   8   9   10  11  12  13  14  15  16  17  18  19  20
TG130 (aa)    M   T   Q   S   H   K   F   M   S   T   S   V   G   D   R   V   S   I   T   C
TG130 (nt)    atg acc cag tct cac aaa ttc atg tcc aca tca gta gga gac agg gtc agc atc acc tgc

                                        CDR1 - IMGT
          21  22  23  24  25  26  27  28  29  30  31  32  33  34  35  36  37  38  39  40
TG130 (aa)    K   A   S   Q   D   V   S   T   A   V   A   W   Y   Q   Q   K   P   G   Q   S
TG130 (nt)    aag gcc agt cag gat gtg agt act gct gta gcc tgg tat caa cag aaa cca gga caa tct

                                                    CDR2 - IMGT
          41  42  43  44  45  46  47  48  49  50  51  52  53  54  55  56  57  58  59  60
TG130 (aa)    P   K   L   L   I   Y   S   A   S   Y   R   Y   T   G   V   P   D   R   F   T
TG130 (nt)    cct aaa cta ctg att tac tcg gca tcc tac cgg tac act gga gtc cct gat cgc ttc act

          61  62  63  64  65  66  67  68  69  70  71  72  73  74  75  76  77  78  79  80
TG130 (aa)    G   S   G   S   G   T   D   F   T   L   T   I   S   N   V   Q   S   E   D   L
TG130 (nt)    ggc agt gga tct ggg acg gat ttc act ctc acc atc agc aat gtg cag tct gaa gac ttg

                                                                CDR3 - IMGT
          81  82  83  84  85  86  87  88  89  90  91  92  93  94  95  96  97  98  99  100
TG130 (aa)    A   E   Y   F   C   Q   Q   Y   N   S   Y   P   Y   T   F   G   A   G   T   K
TG130 (nt)    gca gag tat ttc tgt cag caa tat aac agc tat ccg tac acg ttc ggt gct ggg acc aag

          101 102 103 104
TG130 (aa)    L   E   L   K
TG130 (nt)    ctg gag ctg aaa
```

V_H

```
          1   2   3   4   5   6   7   8   9   10  11  12  13  14  15  16  17  18  19  20
TG130 (aa)    E   V   H   L   V   E   S   G   P   E   L   V   K   P   G   A   S   V   K   I
TG130 (nt)    gag gtg cat ctt gtt gag tca gga cct gag ctg gtg aaa cct ggg gcc tca gtg aag ata

                                    CDR1 - IMGT
          21  22  23  24  25  26  27  28  29  30  31  32  33  34  35  36  37  38  39  40
TG130 (aa)    S   C   K   A   S   G   Y   T   F   T   D   Y   N   M   H   W   V   K   Q   S
TG130 (nt)    tcc tgc aag gct tct gga tac aca ttc act gac tac aac atg cac tgg gtg aag cag agc

                                                        CDR2 - IMGT
          41  42  43  44  45  46  47  48  49  50  51  52  53  54  55  56  57  58  59  60
TG130 (aa)    H   G   K   S   L   E   W   I   G   Y   I   Y   P   Y   N   G   G   T   G   Y
TG130 (nt)    cat gga aag agc ctt gag tgg att gga tat att tat cct tac aat ggt ggt act ggc tac

          61  62  63  64  65  66  67  68  69  70  71  72  73  74  75  76  77  78  79  80
TG130 (aa)    N   Q   K   F   K   S   K   A   T   L   T   V   D   N   S   S   S   T   A   Y
TG130 (nt)    aac cag aag ttc aag agc aag gcc aca ttg act gta gac aat tcc tcc agc aca gcc tac

                                                                        CDR3 - IMGT
          81  82  83  84  85  86  87  88  89  90  91  92  93  94  95  96  97  98  99  100
TG130 (aa)    M   E   L   R   S   L   T   S   E   D   S   A   V   Y   Y   C   A   R   G   D
TG130 (nt)    atg gag ctc cgc agc ctg aca tct gag gac tct gca gtc tat tac tgt gca aga ggg gat

          101 102 103 104 105 106 107 108 109 110 111 112 113 114 115
TG130 (aa)    G   F   A   Y   W   G   Q   G   T   L   V   T   V   S   A
TG130 (nt)    ggg ttt gct tac tgg ggc caa ggg act ctg gtc act gtc tct gca
```

FIGURE 5.2 **Nucleotide and aligned amino acid sequences of V_H and V_L regions of scFv TG130.** Regions mutated from germline origin sequences are boxed in red, and RGYW-motif hotspots are highlighted in yellow. The targeted hotspot mutagenesis is circled in red.

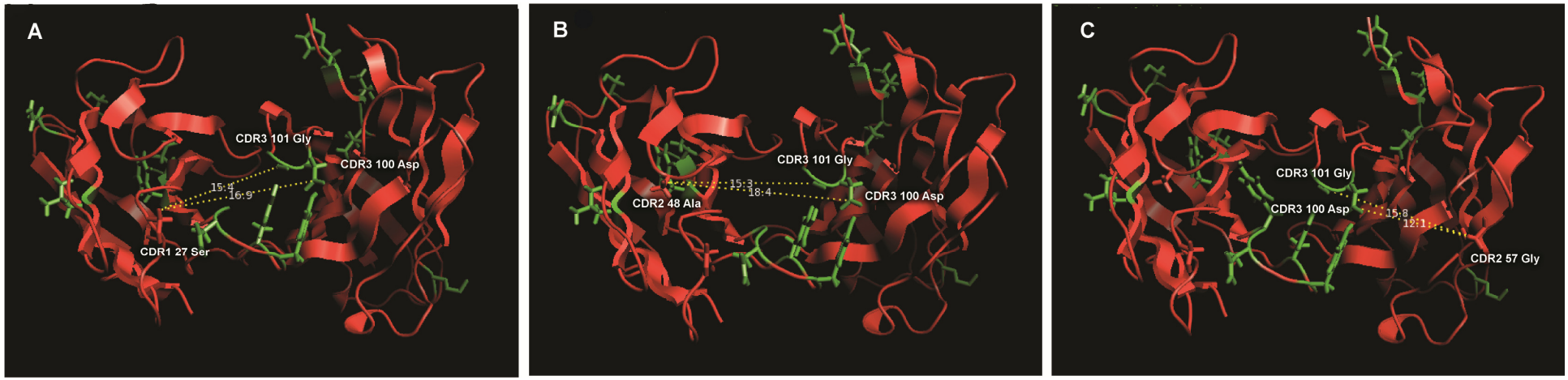

FIGURE 5.3 **Measurements of distance between candidate RGYW hot-spots residues and somatic mutations in V_H CDR3.** The somatic mutations within V_H CDR3 (CDR3 100 Asp and CDR3 101 Gly) are located at the apex of the CDR3 loop, suggesting of its involvement in key antigen-binding interactions. The average distances between the V_H CDR3 apex with V_L CDR1 hot-spot residue (CDR1 27 Ser) is 16.15 Å (A), with V_L CDR2 hot-spot residue (CDR2 48 Ala) is 16.85 Å (B), and with V_H CDR2 hot-spot residue (CDR2 57 Gly) is 13.95 Å (C).
The V_L CDR3 88 Tyr residue in images of panels (A) and (B) is hidden for clarity. All images and measurements were generated with PyMOL.

5.2.2- Generation of an affinity-matured scFv TG130 antibody library by site-directed mutagenesis.

Through an efficient site-directed mutagenesis protocol which was developed, an affinity-matured or second generation TG130 scFv library was able to be generated within a relatively short period of only 2 days. An additional 1 day was required to further sub-clone the randomized-point-mutated TG130 phagemids from *E. coli* XL10-Gold into *E. coli* TG1 to facilitate downstream experiments of phage rescue and biopannings. Several key modifications were introduced into a standard protocol optimized from the Stratagene's QuikChange® Lightning Site-Directed Mutagenesis Kit (Agilent Technologies) manufacturer's conditions to enable the generation of randomized point-mutants. The modifications (indicated by symbol Φ) include a pretreatment with Annealing Buffer and generation of degenerate adapters oligonucleotides (Figure 5.4).

From two point mutagenesis reactions targeted to the RGYW motif within TG130 and two proceeding transformations, a second generation scFv library consisting of a complexity of at least 4.0×10^4 independent clones was obtained. A check of twenty randomly picked clones from the second generation library through PCR showed 100% full-length scFv DNA in all clones (Figure 5.5). A further examination of five randomly picked clones through sequencing found no evidence of truncated clones detectable from this scFv library; which shows that the rational design of degenerate primers done in the present study to introduce randomized mutations at the RGYW motifs was effective at preventing the aberrant encoding of stop codons (UAA – Ochre, UAG – Amber, UGA – Opal) within the antibody fragments. It is important to avoid the incorporation of the stop codons' termination signal in the *in vitro* affinity maturation procedure to circumvent the generation of truncated, loss-of-function antibody molecules which is frequently observed

in *in vivo* systems. To analyze the diversity of the scFv repertoire in the second generation library, the sequencing results of the clones were aligned in BioEdit and compared with the parental TG130 antibody sequence (Appendix XII). Out of a sampling of five random clones examined, four clones had sequences differing from the parental antibody while one clone retained the parental sequence. All five clones had sequences differing from one another, demonstrating that the targeted hot-spot residues were successfully randomized (Table 5.2) (Appendix XII).

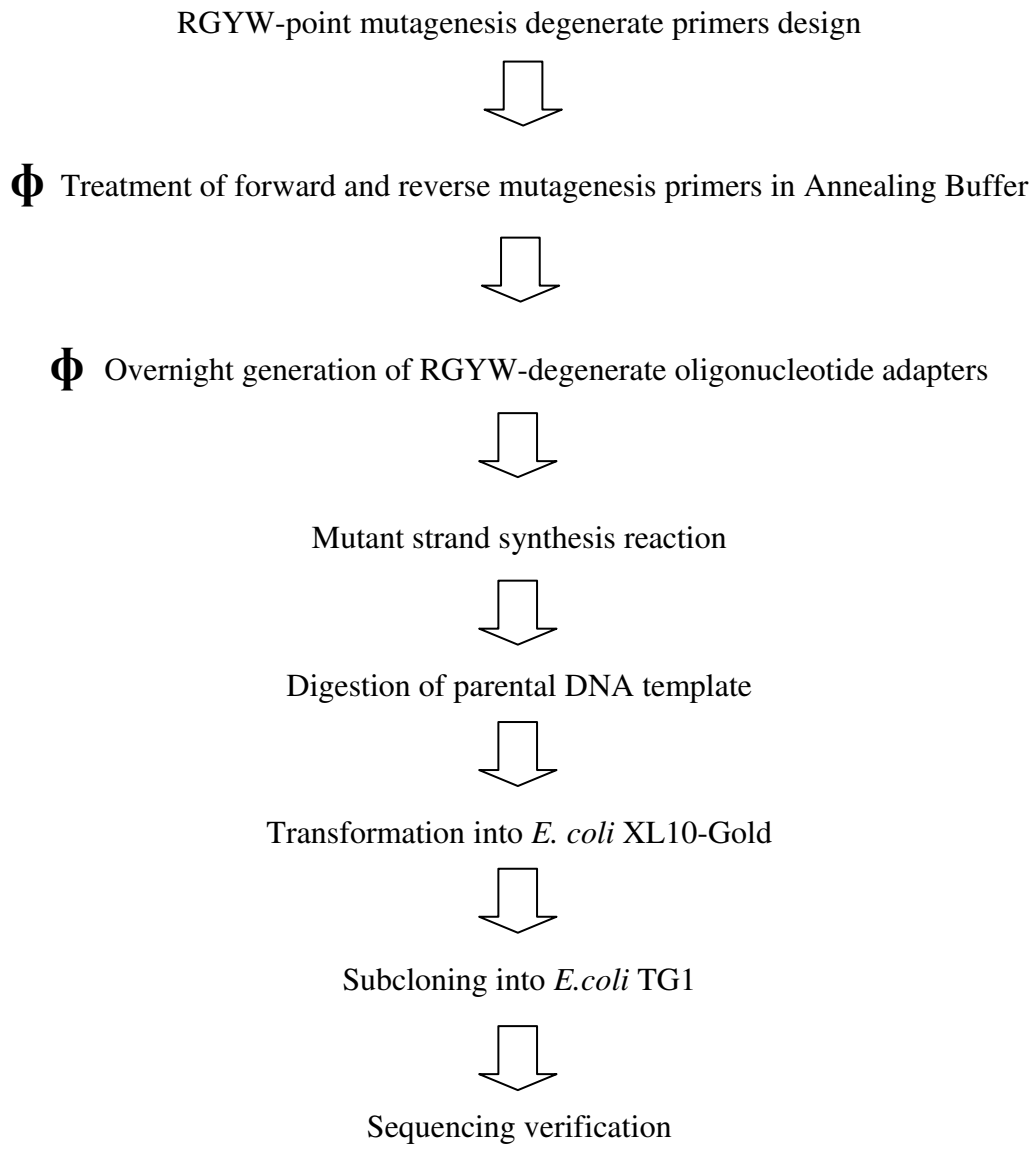

FIGURE 5.4 The modified procedure for the RGYW-site directed mutagenesis of the second generation scFv TG130 library is summarized in this schematic diagram.

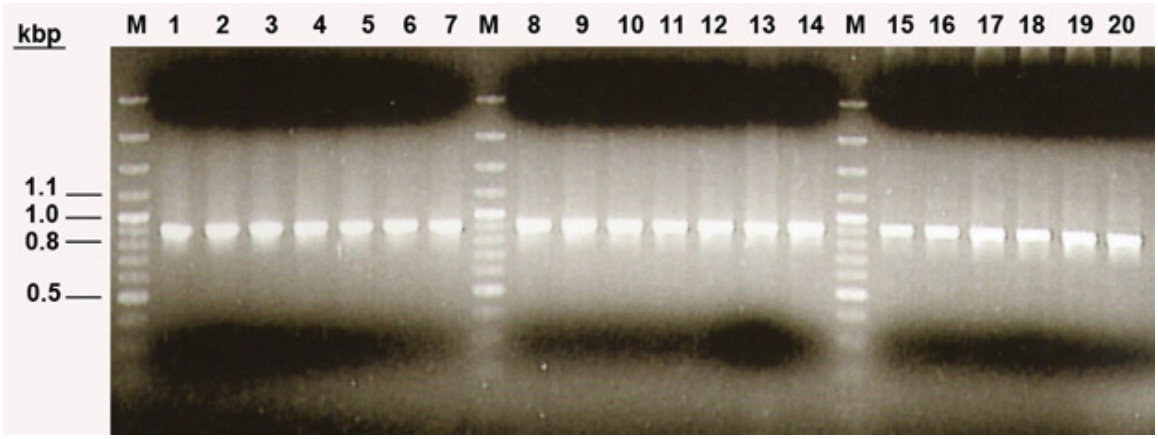

FIGURE 5.5 **PCR verification of *E. coli* TG1-transduced RGYW-mutant scFv within phagemid vector pCANTAB5E.** A sampling of 20 randomly picked mutant clones amplified by colony PCR is shown. All clones showed full-length scFv inserts (approximately 900 bp), and sequencing analysis revealed no occurrence of sequence truncation.

TABLE 5.2 **A sampling of sequence diversity within the RGYW-site-directed mutagenesis of second generation scFv TG130 antibody library.** The four RGYW sequence residues which were targeted for randomization in the present study are indicated in bold, italicized fonts; together with its' corresponding mutated amino acids at positions 27 and 28 of V_L CDR1.

Clone Number	RGYW Mutations	Amino acid Translation	Type
1	***CTG*** ***G***CT	Leu Ala	Non-parental
2	***AGG*** ***T***CT	Arg Ser	Non-parental
3	***ACG*** ***G***CT	Thr Ala	Non-parental
4	***AAC*** ***G***CT	Asn Ala	Non-parental
5	***AGT*** ***A***CT	Ser Thr	Parental

5.2.3- Screening of affinity-matured scFv antibody library for improved antigen binders.

Because the created second generation library is several magnitudes larger than necessary for a four nucleotide mutagenesis and there are no evidence of truncated scFv clones, only one round of selection was performed on *T. gondii* tachyzoites during biopanning. In order to reduce the likelihood of recovering phages that bound non-specifically or weaker binders than the parental antibody, a more stringent biopanning procedure was employed whereby the selective incubation duration with *T. gondii* was halved and washing rounds (off-rate) were doubled, as described in the Methodology section 3.3.d-ii. Through this modified procedure, the total duration of the off-rate selection was at least 100 min, which was double the duration of the primary antibody's screening selection procedure described previously. The biopanning screening of both the secondary antibody library and the originating primary antibody TG130 to *T. gondii* was carried out in parallel. Through this biopanning, it was found that the scFv phage output titer of the secondary library was 6.0×10^3 cfu, while the output titer for the primary antibody was 1.7×10^4 cfu – which is approximately three times higher than the secondary library. Although the secondary antibody library had a lowered phage recovery output compared to the primary scFv, this is not an entirely unexpected result considering the polyclonality of the secondary antibody library versus the monoclonal TG130 antibody. Following the biopanning screening, up to 111 clones were randomly picked and their sequences analyzed to determine the diversity and frequency of binding scFv clones (Table 5.3). Four of the most frequently occurring clones were selected for further characterization. Among the mutant clones recovered from the biopanning was scFv with identical sequences as the parental TG130 antibody. Frequency for these clones was 17 out of 111 clones. But unlike its mutant counterparts, there was no multiple codon usage. The

only codon used for these parental antibody reproductions was the originating germline sequences (AGT A..), indicating a probable bias in the mutant strand synthesis reaction to reproduce the parental sequence, which explains the higher frequency of these clones recaptured from biopanning.

The mutant residues with the highest frequency were found to be Thr^{27}-Pro^{28} and Pro^{27}-Thr^{28}. Each of these clones appeared eight times and five times respectively. More than one codon was used in these clones containing Thr^{27}-Pro^{28} and Pro^{27}-Thr^{28}, suggesting of a strong selection for these amino acid residues. Furthermore, nucleophilic amino acids such as Thr and Ser were conserved in all of these highest occurring scFv binders, except for clone Arg^{27}-Ala^{28}. Multiple codon usage was also observed for all other frequently occurring mutant clones (Table 5.3).

TABLE 5.3 **Sequences of the most frequently occurring RGYW-mutant phage clones obtained after panning.** Amino acid sequences and its corresponding nucleotide codons of mutant phage isolated after an increased off-rate biopanning procedure are listed. Only sequences of clones with a combined frequency higher than 4 are shown.

RGYW Mutation Amino Acids	Nucleotide Sequence	Frequency	Combined Frequency
Thr Pro	ACG C..	4	8
	ACC C..	4	
Pro Thr	CCG A..	4	5
	CCC A..	1	
Arg Ser	AGG T..	2	5
	CGG T..	3	
Thr Ala	ACG G..	4	5
	ACC G..	1	
Arg Ala	AGG G..	3	5
	CGC G..	1	
	CGG G..	1	
Leu Thr	CTG A..	3	4
	CTC A..	1	
Arg Thr	AGG A..	2	4
	CGC A..	2	

5.2.4- Immunofluorescence detection and biopanning of affinity-matured scFv antibodies binding to *T. gondii*.

Following biopanning of the second generation library and sequence analysis of the captured clones, monoclonal scFvs were prepared from several highest occurring phage clones and tested for their ability to bind to *T. gondii* tachyzoites in a binding titer assay. The second generation scFv clones chosen for the monoclonal testings are the Thr-Pro (TP60), Arg-Ser (RS55), Arg-Ala (RA15), Leu-Thr (LT3) and Arg-Thr (RT51) point mutants (Sequencing results in Appendix XII). Following the phage rescue of each of these mutant scFvs and its co-incubation with tachyzoites, binding titers experiments revealed that scFv clone TP60 had the highest binding titers relative to the parental antibody TG130, showing a 1.6-fold increase in averaged binding titer [Figure 5.6, Appendix X (c)]. The remaining four mutant scFvs displayed either lower (RA15, RS55 and RT51) or similar levels (LT3) of *T. gondii* - binding titers to scFv TG130. Confocal microscopy of scFv TP60's reactivity to tachyzoites revealed that the entire surface of extracellular tachyzoites were stained (Figure 5.7). These findings are consistent with the highest frequency of the TP60 mutant clone recovered from selection against the target antigen (Table 5.3). Based on these results, further characterization of the affinity-matured antibody was narrowed down to scFv TP60.

To further determine the binding specificity of the shortlisted scFv clone TP60, the monoclonal antibody fragment was examined for its binding advantage to *T. gondii* compared to negative selection cell line WRL68. Biopanning of scFv TP60 and its parental scFv TG130 revealed that the affinity-matured TP60 antibody demonstrated improved selectivity for its' target antigen *T. gondii*, while having a nearly two-fold increase in its binding titers to the parasite compared to the parental antibody (Figure 5.8), which is a

similar result as obtained in the previous experiment to determine the binding titers of the 5 shortlisted mutant scFvs. However, with an increased off-rate biopanning with a cumulative duration of 100 minutes, it seems the parental antibody TG130 had lost its' binding advantage to *T. gondii* above the negative control cells. Average binding titers of scFv TG130 to negative selection cells WRL68 was found to be 8.9×10^3 cfu, which was slightly higher than the 7.0×10^3 cfu average binding titers to *T. gondii*.

In comparison, with similar stringent biopanning conditions, the affinity matured antibody fragment TP60 demonstrated a statistically significant binding advantage to *T. gondii* compared to the negative control. Average binding titers of scFv TP60 to *T. gondii* was 1.25×10^4 cfu, which is more than a two times greater binding enrichment than its' binding to WRL68 with an average of 6.07×10^3 cfu (Figure 5.8). It is worth noting that the enrichment factors of phage scFvs from cell surface panning is typically lower than with panning on immobilized antigens (Rader et al., 2001), as was also demonstrated by another study by Pansri and co-workers in which phage scFvs showed approximately two times higher binding specificity to a cancer cell surface over negative cell lines (Pansri et al., 2009). This finding indicates that the affinity maturation of antibody fragments by hot-spot mutagenesis can generate mutant scFv that has reduced non-specific binding than the starting molecule. Although obtaining specific antibodies through cell surface panning is generally more difficult due to the complex antigen surface on viable cells, the present study demonstrates that through the advantage of mimicking *in vivo* natural selection of the humoral immune responses against *T. gondii* invasion coupled with *in vitro* affinity maturation; improved antigenic binders to target cells can be achieved.

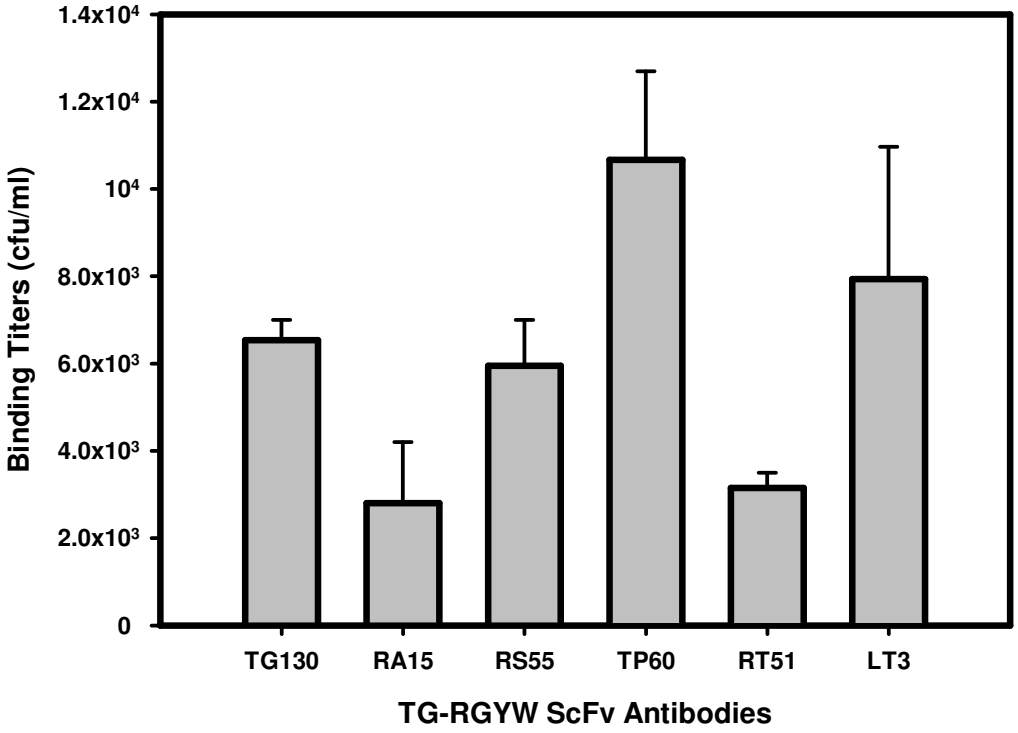

FIGURE 5.6 **Monoclonal TG-RGYW mutant scFv clones binding titer assay.** Five scFv antibodies with the highest occurrence of clones binding to *T. gondii* tachyzoite cells were tested in a binding titer assay to determine its relative binding advantage compared to the parental antibody TG130. Point-mutated scFv TP60 showed the highest binding titers against *T. gondii* relative to scFv TG130, with a 1.6-fold increase in binding. *Error bars*, ± S.E.M. from the means of duplicate or triplicate experiments.

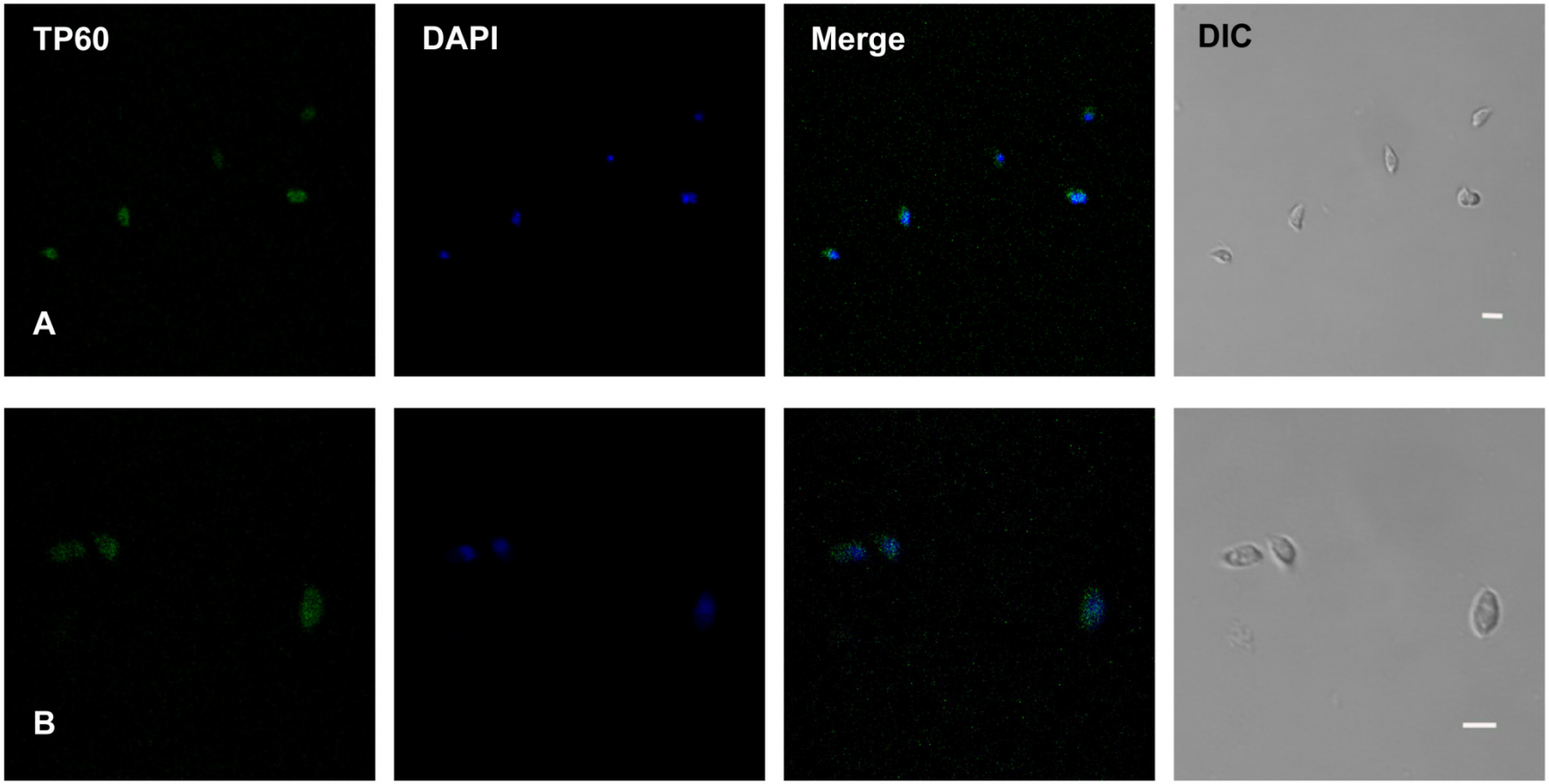

FIGURE 5.7 **Confocal laser-scanning microscopy of the *T. gondii* antigen recognized by affinity-matured scFv TP60.** Fixed extracellular tachyzoites were incubated with phage scFv TP60 and then with Alexa Flour 488-conjugated monoclonal antibody to M13 gp8 (green). Nuclei were ounterstained with DAPI (blue). Both parasite samples in (A) and (B) were processed similarly, with panel (B) showing a magnified view. DAPI, 4',6-diamidino-2-phenylindole; DIC, differential interference contrast. Scale bar, 3 µm.

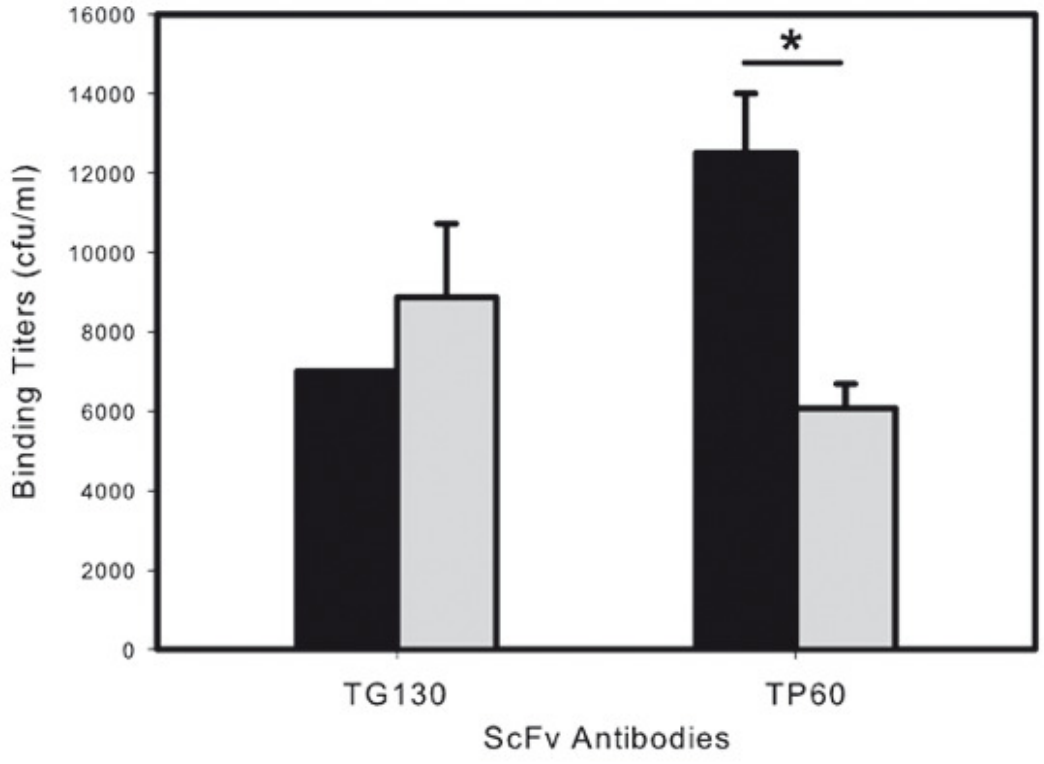

FIGURE 5.8 **Monoclonal phage scFvs of parental antibody TG130 and affinity-matured antibody TP60 were tested for their binding advantage to *T. gondii* tachyzoites.** Phage scFvs were biopanned against *T. gondii* with increased off-rate selection as described under 'Methodology', WRL68 cells were used as negative selection control. Binding titers of monoclonal scFvs to *T. gondii* (black column) and WRL68 (gray column) is shown. Affinity-matured antibody TP60 showed a greater binding specificity to *T. gondii* compared to the parental antibody. Error bars represent the standard deviation for duplicate experiments, and asterisk denotes a statistically significant difference.

5.3 - Discussion

5.3.1- Optimized site-directed mutagenesis of germline hotspots.

Advances in protein engineering have frequently used site-directed mutagenesis to generate randomized amino acid libraries to facilitate the screening and isolation of amino acid combinations that confers the best improvement in activity. However, randomized site-directed mutagenesis is often a process that is laborious and requires the use of ssDNA templates. Alternative random mutagenesis approaches such as error-prone PCR, is designed to introduce single-base mutations and therefore presents inherent limitations as only 5.7 amino acids substitutions on average are accessible from any given amino acid residue (Miyazaki & Arnold, 1999). In order to access a larger fraction of protein sequence space and ideally introduce all 20 amino acid side chains at a targeted site, site-directed saturation mutagenesis is commonly employed (Hogrefe, Cline, Youngblood, & Allen, 2002).

The second generation scFv antibody library generated through the optimized mutagenesis protocol yielded a size of 4.0×10^4 independent transformants. This is a library size that is comparable to that reported using a different kit recommended for use with degenerate primers mutations yielding 8.8×10^4 transformants (Hogrefe et al., 2002). This demonstrates that the protocol used in conjunction with the QuikChange Lightning Site-Directed Mutagenesis (QCM) kit is sufficient to generate a randomized amino acid library. In addition, the optimized protocol enables the construction of the randomized library within 2 days and with just a single PCR amplification, without additional steps required to randomize the amino acids. This is significantly quicker and less laborious compared to conventional PCR / ligation-based protocols which typically requires 5 – 8

days (Table 5.4) (Ling & Robinson, 1997). In the present study, two amino acids were randomized by incorporating the degenerate primers with randomized codons VNSN (Sense) and NSNB (Antisense) (N = A or G or C or T, V = A or C or G, S = C or G, B = C or G or T), and are complementary to one another. These degenerate primers were not only designed to be positioned at the RGYW sequence hot-spot motif, but also to exclude the incorporation of stop codons within the antibody fragment. One of the crucial factors determining the minimum number of clones needed to contain all possible mutations is the frequency of the least represented mutants (Hogrefe et al., 2002). For the VNSN codons, the frequency (f) of the least-represented mutants can be calculated as (⅓×¼×½×¼) = 1/96. Assuming a 100% mutation efficiency, there is a greater than 95% probability of observing all possible mutants in a random sampling of about 300 clones [$0.95 = 1 - (1 - f)^n$, where f = frequency of the least-represented mutants, and n = number of clones screened. (Jeltsch & Lanio, 2002)]. Therefore, the second generation scFv antibody library generated in this study is more than 100 times larger than the minimum size needed to ensure representations of all possible combinations of double amino acid mutants.

Although the primers which were used in this study had a T_m below the ≥ 78°C range recommended by the QCM kit manufacturer (both of the RGYW mutation primers had a T_m of 74.8°C), to decrease the likelihood of primer pairs self-annealing; what the experimental design for this mutagenesis protocol sought out to accomplish instead was actually to form primer dimers from the degenerate oligonucleotides before running the mutagenesis PCR. This approach was based on the postulation that site-directed saturation mutagenesis are often inefficient due to incorrect pairing of degenerate primers on its' DNA template. Therefore, the degenerate primers were pretreated with an Annealing Buffer (Appendix I) and allowed to form complementary oligonucleotide adapters for the mutagenesis reaction in order to create the second generation scFv library. Despite the

lowered T_m primers and the purposeful generation of 'primer dimers' (oligonucleotide adapters), it is shown here that the mutagenesis reaction still worked and generated a randomized antibody library of a robust size. Another study by Zheng L. and co-workers reported the use of partially overlapping degenerate primers instead of completely overlapping primers to construct a site-directed saturation mutagenesis library, as the standard practice of using completely overlapping primers failed to yield mutant strands (Zheng, Baumann, & Reymond, 2004). However, here we show evidence that the utilization of completely overlapping degenerate primers with a lower-than-ideal T_m to encourage sense and antisense primer dimer formations, could efficiently generate a site-directed saturation mutagenesis library with the QCM platform; and that it is not necessary to use partially overlapping primers and purified PCR products as they did. These findings are in good agreement with another publication, with the only difference being in the methodology where the study randomized one amino acid (Steffens & Williams, 2007), while the present study here randomized two amino acids. This simpler protocol reduces both the costs and turnaround time required to produce randomized libraries in directed evolution applications.

TABLE 5.4 **Comparison of major methods of *in vitro* mutagenesis.** (Source: Ling & Robinson, 1997)

	Duration (day)[a]	Man. Time (h)[b]	Advantage	Disadvantage
Connection PCR[c]	6	9 – 10	Good efficiency, fast	Relatively shorter mutant products.
Megaprimer PCR[d]	5	6 – 9	High efficiency, fast, larger mutant products.	Needs careful setup of parameters and conditions.
Inverse PCR	5	6 – 9	High efficiency, fast, simple, mutant product already in a plasmid.	Needs to amplify long PCR products.
Hybrid[e]				
Without selection	5 - 8	15	Mutant product already in a plasmid.	Very low efficiency, lengthy, laborious.
With selection (USE)	7	12 – 14	High efficiency.	Lengthy, laborious, some unique sites not suitable for this method.
Gapped circle	7	13 - 15	Mutant product already in a plasmid.	Relatively poor efficiency, lengthy, laborious, complex.

[a] Duration is the total time from the beginning to the confirmation of mutant clones by sequencing, including waiting time (e.g., *E. coli* growth overnight).
[b] Man. Time (manipulation time) is the time the operator needs to spend on performing all steps of that procedure.
[c] Connection PCR includes ligation, homologous recombination, and overlap extension of two PCR products to form the mutant product.
[d] Only One-STEP version was used for evaluation.
[e] Both methods with and without selection were evaluated. Without selection, the method needs time-consuming screening with radioactive selective hybridization.

5.3.2- *In vitro* antibody affinity maturation.

The results from this study showed that a scFv antibody with improved activity can be generated through an *in vitro* antibody affinity maturation by an evolution strategy targeting intrinsic mutational hot-spots. As previous work has shown that affinity maturation of germline hot-spots are more effective at generating improved antibody affinities compared to non-germline residues (Ho et al., 2005), therefore the V_L CDR1 germline hot spot was selected as target for the affinity maturation exercise.

The mutated hot-spot residues in the evolved antibody TP60 was found to have arisen out of triple mutations at the first, second and third positions in each codon of both variants of the TP60 clone (the ACG-CCT and ACC-CCT variant). This is a very uncommon occurrence in the process of somatic hypermutation of B cells (Jolly et al., 1996). The changing of nucleotide residues from AGT-ACT (Ser^{27} Thr^{28}) in the parental antibody TG130 to ACG-CCT and ACC-CCT (Thr^{27} Pro^{28}) in mutant TP60 involved three nucleotide point mutations, in which nucleotides in the second and third positions in the first codon are mutated and the nucleotide in the first position of the second codon was mutated. Dramatic mutations such as these are highly improbable in the *in vivo* somatic hypermutation process as it normally only mutate one nucleotide in each codon at the hot-spots. This observation lends credence to another published study on the advantages of *in vitro*-based hot-spots antibody affinity maturation as compared with the *in vivo* somatic hypermutation process in expanding the sampling of the mutation points to all 19 other amino acids (Ho et al., 2005).

To further examine the phage-scFv antigen-binding characteristics, the binding titers of both scFv TG130 and affinity-matured scFv TP60 were compared at different off-

rate selection durations of 50.0 min and 100.0 min (Figure 5.9). As was previously discovered, the parental scFv TG130 had a binding enrichment that was more than five times higher for *T. gondii* compared to the negative selection cells WRL68. However, this target-binding selectivity could not be maintained at the 100 min off-rate, where there were nearly similar binding titers for both the intended target antigen and the negative selector at 7.0×10^3 cfu and 8.87×10^3 cfu respectively (Figure 5.9). It is interesting to note that although the affinity matured scFv TP60 showed an initial high background binding to WRL68 (4.94×10^5 cfu/ml) compared to TG130 (9.80×10^4 cfu/ml) at the 50 min selection duration (Figure 5.9a); the antibody demonstrated consistent binding advantage of over two magnitudes to *T. gondii* relative to WRL68 over both the 50 min and 100 min off-rate selection. At 100 min off-rate selection, scFv TP60 also showed a lower binding to WRL68 compared to TG130 at 6.1×10^3 cfu and 8.87×10^3 cfu respectively. This suggests that the mature TP60 antibody does possess a 2-fold higher binding specificity with the ability to distinguish between target parasite cells and non-target cells. In addition, the mature TP60 antibody displayed greater binding titers to *T. gondii* compared to its' parental scFv TG130 over both off-rate selection duration, with a 5-fold and nearly 2-fold enrichment respectively for the 50 min and 100 min off-rate selection. The higher background binding to the non-target cells WRL68 could be due to the inherent problem of non-specific binding and lower enrichment factors associated with cell-surface biopannings (Rader et al., 2001). However, the cell-surface biopanning strategy allows the advantage of screening of antibodies against the native conformational or carbohydrate epitopes of the parasite; which more effectively mimics *in vivo* conditions of the humoral response.

Thus, the affinity maturation of scFv TG130 antibody resulted in the mutant scFv TP60 which had a 1.8-fold increase in binding potency to *T. gondii*, but more than a two-

fold higher specificity for its' target-binding over an extended period of off-rate selection. However, one cannot rule out the possibility that the phage-bound format of the scFv may influence higher background binding to the negative selector cells; as was demonstrated in another study which showed an approximately two-fold higher ELISA signals of target over negative cells binding in the phage-scFv format but a twenty-fold higher ELISA signals with the same test using soluble scFvs (Yu et al., 2005). It is also worth noting that there is a possibility that the apparent flux in specific binding titers of the antibodies to the complex surface of the target is actually resulting from the different expression levels of the recognized antigen (Pansri et al., 2009). Therefore, further characterization of these antibodies and identification of its specifically associated parasite binding ligands are needed to be done. Among some further characterization studies to be carried out would include the production of soluble scFvs, grafting of scFv V-regions into Fab fragments or full-sized IgG molecules, and determination of binding affinities of these antibody modalities to *T. gondii*. These future studies could aid in the evaluation these antibody molecules' utility as diagnostic or therapeutic molecules.

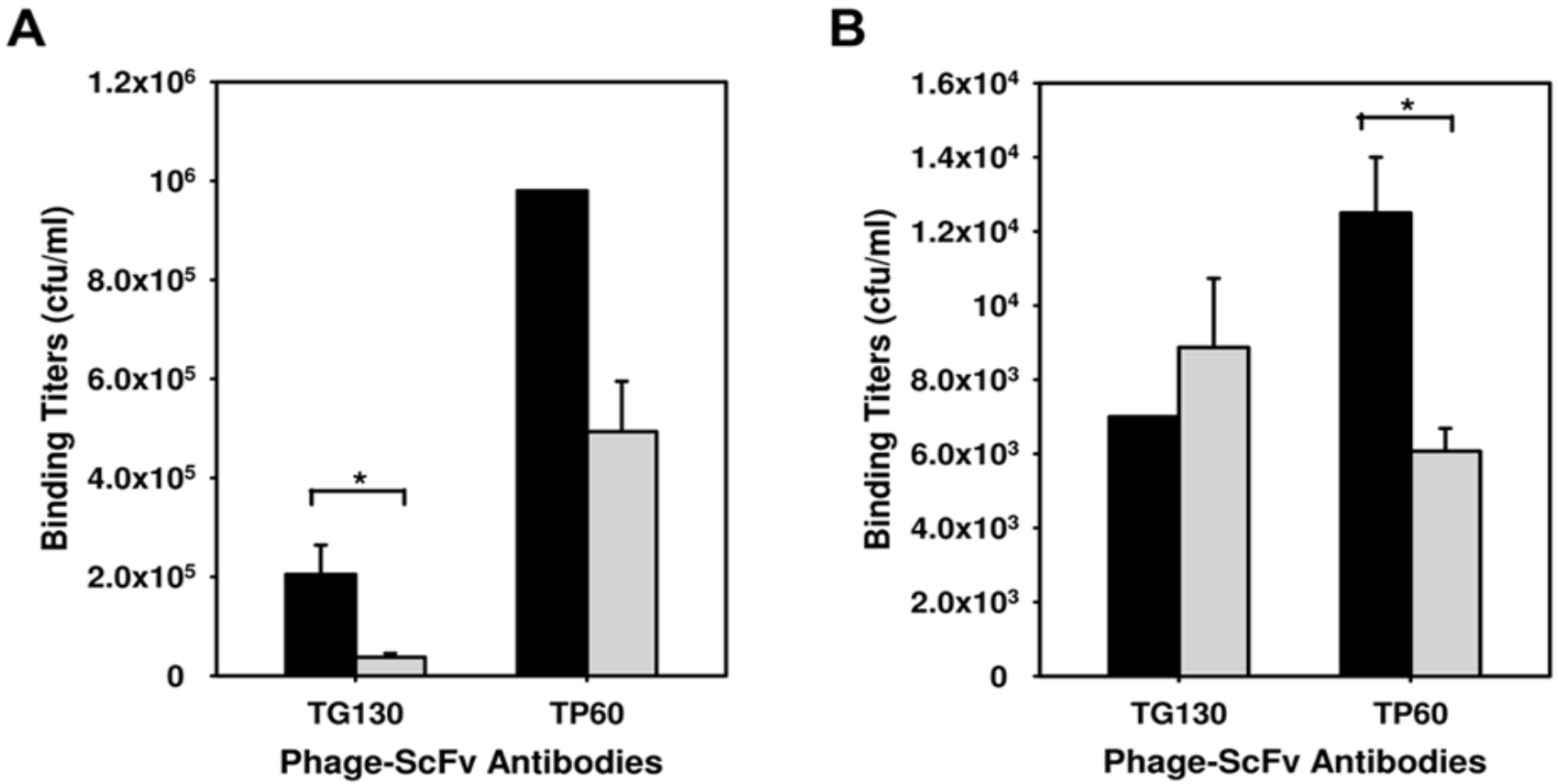

FIGURE 5.9 **Binding selectivity of affinity-matured (TP60) and parental (TG130) scFv antibodies at different off-rates.** The antibody fragments were incubated with either *T. gondii* tachyzoites (black columns) or negative selection cells WRL68 (grey columns) and subjected to off-rate durations of 50.0 min (A) and 100.0 min (B). ScFv TP60 demonstrated better ability at distinguishing between target and non-target cells over both time periods. Asteriks marks statistically significant difference at alpha value = 0.05. Error bars represent the standard error for duplicate experiments.

5.3.3- Structural implications of mutations.

The structural analysis of both the parental scFv TG130 and the mutant scFv TP60 showed that the hotspot mutation site is located at surface-exposed residues positions (Figure 5.11), which is in agreement to a previous publication showing highly-exposed antibody hotspot localization (Ho et al., 2005). Affinity maturation of antibodies by somatic mutations and point mutagenesis is normally a result of the reorganization of hydrogen bonding, electrostatic, and Van der Waals interactions networks between variable region residues. Another study has reported that these affinity-enhancing interactions between variable region amino acid residues can extend over distances of 15 Å (Wedemayer, Patten, Wang, Schultz, & Stevens, 1997). Although Figure 5.11 showed minimal structural deviations in the affinity-matured scFv compared to its' parental counterpart; upon closer examination, it was discovered that there is a closer shift between the mutated residue positions on V_L CDR1 to the V_H CDR3 loop apex. From an initial average distance of 16.15 Å between the molecules in the unmutated parental antibody (Figure 5.2), the average distance has decreased to 11.6 Å in the matured antibody TP60 – bringing the V_L CDR 1 and V_H CDR3 loops closer together by 4.55 Å and within the distance range for effective molecular interactions (Figure 5.11). This may be a contributing factor to the better binding selectivity of the mutated scFv TP60. However, the study currently faces a restriction from finer analysis of the molecular interactions between the scFv antibody and its' antigenic partner as the binding antigen has not been elucidated. Further studies to determine the recognized antigen would prove beneficial in this respect. This can be achieved by immunoprecipitation to pull-down the target antigen via the scFv antibodies, followed by tandem mass spectrometry for the antigen identification.

It is interesting to note that the point mutations in the affinity-matured scFv (Ser^{27} → Thr^{27}, Thr^{28} → Pro^{28}) mimics the trend of sequence changes in the *in vivo* somatic hypermutation process of mouse and human humoral responses (Clark et al., 2006). The published study by Clark and co-workers demonstrated that antibody evolution at hot-spot mutations are not merely random events, but are biased to certain characteristic changes that favours modifications contributing to antibody stability and affinity (Clark et al., 2006). Among the more frequently observable sequence conversions at the antibody-antigen (Ab-Ag) interface are Ser → Thr and Ser → Arg, along with Glu ↔ Asp, Lys → Arg, Asn ↔ Asp and Gln → Glu (Clark et al., 2006). The mutation from Ser^{27} to the larger residue Thr^{27} observed in TP60 in the present study could be due to the conservation of hydrogen bonding at the CDR loops while maintaining solution stability. With due consideration that all except one of the most frequently occurring mutant clones recovered from biopanning of the second generation antibody library showed a conservation of polar nucleophilic amino acids at the hot-spot evolution positions (Table 5.3), it can be postulated that hydrogen bonding interactions may play an essential role in the antigen combining interface. However, the lower binding titers of 3 of the mutant clones (RA15, RS55 and RT51) compared to scFv TG130 may be ascribed to the introduction of the Ser → Arg mutation which could repel antigen binding due to the strongly positive charge of Arginine residue. The large hydrophobic Leucine residue incorporated in mutated scFv clone LT3 may also be responsible for the lack of favourable increase in antibody binding titers to *T. gondii* due to steric hindrance.

It is rare for proline residues to occur in the germline sequences at the Ab-Ag interface of naïve antibodies, but increased proline usage are frequently observed in

matured antibodies (Clark et al., 2006). The second point mutation from Thr^{28} → Pro^{28} in scFv TP60 may contribute to the stabilization of beneficial loop conformations. The stabilizing influence of proline may potentially reduce the entropy cost of antigen binding and increase antibody affinity, which can be seen in the higher antibody binding titers of TP60.

Overall, the results of the present study indicates that with only two amino acid changes within the parental antibody; this has resulted in a small, but appreciable increase in the binding selectivity of affinity-matured antibody TP60. In view of several published observations that the affinity improvement of antibodies is effected by small, additive changes instead of a few large effects (Patten et al., 1996; Wedemayer, Patten et al., 1997; Wedemayer, Wang, Patten, Schultz, & Stevens, 1997), there is a possibility that further improvements of the scFv properties can be made by several more saturation mutagenesis antibody evolutions.

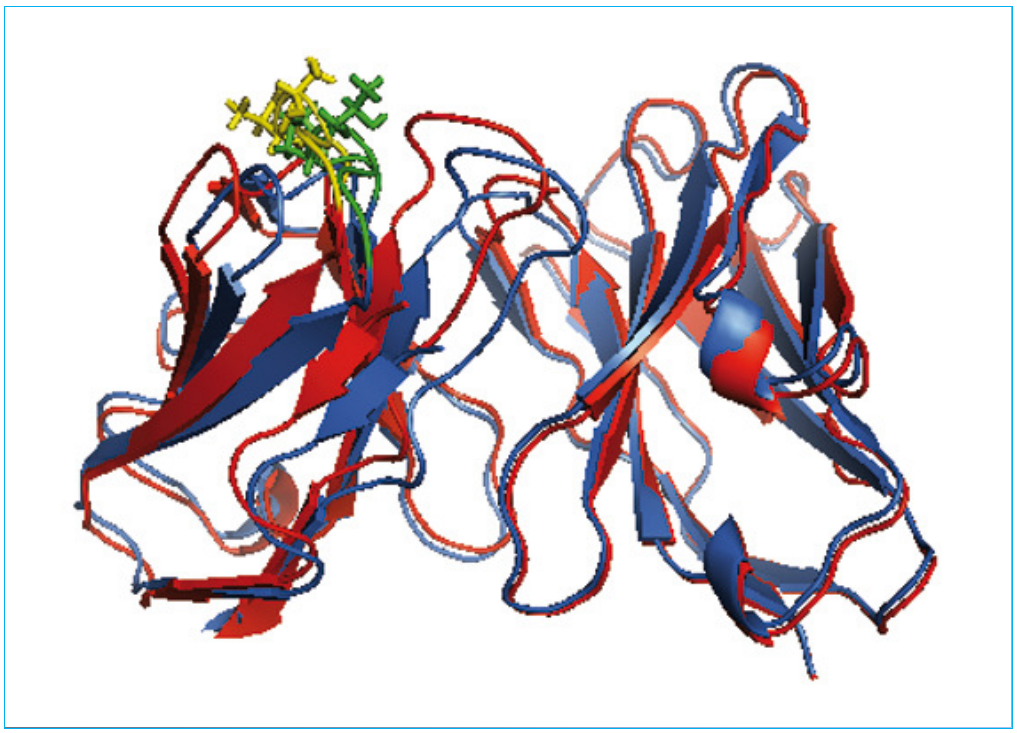

FIGURE 5.10 **Molecular superimposition of scFv TG130 (red) with mutant scFv TP60 (purple).** Alignment of the two antibody structures showed minimal deviations at the RGYW mutation sites at the V_L CDR1 loops. RGYW hot-spot residues Ser^{27}-Thr^{28} in TG130 is shown as yellow side chains, while mutated residues Thr^{27}-Pro^{28} is shown as green side chains. Superimposed structures were generated by PyMOL.

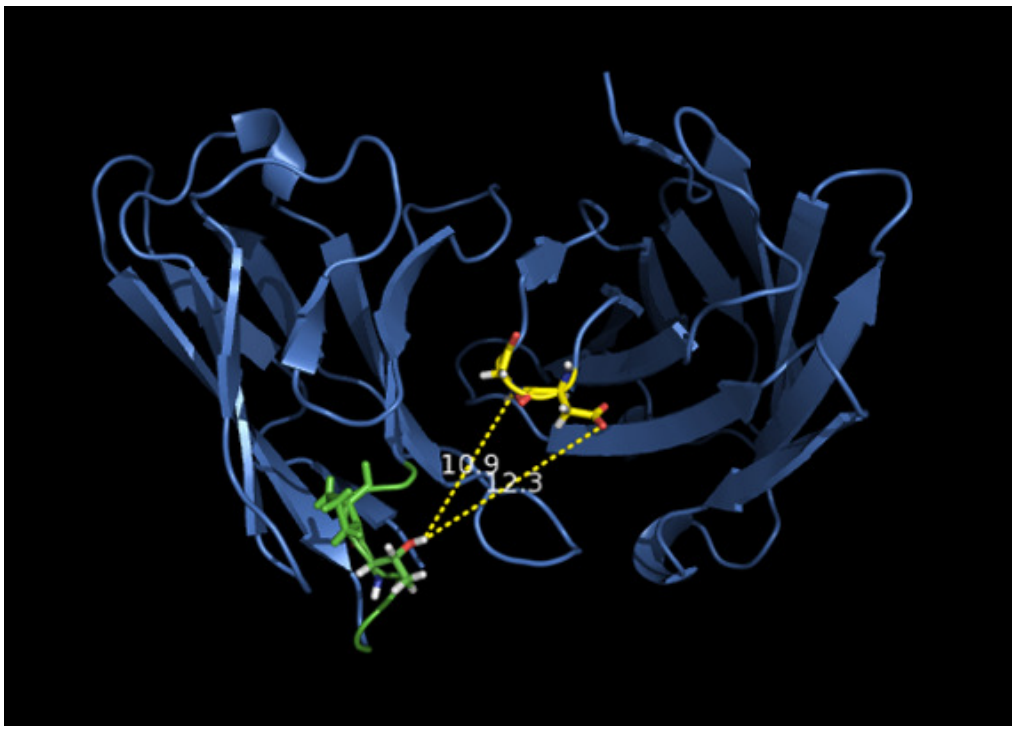

FIGURE 5.11 **Distance measurements of affinity-matured scFv TP60 between V_L CDR1 mutated residue Thr^{27} with the V_H CDR3 apex residues Asp^{100}-Gly^{101}.** The same measurements between the unmutated parental antibody residue Ser^{27} with the V_H CDR3 apex molecules yielded an average distance of 16.15 Å (Figure 5.3). Equivalent measurements done with mutated scFv TP60 shown here revealed a decrease in the average distance between the molecules to 11.6 Å. Mutated V_L CDR1 residues are shown in green while V_H CDR3 apex molecules are shown in yellow. Measurements are taken between atoms likely to contribute to hydrogen bonding. Hydrogen, oxygen and nitrogen atoms of these residues are indicated with white, red and blue colours respectively. View is looking down into the antigen combining site. Measurements are generated through the PyMOL software.

5.4 - General Conclusions

The present study demonstrates the successful application of an *in vitro* site-directed point mutagenesis for the affinity maturation of a scFv antibody fragment targeting *T. gondii* tachyzoites. The optimized saturation mutagenesis protocol described here reduces the time and labour associated with conventional point mutagenesis procedures, whereby the second generation mutated antibody library can be produced within two days with a robust library size and effectively-randomized sequence diversity.

Biopanning of the second generation scFv antibody library resulted in the isolation of the affinity-matured scFv TP60 which displayed only a slight increase in binding potency to *T. gondii*, but an improved robust selectivity for its' target parasite relative to negative selection cells over extended periods of off-rates selection. Although various studies on affinity maturation of antibody variable regions have documented gains of affinity in the order of between 2-fold to 30,000 fold (Ho et al., 2005; Wedemayer, Patten et al., 1997), the modest 2-fold increase in the binding titers of the affinity-matured scFv TP60 to its target may be ascribed to three reasons. First, dramatic gains of affinity are more frequently observed with antibody binding to purified ligands, and not complex cell surfaces (Rader et al., 2001). Second, the parasite binding ligand recognized by the scFv has not been determined; thus the affinity constant for the target epitope cannot be ascertained for direct comparisons. Third, one cannot rule out the possibility that there may in fact be no significant increase in the mutant antibody's affinity, but only an appreciable improvement in binding selectivity – as evidenced in the binding titers assessment. Additional randomization of sequences at remaining antibody hot-spot motifs might be appropriate to further increase the binding

potency of the scFv in a step-wise antibody evolution approach. Furthermore, the antibody hotspots affinity maturation strategy described here could also have potential useful applications for modifications of enzymes, receptors, ligands and other biologically important proteins; as the somatic hypermutation mechanism is a global phenomenon in the genome with DNA hotspots extending beyond immunoglobulin genes (Wang, Harper, & Wabl, 2004).

CHAPTER 6 OVERALL CONCLUSIONS

The present study was undertaken to design and characterize the properties of single-chain variable fragment (scFv) antibodies targeted to *T. gondii*, the etiologic agent of toxoplasmosis infection. A *T. gondii*-immunized scFv antibody library was first generated by PCR assembly of polyclonal V regions harvested from immunized mouse splenic cells. Through this research, an optimized subtractive cell-based biopanning protocol was developed to isolate antibody fragments recognizing *T. gondii* tachyzoites in a solution phase screening. The optimized biopanning protocol involved multiple rounds of negative selection against absorber cells WRL68 to deplete unspecific binders before proceeding with a single round of selection against *T. gondii* to reduce loss of antibody diversity. The first generation scFv antibody library targeted to *T. gondii* was at a complexity of 1.62×10^4 cfu independent transformants. Despite a small library size, this study showed that utilization of this small, immunized library in conjunction with the optimized biopanning protocol was sufficient to isolate a specific scFv antibody against the parasite cells. The isolated phage-scFv antibody, TG130, demonstrated a statistically significant binding specificity to tachyzoite cells with an average binding titer of 5-fold magnitude higher binding advantage relative to negative selection cells. A caveat that needs to be noted regarding the present study is that despite the incorporation of an empirically-determined, optimized negative selection rounds in the biopanning, several unspecific scFv antibodies were still recovered along with specific binders to *T. gondii*. The reasons to this could be that the WRL68 hepatocytes were not entirely suitable as a negative selection cell line, or that the optimized subtractive biopanning procedure wasn't robust enough to completely quench unspecific antibodies. However, in lieu of the successful isolation of specific scFv binders to *T. gondii* shown here, it is proposed that further refinements to the optimized

biopanning protocol would have potential benefits in the rapid isolation of antibody fragments on complex cell surfaces; especially when there is a paucity of defined and purified antigens.

To further enhance the antigen-targeting properties of scFv TG130, an *in vitro* affinity maturation was carried out based on hotspots site-directed mutagenesis. Through this study, an efficient saturation mutagenesis protocol targeted at the antibody's variable region hotspots was developed. The results of this protocol show that the optimized protocol effectively randomized two amino acid positions within the V_L CDR1 fragment and generated a mutated scFv library of a robust size (4.0×10^4 cfu independent transformants) that was approximately 100-fold higher than the minimal requirements. This development has potential implications in providing a rapid and simple saturation mutagenesis protocol that targets multiple amino acid residues simultaneously, with a capability to generate a randomized mutation library within two days, and therefore saving costs, time and labour.

Utilization of the affinity-matured scFv library for biopanning screening for improved target binders resulted in the discovery of scFv clone TP60. The TP60 clone demonstrated binding titers 1.8-fold higher than its parental counterpart TG130, and also a binding advantage that is 2-fold higher for *T. gondii* relative to the negative absorber cell line WRL68, at an extended off-rate selection period of 100.0 min. Evidence of the matured scFv's binding specificity was shown through binding titers experiments as well as immunofluorescence imaging. In comparison, at the same extended off-rate selection parameters, the parental antibody scFv TG130 could not maintain binding selectivity to its' target tachyzoite cells, but showed slightly lower binding titers to *T. gondii* compared to WRL68. This is translated to mean that the

parental antibody TG130 displayed specificity to its target antigen for at least 50.0 min, which was the initial off-rate duration employed in the scFv screenings; but loses its' specificity by the 100^{th} min. Therefore, these findings suggested that the affinity maturation of scFv TG130 into scFv TP60 by mutating two hot-spots amino acids brought modest but appreciable improvements in the scFv antibody's binding affinity and specificity, that was observable over an extended off-rate period of 100.0 min, which was more than eight times longer than the established *in vivo* B-cell receptor (BCR) internalization window period of approximately 12 min. An implication of this is the possibility that further experiments for affinity maturation at alternative V region hot-spots within the antibody could lead to increased improvements in the scFv's binding specificity and potency in a step-wise antibody evolution manner. The current investigation was limited by the identification of the parasite binding partner of these scFv antibodies. Elucidation of the binding antigen could aid in the finer determination of antibody binding affinity constants (K_D) and the rational design of scFv refinements through bioinformatics analysis. Further research might explore this need to identify an antigenic determinant to the developed scFv antibodies, as well as test the soluble scFv expression through an *E. coli* system.

Taken together, the *T. gondii*-targeting scFv antibodies developed through this study could have potential implications to be developed further into potent antibody fragments as an alternative intervention for the disease of toxoplasmosis. At present time, there are no chemotherapeutic agents to completely prevent or cure toxoplasmosis, while vaccine formulations thus far provided partial reduction of parasitaemia but sterile immunity was not achieved (Tan et al., 2010). While a vaccine against *T. gondii* is desirable, this opportunistic infection is problematic in immunocompromised patients due to their reduced cellular immunity. Therefore, a passive immunization strategy

using recombinant antibodies to inhibit parasite-host invasion is a desirable treatment solution. Future work on investigating the reactive properties of these scFv antibodies against *T. gondii* would also be beneficial to evaluate the potential utility of the antibodies as bioimaging or therapeutic ligands. In addition, current treatment regime of toxoplasmosis in pregnant women with the pyrimethamine-sulfadiazine combination drugs is less than ideal due to the teratogenicity of the administered compounds (Gagne, 2001). There is therefore a growing need to develop alternative treatment strategies such as immunotherapeutic antibodies that can decrease parasitaemia and alleviate associated disease pathology in immune-deficient hosts.

These scFv fragments could also be reconstructed into full-length intact IgG for the study of its inhibition of infection by the recruitment of effector functions mediated by the stem Fc domain. While the scFv molecule has the advantage of improved pharmacokinetics, blood clearance properties, simplicity and economically favourable expression and isolation due to its smaller size; the drawback associated with the scFv is its' poorer stability compared to its IgG counterpart. In fact, the intact IgG is often the antibody format of choice used in immunotherapeutics (Holliger & Hudson, 2005). The conversion of the scFv fragments into whole IgG molecules would be an interesting study to explore due to the properties of increased functional affinity, induction of cytotoxic effector functions and high retention times on cell-surface receptors and antigens mediated by a full-length antibody. Immunity to *T. gondii* infection is a combination of cellular and humoral immune responses. B-cell deficient mice are often more susceptible to disease mortality compared to immunocompetent mouse (Johnson & Sayles, 2002; Kang et al., 2000). Therefore, antibodies against toxoplasmosis can be considered as candidates of immune effectors limiting fatal disease *in vivo*. This study reports two scFvs that shows reactivity to the *T. gondii* parasite surface, and it is

believed that these two antibody fragments likely represent only a portion of the parasite binding antibodies occurring in infected mice. The scFv library generated in this study would remain a useful resource for further studies of the humoral immune response to *T. gondii* epitopes.

APPENDICES

Appendix I: Formulations for mini preparation of plasmid DNA, culture media, & other molecular biology reagents.

a) Chemical reagents for mini preparation of plasmid DNA

Solution 1 (per 50 ml)	
1 M Tris.Cl (pH 8.0)	1.25 ml
0.5 M EDTA (pH 8.0)	1.00 ml
Glucose	450 mg

Solution 2 (per 3000 µl)	
10 M NaOH	60 µl
10 % SDS	300 µl
Sterile distilled water	2640 µl

Freshly prepared prior to use

Solution 3 (per 250 ml)	
5 M Potassium acetate	150 ml
Glacial acetic acid	28.75 ml
Sterile distilled water	71.25 ml

b) Miscellaneous molecular biology reagents

Annealing Buffer
10 mM Tris.HCl (pH 7.5)
60 mM NaCl

Biopanning Elution Buffer
0.1 M HCl

Adjusted to pH 2.2 with glycine.

(5%) BSA Blocking Buffer stock (per 100 ml)	
Bovine serum albumin (BSA)	5.00 g
1X PBS	to 100 ml

15 % DMSO (per 20 ml)	
Dimethyl sulfoxide (DMSO, Molecular biology grade)	3.0 ml
1X PBS	17.0 ml

10% NBF (Neutral Buffered Formalin) Fixation Solution (per 100 ml)

Formaldehyde (Molecular Biology grade)	10.0 ml
1X PBS	90.0 ml

10% NBF is equivalent to 4% Formaldehyde fixation solution. Solution is stored at 4°C.

1X PBS (Phosphate-buffered Saline)

137 mM NaCl	10X Stock:	80.00 g of NaCl
2.7 mM KCl		2.00 g of KCl
12 mM Na_2HPO_4		17.00 g of Na_2HPO_4
1.2 mM KH_2PO_4		1.63 g of KH_2PO_4

Adjusted to pH 7.4 with HCl. PBS 10X stock solution was brought to 1 liter with sterile distilled water and autoclaved.

PEG/Nacl (per 250 ml)

Polyethylene glycol 8000	50.00 g
NaCl	36.53 g
Sterile distilled water	to 250 ml

Solution mixture was heated to dissolve before autoclaving.

TB (CaCl2) Solution (for chemical transformation) (per 100 ml)

10 mM PIPES, Sodium salt	0.6706 g
55 mM $MnCl_2.4H_2O$	1.0885 g
15 mM $CaCl_2.2H_2O$	0.2205 g
250 mM KCl	1.8637 g

All the components except for $MnCl_2$ were mixed and the pH was adjusted to 6.7 with KOH.
After adjustment to pH 6.7, $MnCl_2$ was dissolved in and solution was filter-sterilized. TB Solution was stored at 4°C.

Toxoplasma Homegenization Buffer (THB)

20 mM HEPES/KOH (pH 7.0)
50 mM Potassium acetate
10 % (w/v) Sucrose
1 mM EDTA

5X Tris-borate-EDTA buffer (per liter)

Tris base	54.00 g
Boric acid	27.50 g
0.5 M EDTA (pH 8.0)	20 ml
Sterile distilled water	to 1L

Working concentration of TAE buffer is 0.5X.

TE Buffer
10 mM Tris.Cl (pH 8.0)
1 mM EDTA (pH 8.0)

c) Culture media and associated reagents
All media and reagents are sterilized by autoclaving for 15 min at 15 psi on a liquid cycle unless otherwise noted.

LB Medium (per 100 ml)

Bacto-tryptone	1.00 g
Yeast extract	0.50 g
NaCl	0.50 g

For plates, add in 1.5g of Bacto-agar before autoclaving.

LB Top Agar (per 50 ml)

LB medium (Gibco-BRL)	1.25 g
Bacto-agar	0.35 g

Media was autoclaved and stored at 4°C. Before use, it is melted in microwave.

M9 Minimal Medium Plates (per 100 ml)

Bottle A:	
Na_2HPO_4 (dibasic)	0.60 g
KH_2PO_4 (monobasic)	0.30 g
NH_4Cl	0.10 g
Adjust pH to 7.4 with NaOH	
Sterile distilled water	to 50 ml
Bottle B:	
Bacto-agar	1.50 g
Sterile distilled water	to 49 ml

Both bottles were autoclaved simultaneously to sterilize. Bottles were cooled down to 50-60°C and combined. The following pre-filter-sterilized solutions were then added in:

1M $MgCl_2.6H_2O$	100 µl
1M $CaCl_2.2H_2O$	100 µl
1M Thiamine Hydrochloride	100 µl
20 % Glucose	500 µl

Plates were poured immediately.

NZY+ Broth (per 100 ml)

NZ Amine (Casein hydrolysate)	1.00 g
Yeast extract	0.50 g
NaCl	0.50 g

Sterile distilled water was added to ~ 100 ml. The pH was adjusted to 7.5 using NaOH and autoclaved. Media was allowed to cool to 50-60°C, before addition of the following pre-filter-sterilized solutions prior to use:

1M $MgCl_2.6H_20$	1.25 ml
1M $MgSO_4$	1.25 ml
20% (w/v) Glucose	2.00 ml

SOC Medium (per 100 ml)

Bacto-tryptone	2.00 g
Yeast extract	0.50 g
NaCl	0.06 g
250 mM KCl	1.0 ml
1 M $MgCl_2.6H_20$	1.0 ml
1 M $MgSO_4$	1.0 ml
2 M Glucose	1.0 ml

Media was adjusted to pH 7.0 by adding 10 N NaOH prior to autoclaving.
Filter-sterilized 2M Glucose was added after media was autoclaved and cooled down to at least 50°C - 60°C.

SB (Super Broth) (per 100 ml)

MOPS (3(N-Morpholino) propanesulfonic acid)	1.00 g
Bacto-tryptone	3.00 g
Yeast exract	2.00 g

Adjust pH to 7.0.

SOBAG Plates (per 500 ml)

Bacto-tryptone	10.00 g
Yeast extract	2.50 g
NaCl	0.25 g
Bacto-agar	7.50 g

Media was autoclaved and cooled down to 50-60°C before adding in the following pre-filter-sterilized solutions:

1M $MgCl_2.6H_2O$	5.0 ml
2M Glucose	27.8 ml
100 mg/ml Ampicillin	500 µl

2X YT Medium (per 1 L)

Bacto-tryptone	17.00 g
Yeast extract	10.00 g
NaCl	5.00 g

2X YT-AG Medium
2X YT medium containing 100 µg/ml Ampicillin and 2% Glucose.

2X YT-AK Medium
2X YT medium containing 100 µg/ml Ampicillin and 50 µg/ml Kanamycin.

Appendix II: Sterilization procedure for working with phage.
(adapted from General Procedures section in Phage Display: A Laboratory Manual (Barbas et al., 2001))

All plasticware, glassware and complex solutions (such as PEG/NaCl and media) are sterilized in an autoclave that was never used to autoclave biological wastes. This was meant to keep the phage load in the autoclave to a minimum, as phages are known to survive standard autoclaving conditions.

All glass and plasticware to be used or recycled for phage procedures are treated for phage decontamination by heat-treating dry, autoclaved materials in an oven for 4 hours at 105°C, or by simply drying the autoclaved materials overnight at the same temperature.

Appendix III: Table of primer sequences for V_H and V_L regions amplification.

PRIMER	SEQUENCE	D
Vκ 5' / sense (*Sfi* 1)		
MSCVK-1	GGG CCC AGC CGG CCG AGC TCG AYA TCC AGC TGA CTC AGA C	2
MSCVK-2	GGG CCC AGC CGG CCG AGC TCG AYA TTG TTC TCW CCC AGT C	3
MSCVK-3	GGG CCC AGC CGG CCG AGC TCG AYA TTG TGM TMA CTC AGT C	4
MSCVK-4	GGG CCC AGC CGG CCG AGC TCG AYA TTG TGY TRA CAC AGT C	4
MSCVK-5	GGG CCC AGC CGG CCG AGC TCG AYA TTG TRA TGA CMC AGT C	4
MSCVK-6	GGG CCC AGC CGG CCG AGC TCG AYA TTM AGA TRA MCC AGT C	4
MSCVK-7	GGG CCC AGC CGG CCG AGC TCG AYA TTC AGA TGA YDC AGT C	4
MSCVK-8	GGG CCC AGC CGG CCG AGC TCG AYA TYC AGA TGA CAC AGA C	3
MSCVK-9	GGG CCC AGC CGG CCG AGC TCG AYA TTG TTC TCA WCC AGT C	3
MSCVK-10	GGG CCC AGC CGG CCG AGC TCG AYA TTG WGC TSA CCC AAT C	4
MSCVK-11	GGG CCC AGC CGG CCG AGC TCG AYA TTS TRA TGA CCC ART C	5
MSCVK-12	GGG CCC AGC CGG CCG AGC TCG AYR TTK TGA TGA CCC ARA C	5
MSCVK-13	GGG CCC AGC CGG CCG AGC TCG AYA TTG TGA TGA CBC AGK C	4
MSCVK-14	GGG CCC AGC CGG CCG AGC TCG AYA TTG TGA TAA CYC AGG A	3
MSCVK-15	GGG CCC AGC CGG CCG AGC TCG AYA TTG TGA TGA CCC AGW T	3
MSCVK-16	GGG CCC AGC CGG CCG AGC TCG AYA TTG TGA TGA CAC AAC C	2
MSCVK-17	GGG CCC AGC CGG CCG AGC TCG AYA TTT TGC TGA CTC AGT C	2
Vκ 3' / antisense		
MSCJK12-B	GGA AGA TCT AGA GGA ACC ACC TTT KAT TTC CAG YTT GGT CCC	3
MSCJK4-B	GGA AGA TCT AGA GGA ACC ACC TTT TAT TTC CAA CTT TGT CCC	1
MSCJK5-B	GGA AGA TCT AGA GGA ACC ACC TTT CAG CTC CAG CTT GGT CCC	1
Vλ 5'/ sense (*Sfi* 1)		
MSCVL-1	GGG CCC AGC CGG CCG AGC TCG ATG CTG TTG TGA CTC AGG AAT C	1
Vλ 3'/ antisense-short linker		
MSCJKL-B	GGA AGA TCT AGA GGA ACC ACC GCC TAG GAC AGT CAG TTT GG	1
V_H 5' / sense		
MSCVH1	GGT GGT TCC TCT AGA TCT TCC CTC GAG GTR MAG CTT CAG GAG TC	3
MSCVH2	GGT GGT TCC TCT AGA TCT TCC CTC GAG GTB CAG CTB CAG CAG TC	3
MSCVH3	GGT GGT TCC TCT AGA TCT TCC CTC GAG GTG CAG CTG AAG SAS TC	3

PRIMER	SEQUENCE	D
MSCVH4	GGT GGT TCC TCT AGA TCT TCC CTC GAG GTC CAR CTG CAA CAR TC	3
MSCVH5	GGT GGT TCC TCT AGA TCT TCC CTC GAG GTY CAG CTB CAG CAR TC	4
MSCVH6	GGT GGT TCC TCT AGA TCT TCC CTC GAG GTY CAR CTG CAG CAG TC	3
MSCVH7	GGT GGT TCC TCT AGA TCT TCC CTC GAG GTC CAC GTG AAG CAG TC	1
MSCVH8	GGT GGT TCC TCT AGA TCT TCC CTC GAG GTG AAS STG GTG GAA TC	3
MSCVH9	GGT GGT TCC TCT AGA TCT TCC CTC GAG GTG AWG YTG GTG GAG TC	3
MSCVH10	GGT GGT TCC TCT AGA TCT TCC CTC GAG GTG CAG SKG GTG GAG TC	3
MSCVH11	GGT GGT TCC TCT AGA TCT TCC CTC GAG GTG CAM CTG GTG GAG TC	2
MSCVH12	GGT GGT TCC TCT AGA TCT TCC CTC GAG GTG AAG CTG ATG GAR TC	2
MSCVH13	GGT GGT TCC TCT AGA TCT TCC CTC GAG GTG CAR CTT GTT GAG TC	2
MSCVH14	GGT GGT TCC TCT AGA TCT TCC CTC GAG GTR AAG CTT CTC GAG TC	2
MSCVH15	GGT GGT TCC TCT AGA TCT TCC CTC GAG GTG AAR STT GAG GAG TC	3
MSCVH16	GGT GGT TCC TCT AGA TCT TCC CTC GAG GTT ACT CTR AAA GWG TST G	4
MSCVH17	GGT GGT TCC TCT AGA TCT TCC CTC GAG GTC CAA CTV CAG CAR CC	3
MSCVH18	GGT GGT TCC TCT AGA TCT TCC CTC GAG GTG AAG TTG GAA GTG TC	1
MSCVH19	GGT GGT TCC TCT AGA TCT TCC CTC GAG GTG AAG GTG ATC GAG TC	1
V_H 3' / antisense (*Not*1)		
MSCG1ab-B	CCT GCG GCC GCC CAC TAG TGA CAG ATG GGG STG TYG TTT TGG	3
MSCG3-B	CCT GCG GCC GCC CAC TAG TGA CAG ATG GGG CTG TTG TTG T	1
MSC-F	GCG GGG CCC AGC CGG CCG AGC TCG	1
RSC-B	GCC TGC GGC CGC ACT AGT GAC AGA	1

Appendix IV: The map of pCANTAB5E phagemid vector (GE Life Sciences (formerly Amersham Biosciences), Recombinant Phage Antibody System)

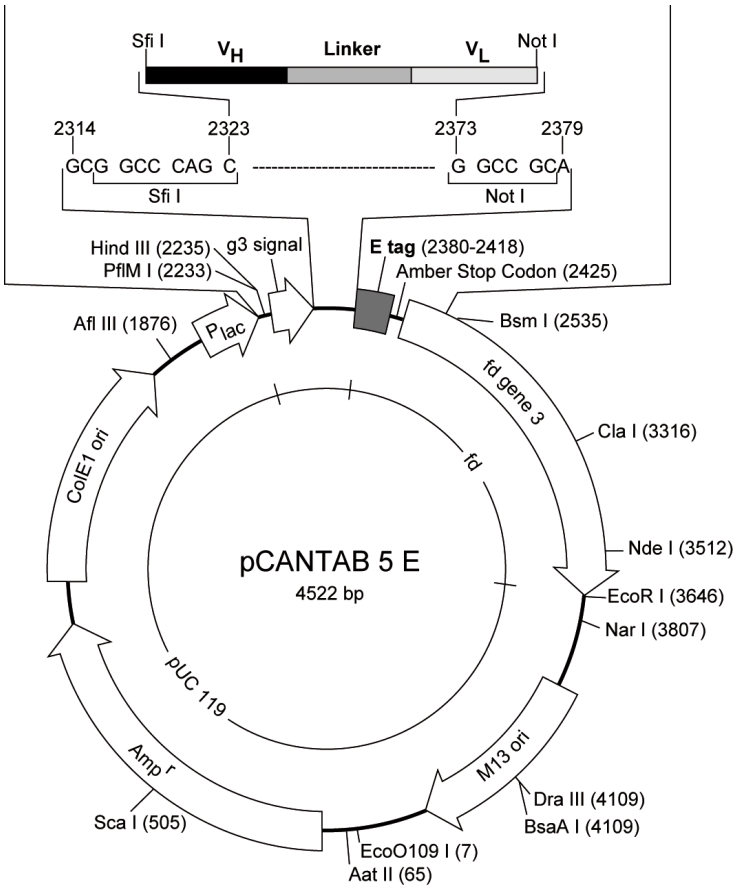

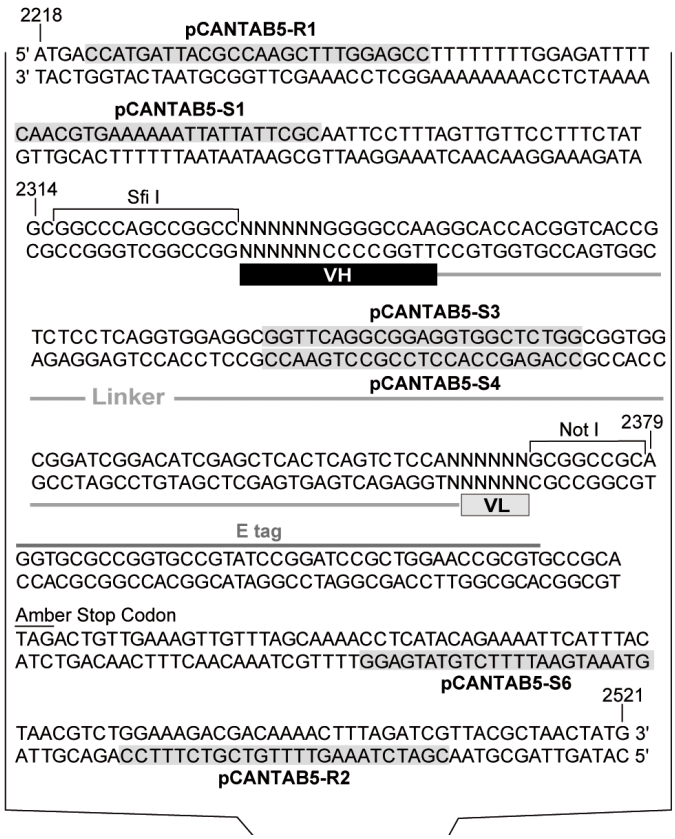

Appendix V: Subtractive biopanning quenching of phage-scFv unspecific paratopes against normal hepatocytes cell line WRL68.

Supplementary Graph: ScFv Subtractive Biopanning Quenching Profile

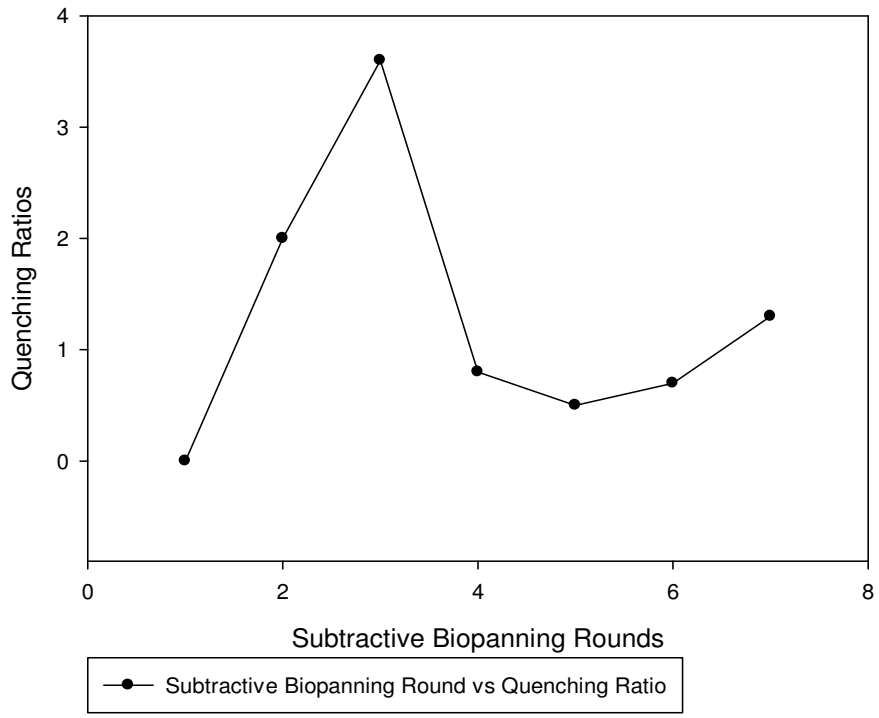

SUBTRACTIVE BIOPANNING ROUND	PHAGE-BINDING TITER (cfu/ml)	QUENCHING RATIO[5]
1	2.2×10^5	-
2	1.1×10^5	2.0
3	3.1×10^4	3.6
4	3.9×10^4	0.8
5	8.0×10^4	0.5
6	1.2×10^4	0.7
7	9.0×10^4	1.3

[5] Quenching ratio = phage titer of previous round / phage titer of test round.

Appendix VI: Chromatograms of scFv sequences

- **Appendix VI-i: Chromatogram of scFv TG64**
- **Appendix VI-ii: Chromatogram of scFv TG69**
- **Appendix VI-iii: Chromatogram of scFv TG116**
- **Appendix VI-iv: Chromatogram of scFv TG130**
- **Appendix VI-v: Protein translation of scFv sequences**

Appendix VI-i : Chromatograms of scFv sequences – scFv TG64

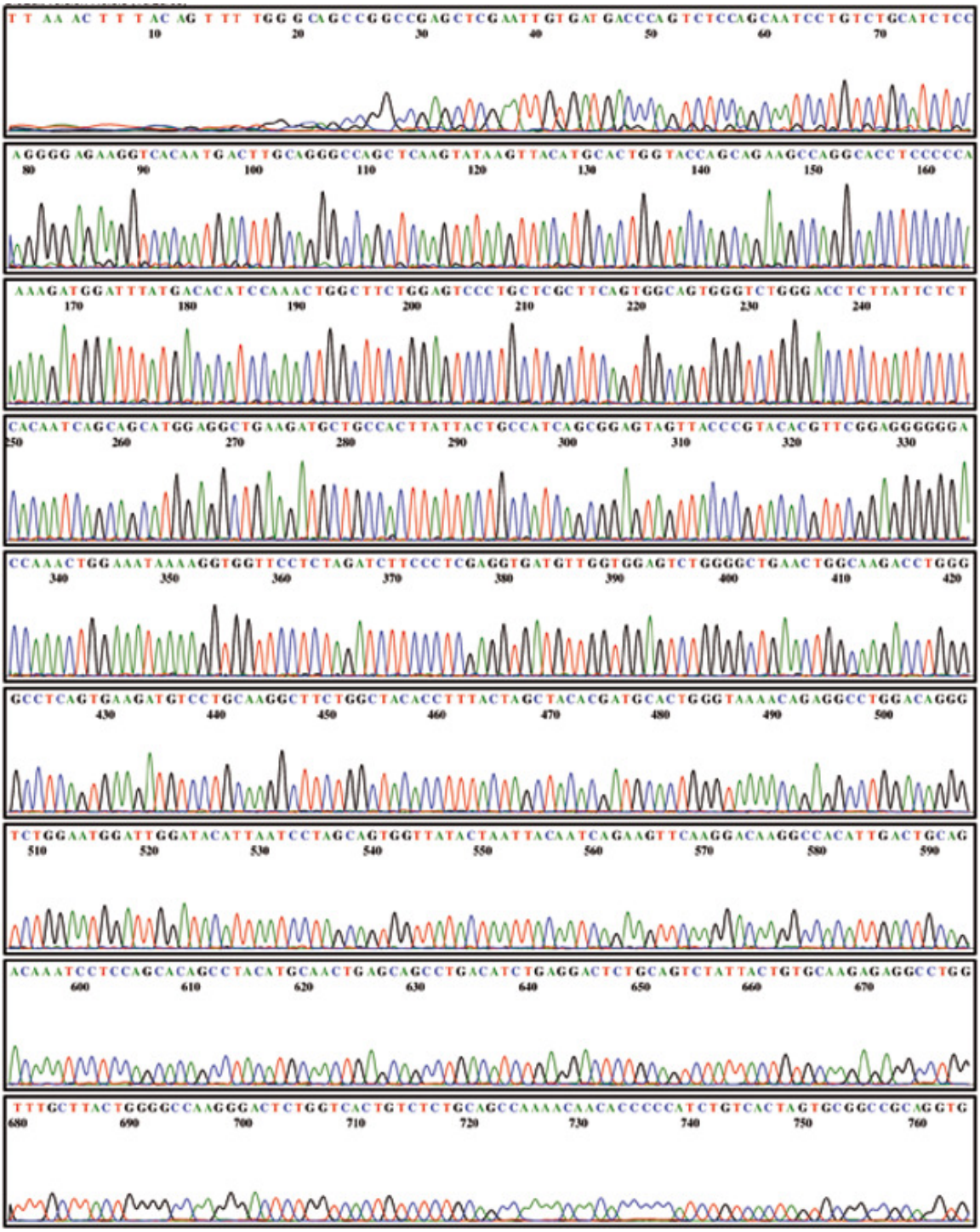

Appendix VI-ii : Chromatograms of scFv sequences – scFv TG69

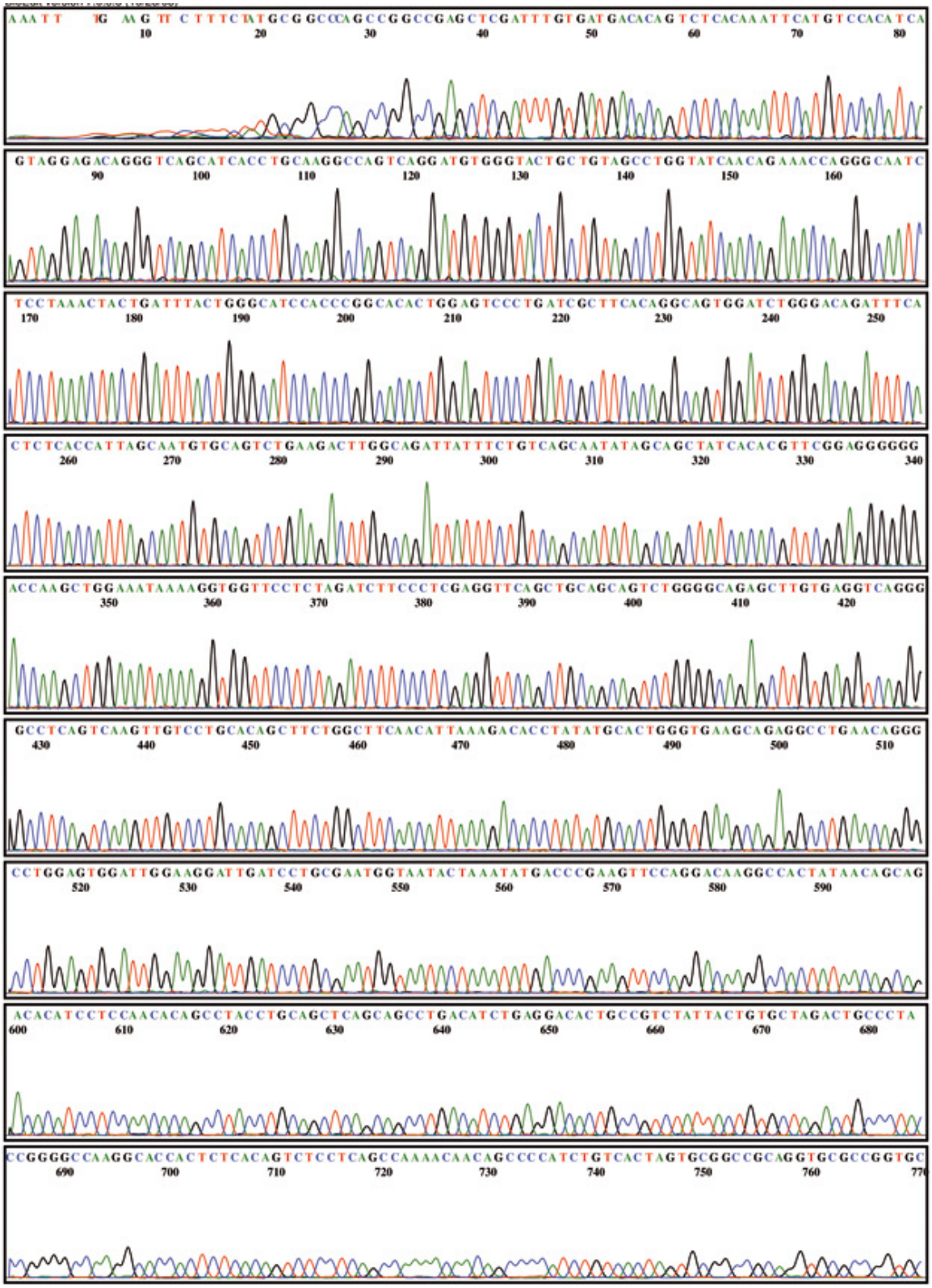

Appendix VI-iii : Chromatograms of scFv sequences – scFv TG116

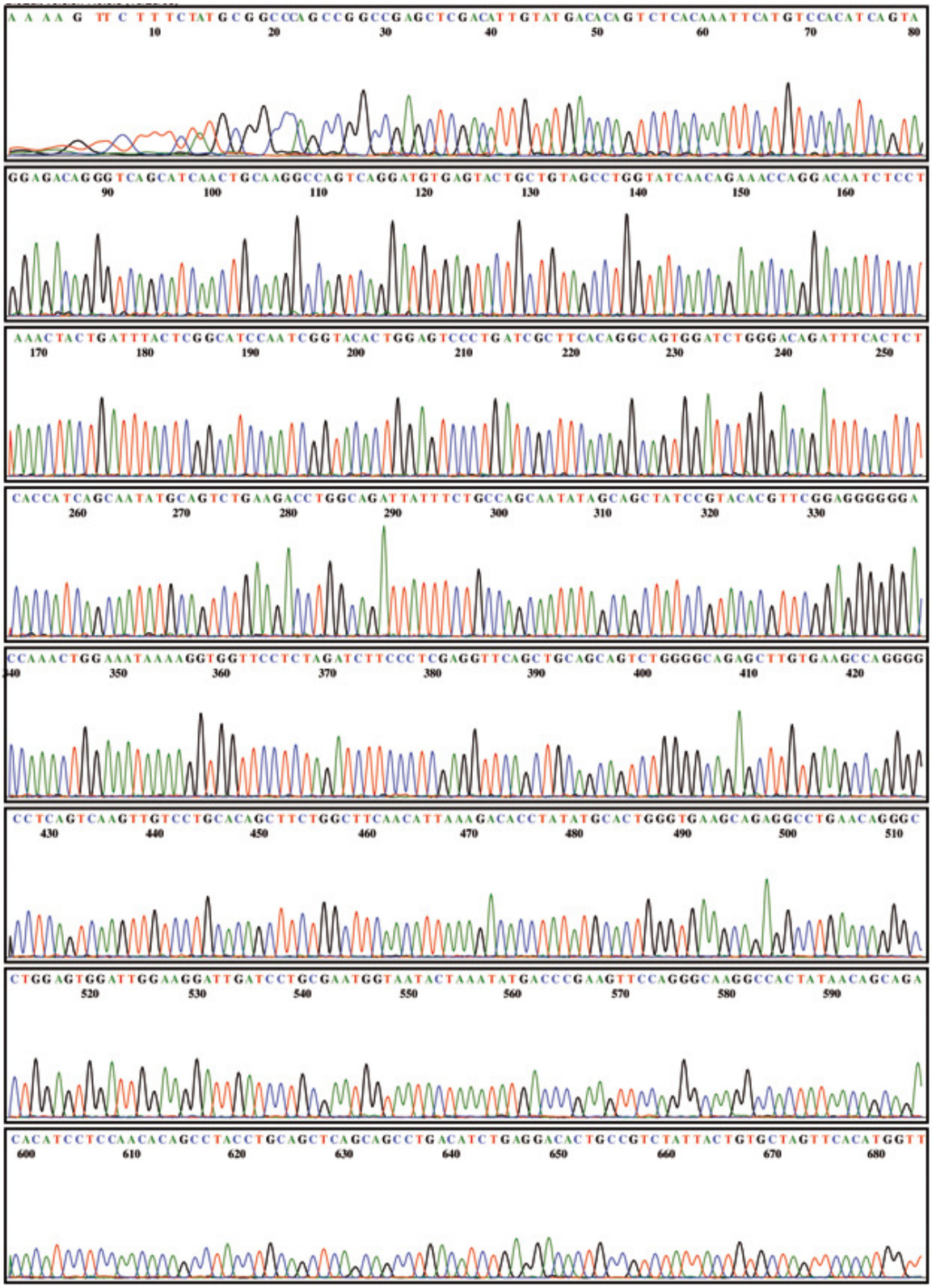

scFv TG116 – continued.

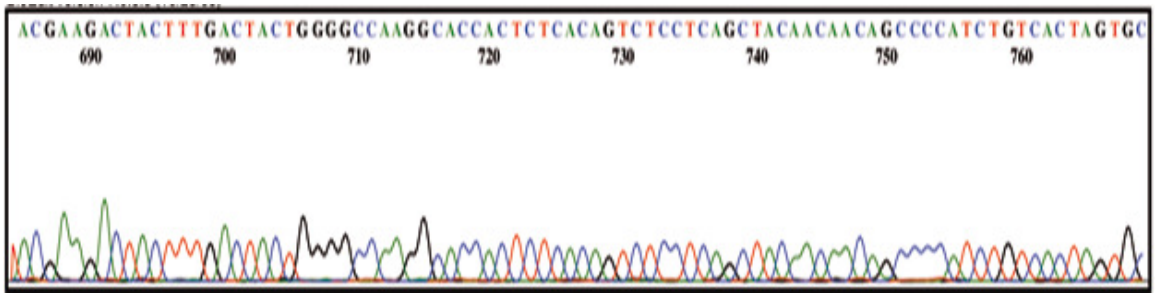

Appendix VI-iv : Chromatograms of scFv sequences – scFv TG130

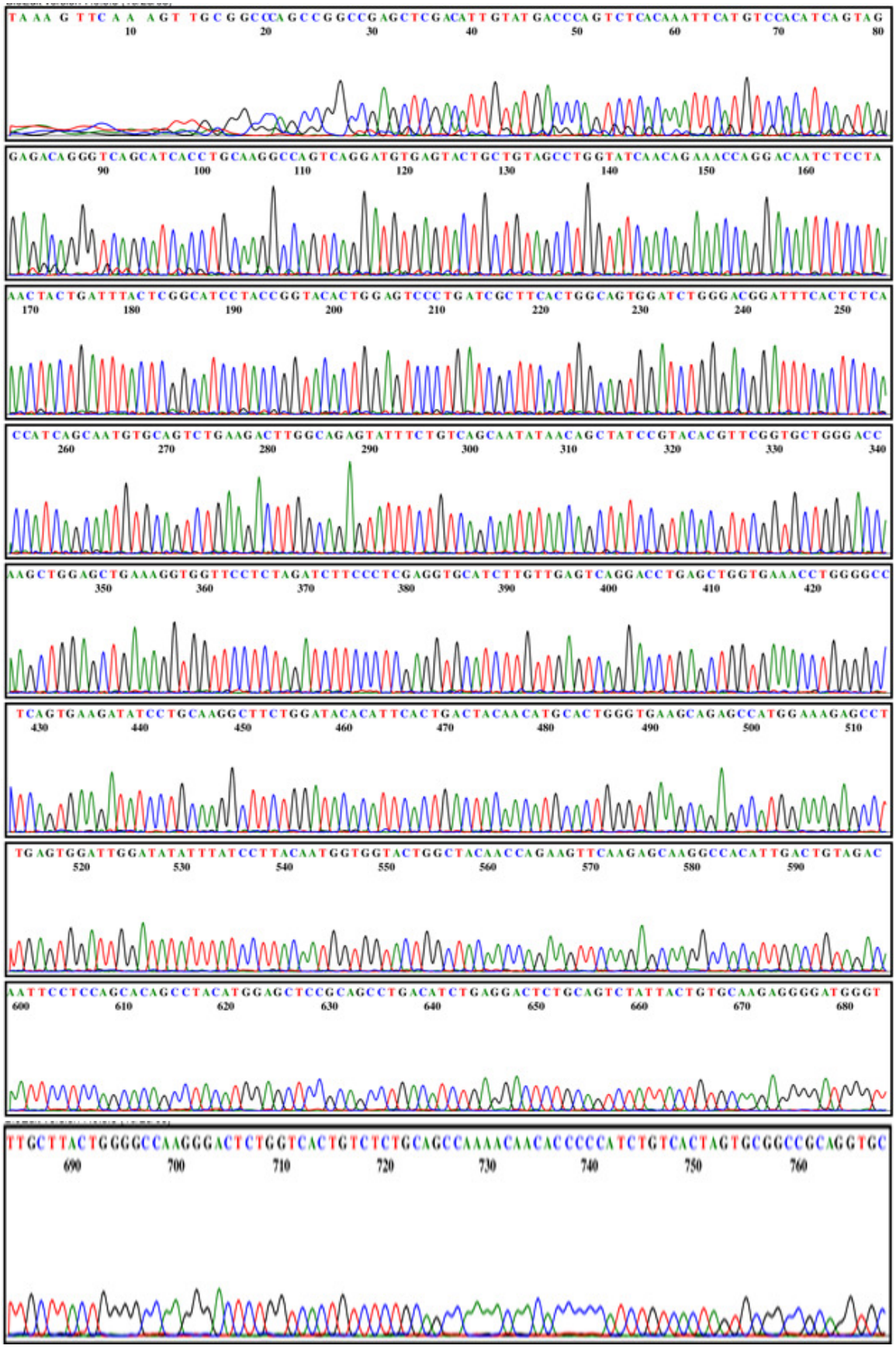

Appendix VI-v : Protein translation of scFv sequences

i. ScFv TG64

M T Q S P A I L S A S P G E K V T M T C R A S S S I S Y M H W Y Q Q K P
G T S P K R W I Y D T S K L A S G V P A R F S G S G S G T S Y S L T I S
S M E A E D A A T Y Y C H Q R S S Y P Y T F G G G T K L E I K G G S S
R S S L E V M L V E S G A E L A R P G A S V K M S C K A S G Y T F T S
Y T M H W V K Q R P G Q G L E W I G Y I N P S S G Y T N Y N Q K F K
D K A T L T A D K S S S T A Y M Q L S S L T S E D S A V Y Y C A R E A
W F A Y W G Q G T L V T V S A

ii. ScFv TG69

M T Q S H K F M S T S V G D R V S I T C K A S Q D V G T A V A W Y Q
Q K P G Q S P K L L I Y W A S T R H T G V P D R F T G S G S G T D F T
L T I S N V Q S E D L A D Y F C Q Q Y S S Y H T F G G G T K L E I K G
G S S R S S L E V Q L Q Q S G A E L V R S G A S V K L S C T A S G F N
I K D T Y M H W V K Q R P E Q G L E W I G R I D P A N G N T K Y D P
K F Q D K A T I T A D T S S N T A Y L Q L S S L T S E D T A V Y Y C A
R L P Y W G Q G T T L T V S S

iii. ScFv TG116

M T Q S H K F M S T S V G D R V S I N C K A S Q D V S T A V A W Y Q
Q K P G Q S P K L L I Y S A S N R Y T G V P D R F T G S G S G T D F T
L T I S N M Q S E D L A D Y F C Q Q Y S S Y P Y T F G G G T K L E I K
G G S S R S S L E V Q L Q Q S G A E L V K P G A S V K L S C T A S G F
N I K D T Y M H W V K Q R P E Q G L E W I G R I D P A N G N T K Y D
P K F Q G K A T I T A D T S S N T A Y L Q L S S L T S E D T A V Y Y C
A S S H G Y E D Y F D Y W G Q G T T L T V S S

iv. ScFv TG130

M T Q S H K F M S T S V G D R V S I T C K A S Q D V S T A V A W Y Q Q
K P G Q S P K L L I Y S A S Y R Y T G V P D R F T G S G S G T D F T L
T I S N V Q S E D L A E Y F C Q Q Y N S Y P Y T F G A G T K L E L K G
G S S R S S L E V H L V E S G P E L V K P G A S V K I S C K A S G Y T
F T D Y N M H W V K Q S H G K S L E W I G Y I Y P Y N G G T G Y N Q
K F K S K A T L T V D N S S S T A Y M E L R S L T S E D S A V Y Y C A
R G D G F A Y W G Q G T L V T V S A

Appendix VII: Chromatograms of truncated scFv sequences

- **Appendix VII-i: Chromatogram of scFv 18**
- **Appendix VII-ii: Chromatogram of scFv 48**
- **Appendix VII-iii: Chromatogram of scFv 103**
- **Appendix VII-iv: Chromatogram of scFv 109**
- **Appendix VII-v: Chromatogram of scFv 118**
- **Appendix VII-vi: Protein translation of truncated scFv sequences**

Appendix VII-i : Chromatograms of truncated scFv sequences – scFv 18 (Stop codon is indicated in red box).

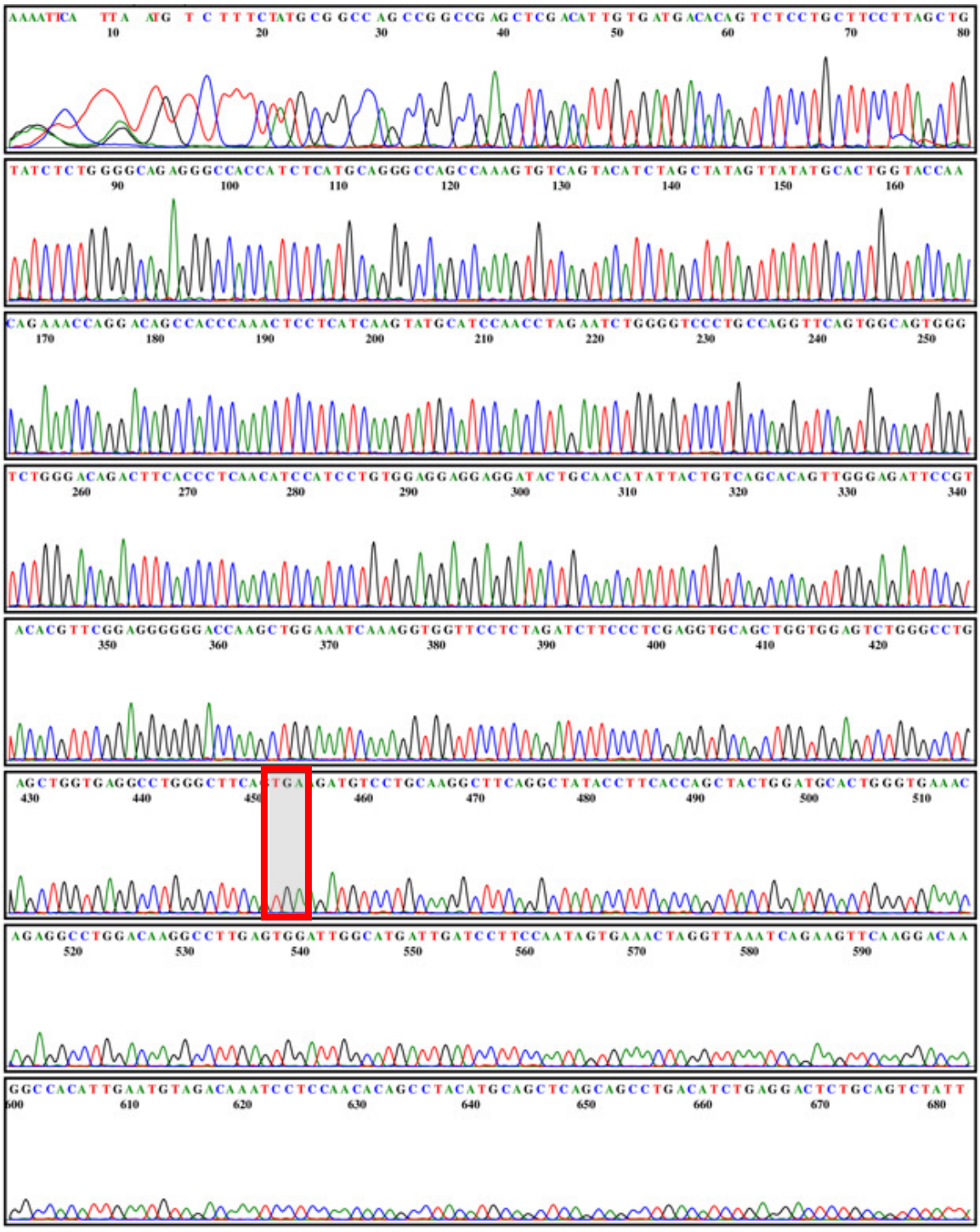

Appendix VII-i i: Chromatograms of truncated scFv sequences – scFv 48 (Stop codon is indicated in red box).

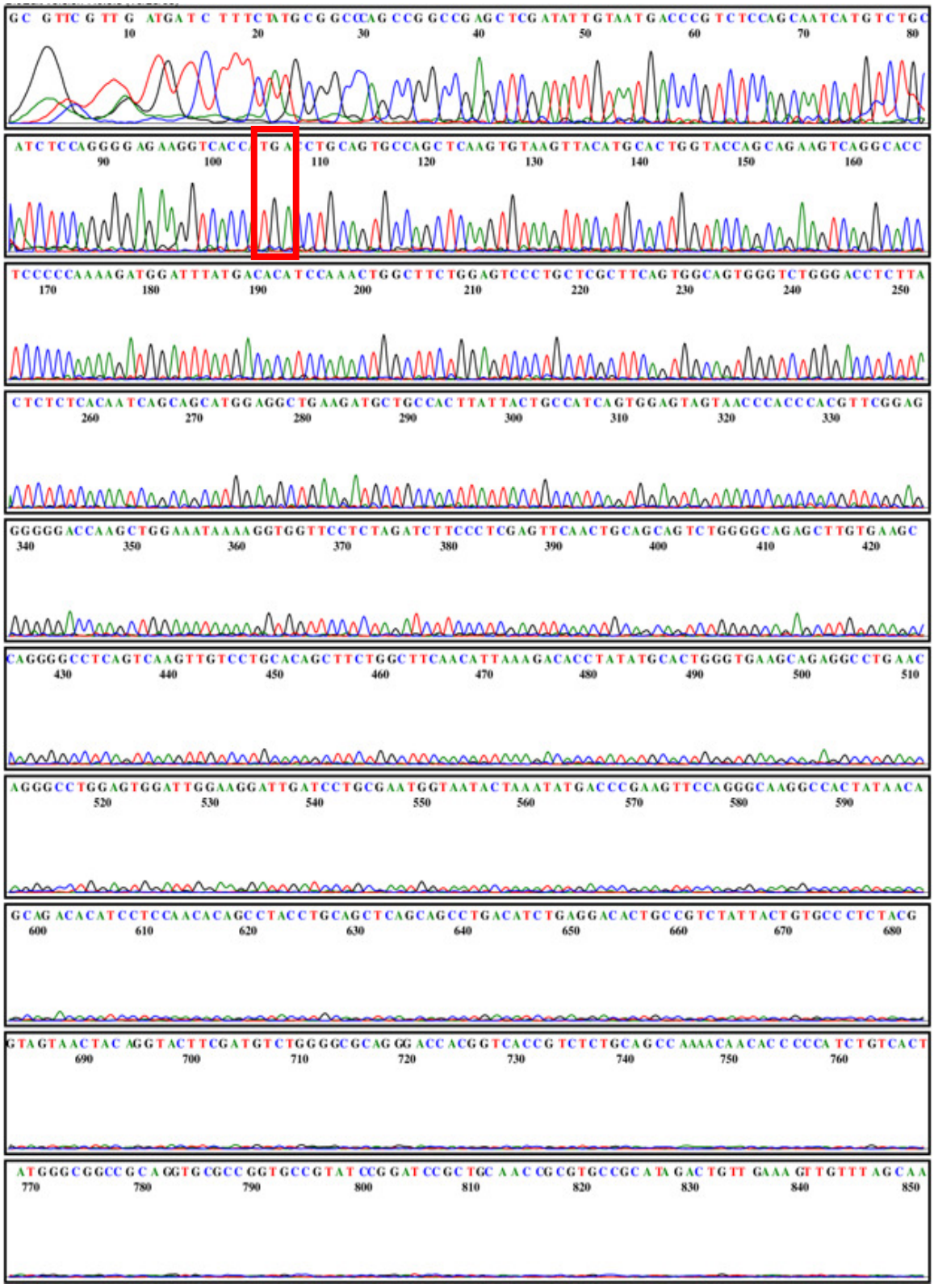

Appendix VII-iii: Chromatograms of truncated scFv sequences – scFv 103 (Stop codon is indicated in red box).

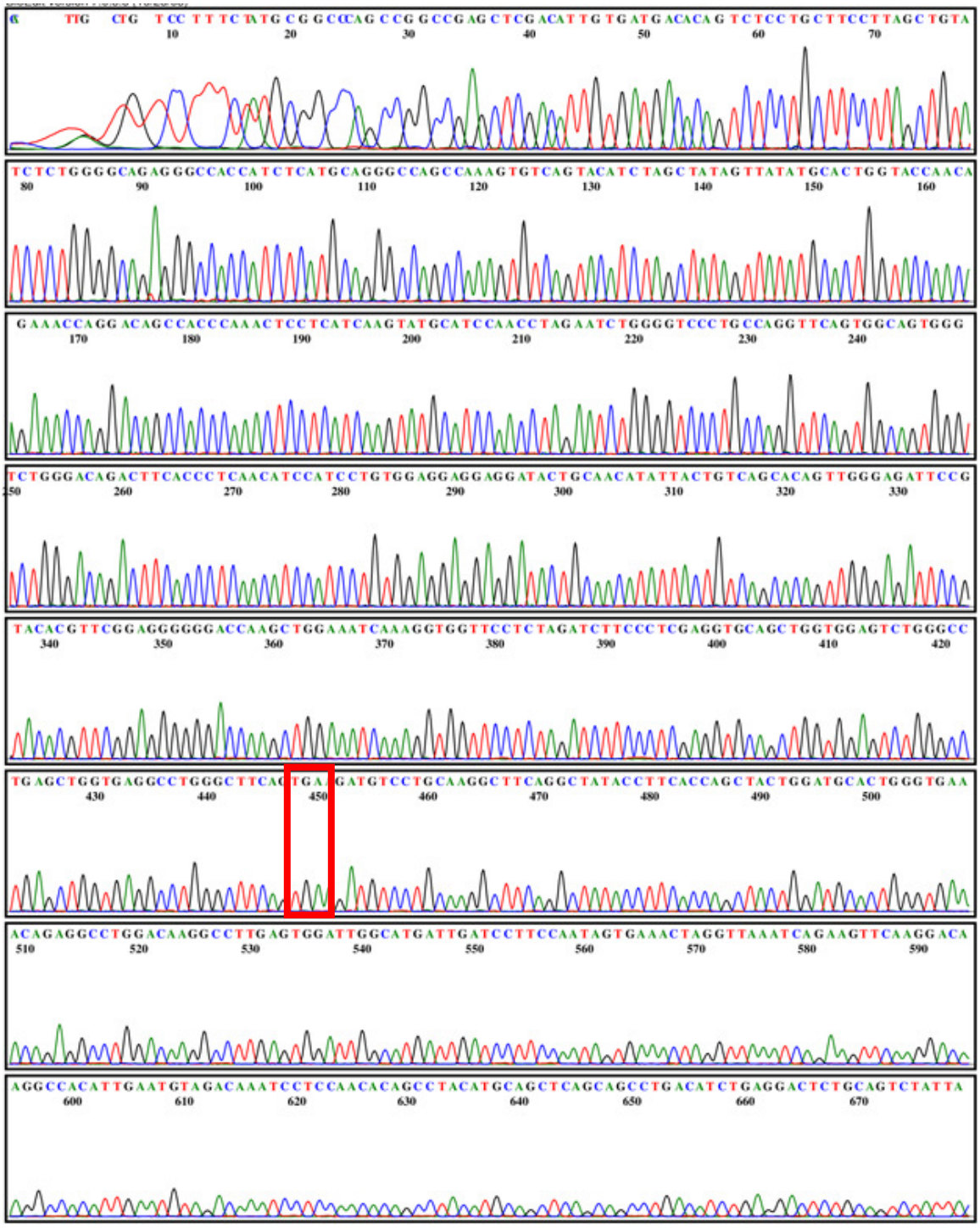

Appendix VII-iv: Chromatograms of truncated scFv sequences – scFv 109 (Stop codon is indicated in red box).

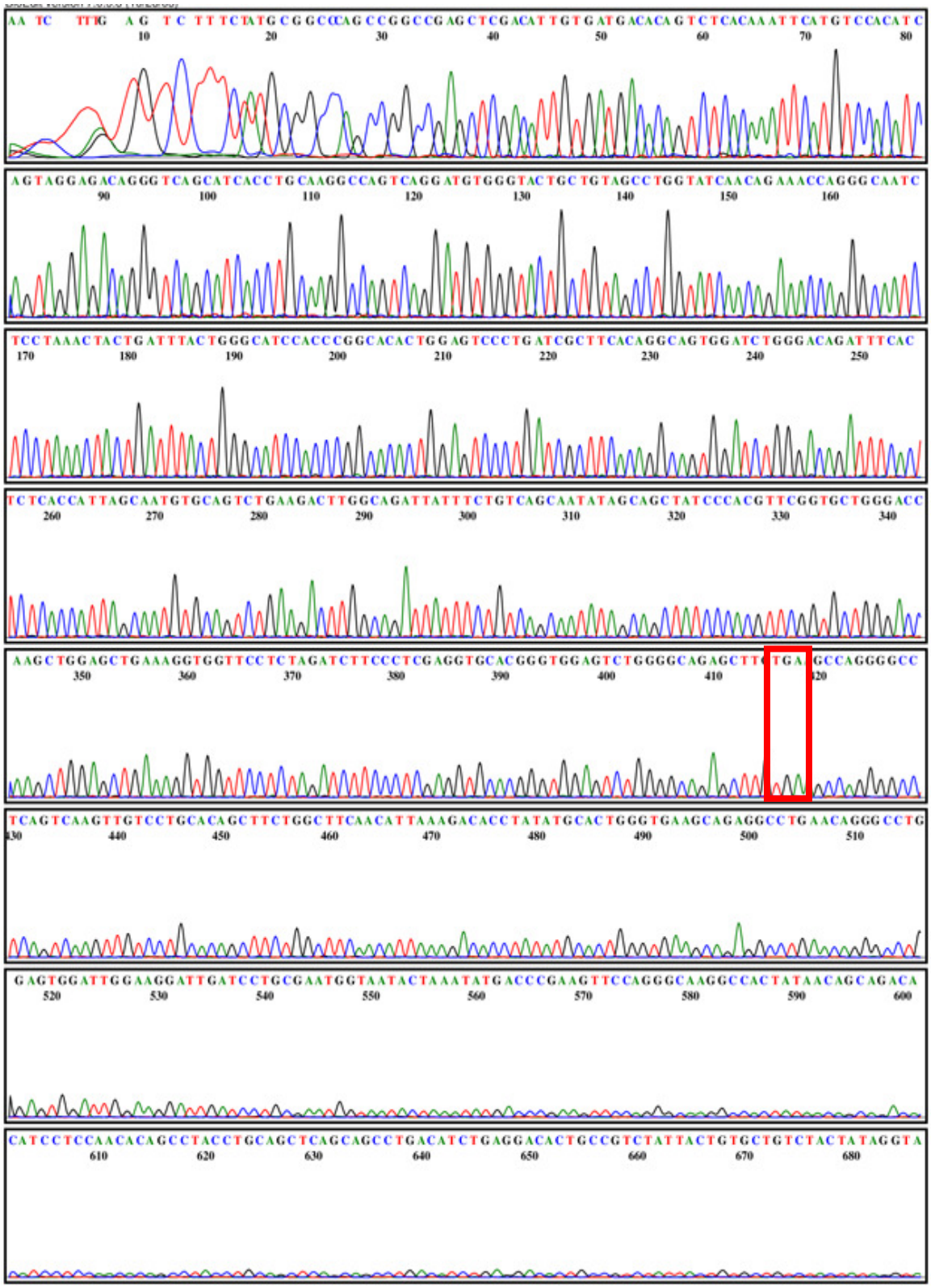

Appendix VII-v: Chromatograms of truncated scFv sequences – scFv 118 (Stop codon is indicated in red box).

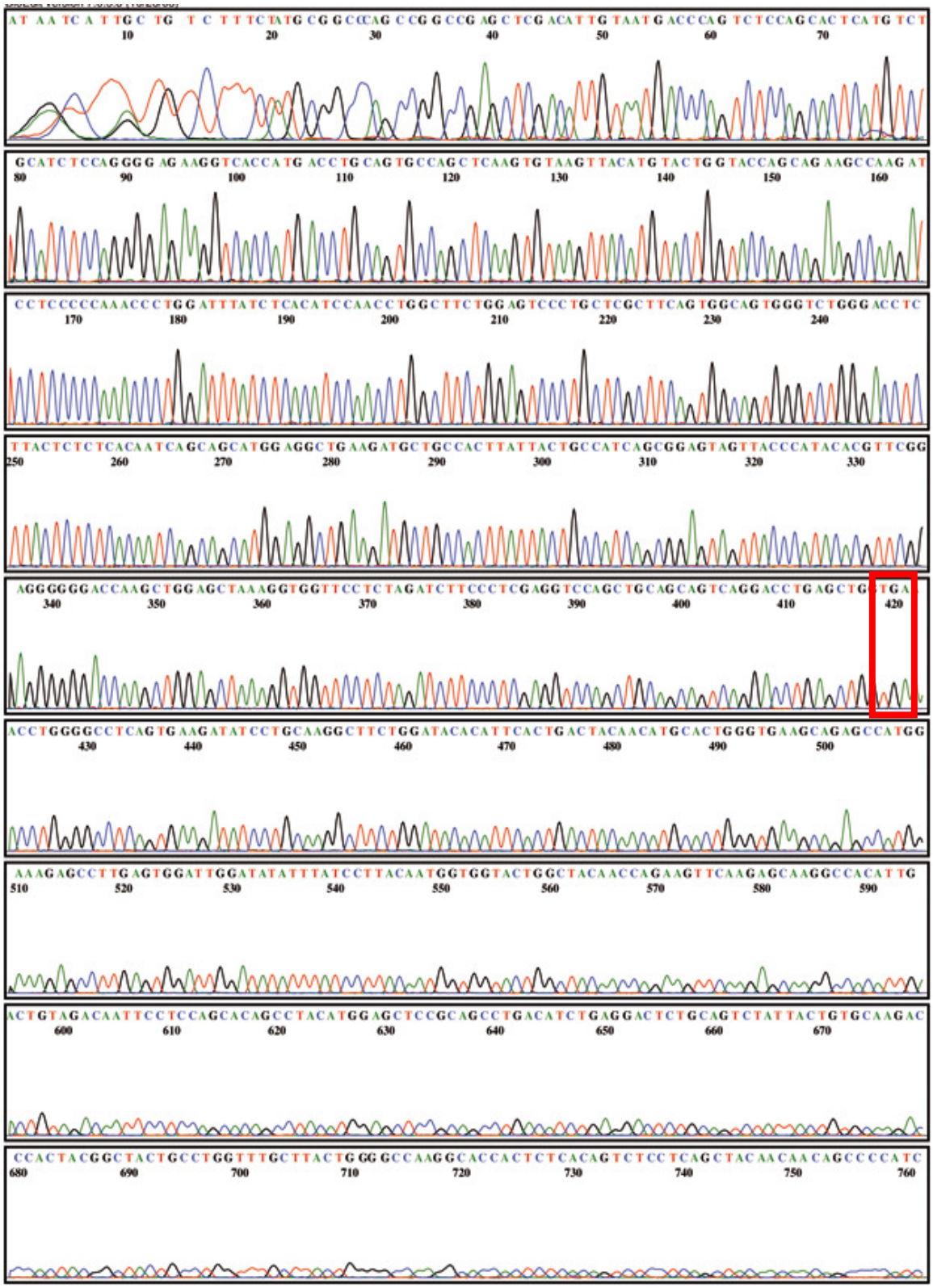

Appendix VII-vi : Protein translation of truncated scFv sequences

scFv 18

MT Q S P A S L A V S L G Q R A T I S C R A S Q S V S T S S Y S YMH
W Y Q Q K P G Q P P K L L I K Y A S N L E S G V P A R F S G S G S G T
D F T L N I H P V E E E D T A T Y Y C Q H S W E I P Y T F G G G T K L
E I K G G S S R S S L E V Q L V E S G P E L V R P G L Q **Stop**

scFv 48

MT R L Q Q S C L H L Q G R R S P **Stop**

scFv 103

MT Q S P A S L A V S L G Q R A T I S C R A S Q S V S T S S Y S YMH
W Y Q Q K P G Q P P K L L I K Y A S N L E S G V P A R F S G S G S G T
D F T L N I H P V E E E D T A T Y Y C Q H S W E I P Y T F G G G T K L
E I K G G S S R S S L E V Q L V E S G P E L V R P G L Q **Stop**

scFv 109

MT Q S H K FMS T S V G D R V S I T C K A S Q D V G T A V A W Y Q
Q K P G Q S P K L L I Y W A S T R H T G V P D R F T G S G S G T D F T
L T I S N V Q S E D L A D Y F C Q Q Y S S Y P T F G A G T K L E L K G
G S S R S S L E V H G W S L G Q S L **Stop**

scFv 118

MT Q S P A LMS A S P G E K V TMT C S A S S S V S YMY W Y Q Q K P
R S S P K P W I Y L T S N L A S G V P A R F S G S G S G T S Y S L T I S
SME A E D A A T Y Y C H Q R S S Y P Y T F G G G T K L E L K V V P L
D L P S R S S C S S Q D L S W **Stop**

Appendix VIII (a): Closest germline sequence homology alignment with biopanned scFv nucleotide and amino acid sequences.

ScFv TG64

V_L

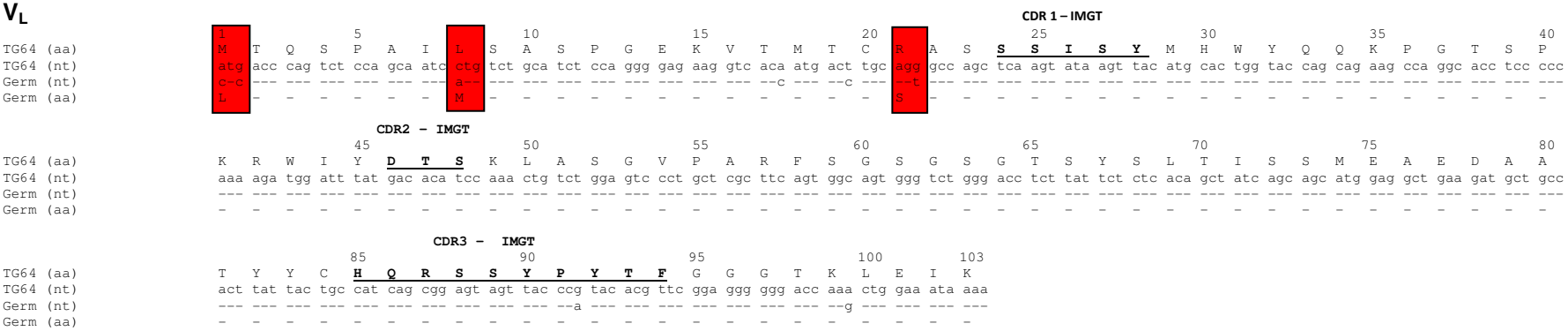

V_H

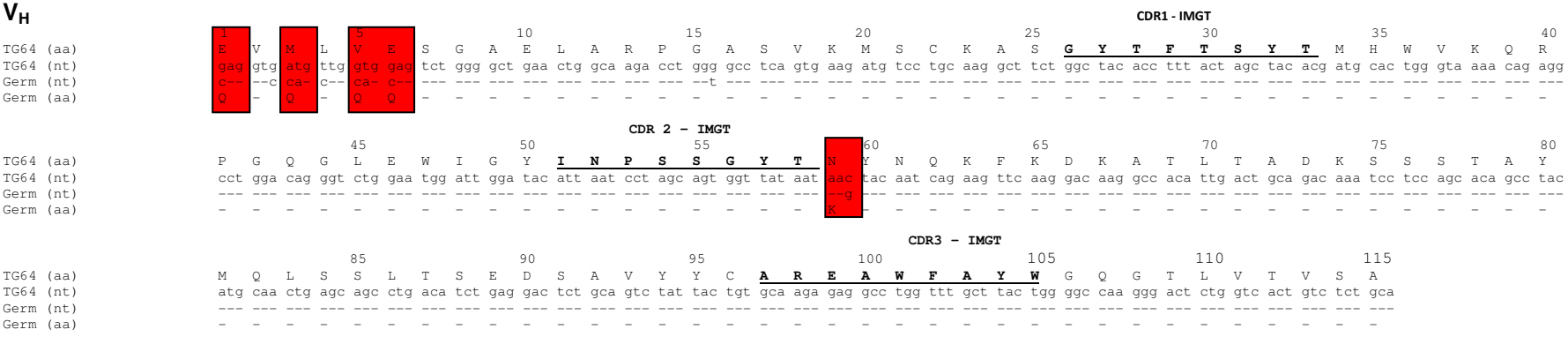

Appendix VIII (b): Closest germline sequence homology alignment with biopanned scFv nucleotide and amino acid sequences.

ScFv TG69

V_L

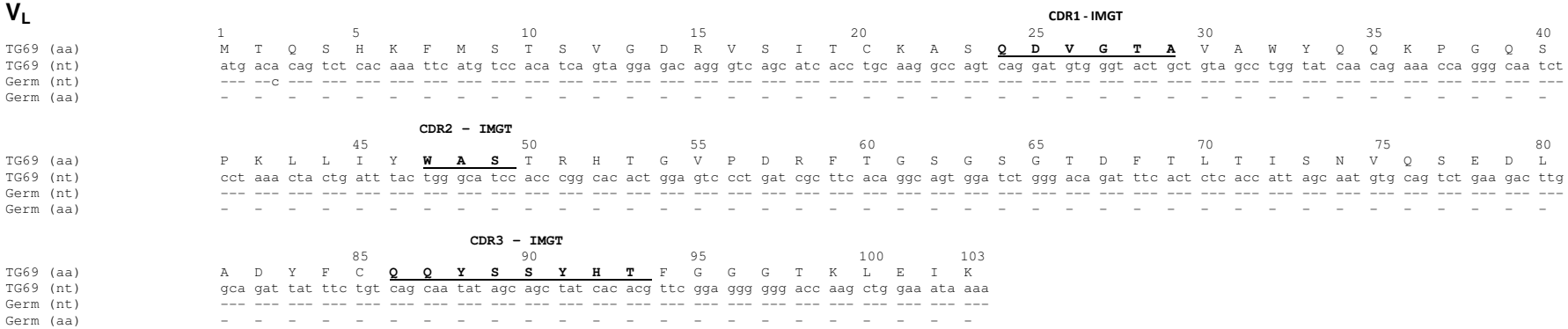

V_H

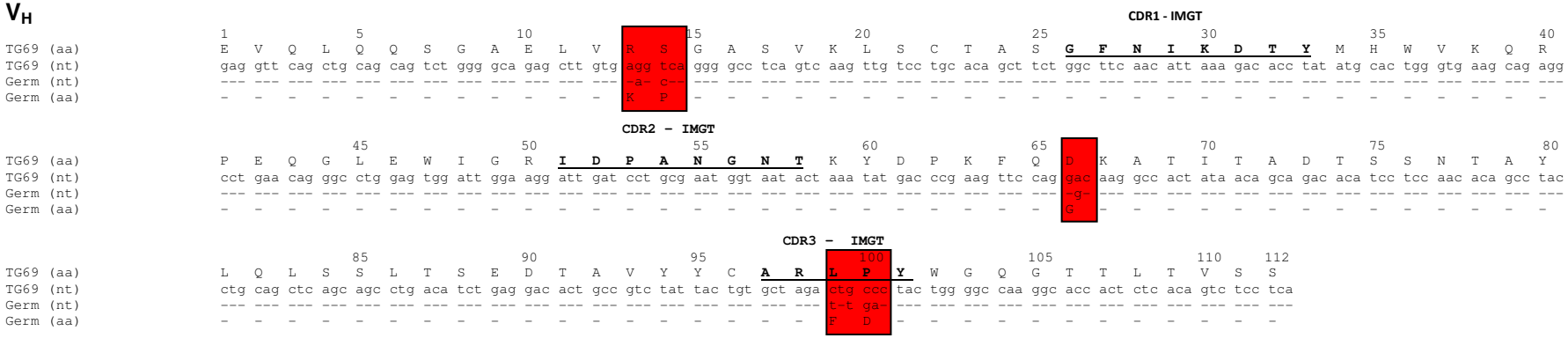

Appendix VIII (c): Closest germline sequence homology alignment with biopanned scFv nucleotide and amino acid sequences.

ScFv TG116

V_L

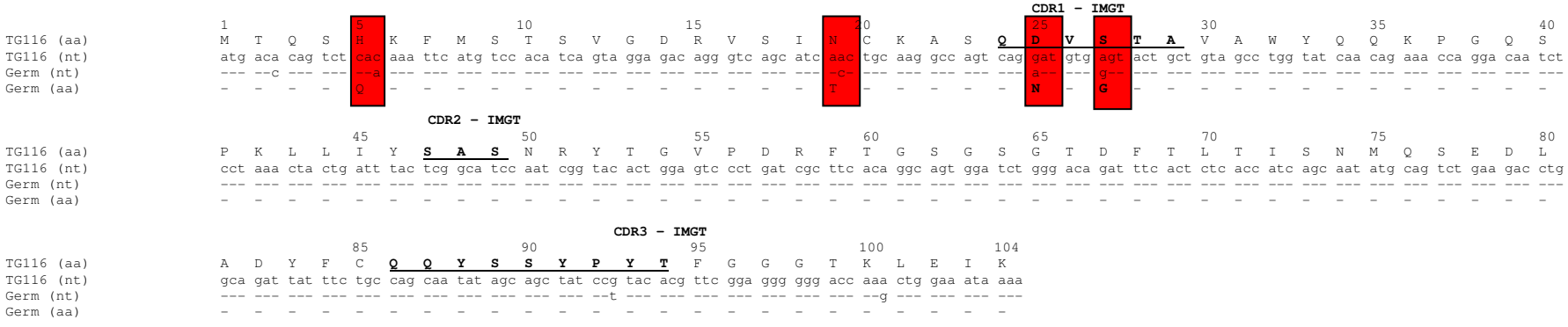

V_H

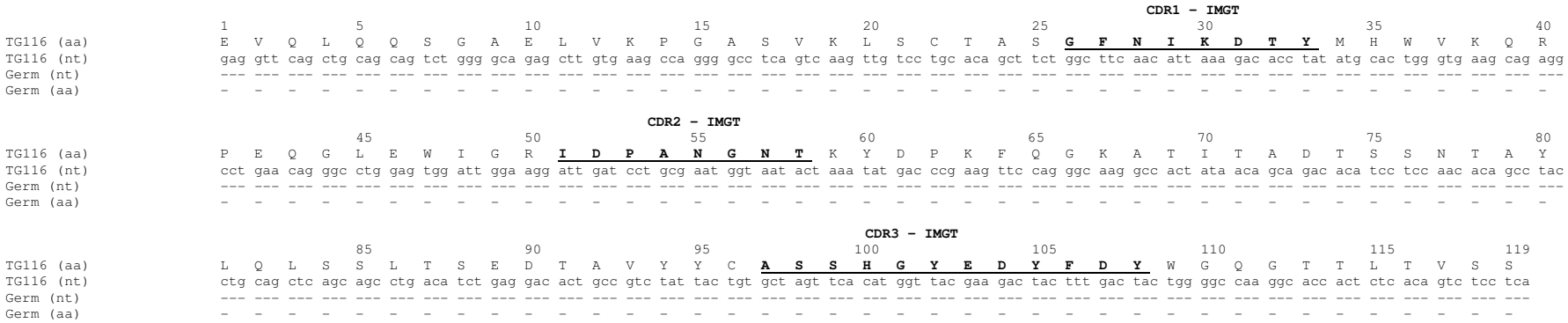

Appendix IX: V-Quest Antibody V-Regions sequence analysis results.

ScFv 64 V_L sequence analysis:

Result summary:	**Productive IGK rearranged sequence** (no stop codon and in-frame junction)		
V-GENE and allele	IGKV4-70*01	score = 1276	identity = **97,75%** (261/267 nt)
J-GENE and allele	IGKJ2*01	score = 176	identity = 97,30% (36/37 nt)
[CDR1-IMGT.CDR2-IMGT.CDR3-IMGT] lengths and AA JUNCTION	[5.3.9]	CHQRSSYPYTF	

ScFv 64 V_H sequence analysis:

Result summary:	**Productive IGH rearranged sequence** (no stop codon and in-frame junction)		
V-GENE and allele	IGHV1-4*01	score = 1345	identity = **96,53%** (278/288 nt)
J-GENE and allele	IGHJ3*01	score = 240	identity = 100,00% (48/48 nt)
D-GENE and allele by IMGT/JunctionAnalysis	No results	-	
[CDR1-IMGT.CDR2-IMGT.CDR3-IMGT] lengths and AA JUNCTION	[8.8.8]	CAREAWFAYW	

ScFv 69 V_L sequence analysis:

Result summary:	**Productive IGK rearranged sequence** (no stop codon and in-frame junction)		
V-GENE and allele	IGKV6-23*01	score = 1336	identity = **99,63%** (269/270 nt)
J-GENE and allele	IGKJ2*01	score = 175	identity = 100,00% (35/35 nt)
[CDR1-IMGT.CDR2-IMGT.CDR3-IMGT] lengths and AA JUNCTION	[6.3.8]	CQQYSSYHTF	

ScFv 69 V_H sequence analysis:

Result summary:	**Productive IGH rearranged sequence** (no stop codon and in-frame junction)		
V-GENE and allele	IGHV14-3*02	score = 1408	identity = **98,96%** (285/288 nt)
J-GENE and allele	IGHJ2*01	score = 179	identity = 90,70% (39/43 nt)
D-GENE and allele by IMGT/JunctionAnalysis	IGHD6-1*01	D-REGION is in reading frame 1	
[CDR1-IMGT.CDR2-IMGT.CDR3-IMGT] lengths and AA JUNCTION	[8.8.5]	CARLPYW	

ScFv 116 V_L sequence analysis:

Result summary:	**Productive IGK rearranged sequence** (no stop codon and in-frame junction)		
V-GENE and allele	IGKV6-13*01	score = 1300	identity = **98,15%** (265/270 nt)
J-GENE and allele	IGKJ2*01	score = 176	identity = 97,30% (36/37 nt)
[CDR1-IMGT.CDR2-IMGT.CDR3-IMGT] lengths and AA JUNCTION	[6.3.9]	CQQYSSYPYTF	

ScFv 116 V_H sequence analysis:

Result summary:	**Productive IGH rearranged sequence** (no stop codon and in-frame junction)		
V-GENE and allele	IGHV14-3*02	score = 1435	identity = **100,00%** (288/288 nt)
J-GENE and allele	IGHJ2*01	score = 240	identity = 100,00% (48/48 nt)
D-GENE and allele by IMGT/JunctionAnalysis	IGHD2-2*01	D-REGION is in reading frame 3	
[CDR1-IMGT.CDR2-IMGT.CDR3-IMGT] lengths and AA JUNCTION	[8.8.12]	CASSHGYEDYFDYW	

ScFv 130 V_L sequence analysis:

Result summary:	**Productive IGK rearranged sequence** (no stop codon and in-frame junction)		
V-GENE and allele	IGKV6-17*01	score = 1255	identity = **95,93%** (259/270 nt)
J-GENE and allele	IGKJ5*01	score = 167	identity = 94,59% (35/37 nt)
[CDR1-IMGT.CDR2-IMGT.CDR3-IMGT] lengths and AA JUNCTION	[6.3.9]	CQQYNSYPYTF	

ScFv 130 V_H sequence analysis:

Result summary:	**Productive IGH rearranged sequence** (no stop codon and in-frame junction)		
V-GENE and allele	IGHV1S29*02	score = 1372	identity = **97,57%** (281/288 nt)
J-GENE and allele	IGHJ3*01	score = 213	identity = 93,75% (45/48 nt)
D-GENE and allele by IMGT/JunctionAnalysis	No results	-	
[CDR1-IMGT.CDR2-IMGT.CDR3-IMGT] lengths and AA JUNCTION	[8.8.8]	CARGDGFAYW	

Appendix X: Data for binding titers of phage-scFv biopanning experiments.

a) ScFv binding titers of monoclonal scFv screenings.

	ScFv Binding Titers (cfu / ml)			
	TG64	**TG69**	**TG116**	**TG130**
Sample 1	3.00×10^5	3.35×10^5	1.25×10^6	4.00×10^5
Sample 2	1.20×10^5	3.50×10^5	6.75×10^5	4.15×10^5
Sample 3	9.60×10^4	3.00×10^5	4.20×10^5	4.00×10^5
Sample 4	1.00×10^6	2.60×10^5	3.00×10^5	1.50×10^5
Sample 5	8.50×10^5	2.40×10^5	1.75×10^5	8.00×10^4
Sample 6	3.50×10^5	3.50×10^5	1.80×10^5	8.70×10^4
Sample 7	2.65×10^5	4.00×10^5	1.46×10^5	5.00×10^4
Sample 8	3.70×10^5	5.40×10^5	1.35×10^6	6.00×10^4
Sample 9	N/D	N/D	N/D	6.00×10^4
Sample 10	N/D	N/D	N/D	4.10×10^4
Sample Mean	**4.19×10^5**	**3.47×10^5**	**5.62×10^5**	**1.74×10^5**
Sample Standard error	1.17×10^5	3.31×10^4	1.72×10^5	5.12×10^4
Negative Control (NC) Mean	**2.90×10^5**	**1.20×10^5**	**6.00×10^5**	**3.75×10^4**
NC Standard error	0.00^{ϕ}	0.00^{ϕ}	0.00^{ϕ}	7.50×10^3

*N/D, not determined.

$^{\phi}$ Although duplicate experiments were carried out for these negative control sets, titers could not be determined due to media plates were confluent with bacterial colonies from the phage-output recovery fraction.

b) ScFv binding titers of parental scFv TG130 and affinity-matured scFv TP60 at different off-rate durations.

	ScFv Binding Titers (cfu / ml)			
	Off-rate 50.0 min		**Off-rate 100.0 min**	
	TG130	**TP60**	**TG130**	**TP60**
Replicate 1	2.73×10^5	9.80×10^5	7.00×10^3	1.40×10^4
Replicate 2	1.61×10^5	N/D*	7.00×10^3	1.10×10^4
Sample Mean	**2.17×10^5**	**9.80×10^5**	**7.00×10^3**	**1.25×10^4**
Sample Standard Error	5.60×10^4	0.00	0.00	1.50×10^3
Negative Control (NC) Mean	**9.80×10^4**	**4.94×10^5**	**8.87×10^3**	**6.07×10^3**
NC Standard Error	0.00	1.02×10^5	1.87×10^3	6.17×10^2

* N/D, not determined. ScFv binding titers could not be determined as media plate was confluent with bacterial colonies from the phage-output recovery fraction.

c) Monoclonal TG-RGYW mutant scFv clones binding titers.

	ScFv Binding Titers (cfu / ml)					
	TG130	**RA15**	**RS55**	**TP60**	**RT51**	**LT3**
Replicate 1	7.00×10^3	1.40×10^3	7.00×10^3	1.40×10^4	3.50×10^3	1.40×10^4
Replicate 2	7.00×10^3	4.20×10^3	4.90×10^3	1.10×10^4	2.80×10^3	4.90×10^3
Replicate 3	5.60×10^3	-	-	7.00×10^3	-	4.90×10^3
Sample Mean	$\mathbf{6.53 \times 10^3}$	$\mathbf{2.80 \times 10^3}$	$\mathbf{5.95 \times 10^3}$	$\mathbf{1.07 \times 10^4}$	$\mathbf{3.15 \times 10^3}$	$\mathbf{7.93 \times 10^3}$
Sample Standard error	4.67×10^2	1.40×10^3	1.05×10^3	2.03×10^3	3.50×10^2	3.03×10^3

Appendix XI: Statistical test results of the difference in scFv TG130 antibody recognition between target antigen *T. gondii* and negative control cell line. Statistical significance comparison between the two test groups were assessed using the non-parametric Wilcoxon Mann-Whitney one-tailed test at alpha value = 0.05, and n = 12. Results were obtained using the Analyse-it for Windows v2.22 statistics software.

Analyse-it v2.22

Test	**Compare Groups - Mann-Whitney test**		
	Groups: ScFv 130 > NC		
Performed by	Sherene	Date	17 September 2010

n	12

Groups	n	Rank sum	Mean rank	U
ScFv 130	10	74.0	7.40	1.0
NC	2	4.0	2.00	19.0

Median difference	4.600E+04	
97.0% CI	5.000E+03 to +∞	(exact)
Mann-Whitney's statistic	1.0	
Z statistic	-	
1-tailed p	0.0303	(exact tables used, 33% ties)

Appendix XII: Sequencing results of TG130-RGYW mutant scFv clones.

- **Appendix XII-i: Alignment of 5 randomly selected RGYW clones.**
- **Appendix XII-ii: Chromatogram of scFv TG130-RGYW 1**
- **Appendix XII-iii: Chromatogram of scFv TG130-RGYW 3**
- **Appendix XII-iv: Chromatogram of scFv TG130-RGYW 4**
- **Appendix XII-v: Chromatogram of scFv TG130-RGYW 21**
- **Appendix XII-vi: Chromatogram of scFv TG130-RGYW 27**
- **Appendix XII-vii: Alignment of 5 selected RGYW scFv clones from biopanning**
- **Appendix XII-viii: Chromatogram of scFv TP60**
- **Appendix XII-ix: Chromatogram of scFv RA15**
- **Appendix XII-x: Chromatogram of scFv RS55**
- **Appendix XII-xi: Chromatogram of scFv RT51**
- **Appendix XII-xii: Chromatogram of scFv LT3**

Appendix XII-i: Alignment of 5 randomly selected RGYW clones.

```
Alignment: C:\Users\Sherene\Desktop\ScFv Thesis & Papers\scFv Sequences_
RGYW Mutants\TG130 RGYW alignment.fas

                ....|....| ....|....| ....|....| ....|....| ....|....|
                      10         20         30         40         50
RGYW2-1_pC      ATGACCCAGT CTCACAAATT CATGTCCACA TCAGTAGGAG ACAGGGTCAG
RGYW2-3_pC      ATGACCCAGT CTCACAAATT CATGTCCACA TCAGTAGGAG ACAGGGTCAG
RGYW2-4_pC      ATGACCCAGT CTCACAAATT CATGTCCACA TCAGTAGGAG ACAGGGTCAG
RGYW2-27_p      ATGACCCAGT CTCACAAATT CATGTCCACA TCAGTAGGAG ACAGGGTCAG
RGYW2-21_p      ATGACCCAGT CTCACAAATT CATGTCCACA TCAGTAGGAG ACAGGGTCAG

                ....|....| ....|....| ....|....| ....|....| ....|....|
                      60         70         80         90        100
RGYW2-1_pC      CATCACCTGC AAGGCCAGTC AGGATGTGCT GGCTGCTGTA GCCTGGTATC
RGYW2-3_pC      CATCACCTGC AAGGCCAGTC AGGATGTGAG GTCTGCTGTA GCCTGGTATC
RGYW2-4_pC      CATCACCTGC AAGGCCAGTC AGGATGTGAC GGCTGCTGTA GCCTGGTATC
RGYW2-27_p      CATCACCTGC AAGGCCAGTC AGGATGTGAA CGCTGCTGTA GCCTGGTATC
RGYW2-21_p      CATCACCTGC AAGGCCAGTC AGGATGTGAG TACTGCTGTA GCCTGGTATC

                ....|....| ....|....| ....|....| ....|....| ....|....|
                     110        120        130        140        150
RGYW2-1_pC      AACAGAAACC AGGACAATCT CCTAAACTAC TGATTTACTC GGCATCCTAC
RGYW2-3_pC      AACAGAAACC AGGACAATCT CCTAAACTAC TGATTTACTC GGCATCCTAC
RGYW2-4_pC      AACAGAAACC AGGACAATCT CCTAAACTAC TGATTTACTC GGCATCCTAC
RGYW2-27_p      AACAGAAACC AGGACAATCT CCTAAACTAC TGATTTACTC GGCATCCTAC
RGYW2-21_p      AACAGAAACC AGGACAATCT CCTAAACTAC TGATTTACTC GGCATCCTAC

                ....|....| ....|....| ....|....| ....|....| ....|....|
                     160        170        180        190        200
RGYW2-1_pC      CGGTACACTG GAGTCCCTGA TCGCTTCACT GGCAGTGGAT CTGGGACGGA
RGYW2-3_pC      CGGTACACTG GAGTCCCTGA TCGCTTCACT GGCAGTGGAT CTGGGACGGA
RGYW2-4_pC      CGGTACACTG GAGTCCCTGA TCGCTTCACT GGCAGTGGAT CTGGGACGGA
RGYW2-27_p      CGGTACACTG GAGTCCCTGA TCGCTTCACT GGCAGTGGAT CTGGGACGGA
RGYW2-21_p      CGGTACACTG GAGTCCCTGA TCGCTTCACT GGCAGTGGAT CTGGGACGGA

                ....|....| ....|....| ....|....| ....|....| ....|....|
                     210        220        230        240        250
RGYW2-1_pC      TTTCACTCTC ACCATCAGCA ATGTGCAGTC TGAAGACTTG GCAGAGTATT
RGYW2-3_pC      TTTCACTCTC ACCATCAGCA ATGTGCAGTC TGAAGACTTG GCAGAGTATT
RGYW2-4_pC      TTTCACTCTC ACCATCAGCA ATGTGCAGTC TGAAGACTTG GCAGAGTATT
RGYW2-27_p      TTTCACTCTC ACCATCAGCA ATGTGCAGTC TGAAGACTTG GCAGAGTATT
RGYW2-21_p      TTTCACTCTC ACCATCAGCA ATGTGCAGTC TGAAGACTTG GCAGAGTATT

                ....|....| ....|....| ....|....| ....|....| ....|....|
                     260        270        280        290        300
RGYW2-1_pC      TCTGTCAGCA ATATAACAGC TATCCGTACA CGTTCGGTGC TGGGACCAAG
RGYW2-3_pC      TCTGTCAGCA ATATAACAGC TATCCGTACA CGTTCGGTGC TGGGACCAAG
RGYW2-4_pC      TCTGTCAGCA ATATAACAGC TATCCGTACA CGTTCGGTGC TGGGACCAAG
RGYW2-27_p      TCTGTCAGCA ATATAACAGC TATCCGTACA CGTTCGGTGC TGGGACCAAG
RGYW2-21_p      TCTGTCAGCA ATATAACAGC TATCCGTACA CGTTCGGTGC TGGGACCAAG

                ....|....| ....|....| ....|....| ....|....| ....|....|
                     310        320        330        340        350
RGYW2-1_pC      CTGGAGCTGA AAGGTGGTTC CTCTAGATCT TCCCTCGAGG TGCATCTTGT
RGYW2-3_pC      CTGGAGCTGA AAGGTGGTTC CTCTAGATCT TCCCTCGAGG TGCATCTTGT
RGYW2-4_pC      CTGGAGCTGA AAGGTGGTTC CTCTAGATCT TCCCTCGAGG TGCATCTTGT
RGYW2-27_p      CTGGAGCTGA AAGGTGGTTC CTCTAGATCT TCCCTCGAGG TGCATCTTGT
RGYW2-21_p      CTGGAGCTGA AAGGTGGTTC CTCTAGATCT TCCCTCGAGG TGCATCTTGT

                ....|....| ....|....| ....|....| ....|....| ....|....|
                     360        370        380        390        400
RGYW2-1_pC      TGAGTCAGGA CCTGAGCTGG TGAAACCTGG GGCCTCAGTG AAGATATCCT
RGYW2-3_pC      TGAGTCAGGA CCTGAGCTGG TGAAACCTGG GGCCTCAGTG AAGATATCCT
RGYW2-4_pC      TGAGTCAGGA CCTGAGCTGG TGAAACCTGG GGCCTCAGTG AAGATATCCT
```

```
RGYW2-27_p    TGAGTCAGGA CCTGAGCTGG TGAAACCTGG GGCCTCAGTG AAGATATCCT
RGYW2-21_p    TGAGTCAGGA CCTGAGCTGG TGAAACCTGG GGCCTCAGTG AAGATATCCT

                        410        420        430        440        450
RGYW2-1_pC    GCAAGGCTTC TGGATACACA TTCACTGACT ACAACATGCA CTGGGTGAAG
RGYW2-3_pC    GCAAGGCTTC TGGATACACA TTCACTGACT ACAACATGCA CTGGGTGAAG
RGYW2-4_pC    GCAAGGCTTC TGGATACACA TTCACTGACT ACAACATGCA CTGGGTGAAG
RGYW2-27_p    GCAAGGCTTC TGGATACACA TTCACTGACT ACAACATGCA CTGGGTGAAG
RGYW2-21_p    GCAAGGCTTC TGGATACACA TTCACTGACT ACAACATGCA CTGGGTGAAG

                        460        470        480        490        500
RGYW2-1_pC    CAGAGCCATG GAAAGAGCCT TGAGTGGATT GGATATATTT ATCCTTACAA
RGYW2-3_pC    CAGAGCCATG GAAAGAGCCT TGAGTGGATT GGATATATTT ATCCTTACAA
RGYW2-4_pC    CAGAGCCATG GAAAGAGCCT TGAGTGGATT GGATATATTT ATCCTTACAA
RGYW2-27_p    CAGAGCCATG GAAAGAGCCT TGAGTGGATT GGATATATTT ATCCTTACAA
RGYW2-21_p    CAGAGCCATG GAAAGAGCCT TGAGTGGATT GGATATATTT ATCCTTACAA

                        510        520        530        540        550
RGYW2-1_pC    TGGTGGTACT GGCTACAACC AGAAGTTCAA GAGCAAGGCC ACATTGACTG
RGYW2-3_pC    TGGTGGTACT GGCTACAACC AGAAGTTCAA GAGCAAGGCC ACATTGACTG
RGYW2-4_pC    TGGTGGTACT GGCTACAACC AGAAGTTCAA GAGCAAGGCC ACATTGACTG
RGYW2-27_p    TGGTGGTACT GGCTACAACC AGAAGTTCAA GAGCAAGGCC ACATTGACTG
RGYW2-21_p    TGGTGGTACT GGCTACAACC AGAAGTTCAA GAGCAAGGCC ACATTGACTG

                        560        570        580        590        600
RGYW2-1_pC    TAGACAATTC CTCCAGCACA GCCTACATGG AGCTCCGCAG CCTGACATCT
RGYW2-3_pC    TAGACAATTC CTCCAGCACA GCCTACATGG AGCTCCGCAG CCTGACATCT
RGYW2-4_pC    TAGACAATTC CTCCAGCACA GCCTACATGG AGCTCCGCAG CCTGACATCT
RGYW2-27_p    TAGACAATTC CTCCAGCACA GCCTACATGG AGCTCCGCAG CCTGACATCT
RGYW2-21_p    TAGACAATTC CTCCAGCACA GCCTACATGG AGCTCCGCAG CCTGACATCT

                        610        620        630        640        650
RGYW2-1_pC    GAGGACTCTG CAGTCTATTA CTGTGCAAGA GGGGATGGGT TTGCTTACTG
RGYW2-3_pC    GAGGACTCTG CAGTCTATTA CTGTGCAAGA GGGGATGGGT TTGCTTACTG
RGYW2-4_pC    GAGGACTCTG CAGTCTATTA CTGTGCAAGA GGGGATGGGT TTGCTTACTG
RGYW2-27_p    GAGGACTCTG CAGTCTATTA CTGTGCAAGA GGGGATGGGT TTGCTTACTG
RGYW2-21_p    GAGGACTCTG CAGTCTATTA CTGTGCAAGA GGGGATGGGT TTGCTTACTG

                        660        670        680
RGYW2-1_pC    GGGCCAAGGG ACTCTGGTCA CTGTCTCTGC A
RGYW2-3_pC    GGGCCAAGGG ACTCTGGTCA CTGTCTCTGC A
RGYW2-4_pC    GGGCCAAGGG ACTCTGGTCA CTGTCTCTGC A
RGYW2-27_p    GGGCCAAGGG ACTCTGGTCA CTGTCTCTGC A
RGYW2-21_p    GGGCCAAGGG ACTCTGGTCA CTGTCTCTGC A
```

Appendix XII-ii: Chromatogram of scFv TG130-RGYW 1.

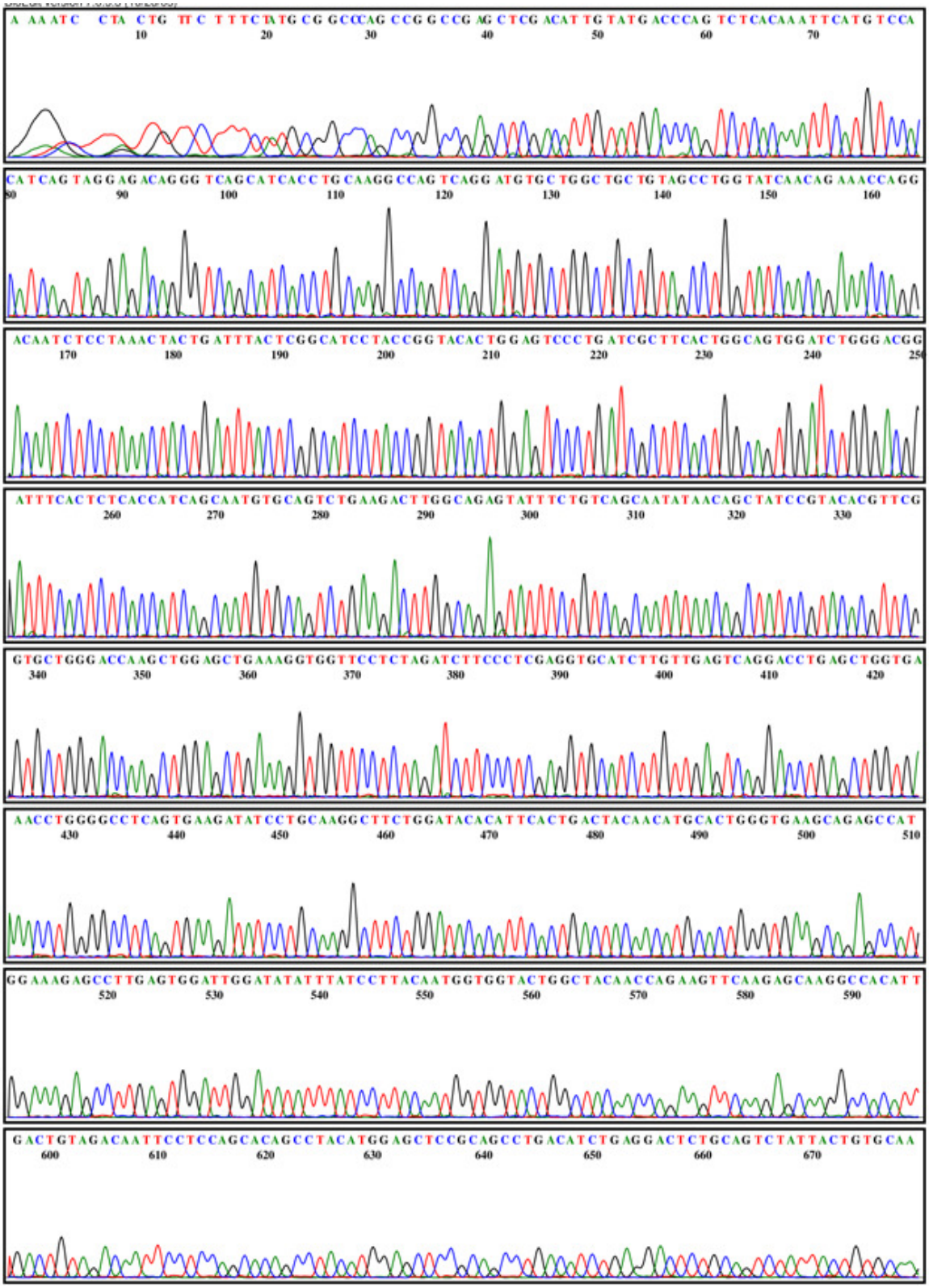

Appendix XII-ii: Chromatogram of scFv TG130-RGYW 1 (*continued*).

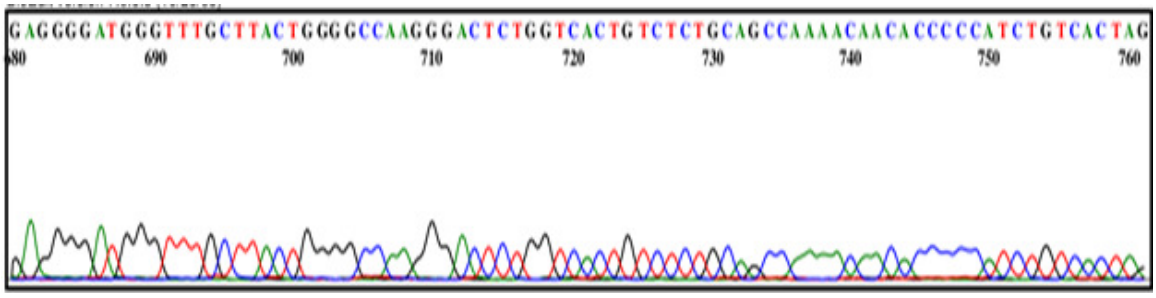

Appendix XII-iii: Chromatogram of scFv TG130-RGYW 3

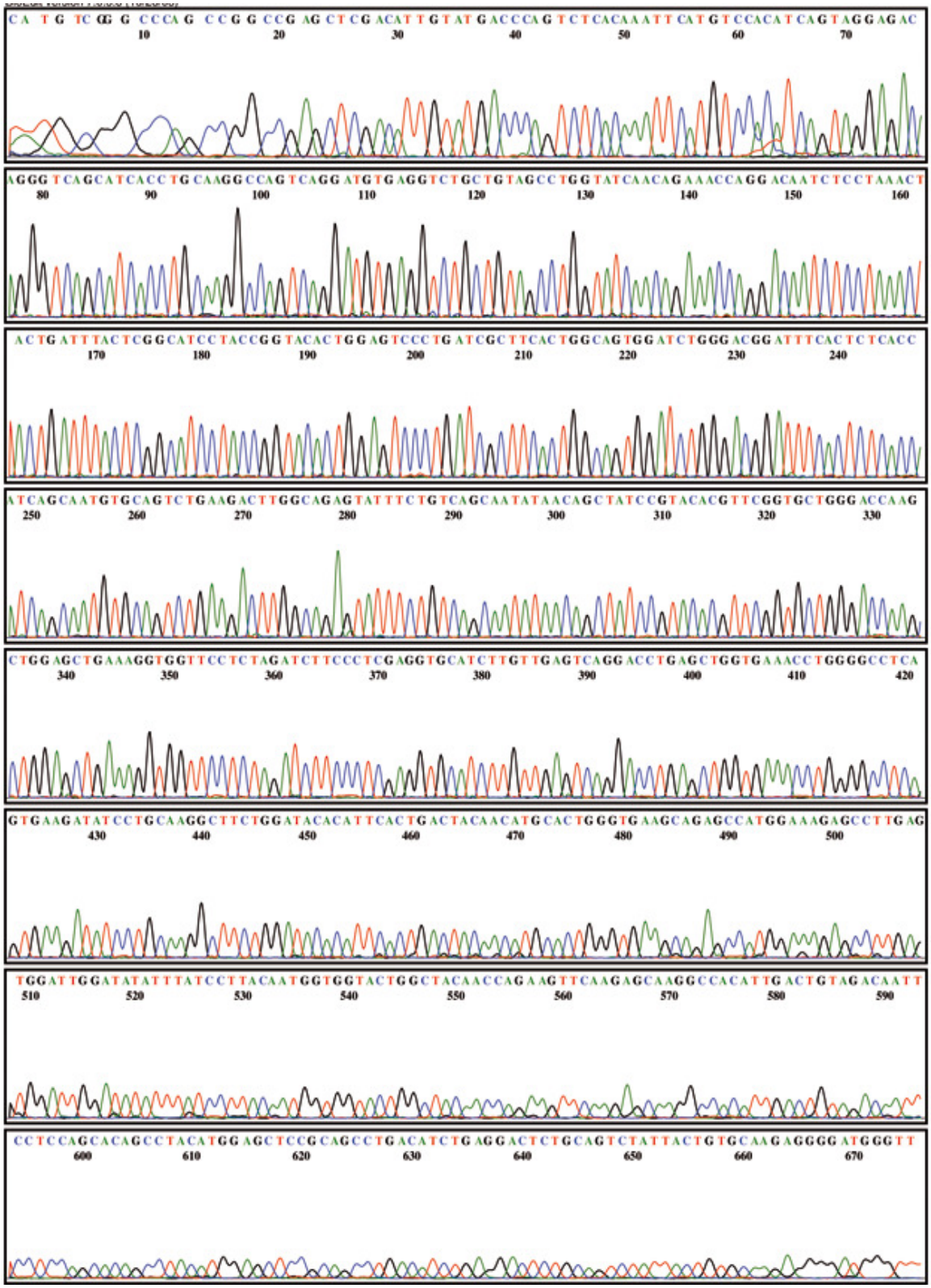

Appendix XII-iii: Chromatogram of scFv TG130-RGYW 3 (*continued*)

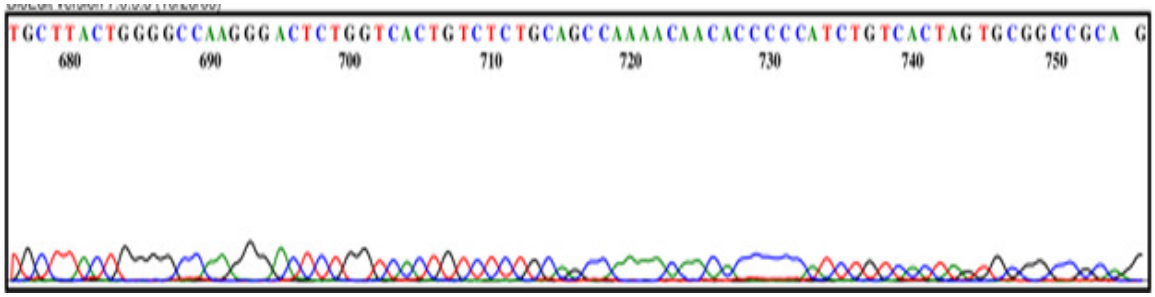

Appendix XII-iv: Chromatogram of scFv TG130-RGYW 4.

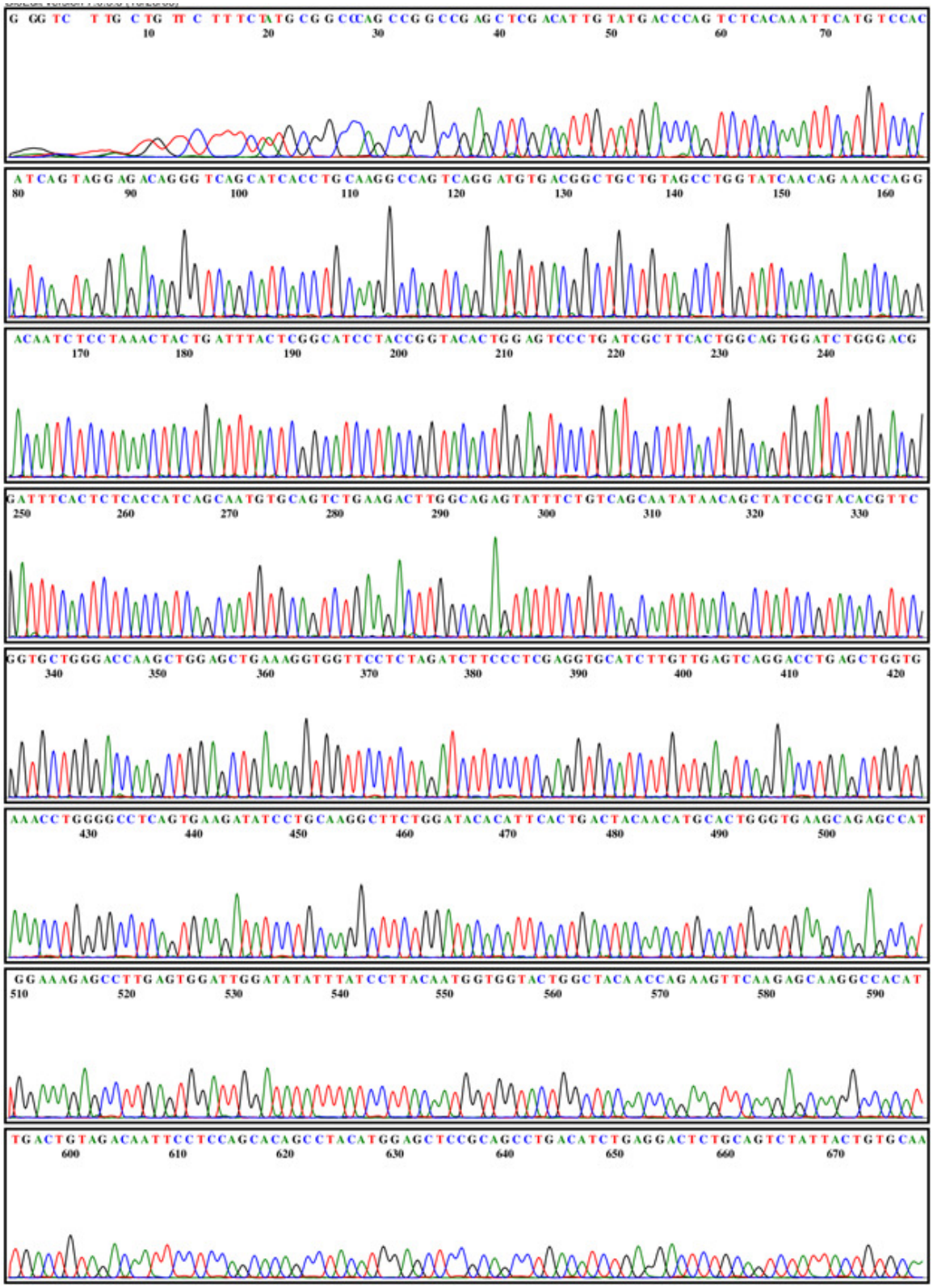

Appendix XII-iv: Chromatogram of scFv TG130-RGYW 4 (*continued*)

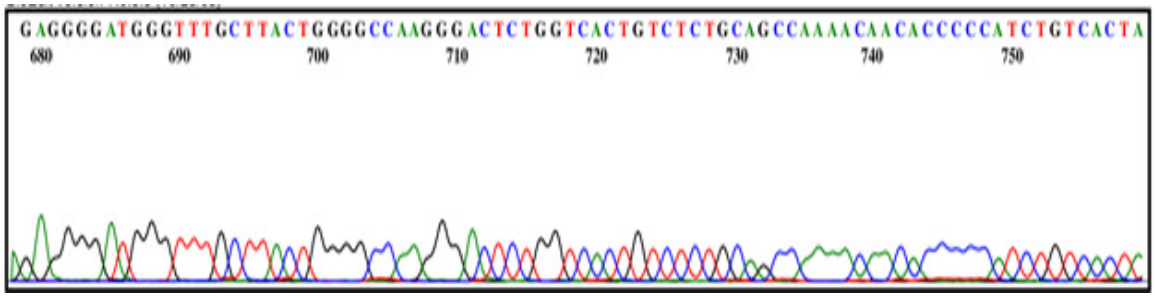

Appendix XII-v: Chromatogram of scFv TG130-RGYW 21.

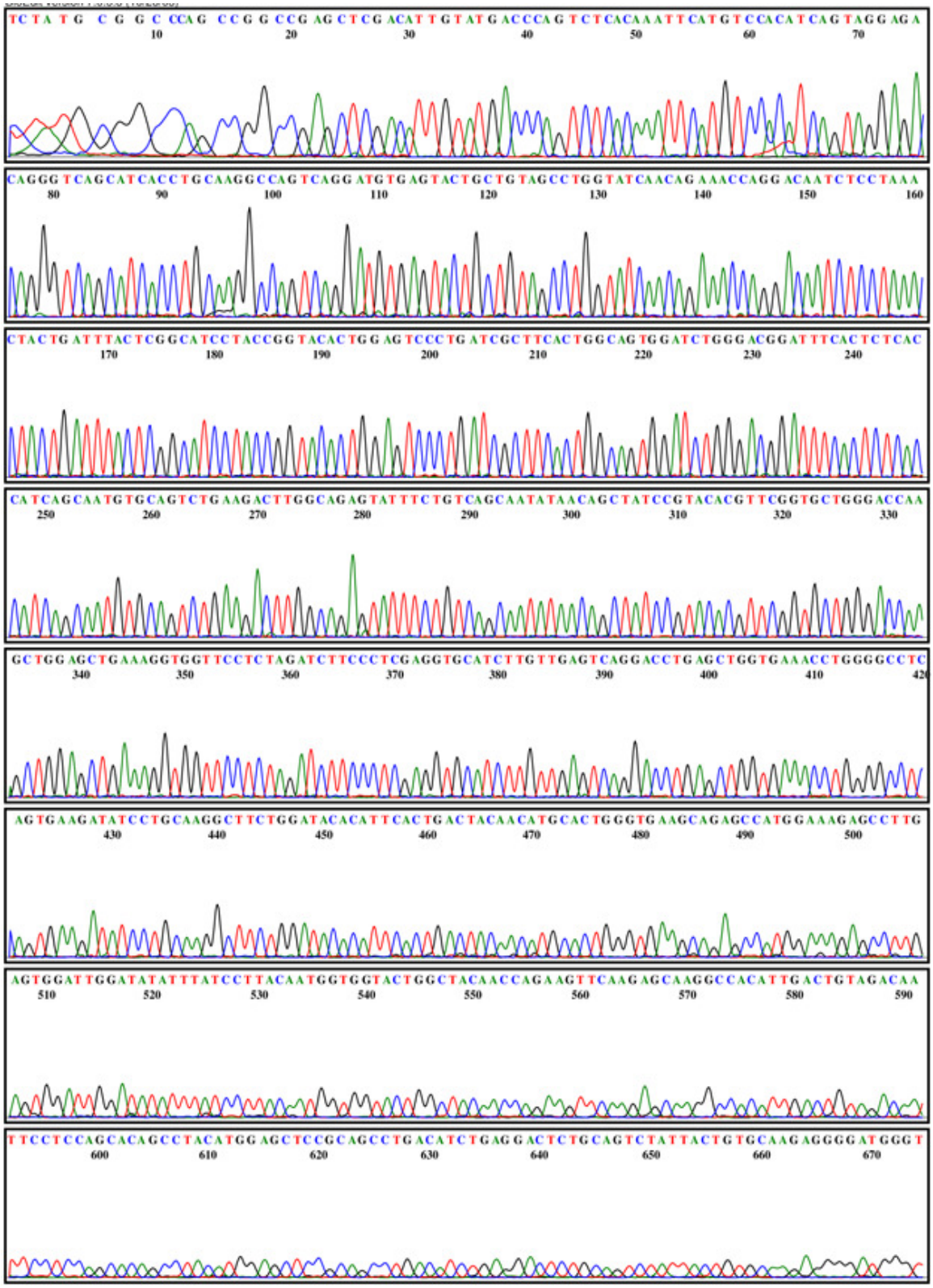

Appendix XII-v: Chromatogram of scFv TG130-RGYW 21 (*continued*)

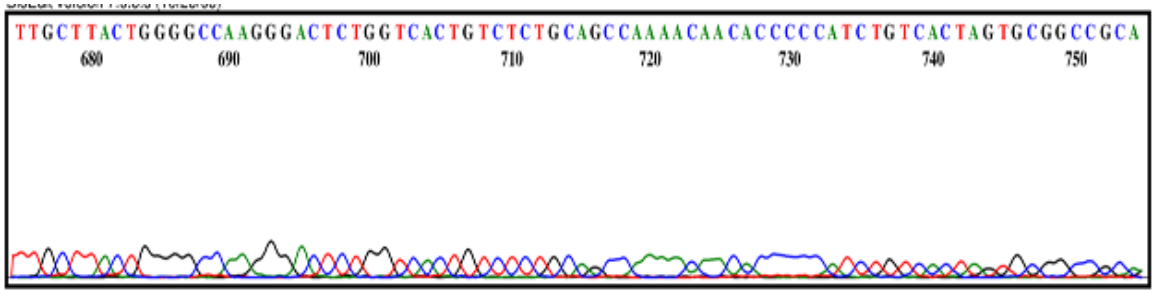

Appendix XII-vi: Chromatogram of scFv TG130-RGYW 27.

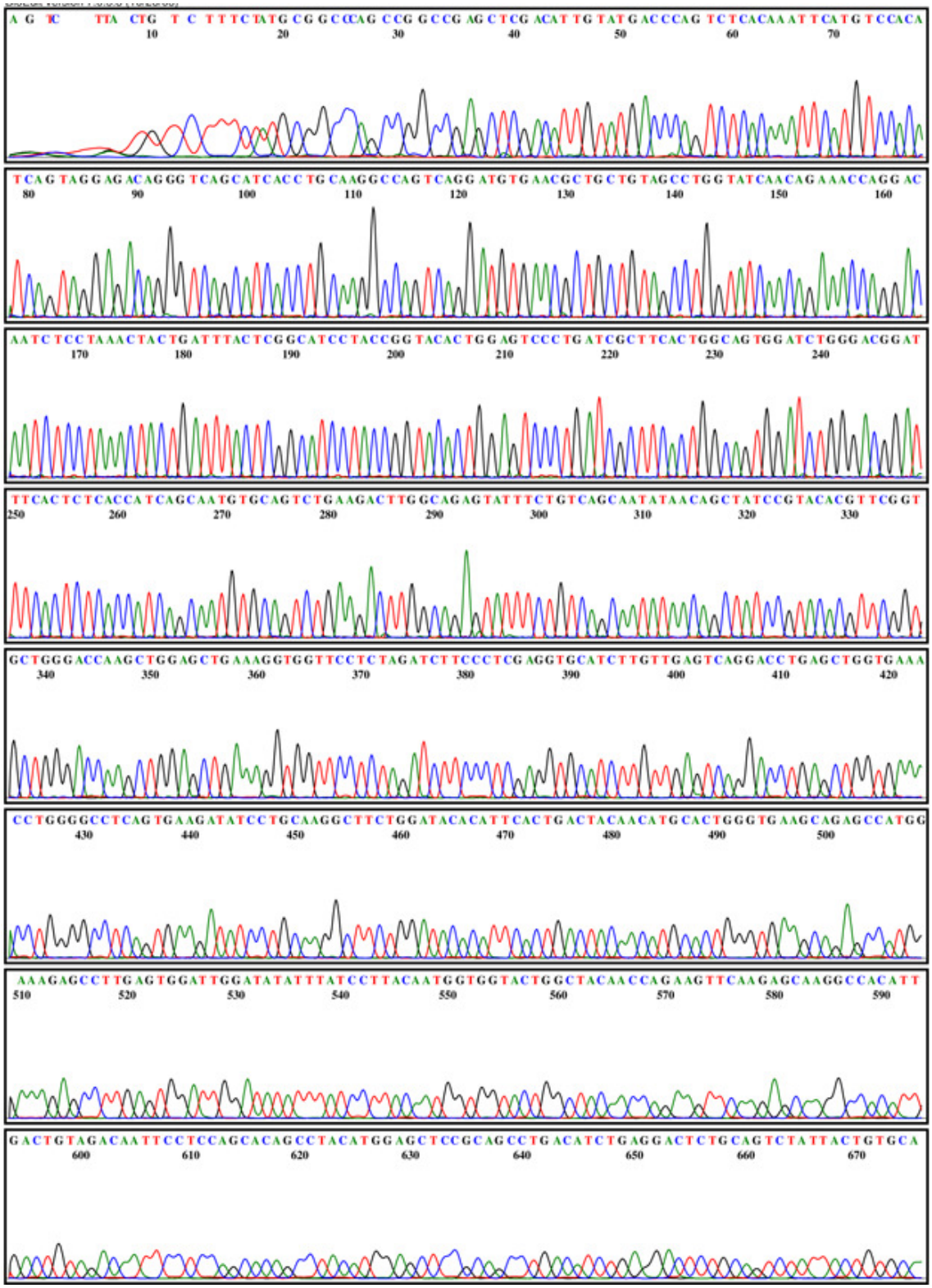

Appendix XII-vi: Chromatogram of scFv TG130-RGYW 27 (*continued*)

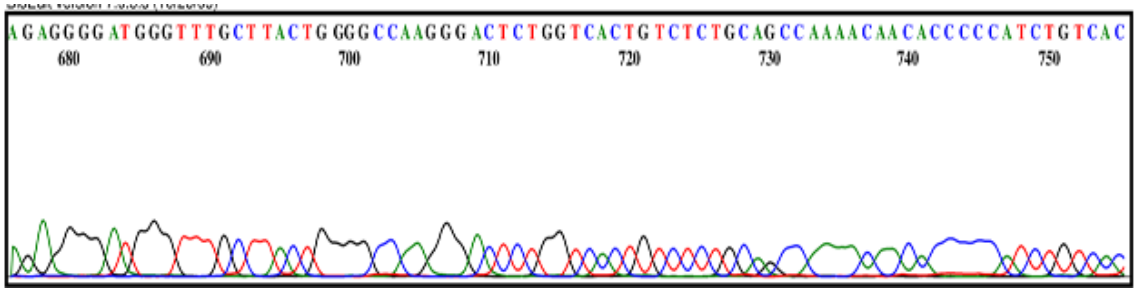

Appendix XII-vii: Alignment of 5 selected RGYW scFv clones from biopanning.

```
Alignment: C:\Users\Sherene\Desktop\ScFv Thesis & Papers\scFv Sequences,
clones\Shortlisted TG130-RGYW alignment.fas

                ....|....| ....|....| ....|....| ....|....| ....|....|
                        10         20         30         40         50
SCFV130_pC      ATGACCCAGT CTCACAAATT CATGTCCACA TCAGTAGGAG ACAGGGTCAG
RA15            ATGACCCAGT CTCACAAATT CATGTCCACA TCAGTAGGAG ACAGGGTCAG
RS55            ATGACCCAGT CTCACAAATT CATGTCCACA TCAGTAGGAG ACAGGGTCAG
RT51            ATGACCCAGT CTCACAAATT CATGTCCACA TCAGTAGGAG ACAGGGTCAG
LT3             ATGACCCAGT CTCACAAATT CATGTCCACA TCAGTAGGAG ACAGGGTCAG
TP60            ATGACCCAGT CTCACAAATT CATGTCCACA TCAGTAGGAG ACAGGGTCAG

                ....|....| ....|....| ....|....| ....|....| ....|....|
                        60         70         80         90        100
SCFV130_pC      CATCACCTGC AAGGCCAGTC AGGATGTGAG TACTGCTGTA GCCTGGTATC
RA15            CATCACCTGC AAGGCCAGTC AGGATGTGAG GGCTGCTGTA GCCTGGTATC
RS55            CATCACCTGC AAGGCCAGTC AGGATGTGCG GTCTGCTGTA GCCTGGTATC
RT51            CATCACCTGC AAGGCCAGTC AGGATGTGCG CACTGCTGTA GCCTGGTATC
LT3             CATCACCTGC AAGGCCAGTC AGGATGTGCT GACTGCTGTA GCCTGGTATC
TP60            CATCACCTGC AAGGCCAGTC AGGATGTGAC CCCTGCTGTA GCCTGGTATC

                ....|....| ....|....| ....|....| ....|....| ....|....|
                       110        120        130        140        150
SCFV130_pC      AACAGAAACC AGGACAATCT CCTAAACTAC TGATTTACTC GGCATCCTAC
RA15            AACAGAAACC AGGACAATCT CCTAAACTAC TGATTTACTC GGCATCCTAC
RS55            AACAGAAACC AGGACAATCT CCTAAACTAC TGATTTACTC GGCATCCTAC
RT51            AACAGAAACC AGGACAATCT CCTAAACTAC TGATTTACTC GGCATCCTAC
LT3             AACAGAAACC AGGACAATCT CCTAAACTAC TGATTTACTC GGCATCCTAC
TP60            AACAGAAACC AGGACAATCT CCTAAACTAC TGATTTACTC GGCATCCTAC

                ....|....| ....|....| ....|....| ....|....| ....|....|
                       160        170        180        190        200
SCFV130_pC      CGGTACACTG GAGTCCCTGA TCGCTTCACT GGCAGTGGAT CTGGGACGGA
RA15            CGGTACACTG GAGTCCCTGA TCGCTTCACT GGCAGTGGAT CTGGGACGGA
RS55            CGGTACACTG GAGTCCCTGA TCGCTTCACT GGCAGTGGAT CTGGGACGGA
RT51            CGGTACACTG GAGTCCCTGA TCGCTTCACT GGCAGTGGAT CTGGGACGGA
LT3             CGGTACACTG GAGTCCCTGA TCGCTTCACT GGCAGTGGAT CTGGGACGGA
TP60            CGGTACACTG GAGTCCCTGA TCGCTTCACT GGCAGTGGAT CTGGGACGGA

                ....|....| ....|....| ....|....| ....|....| ....|....|
                       210        220        230        240        250
SCFV130_pC      TTTCACTCTC ACCATCAGCA ATGTGCAGTC TGAAGACTTG GCAGAGTATT
RA15            TTTCACTCTC ACCATCAGCA ATGTGCAGTC TGAAGACTTG GCAGAGTATT
RS55            TTTCACTCTC ACCATCAGCA ATGTGCAGTC TGAAGACTTG GCAGAGTATT
RT51            TTTCACTCTC ACCATCAGCA ATGTGCAGTC TGAAGACTTG GCAGAGTATT
LT3             TTTCACTCTC ACCATCAGCA ATGTGCAGTC TGAAGACTTG GCAGAGTATT
TP60            TTTCACTCTC ACCATCAGCA ATGTGCAGTC TGAAGACTTG GCAGAGTATT

                ....|....| ....|....| ....|....| ....|....| ....|....|
                       260        270        280        290        300
SCFV130_pC      TCTGTCAGCA ATATAACAGC TATCCGTACA CGTTCGGTGC TGGGACCAAG
RA15            TCTGTCAGCA ATATAACAGC TATCCGTACA CGTTCGGTGC TGGGACCAAG
RS55            TCTGTCAGCA ATATAACAGC TATCCGTACA CGTTCGGTGC TGGGACCAAG
RT51            TCTGTCAGCA ATATAACAGC TATCCGTACA CGTTCGGTGC TGGGACCAAG
LT3             TCTGTCAGCA ATATAACAGC TATCCGTACA CGTTCGGTGC TGGGACCAAG
TP60            TCTGTCAGCA ATATAACAGC TATCCGTACA CGTTCGGTGC TGGGACCAAG

                ....|....| ....|....| ....|....| ....|....| ....|....|
                       310        320        330        340        350
SCFV130_pC      CTGGAGCTGA AAGGTGGTTC CTCTAGATCT TCCCTCGAGG TGCATCTTGT
RA15            CTGGAGCTGA AAGGTGGTTC CTCTAGATCT TCCCTCGAGG TGCATCTTGT
RS55            CTGGAGCTGA AAGGTGGTTC CTCTAGATCT TCCCTCGAGG TGCATCTTGT
RT51            CTGGAGCTGA AAGGTGGTTC CTCTAGATCT TCCCTCGAGG TGCATCTTGT
LT3             CTGGAGCTGA AAGGTGGTTC CTCTAGATCT TCCCTCGAGG TGCATCTTGT
TP60            CTGGAGCTGA AAGGTGGTTC CTCTAGATCT TCCCTCGAGG TGCATCTTGT
```

Alignment (page 2 of 2)

```
                ....|....| ....|....| ....|....| ....|....| ....|....|
                       360        370        380        390        400
SCFV130_pC      TGAGTCAGGA CCTGAGCTGG TGAAACCTGG GGCCTCAGTG AAGATATCCT
RA15            TGAGTCAGGA CCTGAGCTGG TGAAACCTGG GGCCTCAGTG AAGATATCCT
RS55            TGAGTCAGGA CCTGAGCTGG TGAAACCTGG GGCCTCAGTG AAGATATCCT
RT51            TGAGTCAGGA CCTGAGCTGG TGAAACCTGG GGCCTCAGTG AAGATATCCT
LT3             TGAGTCAGGA CCTGAGCTGG TGAAACCTGG GGCCTCAGTG AAGATATCCT
TP60            TGAGTCAGGA CCTGAGCTGG TGAAACCTGG GGCCTCAGTG AAGATATCCT

                ....|....| ....|....| ....|....| ....|....| ....|....|
                      410        420        430        440        450
SCFV130_pC      GCAAGGCTTC TGGATACACA TTCACTGACT ACAACATGCA CTGGGTGAAG
RA15            GCAAGGCTTC TGGATACACA TTCACTGACT ACAACATGCA CTGGGTGAAG
RS55            GCAAGGCTTC TGGATACACA TTCACTGACT ACAACATGCA CTGGGTGAAG
RT51            GCAAGGCTTC TGGATACACA TTCACTGACT ACAACATGCA CTGGGTGAAG
LT3             GCAAGGCTTC TGGATACACA TTCACTGACT ACAACATGCA CTGGGTGAAG
TP60            GCAAGGCTTC TGGATACACA TTCACTGACT ACAACATGCA CTGGGTGAAG

                ....|....| ....|....| ....|....| ....|....| ....|....|
                      460        470        480        490        500
SCFV130_pC      CAGAGCCATG GAAAGAGCCT TGAGTGGATT GGATATATTT ATCCTTACAA
RA15            CAGAGCCATG GAAAGAGCCT TGAGTGGATT GGATATATTT ATCCTTACAA
RS55            CAGAGCCATG GAAAGAGCCT TGAGTGGATT GGATATATTT ATCCTTACAA
RT51            CAGAGCCATG GAAAGAGCCT TGAGTGGATT GGATATATTT ATCCTTACAA
LT3             CAGAGCCATG GAAAGAGCCT TGAGTGGATT GGATATATTT ATCCTTACAA
TP60            CAGAGCCATG GAAAGAGCCT TGAGTGGATT GGATATATTT ATCCTTACAA

                ....|....| ....|....| ....|....| ....|....| ....|....|
                      510        520        530        540        550
SCFV130_pC      TGGTGGTACT GGCTACAACC AGAAGTTCAA GAGCAAGGCC ACATTGACTG
RA15            TGGTGGTACT GGCTACAACC AGAAGTTCAA GAGCAAGGCC ACATTGACTG
RS55            TGGTGGTACT GGCTACAACC AGAAGTTCAA GAGCAAGGCC ACATTGACTG
RT51            TGGTGGTACT GGCTACAACC AGAAGTTCAA GAGCAAGGCC ACATTGACTG
LT3             TGGTGGTACT GGCTACAACC AGAAGTTCAA GAGCAAGGCC ACATTGACTG
TP60            TGGTGGTACT GGCTACAACC AGAAGTTCAA GAGCAAGGCC ACATTGACTG

                ....|....| ....|....| ....|....| ....|....| ....|....|
                      560        570        580        590        600
SCFV130_pC      TAGACAATTC CTCCAGCACA GCCTACATGG AGCTCCGCAG CCTGACATCT
RA15            TAGACAATTC CTCCAGCACA GCCTACATGG AGCTCCGCAG CCTGACATCT
RS55            TAGACAATTC CTCCAGCACA GCCTACATGG AGCTCCGCAG CCTGACATCT
RT51            TAGACAATTC CTCCAGCACA GCCTACATGG AGCTCCGCAG CCTGACATCT
LT3             TAGACAATTC CTCCAGCACA GCCTACATGG AGCTCCGCAG CCTGACATCT
TP60            TAGACAATTC CTCCAGCACA GCCTACATGG AGCTCCGCAG CCTGACATCT

                ....|....| ....|....| ....|....| ....|....| ....|....|
                      610        620        630        640        650
SCFV130_pC      GAGGACTCTG CAGTCTATTA CTGTGCAAGA GGGGATGGGT TTGCTTACTG
RA15            GAGGACTCTG CAGTCTATTA CTGTGCAAGA GGGGATGGGT TTGCTTACTG
RS55            GAGGACTCTG CAGTCTATTA CTGTGCAAGA GGGGATGGGT TTGCTTACTG
RT51            GAGGACTCTG CAGTCTATTA CTGTGCAAGA GGGGATGGGT TTGCTTACTG
LT3             GAGGACTCTG CAGTCTATTA CTGTGCAAGA GGGGATGGGT TTGCTTACTG
TP60            GAGNACTCTG CAGTCTATTA CTGTGCAAGA GGGGATGGGT TTGCTTACTG

                ....|....| ....|....| ....|....| ....|....| ....|....|
                      660        670        680        690        700
SCFV130_pC      GGGCCAAGGG ACTCTGGTCA CTGTCTCTGC AGCCAAAACA ACACCCCCAT
RA15            GGGCCAAGGG ACTCTGGTCA CTGTCTCTGC A..........  ..........
RS55            GGGCCAAGGG ACTCTGGTCA CTGTCTCTGC A..........  ..........
RT51            GGGCCAAGGG ACTCTGGTCA CTGTCTCTGC A..........  ..........
LT3             GGGCCAAGGG ACTCTGGTCA CTGTCTCTGC A..........  ..........
TP60            GGGCCAAGGG ACTCTGGTCA CTGTCTCTGC A..........  ..........
```

Appendix XII-viii: Chromatogram of scFv TP60.

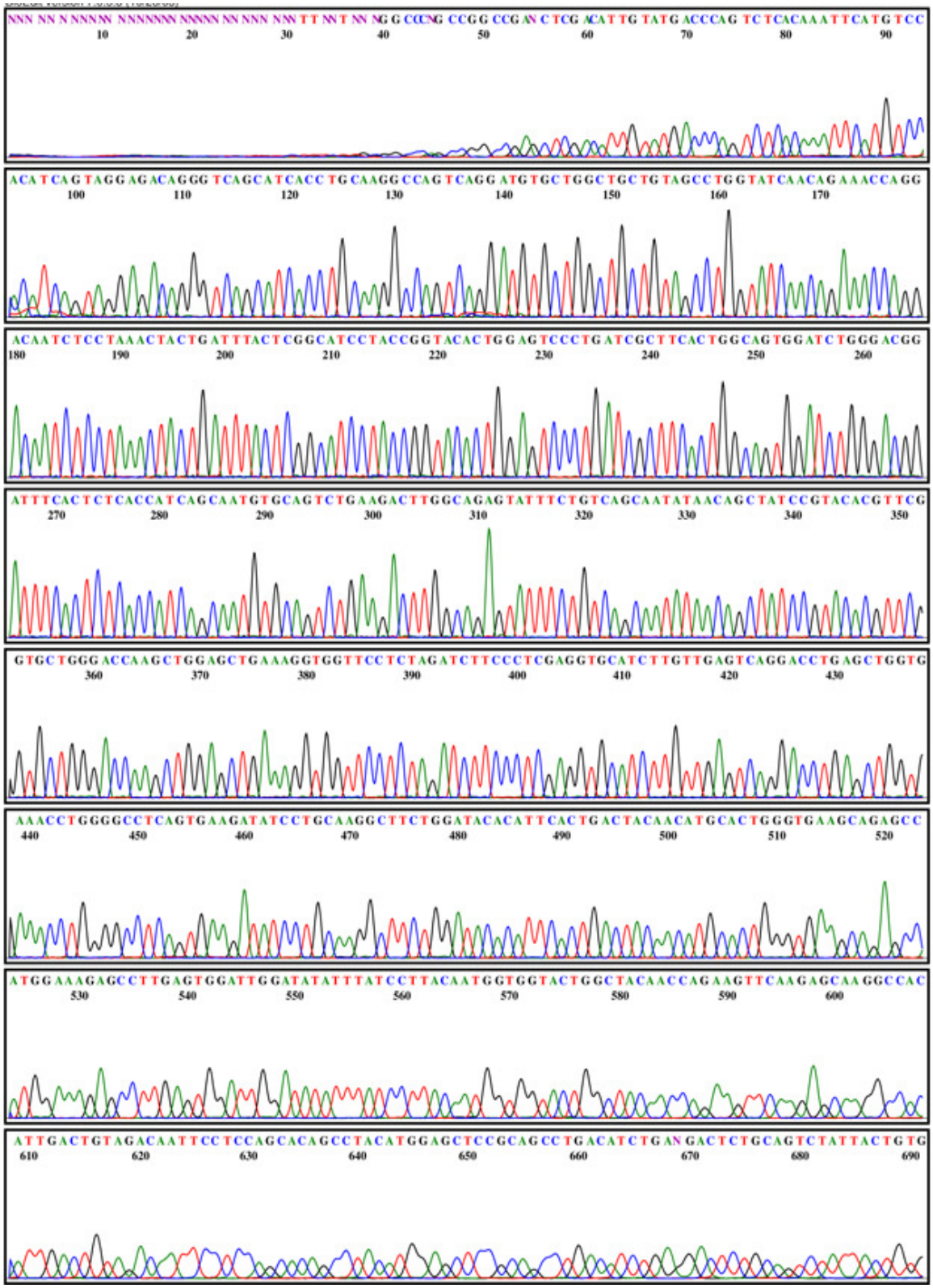

Appendix XII-viii: Chromatogram of scFv TP60 (*continued*)

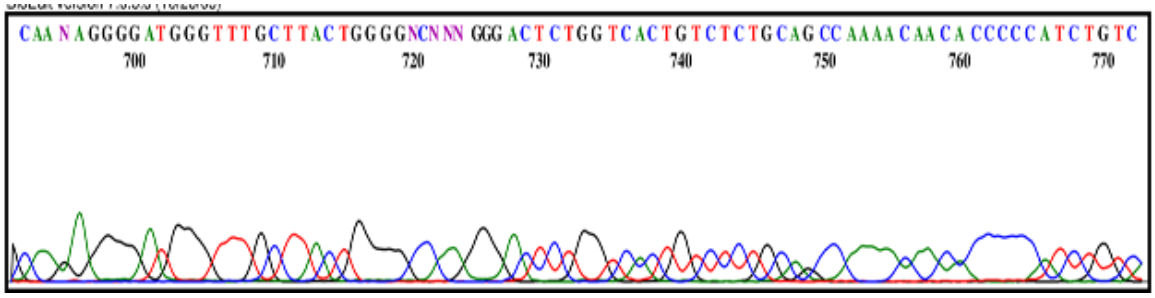

Appendix XII-ix: Chromatogram of scFv RA15.

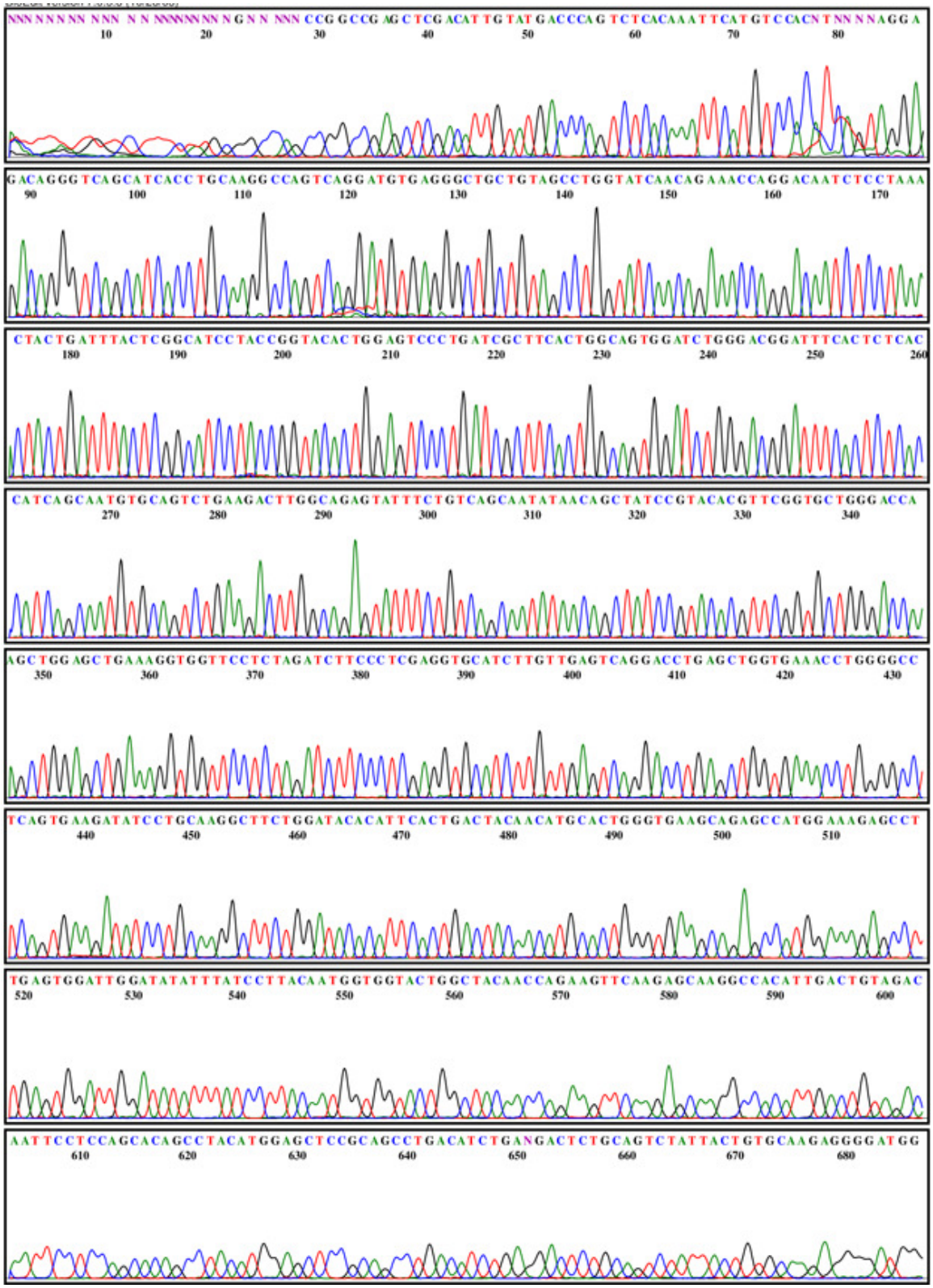

Appendix XII-ix: Chromatogram of scFv RA15 (*continued*)

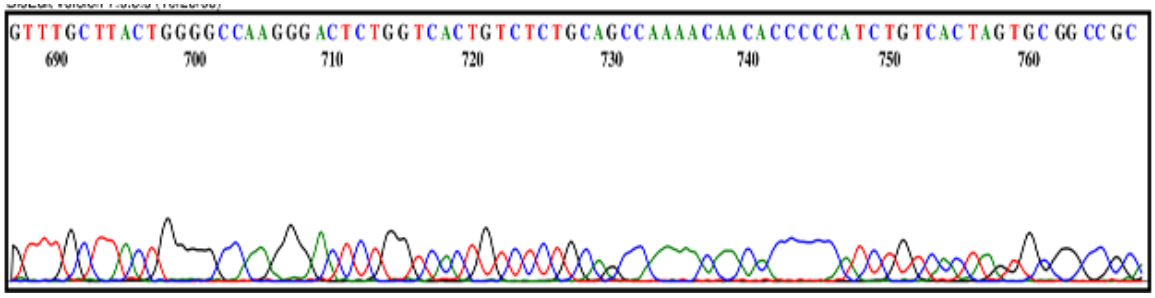

Appendix XII-x: Chromatogram of scFv RS55.

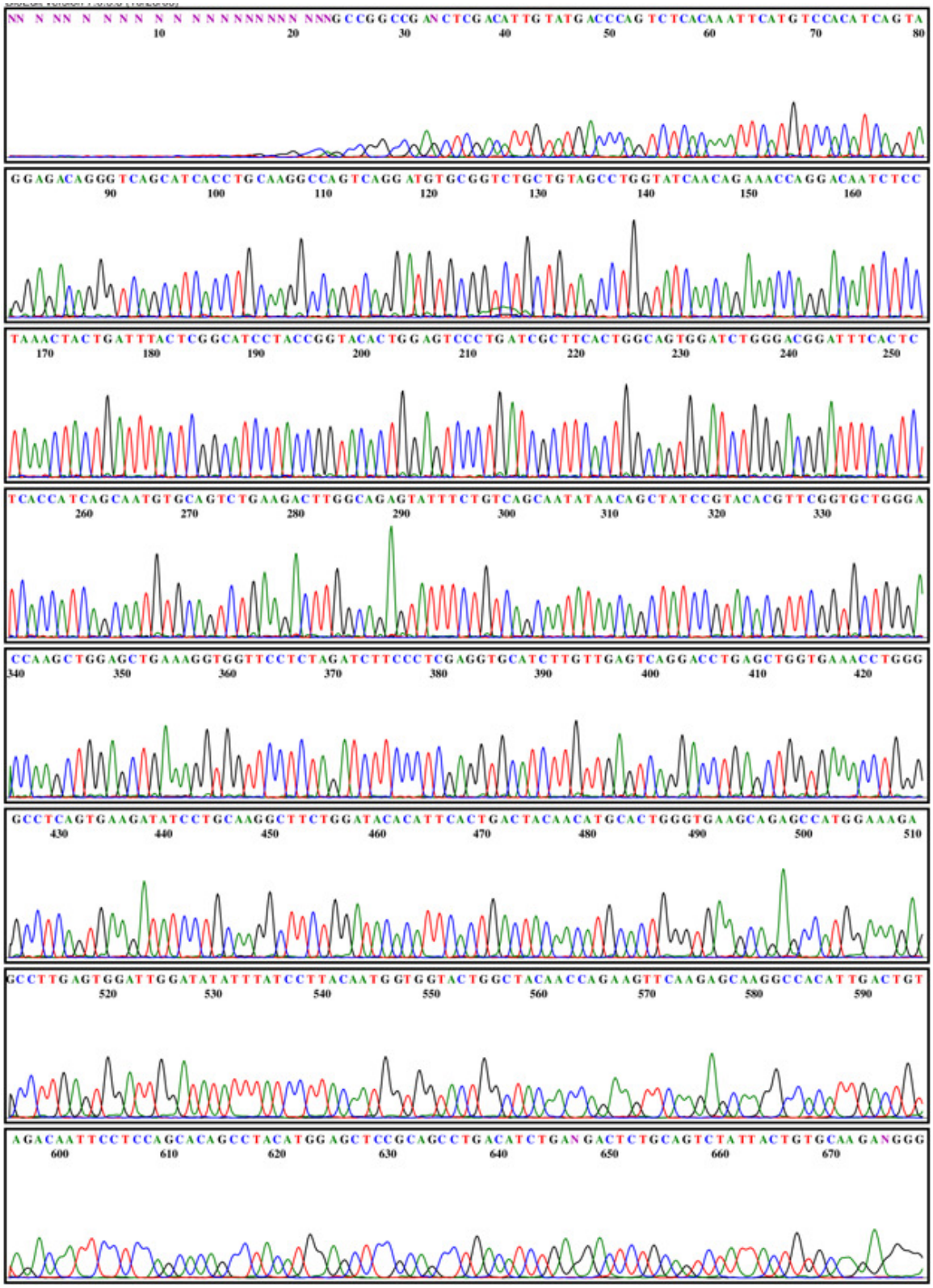

Appendix XII-x: Chromatogram of scFv RS55 (*continued*)

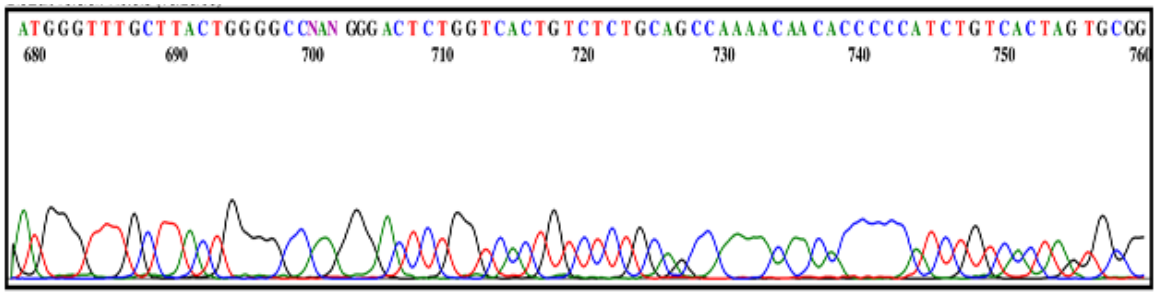

Appendix XII-xi: Chromatogram of scFv RT51.

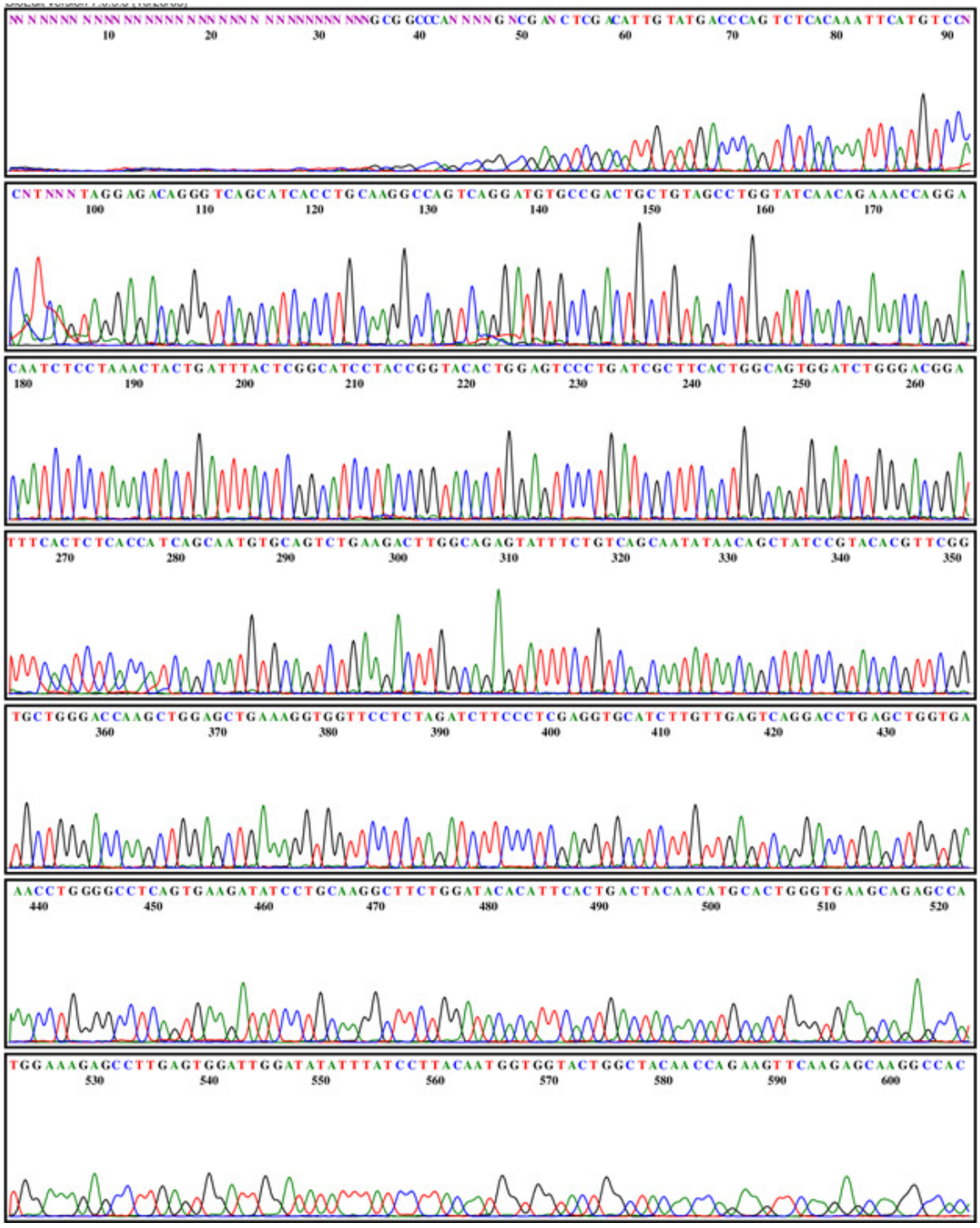

Appendix XII-xi: Chromatogram of scFv RT51 (*continued*)

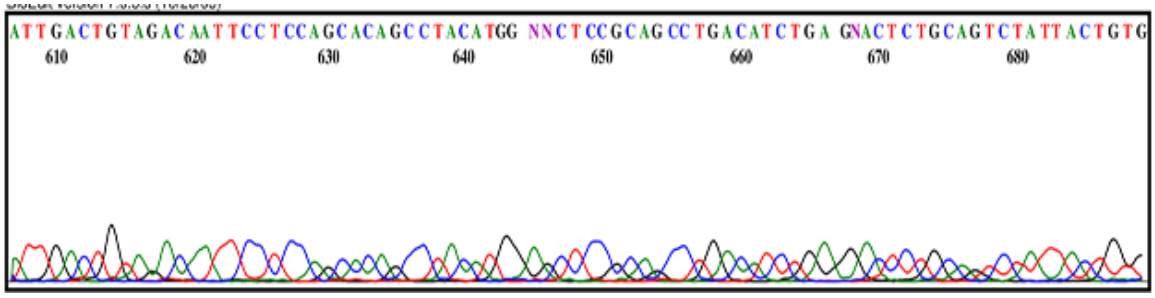

Appendix XII-xii: Chromatogram of scFv LT3.

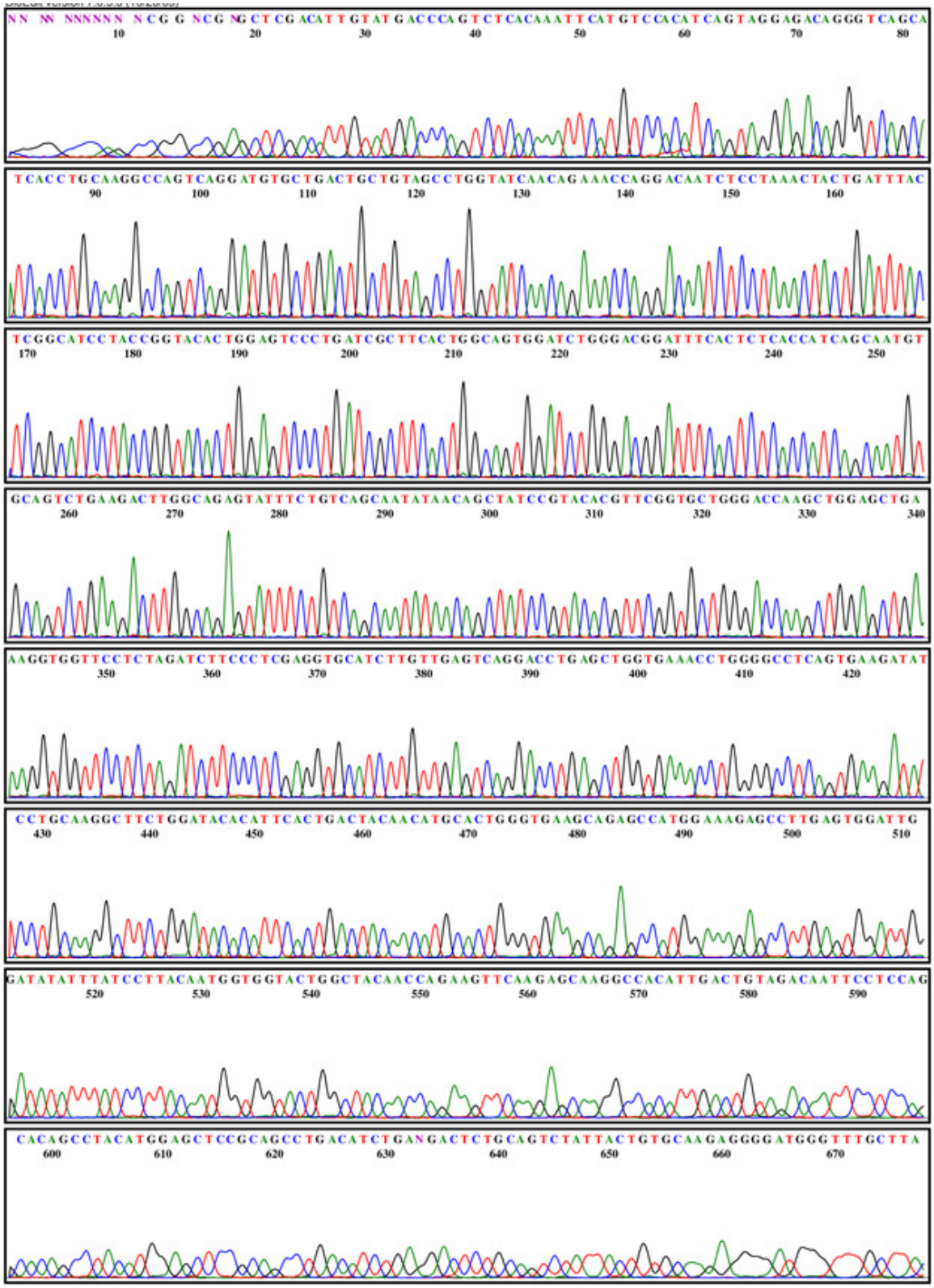

Appendix XII-xii: Chromatogram of scFv LT3 (*continued*)

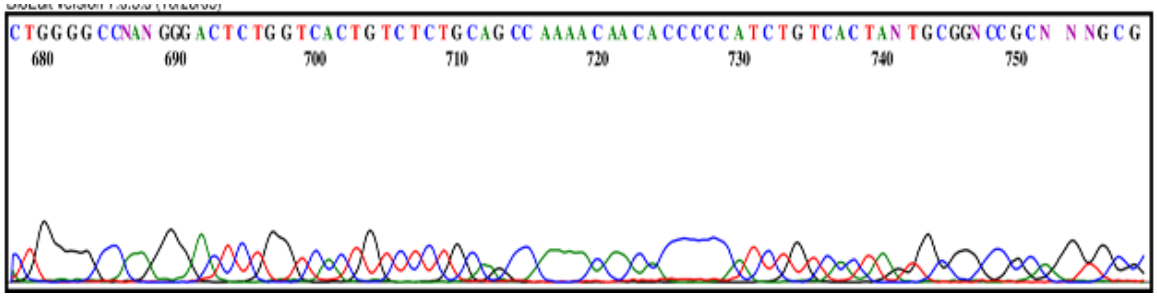

Appendix XIII: Statistical test results output of the difference in affinity-matured scFv TP60 antibody recognition between target antigen *T. gondii* and negative control cell line. A t-test comparison between the binding titer readings of both test groups was performed at alpha value = 0.05 using the SigmaPlot 11.0 statistical software programme. The test result shows a statistically significant difference between the binding titers of antibody TP60 and the negative control cell line.

t-test Thursday, November 10, 2011, 2:11:22 PM

Data source: Data 1 in ScFv TG-RGYW Monoclonal Screening_101111

Normality Test: Passed (P = 0.540)

Equal Variance Test: Passed (P = 0.327)

Group Name	N	Missing	Mean	Std Dev	SEM
TP60-TGRH	2	0	12500.000	2121.320	1500.000
TP60-WRL68	3	0	6066.667	1069.268	617.342

Difference 6433.333

t = 4.686 with 3 degrees of freedom. (P = 0.018)

95 percent confidence interval for difference of means: 2063.785 to 10802.882

The difference in the mean values of the two groups is greater than would be expected by chance; there is a statistically significant difference between the input groups (P = 0.018).

Power of performed test with alpha = 0.050: 0.852

Appendix XIV: Table of sequences of 2nd generation mutant scFv antibody clones (TG-RGYW library) recovered from biopanning to *T. gondii*. Clones were randomly selected and only mutated regions with its' corresponding amino acid residues are shown. Most frequently occurring clones (≥ 4) are highlighted in yellow. Legend for amino acid structures are S – small, N – nucleophilic, H – hydrophobic, A – acidic, B – basic and AM – amide.

Clone Number	Nucleotide Sequence	Amino Acid Translation	Amino Acid Structures
1	GCC T	A S	S N
2	GCC T	A S	S N
3	GCC A	A T	S N
4	GCG A	A T	S N
5	GAC G	D A	A S
6	GAC G	D A	A S
7	GAC C	D P	A H
8	GAC T	D S	A N
9	GAC T	D S	A N
10	GAC A	D T	A N
11	GAG C	E P	A H
12	GAG C	E P	A H
13	GAG T	E S	A N
14	GGG G	G A	S S
15	GGG G	G A	S S
16	GGG T	G S	S N
17	GGG T	G S	S N
18	GGC A	G T	S N
19	CAC G	H A	B S
20	CAC G	H A	B S
21	CAC C	H P	B H
22	CAC A	H T	B N
23	CAC A	H T	B N
24	ATC C	I P	H H
25	ATC T	I S	H H
26	ATC A	I T	H N
27	AAG G	K A	B S
28	CTG G	L A	H S
29	CTG C	L P	H H
30	CTG C	L P	H H
31	CTC T	L S	H N
32	CTC T	L S	H N
33	CTC A	L T	H N
34	CTG A	L T	H N
35	CTG A	L T	H N
36	CTG A	L T	H N
37	ATG G	M A	H S
38	ATG C	M P	H H

Clone Number	Nucleotide Sequence	Amino Acid Translation	Amino Acid Structures
39	AAC C	N P	AM H
40	GAC A	N T	AM N
41	AAC A	N T	AM N
42	CCG G	P A	H S
43	CCG G	P A	H S
44	CCC T	P S	H N
45	CCC A	P T	H N
46	CCG A	P T	H N
47	CCG A	P T	H N
48	CCG A	P T	H N
49	CCG A	P T	H N
50	CAG G	Q A	AM S
51	CAG C	Q P	AM H
52	CAG T	Q S	AM N
53	CAG T	Q S	AM N
54	CAG A	Q T	AM N
55	AGG G	R A	B S
56	AGG G	R A	B S
57	CGC G	R A	B S
58	AGG G	R A	B S
59	CGG G	R A	B S
60	AGG C	R P	B H
61	CGC C	R P	B H
62	CGG T	R S	B N
63	CGG T	R S	B N
64	AGG T	R S	B N
65	AGG T	R S	B N
66	CGG T	R S	B N
67	AGG A	R T	B N
68	AGG A	R T	B N
69	CGC A	R T	B N
70	CGC A	R T	B N
71	AGC G	S A	N S
72	AGC G	S A	N S
73	AGC T	S S	N N
74	AGC T	S S	N N
75	ACG G	T A	N S
76	ACG G	T A	N S
77	ACC G	T A	N S
78	ACG G	T A	N S
79	ACG G	T A	N S
80	ACG C	T P	N H
81	ACC C	T P	N H
82	ACG C	T P	N H
83	ACC C	T P	N H

Clone Number	Nucleotide Sequence	Amino Acid Translation	Amino Acid Structures
84	ACC C	T P	N H
85	ACG C	T P	N H
86	ACG C	T P	N H
87	ACC C	T P	N H
88	ACG T	T S	N N
89	ACG T	T S	N N
90	ACG A	T T	N N
91	GTG G	V A	H S
92	GTC G	V A	H S
93	GTC C	V P	H H
94	GTC A	V T	H N

Appendix XV: Useful website and links.

For up-to-date information and news regarding the protozoan parasite *Toxoplasma gondii:*

- http://toxoplasmaparasite.blogspot.com/

For protein translation tool:

- http://web.expasy.org/translate/

For downloading the BioEdit sequence analysis and alignment software:

- http://en.bio-soft.net/format/BioEdit.html

For analyzing and aligning antibody sequences software:

- V-QUEST (http://www.imgt.org/IMGT_vquest/share/textes/)
- Igblast (human and mouse antibody gene sequences (http://www.ncbi.nlm.nih.gov/igblast/)

For visualizing, analyzing, and superimposition of antibody molecular structures:

- VMD version 1.8.7 (2009) (www.ks.uiuc.edu/)
- SwissPdb-Viewer (DeepView) version 4.0.1 (2008) (http://spdbv.vital-it.ch/)
- PyMOL v1.4.1 software (http://pymol.org/educational/)

For homology modelling of antibody structures:

- Rosetta Antibody: Structure Prediction server, by the Department of Chemical and Biomolecular Engineering, Johns Hopkins University (http://antibody.graylab.jhu.edu/)

- Web Antibody Modelling (WAM) server (http://antibody.bath.ac.uk/)

Bibliography

Abu-Madi, M. A., Behnke, J. M., & Dabritz, H. A. (2010). *Toxoplasma gondii* Seropositivity and Co-Infection with TORCH Pathogens in High-Risk Patients from Qatar. *Am J Trop Med Hyg, 82*(4), 626-633.

Adams, G. P., McCartney, J. E., Tai, M.-S., Oppermann, H., Huston, J. S., Stafford, W. F., et al. (1993). Highly Specific *in Vivo* Tumor Targeting by Monovalent and Divalent Forms of 741F8 Anti-c-erbB-2 Single-Chain Fv. *Cancer Research, 53*(17), 4026-4034.

Adey, N. B., Mataragnon, A. H., Rider, J. E., Carter, J. M., & Kay, B. K. (1995). Characterization of phage that bind plastic from phage-displayed random peptide libraries. *Gene, 156*(1), 27-31.

Adomako-Ankomah, Y., Wier, G. M., & Boyle, J. P. (2011). Beyond the genome: Recent advances in *Toxoplasma gondii* functional genomics. *Parasite Immunology*, Accepted manuscript online.

.

Ajioka, J. W., Boothroyd, J. C., Brunk, B. P., Hehl, A., Hillier, L., Manger, I. D., et al. (1998a). Gene Discovery by EST Sequencing in *Toxoplasma gondii* Reveals Sequences Restricted to the Apicomplexa. *Genome Research, 8*(1), 18-28.

Ajioka, J. W., Boothroyd, J. C., Brunk, B. P., Hehl, A., Hillier, L., Manger, I. D., et al. (1998b). Gene Discovery by EST Sequencing in *Toxoplasma gondii*Reveals Sequences Restricted to the Apicomplexa. *Genome Research, 8*(1), 18-28.

Alexander, D. L., Mital, J., Ward, G. E., Bradley, P., & Boothroyd, J. C. (2005). Identification of the Moving Junction Complex of *Toxoplasma gondii*: A Collaboration between Distinct Secretory Organelles. *PLoS Pathog, 1*(2), e17.

Anderson, S. E. J., Bautista, S. C., & Remington, J. S. (1976). Specific antibody-dependent killing of *Toxoplasma gondii* by normal macrophages. *Clin Exp Immunol., 26*(3), 375-380.

Andris-Widhopf, J., Rader, C., & Barbas, C. F. I. (2001). Generation of Antibody Libraries: Immunization, RNA Preparation, and cDNA Synthesis. In C. F. I. Barbas, D. R. Burton, J. K. Scott & G. J. Silverman (Eds.), *Phage Display - A Laboratory Manual* (pp. 8.1-8.3). New York: Cold Spring Harbor Laboratory Press.

Arap, M. A. (2005). Phage display technology: applications and innovations. *Genet. Mol. Biol., 28*, 1-9.

Arap, W., Haedicke, W., Bernasconi, M., Kain, R., Rajotte, D., Krajewski, S., et al. (2002). Targeting the prostate for destruction through a vascular address. *Proceedings of the National Academy of Sciences, 99*(3), 1527-1531.

Araujo, F. G., Suzuki, Y., & Remington, J. S. (1996). Use of rifabutin in combination with atovaquone, clindamycin, pyrimethamine, or sulfadiazine for treatment of toxoplasmic encephalitis in mice. *European Journal of Clinical Microbiology & Infectious Diseases, 15*(5), 394-397.

Ardelt, P. U., Wood, C. G., Chen, L., Mintz, P. J., Moya, C., Arap, M. A., et al. (2003). Targeting Urothelium: *Ex Vivo* Assay Standardization and Selection of Internalizing Ligands. *The Journal of urology, 169*(4), 1535-1540.

Asai, T., Miura, S., Sibley, L. D., Okabayashi, H., & Takeuchi, T. (1995). Biochemical and molecular characterization of nucleoside triphosphate hydrolase isozymes from the parasitic protozoan *Toxoplasma gondii*. *Journal of Biological Chemistry, 270*(19), 11391-11397.

Asai, T., O'Sullivan, W. J., & Tatibana, M. (1983). A potent nucleoside triphosphate hydrolase from the parasitic protozoan *Toxoplasma gondii*. Purification, some properties, and activation by thiol compounds. *Journal of Biological Chemistry, 258*(11), 6816-6822.

Azmi, M. N., Fong, M., Init, I., Rohela, M., Anuar, A. K., Quek, K., et al. (2003). Toxoplasmosis: prevalence and risk factors. *Journal of Obstetrics & Gynaecology, 23*, 618-624.

Baggish, A. L., & Hill, D. R. (2002). Antiparasitic Agent Atovaquone. *Antimicrob. Agents Chemother., 46*(5), 1163-1173.

Bang, S., Nagata, S., Onda, M., Kreitman, R. J., & Pastan, I. (2005). HA22 (R490A) Is a Recombinant Immunotoxin with Increased Antitumor Activity without an Increase in Animal Toxicity. *Clinical Cancer Research, 11*(4), 1545-1550.

Barbas, C. F., Burton, D., Scott, J. K., & Silverman, G. J. (2001). *Phage Display: A Laboratory Manual*. New York: Cold Spring Harbor Laboratory Press.

Barragan, A., Brossier, F., & Sibley, L. D. (2005). Transepithelial migration of *Toxoplasma gondii* involves an interaction of intercellular adhesion molecule 1 (ICAM-1) with the parasite adhesin MIC2. *Cellular Microbiology, 7*(4), 561-568.

Barragan, A., & Sibley, L. D. (2002). Transepithelial Migration of *Toxoplasma gondii* Is Linked to Parasite Motility and Virulence. *The Journal of Experimental Medicine, 195*(12), 1625-1633.

Batista, F. D., & Neuberger, M. S. (1998). Affinity Dependence of the B Cell Response to Antigen: A Threshold, a Ceiling, and the Importance of Off-Rate. *Immunity, 8*(6), 751-759.

Beck, A., Wurch, T., Bailly, C., & Corvaia, N. (2012). Strategies and challenges for the next generation of therapeutic antibodies. *Nat Rev Immunol, 10*(5), 345-352.

Beckers, C. J., Dubremetz, J. F., Mercereau-Puijalon, O., & Joiner, K. A. (1994). The *Toxoplasma gondii* rhoptry protein ROP 2 is inserted into the parasitophorous vacuole membrane, surrounding the intracellular parasite, and is exposed to the host cell cytoplasm. *The Journal of Cell Biology, 127*(4), 947-961.

Billker, O., Lourido, S., & Sibley, L. D. (2009). Calcium-Dependent Signaling and Kinases in Apicomplexan Parasites. *Cell host & microbe, 5*(6), 612-622.

Black, M. W., & Boothroyd, J. C. (2000). Lytic Cycle of *Toxoplasma gondii*. *Microbiol. Mol. Biol. Rev., 64*(3), 607-623.

Boder, E. T., Midelfort, K. S., & Wittrup, K. D. (2000). Directed evolution of antibody fragments with monovalent femtomolar antigen-binding affinity. *Proceedings of the National Academy of Sciences of the United States of America, 97*(20), 10701-10705.

Boel, E., Verlaan, S., Poppelier, M. J. J. G., Westerdaal, N. A. C., Van Strijp, J. A. G., & Logtenberg, T. (2000). Functional human monoclonal antibodies of all isotypes constructed from phage display library-derived single-chain Fv antibody fragments. *Journal of Immunological Methods, 239*(1-2), 153-166.

Bohne, W., Heesemann, J., & Gross, U. (1994). Reduced replication of *Toxoplasma gondii* is necessary for induction of bradyzoite-specific antigens: a possible role for nitric oxide in triggering stage conversion. *Infect. Immun., 62*(5), 1761-1767.

Boothroyd, J. C., & Dubremetz, J.-F. (2008). Kiss and spit: the dual roles of Toxoplasma rhoptries. *Nat Rev Micro, 6*(1), 79-88.

Boothroyd, J. C., Hehl, A., Knoll, L. J., & Manger, I. D. (1998). The surface of toxoplasma: More and Less. *International Journal for Parasitology, 28*(1), 3-9.

Bradbury, A. R. M., & Marks, J. D. (2004). Review: Antibodies from phage antibody libraries. *Journal of Immunological Methods, 290*, 29-49.

Brammer, L. A., Bolduc, B., Kass, J. L., Felice, K. M., Noren, C. J., & Hall, M. F. (2008). A target-unrelated peptide in an M13 phage display library traced to an advantageous mutation in the gene II ribosome-binding site. *Analytical Biochemistry, 373*(1), 88-98.

Brindle, R., Holliman, R., Gilks, C., & Waiyaki, P. (1991). Toxoplasma antibodies in HIV-positive patients from Nairobi. *Transactions of the Royal Society of Tropical Medicine and Hygiene, 85*(6), 750-751.

Brooks, R. G., & Remington, J. S. (1986). Transplant-related infections. In J. V. Bennett & P. S. Brachman (Eds.), *Hospital Infections* (2nd ed., pp. 581-618). Boston: Little, Brown and Co.

Brossier, F., Jewett, T. J., Sibley, L. D., & Urban, S. (2005). A spatially localized rhomboid protease cleaves cell surface adhesins essential for invasion by Toxoplasma. *Proceedings of the National Academy of Sciences of the United States of America, 102*(11), 4146-4151.

Bruccoleri, R. E., & Karplus, M. (1987). Prediction of the folding of short polypeptide segments by uniform conformational sampling. *Biopolymers, 26*(1), 137-168.

Brydges, S. D., Harper, J. M., Parussini, F., Coppens, I., & Carruthers, V. B. (2008). A transient forward-targeting element for microneme-regulated secretion in *Toxoplasma gondii*. *Biology of the Cell, 100*(4), 253-264.

Burg, J. L., Grover, C. M., Pouletty, P., & Boothroyd, J. C. (1989). Direct and sensitive detection of a pathogenic protozoan, *Toxoplasma gondii*, by polymerase chain reaction. *J. Clin. Microbiol., 27*(8), 1787-1792.

Burton, D. R. (2001). Antibody Libraries. In C. F. I. Barbas, D. R. Burton, J. K. Scott & G. J. Silverman (Eds.), *Phage Display - A Laboratory Manual* (pp. 3.1-3.11). New York: Cold Spring Harbor Laboratory Press.

Butcher, B. A., Kim, L., Johnson, P. F., & Denkers, E. Y. (2001). *Toxoplasma gondii* Tachyzoites Inhibit Proinflammatory Cytokine Induction in Infected Macrophages by Preventing Nuclear Translocation of the Transcription Factor NF-κB. *The Journal of Immunology, 167*(4), 2193-2201.

Buzby, J. C., & Roberts, T. (1996). ERS Updates U.S. Foodborne Disease Costs for Seven Pathogens. *Food Review, (Sept - Dec)*, 20-25.

Buzoni-Gatel, D., Debbabi, H., Mennechet, F. J. D., Martin, V., Lepage, A. C., Schwartzman, J. D., et al. (2001). Murine ileitis after intracellular parasite infection is controlled by TGF-β-producing intraepithelial lymphocytes. *Gastroenterology, 120*(4), 914-924.

Cai, X., & Garen, A. (1995). Anti-melanoma antibodies from melanoma patients immunized with genetically modified autologous tumor cells: selection of specific antibodies from single-chain Fv fusion phage libraries. *Proc. Natl. Acad. of Sci. , 92*(14), 6537-6541.

Cardoso, R. M. F., Zwick, M. B., Stanfield, R. L., Kunert, R., Binley, J. M., Katinger, H., et al. (2005). Broadly Neutralizing Anti-HIV Antibody 4E10 Recognizes a Helical Conformation of a Highly Conserved Fusion-Associated Motif in gp41. *Immunity, 22*(2), 163-173.

Carmen, J. C., Hardi, L., & Sinai, A. P. (2006). *Toxoplasma gondii* inhibits ultraviolet light-induced apoptosis through multiple interactions with the mitochondrion-dependent programmed cell death pathway. *Cellular Microbiology, 8*(2), 301-315.

Carruthers, V. B. (1999). Armed and dangerous: *Toxoplasma gondii* uses an arsenal of secretory proteins to infect host cells. *Parasitol Int, 48*, 1-10.

Carruthers, V. B. (2002). Host cell invasion by the opportunistic pathogen *Toxoplasma gondii*. *Acta Tropica, 81*(2), 111-122.

Carruthers, V. B., & Blackman, M. J. (2005). MicroReview: A new release on life: emerging concepts in proteolysis and parasite invasion. *Molecular Microbiology, 55*(6), 1617-1630.

Carruthers, V. B., Giddings, O. K., & Sibley, L. D. (1999). Secretion of micronemal proteins is associated with toxoplasma invasion of host cells. *Cellular Microbiology, 1*(3), 225-235.

Carruthers, V. B., Hakansson, S., Giddings, O. K., & Sibley, L. D. (2000). *Toxoplasma gondii* Uses Sulfated Proteoglycans for Substrate and Host Cell Attachment. *Infect. Immun., 68*(7), 4005-4011.

Carruthers, V. B., Moreno, S. N. J., & Sibley, L. D. (1999). Ethanol and acetaldehyde elevate intracellular Ca2+ and stimulate microneme discharge in *Toxoplasma gondii*. *Biochemical Journal, 342*(2), 379-386.

Carruthers, V. B., & Sibley, L. D. (1999). Mobilization of intracellular calcium stimulates microneme discharge in *Toxoplasma gondii*. *Molecular Microbiology, 31*(2), 421-428.

Carter, P. J. (2006). Potent antibody therapeutics by design. *Nat Rev Immunol, 6*(5), 343-357.

Catherine, L., Francois, R., Sophie, M., Christine, K., Bernard, R., Adrien, G. S., et al. (1988). Treatment of central nervous system toxoplasmosis with pyrimethamine/sulfadiazine combination in 35 patients with the acquired immunodeficiency syndrome: Efficacy of long-term continuous therapy. *The American journal of medicine, 84*(1), 94-100.

Cesbron-Delauw, M. F. (1994). Dense-granule organelles of *Toxoplasma gondii*: Their role in the host-parasite relationship. *Parasitology Today, 10*(8), 293-296.

Cesbron-Delauw, M. F., Guy, B., Torpier, G., Pierce, R. J., Lenzen, G., Cesbron, J. Y., et al. (1989). Molecular characterization of a 23-kilodalton major antigen secreted by *Toxoplasma gondii*. *Proceedings of the National Academy of Sciences of the United States of America, 86*(19), 7537-7541.

Chang, T. Y., & Siegel, D. L. (2001). Isolation of an IgG anti-B from a human Fab-phage display library. *Transfusion, 41*(1), 6-12.

Chen, M., Aosai, F., Norose, K., Mun, H.-S., & Yano, A. (2003). The role of anti-HSP70 autoantibody-forming VH1-JH1 B-1 cells in *Toxoplasma gondii*-infected mice. *International Immunology, 15*(1), 39-47.

Chen, W., & Dimitrov, D. S. (2009). Human monoclonal antibodies and engineered antibody domains as HIV-1 entry inhibitors. *Current Opinion in HIV and AIDS, 4*(2), 112-117 110.1097/COH.1090b1013e328322f328395e.

Chiappino, M. L., Nichols, B. A., & O'Connor, G. R. (1984). Scanning Electron Microscopy of *Toxoplasma gondii*: Parasite Torsion and Host-Cell Responses during Invasion1. *Journal of Eukaryotic Microbiology, 31*(2), 288-292.

Chirgwin, K., Hafner, R., Leport, C., Remington, J., Andersen, J., Bosler, E. M., et al. (2002). Randomized Phase II Trial of Atovaquone with Pyrimethamine or Sulfadiazine for Treatment of Toxoplasmic Encephalitis in Patients with Acquired Immunodeficiency Syndrome: ACTG 237/ANRS 039 Study. *Clinical Infectious Diseases, 34*(9), 1243-1250.

Chowdhury, P. S., & Pastan, I. (1999). Improving antibody affinity by mimicking somatic hypermutation *in vitro*. *Nat Biotech, 17*(6), 568-572.

Clackson, T., Hoogenboom, H. R., Griffiths, A. D., & Winter, G. (1991). Making antibody fragments using phage display libraries. *Nature, 352*(6336), 624-628.

Clark, L. A., Ganesan, S., Papp, S., & van Vlijmen, H. W. T. (2006). Trends in Antibody Sequence Changes during the Somatic Hypermutation Process. *The Journal of Immunology, 177*(1), 333-340.

Coppens, I., Dunn, J. D., Romano, J. D., Pypaert, M., Zhang, H., Boothroyd, J. C., et al. (2006). *Toxoplasma gondii* Sequesters Lysosomes from Mammalian Hosts in the Vacuolar Space. *Cell, 125*(2), 261-274.

Coppens, I., & Joiner, K. A. (2001). Parasite-host cell interactions in toxoplasmosis: new avenues for intervention? *Expert Reviews in Molecular Medicine, 3*(02), 1-20.

Costa, J. M., Munoz, C., Kruger, D., Martino, R., Held, T. K., Darde, M.-L., et al. (2001). Quality control for the diagnosis of *Toxoplasma gondii* reactivation in SCT patients using PCR assays. *Bone Marrow Transpl, 28*(5), 527-528.

Couper, K. N., Roberts, C. W., Brombacher, F., Alexander, J., & Johnson, L. L. (2005). *Toxoplasma gondii*-Specific Immunoglobulin M Limits Parasite Dissemination by Preventing Host Cell Invasion. *Infect. Immun., 73*(12), 8060-8068.

Courret, N., Darche, S., Sonigo, P., Milon, G., Buzoni-Gatel, D., & Tardieux, I. (2006). CD11c- and CD11b-expressing mouse leukocytes transport single *Toxoplasma gondii* tachyzoites to the brain. *Blood, 107*(1), 309-316.

Crncic, T. B., Laskarin, G., Juretic, K., Strbo, N., Dupor, J., Srsen, S., et al. (2005). Perforin and Fas/FasL Cytolytic Pathways at the Maternal–Fetal Interface. *American Journal of Reproductive Immunology, 54*(5), 241-248.

Crothers, D. M., & Metzger, H. (1972). The influence of polyvalency on the binding properties of antibodies. *Immunochemistry, 9*(3), 341-357.

Dabil, H., Boley, M. L., Schmitz, T. M., & Van Gelder, R. N. (2001). Validation of a Diagnostic Multiplex Polymerase Chain Reaction Assay for Infectious Posterior Uveitis. *Arch Ophthalmol, 119*(9), 1315-1322.

Dannemann, B., McCutchan, J. A., Israelski, D., Antoniskis, D., Leport, C., Luft, B., et al. (1992). Treatment of Toxoplasmic Encephalitis in Patients with AIDS. *Annals of Internal Medicine, 116*(1), 33-43.

Darde, M.-L. (2004). Genetic analysis of the diversity in *Toxoplasma gondii*. *Ann Ist Super Sanita, 40*(1), 57-63.

David, D., Goossens, D., Desgranges, C., Thèze, J., & Zouali, M. (1995). Molecular characterization of human monoclonal antibodies specific for several HIV proteins: analysis of the VH3 family expression. *Immunology Letters, 47*(1-2), 107-112.

De Genst, E., Handelberg, F., Van Meirhaeghe, A., Vynck, S., Loris, R., Wyns, L., et al. (2004). Chemical Basis for the Affinity Maturation of a Camel Single Domain Antibody. *Journal of Biological Chemistry, 279*(51), 53593-53601.

De Genst, E., Silence, K., Ghahroudi, M. A., Decanniere, K., Loris, R., Kinne, J. r., et al. (2005). Strong in Vivo Maturation Compensates for Structurally Restricted H3 Loops in Antibody Repertoires. *Journal of Biological Chemistry, 280*(14), 14114-14121.

de Kruif, J., Terstappen, L., Boel, E., & Logtenberg, T. (1995). Rapid selection of cell subpopulation-specific human monoclonal antibodies from a synthetic phage antibody library. *Proc. Natl. Acad. Sci. , 92*(9), 3938-3942.

Dempster, R. P. (1984). *Toxoplasma gondii*: Purification of zoites from peritoneal exudates by eight methods. *Exp. Parasitol., 57*(2), 195-207.

Denkers, E. Y., Yap, G., SchartonKersten, T., Charest, H., Butcher, B. A., Caspar, P., et al. (1997). Perforin-mediated cytolysis plays a limited role in host resistance to *Toxoplasma gondii*. *Journal of Immunology, 159*(4), 1903-1908.

Desiderio, A., Franconi, R., Lopez, M., Villani, M. E., Viti, F., Chiaraluce, R., et al. (2001). A semi-synthetic repertoire of intrinsically stable antibody fragments derived from a single-framework scaffold. *Journal of Molecular Biology, 310*(3), 603-615.

Dlugonska, H. (2008). Toxoplasma Rhoptries: Unique Secretory Organelles and Source of Promising Vaccine Proteins for Immunoprevention of Toxoplasmosis. *Journal of Biomedicine and Biotechnology, 2008*, Article ID 632424.

Dobrowolski, J. M., Carruthers, V. B., & Sibley, L. D. (1997). Participation of myosin in gliding motility and host cell invasion by *Toxoplasma gondii*. *Molecular Microbiology, 26*(1), 163-173.

Dobrowolski, J. M., & Sibley, L. D. (1996). Toxoplasma invasion of mammalian cells is powered by the actin cytoskeleton of the parasite. *Cell, 84*(6), 933-939.

Dockrell, D. H. (2003). The multiple roles of Fas ligand in the pathogenesis of infectious diseases. *Clinical Microbiology and Infection, 9*(8), 766-779.

Dooley, H., & Flajnik, M. F. (2005). Shark immunity bites back: affinity maturation and memory response in the nurse shark, Ginglymostoma cirratum. *European Journal of Immunology, 35*(3), 936-945.

Doorbar, J., & Winter, G. (1994). Isolation of a Peptide Antagonist to the Thrombin Receptor using Phage Display. *Journal of Molecular Biology, 244*(4), 361-369.

Dowse, T., & Soldati, D. (2004). Host cell invasion by the apicomplexans: the significance of microneme protein proteolysis. *Current Opinion in Microbiology, 7*(4), 388-396.

Dubey, J. P. (1996). *Toxoplasma gondii*. In S. Baron (Ed.), *Medical Microbiology* (4th ed.). Galveston, TX: The University of Texas Medical Branch at Galveston.

Dubey, J. P. (2007). The History and Life Cycle of *Toxoplasma gondii* (Diagnosis). In L. M. Weiss & K. Kim (Eds.), *Toxoplasma gondii: the model apicomplexan: perspectives and methods* (1st ed., pp. 10-11). London: Academic Press, Elsevier Ltd.

Dubey, J. P., & Beattie, C. P. (1988). *Toxoplasmosis of animals and man*. Boca Raton, FL.: CRC Press.

Dubey, J. P., & Jones, J. L. (2008). *Toxoplasma gondii* infection in humans and animals in the United States. *International Journal for Parasitology, 38*(11), 1257-1278.

Dubey, J. P., Lindsay, D. S., & Speer, C. A. (1998). Structures of *Toxoplasma gondii* Tachyzoites, Bradyzoites, and Sporozoites and Biology and Development of Tissue Cysts. *Clin. Microbiol. Rev., 11*(2), 267-299.

Dubey, J. P., Miller, N. L., & Frenkel, J. K. (1970). The *Toxoplasma gondii* oocyst from cat feces. *The Journal of Experimental Medicine, 132*(4), 636-662.

Dubey, J. P., Miller, S., Desmonts, G., Thulliez, P., & Anderson, W. R. (1986). *Toxoplasma gondii*-induced abortion in dairy goats. *J. Am. Vet. Med. Assoc., 188*(2), 159-162.

Dubey, J. P., Murrell, K. D., Fayer, R., & Schad, G. A. (1986). Distribution of *Toxoplasma gondii* tissue cysts in commercial cuts of pork. *J. Am. Vet. Med. Assoc., 188*(9), 1035-1037.

Dubremetz, J. F. (1998). Host cell invasion by *Toxoplasma gondii*. *Trends in Microbiology, 6*(1), 27-30.

Dubremetz, J. F., Rodriguez, C., & Ferreira, E. (1985). *Toxoplasma gondii*: Redistribution of monoclonal antibodies on tachyzoites during host cell invasion. *Experimental Parasitology, 59*(1), 24-32.

Dunn, D., Wallon, M., Peyron, F., Petersen, E., Peckham, C., & Gilbert, R. (1999). Mother-to-child transmission of toxoplasmosis: Risk estimates for clinical counselling. *Lancet, 353*(9167), 1829-1833.

Edelhofer, R. (1994). Prevalence of antibodies against *Toxoplasma gondii* in pigs in Austria - an evaluation of data from 1982 and 1992. *Parasitology Research, 80*(8), 642-644.

Edwards, B. M., Barash, S. C., Main, S. H., Choi, G. H., Minter, R., Ullrich, S., et al. (2003). The Remarkable Flexibility of the Human Antibody Repertoire; Isolation of Over One Thousand Different Antibodies to a Single Protein, BLyS. *Journal of Molecular Biology, 334*(1), 103-118.

Eisenhardt, S. U., Schwarz, M., Bassler, N., & Peter, K. (2007). Subtractive single-chain antibody (scFv) phage-display: tailoring phage-display for high specificity against function-specific conformations of cell membrane molecules. *Nat. Protocols, 2*(12), 3063-3073.

Ellis, J., Sinclair, D., & Morrison, D. (2004). Microarrays and stage conversion in *Toxoplasma gondii*. *Trends in Parasitology, 20*(6), 288-295.

Elsheikha, H. M., & Khan, N. A. (2010). Protozoa traversal of the blood–brain barrier to invade the central nervous system. *FEMS Microbiology Reviews, 34*(4), 532-553.

Endo, T., Sethi, K. K., & Piekarski, G. (1982). *Toxoplasma gondii*: Calcium lonophore A23187-mediated exit of trophozoites from infected murine macrophages. *Experimental Parasitology, 53*(2), 179-188.

Ewert, S., Honegger, A., & Plückthun, A. (2004). Stability improvement of antibodies for extracellular and intracellular applications: CDR grafting to stable frameworks and structure-based framework engineering. *Methods, 34*(2), 184-199.

Ewert, S., Huber, T., Honegger, A., & Plückthun, A. (2003). Biophysical Properties of Human Antibody Variable Domains. *Journal of Molecular Biology, 325*(3), 531-553.

Ferguson, D. J. P., & Hutchison, W. M. (1987). An ultrastructural study of the early development and tissue cyst formation of *Toxoplasma gondii* in the brains of mice. *Parasitology Research, 73*(6), 483-491.

Fernandez-Martin, J., Leport, C., Morlat, P., Meyohas, M. C., Chauvin, J. P., & Vilde, J. L. (1991). Pyrimethamine-clarithromycin combination for therapy of acute Toxoplasma encephalitis in patients with AIDS. *Antimicrob. Agents Chemother., 35*(10), 2049-2052.

Fischer, H.-G., Nitzgen, B., Reichmann, G., Groß, U., & Hadding, U. (1997). Host cells of *Toxoplasma gondii* encystation in infected primary culture from mouse brain. *Parasitology Research, 83*(7), 637-641.

Fishback;, J., & Frenkel, J. (1991). Toxoplasmosis. *Semin Vet Med Surg (Small Anim), 6*(3), 219-226.

Folgori, A., Tafi, R., Meola, A., Felici, F., Galfre, G., Cortese, R., et al. (1994). A general strategy to identify mimotopes of pathological antigens using only random peptide libraries and human sera. *EMBO J., 13*(9), 2236-2243.

Foote, J., & Eisen, H. N. (1995). Kinetic and affinity limits on antibodies produced during immune responses. *Proceedings of the National Academy of Sciences, 92*(5), 1254-1256.

Foulon, W., Pinon, J.-M., Stray-Pedersen, B., Pollak, A., Lappalainen, M., Decoster, A., et al. (1999). Prenatal diagnosis of congenital toxoplasmosis: A multicenter evaluation of

different diagnostic parameters. *American Journal of Obstetrics and Gynecology, 181*(4), 843-847.

French, D. L., Laskov, R., & Scharff, M. D. (1989). The role of somatic hypermutation in the generation of antibody diversity. *Science, 244*(4909), 1152-1157.

Fu, Y.-F., Feng, M., Ohnishi, K., Kimura, T., Itoh, J., Cheng, X.-J., et al. (2011). Generation of a Neutralizing Human Monoclonal Antibody Fab Fragment to Surface Antigen 1 of Toxoplasma gondii Tachyzoites. *Infection and Immunity, 79*(1), 512-517.

Fuhrman, S. A., & Joiner, K. A. (1989). *Toxoplasma gondii*: mechanism of resistance to complement-mediated killing. *The Journal of Immunology, 142*(3), 940-947.

Furtado, G. C., Slowik, M., Kleinman, H. K., & Joiner, K. A. (1992). Laminin enhances binding of *Toxoplasma gondii* tachyzoites to J774 murine macrophage cells. *Infect. Immun., 60*(6), 2337-2342.

Gagne, S. S. (2001). Toxoplasmosis. *Primary Care Update for OB/GYNS, 8*(3), 122-126.

Galanis, M., Irving, R. A., & Hudson, P. J. (2001). Bacteriophage Library Construction and Selection of Recombinant Antibodies. In *Current Protocols in Immunology*: John Wiley & Sons, Inc.

Gavrilescu, L. C., & Denkers, E. Y. (2001). IFN-γ Overproduction and High Level Apoptosis Are Associated with High but Not Low Virulence *Toxoplasma gondii* Infection. *The Journal of Immunology, 167*(2), 902-909.

Ghosh, S., & Karin, M. (2002). Missing Pieces in the NF-ºB Puzzle. *Cell, 109*(2), S81-S96.

Gigley, J. P., Fox, B. A., & Bzik, D. J. (2009). Cell-Mediated Immunity to *Toxoplasma gondii* Develops Primarily by Local Th1 Host Immune Responses in the Absence of Parasite Replication. *The Journal of Immunology, 182*(2), 1069-1078.

Giordano, R. J., Cardo-Vila, M., Lahdenranta, J., Pasqualini, R., & Arap, W. (2001). Biopanning and rapid analysis of selective interactive ligands. *Nat Med, 7*(11), 1249-1253.

Grimwood, J., & Smith, J. E. (1996). *Toxoplasma gondii:* the role of parasite surface and secreted proteins in host cell invasion. *International Journal for Parasitology, 26*(2), 169-173.

Guerina, N. G., Hsu, H.-W., Meissner, H. C., Maguire, J. H., Lynfield, R., Stechenberg, B., et al. (1994). Neonatal Serologic Screening and Early Treatment for Congenital *Toxoplasma gondii* Infection. *New England Journal of Medicine, 330*(26), 1858-1863.

Hagberg, L., Palmertz, B., & Lindberg, J. (1993). Doxycycline and Pyrimethamine for Toxoplasmic Encephalitis. *Scandinavian Journal of Infectious Diseases, 25*(1), 157-160.

Hakansson, S., Charron, A. J., & Sibley, L. D. (2001). Toxoplasma evacuoles: a two-step process of secretion and fusion forms the parasitophorous vacuole. *EMBO J, 20*(12), 3132-3144.

Halin, C., Rondini, S., Nilsson, F., Berndt, A., Kosmehl, H., Zardi, L., et al. (2002). Enhancement of the antitumor activity of interleukin-12 by targeted delivery to neovasculature. *Nat Biotech, 20*(3), 264-269.

Hall, T. A. (1999). BioEdit: a user-friendly biological sequence alignment editor and analysis program for Windows 95/98/NT. *Nucleic Acids Symposium Series, 41*, 95-98.

Hammer, J., Takacs, B., & Sinigaglia, F. (1992). Identification of a motif for HLA-DR1 binding peptides using M13 display libraries. *J Exp Med, 176*(4), 1007-1013.

Hansen, M. H., Nielsen, H. V., & Ditzel, H. J. (2002). Translocation of an Intracellular Antigen to the Surface of Medullary Breast Cancer Cells Early in Apoptosis Allows for an Antigen-Driven Antibody Response Elicited by Tumor-Infiltrating B Cells. *The Journal of Immunology, 169*(5), 2701-2711.

He, X.-l., Grigg, M. E., Boothroyd, J. C., & Garcia, K. C. (2002). Structure of the immunodominant surface antigen from the *Toxoplasma gondii* SRS superfamily. *Nat Struct Mol Biol, 9*(8), 606-611.

Hehl, A. B., Lekutis, C., Grigg, M. E., Bradley, P. J., Dubremetz, J.-F., Ortega-Barria, E., et al. (2000). *Toxoplasma gondii* Homologue of Plasmodium Apical Membrane Antigen 1 Is Involved in Invasion of Host Cells. *Infect. Immun., 68*(12), 7078-7086.

Hill, D., & Dubey, J. P. (2002). *Toxoplasma gondii*: transmission, diagnosis and prevention. *Clinical Microbiology and Infection, 8*(10), 634-640.

Ho, M., Kreitman, R. J., Onda, M., & Pastan, I. (2005). In vitro antibody evolution targeting germline hot spots to increase activity of an anti-CD22 immunotoxin. *J Biol Chem, 280*(1), 607-617.

Hoe, L. N., Wan, K. L., & Nathan, S. (2005). Construction and characterization of recombinant single-chain variable fragment antibodies against *Toxoplasma gondii* MIC2 protein. *Parasitology, 131*(06), 759-768.

Hof, D. l., Cheung, K., Roossien, H. E., Pruijn, G. J. M., & Raats, J. M. H. (2006). A Novel Subtractive Antibody Phage Display Method to Discover Disease Markers. *Molecular & Cellular Proteomics, 5*(2), 245-255.

Hogrefe, H. H., Cline, J., Youngblood, G. L., & Allen, R. M. (2002). Creating Randomized Amino Acid Libraries with the QuikChange Multi Site-Directed Mutagenesis Kit. *BioTechniques, 33*(5), 1158-1165.

Hohlfeld, P., Daffos, F., Costa, J.-M., Thulliez, P., Forestier, F., & Vidaud, M. (1994). Prenatal Diagnosis of Congenital Toxoplasmosis with a Polymerase-Chain-Reaction Test on Amniotic Fluid. *New England Journal of Medicine, 331*(11), 695-699.

Hokelek, M. (2009, Jan 27, 2009). Toxoplasmosis: Treatment & Medication. *Parasitic Infections*, from http://emedicine.medscape.com/article/229969-treatment

Holliger, P., & Hudson, P. J. (2005). Engineered antibody fragments and the rise of single domains. *Nat Biotech, 23*(9), 1126-1136.

Holliger, P., Wing, M., Pound, J. D., Bohlen, H., & Winter, G. (1997). Retargeting serum immunoglobulin with bispecific diabodies. *Nat Biotech, 15*(7), 632-636.

Holliman, R. E. (1995). Congenital toxoplasmosis: prevention, screening and treatment. *Journal of Hospital Infection, 30*(Supplement 1), 179-190.

Hoogenboom, H. R. (2005). Selecting and screening recombinant antibody libraries. *Nat Biotech, 23*(9), 1105-1116.

Hoppe, H. C., Ngo, H. M., Yang, M., & Joiner, K. A. (2000). Targeting to rhoptry organelles of *Toxoplasma gondii* involves evolutionarily conserved mechanisms. *Nat Cell Biol, 2*(7), 449-456.

Huang, J., Ru, B., Li, S., Lin, H., & Guo, F.-B. (2010). SAROTUP: Scanner and Reporter of Target-Unrelated Peptides. *Journal of Biomedicine and Biotechnology, 2010*.

Hudson, P. J., & Souriau, C. (2003). Engineered antibodies. *Nat Med, 9*(1), 129-134.

Huhalov, A., & K.A., C. (2004). Engineered single chain antibody fragments for radioimmunotherapy. *Q. J. Nucl. Med. Mol. Imaging, 48*(4), 279-288.

Huynh, M.-H., & Carruthers, V. B. (2006). Toxoplasma MIC2 Is a Major Determinant of Invasion and Virulence. *PLoS Pathog, 2*(8), e84.

Huynh, M.-H., Rabenau, K. E., Harper, J. M., Beatty, W. L., Sibley, L. D., & Carruthers, V. B. (2003). Rapid invasion of host cells by Toxoplasma requires secretion of the MIC2-M2AP adhesive protein complex. *EMBO J, 22*(9), 2082-2090.

Igonet, S., Vulliez-Le Normand, B., Faure, G., Riottot, M.-M., Kocken, C. H. M., Thomas, A. W., et al. (2007). Cross-reactivity Studies of an Anti-*Plasmodium vivax* Apical Membrane Antigen 1 Monoclonal Antibody: Binding and Structural Characterisation. *Journal of Molecular Biology, 366*(5), 1523-1537.

Israelski, D. M., Chmiel, J. S., Poggensee, L., Phair, J. P., & Remington, J. S. (1993). Prevalence of Toxoplasma infection in a cohort of homosexual men at risk of AIDS and toxoplasmic encephalitis. *Journal of Acquired Immune Deficiency Syndromes, 6*(4), 414-418.

Jacobs, L., Remington, J. S., & Melton, M. L. (1960). The resistance of the encysted form of *Toxoplasma gondii*. *The Journal of Parasitology, 46*(1), 11-21.

Jeltsch, A., & Lanio, T. (2002). Site-directed mutagenesis by polymerase chain reaction. In J. Braman (Ed.), *Methods in Molecular Biology* (2nd ed.). Totowa, NJ: Humana Press.

Jenum, P. A., Stray-Pedersen, B., & Gundersen, A. G. (1997). Improved diagnosis of primary *Toxoplasma gondii* infection in early pregnancy by determination of antitoxoplasma immunoglobulin G avidity. *J. Clin. Microbiol., 35*(8), 1972-1977.

Jespers, L., Schon, O., James, L. C., Veprintsev, D., & Winter, G. (2004). Crystal Structure of HEL4, a Soluble, Refoldable Human VH Single Domain with a Germ-line Scaffold. *Journal of Molecular Biology, 337*(4), 893-903.

Johnson, L. L., & Sayles, P. C. (2002). Deficient Humoral Responses Underlie Susceptibility to *Toxoplasma gondii* in CD4-Deficient Mice. *Infect. Immun., 70*(1), 185-191.

Joiner, K. A., Fuhrman, S. A., Miettinen, H. M., Kasper, L. H., & Mellman, I. (1990). *Toxoplasma gondii*: fusion competence of parasitophorous vacuoles in Fc receptor-transfected fibroblasts. *Science, 249*(4969), 641-646.

Jolly, C. J., Wagner, S. D., Rada, C., Klix, N., Milstein, C. s., & Neuberger, M. S. (1996). The targeting of somatic hypermutation. *Seminars in Immunology, 8*(3), 159-168.

Jones, J., Lopez, A., & Wilson, M. (2003). Congenital Toxoplasmosis. *Am Fam Phys, 67*, 2131-2138.

Jones, T. C., Yeh, S., & Hirsch, J. G. (1972). The interaction between *Toxoplasma gondii* and mammalian cells : I. Mechanism of entry and intracellular fate of the parasite. *J Exp Med., 136*(5), 1157-1172.

Jung, C., Lee, C. Y. F., & Grigg, M. E. (2004). The SRS superfamily of Toxoplasma surface proteins. *International Journal for Parasitology, 34*(3), 285-296.

Kabir, M. E., Krishnaswamy, S., Miyamoto, M., Furuichi, Y., & Komiyama, T. (2009). An improved phage-display panning method to produce an HM-1 killer toxin anti-idiotypic antibody. *BMC Biotechnology, 9*(1), 99.

Kamal. *Toxoplasma gondii*: Rosette formation. from http://www.einstein.yu.edu/aif/page.aspx?id=22505

Kang, H., Remington, J. S., & Suzuki, Y. (2000). Decreased Resistance of B Cell-Deficient Mice to Infection with *Toxoplasma gondii* Despite Unimpaired Expression of IFN-γ, TNF-α, and Inducible Nitric Oxide Synthase. *The Journal of Immunology, 164*(5), 2629-2634.

Keller, P., Schaumburg, F., Fischer, S. F., Häcker, G., Groß, U., & Lüder, C. G. K. (2006). Direct inhibition of cytochrome c-induced caspase activation *in vitro* by *Toxoplasma gondii* reveals novel mechanisms of interference with host cell apoptosis. *FEMS Microbiology Letters, 258*(2), 312-319.

Kieschnick, H., Wakefield, T., Narducci, C. A., & Beckers, C. (2001). *Toxoplasma gondii* Attachment to Host Cells Is Regulated by a Calmodulin-like Domain Protein Kinase. *Journal of Biological Chemistry, 276*(15), 12369-12377.

Kim, J.-H., Kang, K.-I., Kang, W.-C., Sohn, H.-J., Jean, Y.-H., Park, B. K., et al. (2009). Porcine abortion outbreak associated with *Toxoplasma gondii* in Jeju Island, Korea. *J Vet Sci, 10*(2), 147-151.

Kim, J. Y., Ahn, H.-J., Ryu, K. J., & Nam, H.-W. (2008). Interaction between Parasitophorous Vacuolar Membrane-associated GRA3 and Calcium Modulating Ligand of Host Cell Endoplasmic Reticulum in the Parasitism of *Toxoplasma gondii*. *Korean J Parasitol, 46*(4), 209-216.

Kim, L., & Denkers, E. Y. (2006). *Toxoplasma gondii* triggers Gi-dependent PI 3-kinase signaling required for inhibition of host cell apoptosis. *J Cell Sci, 119*(10), 2119-2126.

Kim, S.-K., Fouts, A. E., & Boothroyd, J. C. (2007). *Toxoplasma gondii* Dysregulates IFN-γ-Inducible Gene Expression in Human Fibroblasts: Insights from a Genome-Wide Transcriptional Profiling. *The Journal of Immunology, 178*(8), 5154-5165.

Knight, D. M., Jordan, R. E., Kruszynski, M., Tam, S. H., Giles-Komar, J., Treacy, G., et al. (2004). Pharmacodynamic enhancement of the anti-platelet antibody Fab abciximab by site-specific pegylation. *Platelets, 15*(7), 409-418.

Kola, I., & Landis, J. (2004). Can the pharmaceutical industry reduce attrition rates? *Nat Rev Drug Discov, 3*(8), 711-716.

Kolonin, M. G., Saha, P. K., Chan, L., Pasqualini, R., & Arap, W. (2004). Reversal of obesity by targeted ablation of adipose tissue. *Nature Medicine, 10*(6), 625-632.

Kramer, R. A., Cox, F., van der Horst, M., van den Oudenrijn, S., Res, P. C. M., Bia, J., et al. (2003). A novel helper phage that improves phage display selection efficiency by preventing the amplification of phages without recombinant protein. *Nucleic Acids Research, 31*(11), e59.

Krammer, P. H. (2000). CD95's deadly mission in the immune system. *Nature, 407*(6805), 789-795.

Krauss, J., Arndt, M. A. E., Vu, B. K., Newton, D. L., & Rybak, S. M. (2005). Targeting malignant B-cell lymphoma with a humanized anti-CD22 scFv-angiogenin immunoenzyme. *British Journal of Haematology, 128*(5), 602-609.

Krumpe, L. R. H., Atkinson, A. J., Smythers, G. W., Kandel, A., Schumacher, K. M., McMahon, J. B., et al. (2006). T7 lytic phage-displayed peptide libraries exhibit less sequence bias than M13 filamentous phage-displayed peptide libraries. *Proteomics, 6*(15), 4210-4222.

Kupsch, J. r.-M., Tidman, N. H., Kang, N. V., Truman, H., Hamilton, S., Patel, N., et al. (1999). Isolation of Human Tumor-specific Antibodies by Selection of an Antibody Phage Library on Melanoma Cells. *Clinical Cancer Research, 5*(4), 925-931.

Laemmli, U. K. (1970). Cleavage of Structural Proteins during the Assembly of the Head of Bacteriophage T4. *Nature, 227*(5259), 680-685.

Laliberté, J., & Carruthers, V. (2008). Host cell manipulation by the human pathogen *Toxoplasma gondii*. *Cellular and Molecular Life Sciences, 65*(12), 1900-1915.

Lambert, H., & Barragan, A. (2010). Modelling parasite dissemination: host cell subversion and immune evasion by *Toxoplasma gondii*. *Cellular Microbiology, 12*(3), 292-300.

Lambert, H., Hitziger, N., Dellacasa, I., Svensson, M., & Barragan, A. (2006). Induction of dendritic cell migration upon *Toxoplasma gondii* infection potentiates parasite dissemination. *Cellular Microbiology, 8*(10), 1611-1623.

Lambert, H., Vutova, P. P., Adams, W. C., Lore, K., & Barragan, A. (2009). The *Toxoplasma gondii*-Shuttling Function of Dendritic Cells Is Linked to the Parasite Genotype. *Infect. Immun., 77*(4), 1679-1688.

Lang, C., Groß, U., & Lüder, C. (2007). Subversion of innate and adaptive immune responses by *Toxoplasma Gondii*. *Parasitology Research, 100*(2), 191-203.

Lazar, G. A., Dang, W., Karki, S., Vafa, O., Peng, J. S., Hyun, L., et al. (2006). Engineered antibody Fc variants with enhanced effector function. *Proceedings of the National Academy of Sciences of the United States of America, 103*(11), 4005-4010.

Lazarou, M., Patino, J. A. G., Jennings, R. M., McIntosh, R. S., Shi, J., Howell, S., et al. (2009). Inhibition of Erythrocyte Invasion and *Plasmodium falciparum* Merozoite Surface Protein 1 Processing by Human Immunoglobulin G1 (IgG1) and IgG3 Antibodies. *Infection and Immunity, 77*(12), 5659-5667.

Lefranc, M.-P. (2001). IMGT, the international ImMunoGeneTics database. *Nucleic Acids Res., 29*(1), 207-209.

Lefranc, M.-P., Pommié, C., Ruiz, M., Giudicelli, V., Foulquier, E., Truong, L., et al. (2003). IMGT unique numbering for immunoglobulin and T cell receptor variable domains and Ig superfamily V-like domains. *Developmental & Comparative Immunology, 27*(1), 55-77.

Lemasters, J. J., Qian, T., Bradham, C. A., Brenner, D. A., Cascio, W. E., Trost, L. C., et al. (1999). Mitochondrial Dysfunction in the Pathogenesis of Necrotic and Apoptotic Cell Death. *Journal of Bioenergetics and Biomembranes, 31*(4), 305-319.

Li, Z., Woo, C. J., Iglesias-Ussel, M. D., Ronai, D., & Scharff, M. D. (2004). The generation of antibody diversity through somatic hypermutation and class switch recombination. *Genes & Development, 18*(1), 1-11.

Lieberman, J. (2003). The ABCs of granule-mediated cytotoxicity: New weapons in the arsenal. *Nature Reviews Immunology, 3*(5), 361-370.

Liesenfeld, O., Montoya, J. G., Tathineni, N. J., Davis, M., Brown, B. W., Cobb, K. L., et al. (2001). Confirmatory serologic testing for acute toxoplasmosis and rate of induced abortions among women reported to have positive Toxoplasma immunoglobulin M antibody titers. *American Journal of Obstetrics and Gynecology, 184*(2), 140-145.

Ling, M. M., & Robinson, B. H. (1997). Approaches to DNA Mutagenesis: An Overview. *Analytical Biochemistry, 254*(2), 157-178.

Linsley, P. S. (2005). New look at an old costimulator. *Nat Immunol, 6*(3), 231-232.

Lopez, A., Dietz, V. J., Wilson, M., Navin, T. R., & Jones, J. L. (2000). *Preventing Congenital Toxoplasmosis* (No. 49/RR02). Atlanta: Mortality and Morbidity Weekly Report (MMWR), Centers for Disease Control and Prevention (CDC)o. Document Number)

Lowe, D., & Jermutus, L. (2004). Combinatorial Protein Biochemistry for Therapeutics and Proteomics. *Current Pharmaceutical Biotechnology, 5*(1), 17-27.

Lu, D., Shen, J., Vil, M. D., Zhang, H., Jimenez, X., Bohlen, P., et al. (2003). Tailoring in Vitro Selection for a Picomolar Affinity Human Antibody Directed against Vascular Endothelial Growth Factor Receptor 2 for Enhanced Neutralizing Activity. *Journal of Biological Chemistry, 278*(44), 43496-43507.

Luangsay, S., Kasper, L. H., Rachinel, N., Minns, L. A., Mennechet, F. J. D., Vandewalle, A., et al. (2003). CCR5 mediates specific migration of *Toxoplasma gondii*-primed CD8+ lymphocytes to inflammatory intestinal epithelial cells. *Gastroenterology, 125*(2), 491-500.

Lüder, C. G. K., Algner, M., Lang, C., Bleicher, N., & Gro, U. (2003). Reduced expression of the inducible nitric oxide synthase after infection with *Toxoplasma gondii* facilitates parasite replication in activated murine macrophages. *International Journal for Parasitology, 33*(8), 833-844.

Lüder, C. G. K., Giraldo-Velásquez, M., Sendtner, M., & Gross, U. (1999). *Toxoplasma gondii* in Primary Rat CNS Cells: Differential Contribution of Neurons, Astrocytes, and Microglial Cells for the Intracerebral Development and Stage Differentiation. *Experimental Parasitology, 93*(1), 23-32.

Luft, B. J., Hafner, R., Korzun, A. H., Leport, C., Antoniskis, D., Bosler, E. M., et al. (1993). Toxoplasmic encephalitis in patients with the acquired immunodeficiency syndrome. *New England Journal of Medicine, 329*(14), 995-1000.

Luft, B. J., & Remington, J. S. (1992). Toxoplasmic Encephalitis in AIDS. *Clinical Infectious Diseases, 15*(2), 211-222.

Lycke, E., & Norrby, R. (1966). Demonstration of a factor of *Toxoplasma gondii* enhancing the penetration of toxoplasma parasites into cultured host cells. *Br. J. Exp. Pathol., 47*, 248-256.

Machado, F., & Aliberti, J. (2006). Impact of lipoxin-mediated regulation on immune response to infectious disease. *Immunologic Research, 35*(3), 209-218.

MacLennan, I. C. M. (1994). Germinal Centers. *Annual Review of Immunology, 12*(1), 117-139.

Maggon, K. (18 March 2012). Top Ten Monoclonal Antibodies 2011. *Monoclonal Antibodies Market 2008 - 2011* Retrieved 18 March 2012, 2012, from http://monoclonalantibodies.wordpress.com/2012/03/18/top-ten-mabs-2011/

Manger, I. D., Hehl, A. B., & Boothroyd, J. C. (1998). The Surface of Toxoplasma Tachyzoites Is Dominated by a Family of Glycosylphosphatidylinositol-Anchored Antigens Related to SAG1. *Infect. Immun., 66*(5), 2237-2244.

Marks, C., & Marks, J. D. (1996). Phage Libraries - A New Route to Clinically Useful Antibodies. *New England Journal of Medicine, 335*(10), 730-733.

Marks, J. D., Ouwehand, W. H., Bye, J. M., Finnern, R., Gorick, B. D., Voak, D., et al. (1993). Human Antibody Fragments Specific for Human Blood Group Antigens from a Phage Display Library. *Nat Biotech, 11*(10), 1145-1149.

McCafferty, J., Griffiths, A. D., Winter, G., & Chiswell, D. J. (1990). Phage antibodies: filamentous phage displaying antibody variable domains. *Nature, 348*(6301), 552-554.

McCoy, K. D., Stoel, M., Stettler, R., Merky, P., Fink, K., Senn, B. M., et al. (2008). Polyclonal and Specific Antibodies Mediate Protective Immunity against Enteric Helminth Infection. *Cell Host & Microbe, 4*(4), 362-373.

Mead, P. S., Slutsker, L., Dietz, V., McCaig, L. F., Bresee, J. S., Shapiro, C., et al. (1999). Food-related illness and death in the United States. *Emerg. Infect. Dis., 5*, 841-842.

Meissner, M., Reiss, M., Viebig, N., Carruthers, V. B., Toursel, C., Tomavo, S., et al. (2002). A family of transmembrane microneme proteins of *Toxoplasma gondii* contain EGF-like domains and function as escorters. *J Cell Sci, 115*(3), 563-574.

Mercier, C., Howe, D. K., Mordue, D., Lingnau, M., & Sibley, L. D. (1998). Targeted Disruption of the GRA2 Locus in *Toxoplasma gondii* Decreases Acute Virulence in Mice. *Infect. Immun., 66*(9), 4176-4182.

Midelfort, K. S., Hernandez, H. H., Lippow, S. M., Tidor, B., Drennan, C. L., & Wittrup, K. D. (2004). Substantial Energetic Improvement with Minimal Structural Perturbation in a High Affinity Mutant Antibody. *Journal of Molecular Biology, 343*(3), 685-701.

Milroy, D. (2006). Monoclonal antibody therapeutics: The next generation. *Innovations in Pharmaceutical Technology: Biotechnology, 20*, 40-44.

Mintz, P. J., Kim, J., Do, K.-A., Wang, X., Zinner, R. G., Cristofanilli, M., et al. (2003). Fingerprinting the circulating repertoire of antibodies from cancer patients. *Nature Biotechnology, 21*(1), 57-63.

Miro, J. M., & Alvarez-Martinez, M. J. (2011). Parasitic infections in HIV-infected Patients: Toxoplasmosis. In J. J. Eron, K. Y. Smith & K. E. Squires (Eds.), *CCO HIV inPractice*. Reston, VA.: Clinical Care Options.

Miyazaki, K., & Arnold, F. H. (1999). Exploring Nonnatural Evolutionary Pathways by Saturation Mutagenesis: Rapid Improvement of Protein Function. *Journal of Molecular Evolution, 49*(6), 716-720.

Molestina, R. E., Payne, T. M., Coppens, I., & Sinai, A. P. (2003). Activation of NF-{kappa}B by *Toxoplasma gondii* correlates with increased expression of antiapoptotic genes and localization of phosphorylated I{kappa}B to the parasitophorous vacuole membrane. *J Cell Sci, 116*(21), 4359-4371.

Molestina, R. E., & Sinai, A. P. (2005). Host and parasite-derived IKK activities direct distinct temporal phases of NF-{kappa}B activation and target gene expression following Toxoplasma gondii infection. *J Cell Sci, 118*(24), 5785-5796.

Mondragon, R., & Frixione, E. (1996). Ca^{2+}-Dependence of Conoid Extrusion in *Toxoplasma gondii* Tachyzoites. *Journal of Eukaryotic Microbiology, 43*(2), 120-127.

Mondragon, R., Meza, I., & Frixione, E. (1994). Divalent Cation and ATP Dependent Motility of *Toxoplasma gondii* Tachyzoites After Mild Treatment with Trypsin. *Journal of Eukaryotic Microbiology, 41*(4), 330-337.

Montoya, J. G., & Liesenfeld, O. (2004). Toxoplasmosis. *The Lancet, 363*(9425), 1965-1976.

Montoya, J. G., & Remington, J. S. (2000). *Toxoplasma gondii*. In G. L. Mandell, R. G. Douglas, J. E. Bennett & R. Dolin (Eds.), *Mandell, Douglas and Bennett's Principles and Practice of Infectious Diseases* (5th ed., pp. 2858-2888). Philadelphia: Churchill Livingstone.

Mordue, D. G., Desai, N., Dustin, M., & Sibley, L. D. (1999). Invasion by *Toxoplasma gondii* Establishes a Moving Junction That Selectively Excludes Host Cell Plasma Membrane Proteins on the Basis of Their Membrane Anchoring. *The Journal of Experimental Medicine, 190*(12), 1783-1792.

Mordue, D. G., Håkansson, S., Niesman, I., & David Sibley, L. (1999). *Toxoplasma gondii* Resides in a Vacuole That Avoids Fusion with Host Cell Endocytic and Exocytic Vesicular Trafficking Pathways. *Experimental Parasitology, 92*(2), 87-99.

Mordue, D. G., Monroy, F., La Regina, M., Dinarello, C. A., & Sibley, L. D. (2001). Acute Toxoplasmosis Leads to Lethal Overproduction of Th1 Cytokines. *The Journal of Immunology, 167*(8), 4574-4584.

Mota, M. M., Pradel, G., Vanderberg, J. P., Hafalla, J. C. R., Frevert, U., Nussenzweig, R. S., et al. (2001). Migration of Plasmodium Sporozoites Through Cells Before Infection. *Science, 291*(5501), 141-144.

Mourez, M., Kane, R. S., Mogridge, J., Metallo, S., Deschatelets, P., Sellman, B. R., et al. (2001). Designing a polyvalent inhibitor of anthrax toxin. *Nat Biotech, 19*(10), 958-961.

Muraoka, S., Ito, Y., Kamimura, M., Baba, M., Arima, N., Suda, Y., et al. (2009). Effective Induction of Cell Death on Adult T-Cell Leukaemia Cells by HLA-DRÎ²-Specific Small Antibody Fragment Isolated from Human Antibody Phage Library. *J Biochem, 145*(6), 799-810.

Nakaar, V., Ngo, H. M., Aaronson, E. P., Coppens, I., Stedman, T. T., & Joiner, K. A. (2003). Pleiotropic effect due to targeted depletion of secretory rhoptry protein ROP2 in *Toxoplasma gondii. J Cell Sci, 116*(11), 2311-2320.

Nakamura, T., Peng, K.-W., Vongpunsawad, S., Harvey, M., Mizuguchi, H., Hayakawa, T., et al. (2004). Antibody-targeted cell fusion. *Nat Biotech, 22*(3), 331-336.

Nathan, S., Li, H., Mohamed, R., & Embi, N. (2002). Phage display of recombinant antibodies toward *Burkholderia pseudomallei* exotoxin. *J Biochem Mol Biol Biophys. , 6*(1), 45-53.

Neri, D., Montigiani, S., & Kirkham, P. M. (1996). Biophysical methods for the determination of antibody-antigen affinities. *Trends in Biotechnology, 14*(12), 465-470.

Neuberger, M. S., Ehrenstein, M. K., Klix, N., Jolly, C. J., Yélamos, J., Rada, C., et al. (1998). Monitoring and interpreting the intrinsic features of somatic hypermutation. *Immunological Reviews, 162*(1), 107-116.

Neuberger, M. S., & Milstein, C. (1995). Somatic hypermutation. *Current Opinion in Immunology, 7*(2), 248-254.

Newton, E. R. (1999). Diagnosis of Perinatal TORCH Infections. *Clinical Obstetrics and Gynecology, 42*(1), 59-70.

Nichols, B. A., Chiappino, M. L., & O'Connor, G. R. (1983). Secretion from the Rhoptries of *Toxoplasma gondii* during host-cell invasion. *Journal of Ultrastructure Research, 83*(1), 85-98.

Nichols, B. A., Chiappino, M. L., & O'Connor, G. R. (1983). Secretion from the rhoptries of *Toxoplasma gondii* during host-cell invasion. *J. Ultrastruct. Res., 83*, 85-98.

Nielsen, U. B., Adams, G. P., Weiner, L. M., & Marks, J. D. (2000). Targeting of Bivalent Anti-ErbB2 Diabody Antibody Fragments to Tumor Cells Is Independent of the Intrinsic Antibody Affinity. *Cancer Research, 60*(22), 6434-6440.

Nissapatorn, V., & Abdullah, K. A. (2004). Review on human toxoplasmosis in Malaysia: The past, present and prospective future. *Southeast Asian J. Trop. Med. Public Health, 35*(1), 24-30.

Nissapatorn, V., Lee, C., Quek, K. F., Leong, C. L., Mahmud, R., & Abdulah, K. A. (2004). Toxoplasmosis in HIV/AIDS patients: A current situation. *Jpn. J. Infect. Dis., 57*, 160-165.

Nissapatorn, V., Lee, C. K. C., & Cho, S. M. (2003). Toxoplasmosis in HIV/AIDS patients in Malaysia. *Southeast Asian J. Trop. Med. Public Health, 34*(2), 80-85.

O'Neil, K. T., & Hoess, R. H. (1995). Phage display: protein engineering by directed evolution. *Curr Opin Struct Biol, 5*(4), 443-449.

Opitz, C., Cristina, M. D., Reiss, M., Ruppert, T., Crisanti, A., & Soldati, D. (2002). Intramembrane cleavage of microneme proteins at the surface of the apicomplexan parasite *Toxoplasma gondii*. *EMBO J, 21*(7), 1577-1585.

Pansri, P., Jaruseranee, N., Rangnoi, K., Kristensen, P., & Yamabhai, M. (2009). A compact phage display human scFv library for selection of antibodies to a wide variety of antigens. *BMC Biotechnology, 9*(1), 6.

Pastorek, J. G. (1994). *Obstetric and gynecologic infectious disease*. New York: Raven Press.

Patten, P. A., Gray, N. S., Yang, P. L., Marks, C. B., Wedemayer, G. J., Boniface, J. J., et al. (1996). The Immunological Evolution of Catalysis. *Science, 271*(5252), 1086-1091.

Pedersen, H., Holder, S., Sutherlin, D. P., Schwitter, U., King, D. S., & Schultz, P. G. (1998). A method for directed evolution and functional cloning of enzymes. *PNAS, 95*(18), 10523-10528.

Pereira-Bueno, J., Quintanilla-Gozalo, A., Pérez-Pérez, V., Álvarez-García, G., Collantes-Fernández, E., & Ortega-Mora, L. M. (2004). Evaluation of ovine abortion associated with *Toxoplasma gondii* in Spain by different diagnostic techniques. *Veterinary Parasitology, 121*(1-2), 33-43.

Persson, C. M., Lambert, H., Vutova, P. P., Dellacasa-Lindberg, I., Nederby, J., Yagita, H., et al. (2009). Transmission of *Toxoplasma gondii* from Infected Dendritic Cells to Natural Killer Cells. *Infect. Immun., 77*(3), 970-976.

Persson, E. K., Agnarson, A. M., Lambert, H., Hitziger, N., Yagita, H., Chambers, B. J., et al. (2007). Death Receptor Ligation or Exposure to Perforin Trigger Rapid Egress of the Intracellular Parasite *Toxoplasma gondii*. *The Journal of Immunology, 179*(12), 8357-8365.

Pfefferkorn, E. R., & Pfefferkorn, L. G. (1976). *Toxoplasma gondii*: Isolation and preliminary characterization of temperature-sensitive mutants. *Exp. Parasitol., 39*(3), 365-376.

Pini, A., Giuliani, A., Ricci, C., Runci, Y., & Bracci, L. (2004). Strategies for the Construction and Use of Peptide and Antibody Libraries Displayed on Phages. *Current Protein and Peptide Science, 5*(6), 487-496.

Piper, J. M., & Wen, T. S. (1999). Perinatal Cytomegalovirus and Toxoplasmosis: Challenges of Antepartum Therapy. *Clinical Obstetrics and Gynecology, 42*(1), 81-96.

Popkov, M., Jendreyko, N., Gonzalez-Sapienza, G., Mage, R. G., Rader, C., & Barbas, C. F. (2004). Human/mouse cross-reactive anti-VEGF receptor 2 recombinant antibodies selected from an immune b9 allotype rabbit antibody library. *Journal of Immunological Methods, 288*(1-2), 149-164.

Porter, S. B., & Sande, M. A. (1992). Toxoplasmosis of the Central Nervous System in the Acquired Immunodeficiency Syndrome. *New England Journal of Medicine, 327*(23), 1643-1648.

Power, B. E., Caine, J. M., Burns, J. E., Shapira, D. R., Hattarki, M. K., Tahtis, K., et al. (2001). Construction, expression and characterisation of a single-chain diabody derived from a humanised anti-Lewis Y cancer targeting antibody using a heat-inducible bacterial secretion vector. *Cancer Immunology, Immunotherapy, 50*(5), 241-250.

Pressman, B. C. (1976). Biological Applications of Ionophores. *Annual Review of Biochemistry, 45*(1), 501-530.

Qiu, W., Wernimont, A., Tang, K., Taylor, S., Lunin, V., Schapira, M., et al. (2009). Novel structural and regulatory features of rhoptry secretory kinases in *Toxoplasma gondii*. *EMBO J, 28*(7), 969-979.

Rabenau, K. E., Sohrabi, A., Tripathy, A., Reitter, C., Ajioka, J. W., Tomley, F. M., et al. (2001). TgM2AP participates in *Toxoplasma gondii* invasion of host cells and is tightly associated with the adhesive protein TgMIC2. *Molecular Microbiology, 41*(3), 537-547.

Rader, C., Steinberger, P., & Barbas, C. F. I. (2001). Selection from Antibody Libraries. In C. F. I. Barbas, D. R. Burton, J. K. Scott & G. J. Silverman (Eds.), *Phage Display - A Laboratory Manual* (pp. 10.10-10.11). New York: Cold Spring Harbor Laboratory Press.

Rajotte, D., Arap, W., Hagedorn, M., Koivunen, E., Pasqualini, R., & Ruoslahti, E. (1998). Molecular heterogeneity of the vascular endothelium revealed by *in vivo* phage display. *The Journal of Clinical Investigation, 102*(2), 430-437.

Ray, K., Embleton, M. J., Jailkhani, B. L., Bhan, M. K., & Kumar, R. (2001). Selection of single chain variable fragments (scFv) against the glycoprotein antigen of the rabies virus from a human synthetic scFv phage display library and their fusion with the Fc region of human IgG1. *Clinical & Experimental Immunology, 125*(1), 94-101.

Reiche, E. M. V., Morimoto, H. K., Farias, G. N., Hisatsugu, K. R., Geller, L., Gomes, A. C. L. F., et al. (2000). Prevalência de tripanossomíase americana, sífilis, toxoplasmose, rubéola, hepatite B, hepatite C e da infecção pelo vírus da imunodeficiência humana, avaliada

por intermédio de testes sorológicos, em gestantes atendidas no período de 1996 a 1998 no Hospital Universitário Regional Norte do Paraná (Universidade Estadual de Londrina, Paraná, Brasil). *Revista da Sociedade Brasileira de Medicina Tropical, 33*, 519-527.

Reichert, J. M., Rosensweig, C. J., Faden, L. B., & Dewitz, M. C. (2005). Monoclonal antibody successes in the clinic. *Nat Biotech, 23*(9), 1073-1078.

Reiss, M., Viebig, N., Brecht, S., Fourmaux, M.-N., Soete, M., Di Cristina, M., et al. (2001). Identification and Characterization of an Escorter for Two Secretory Adhesins in *Toxoplasma gondii*. *The Journal of Cell Biology, 152*(3), 563-578.

Remington, J. S., & Gentry, L. O. (1970). Acquired Toxoplasmosis: Infection versus disease. *Annals of the New York Academy of Sciences, 174*(2), 1006-1017.

Remington, J. S., McLeod, R., Thulliez, P., & Desmonts, G. (2001). Toxoplasmosis. In J. S. Remington & J. O. Klein (Eds.), *Infectious diseases of the fetus and newborn infant* (pp. 205-346). Philadelphia: Saunders.

Remington, J. S., & Miller, M. J. (1966). 19S and 7S anti-Toxoplasma antibodies in diagnosis of acute congenital and acquired toxoplasmosis. *Proc. Soc. Exp. Biol. Med., 121*, 357-363.

Rhyner, C., Weichel, M., Fluckiger, S., Hemmann, S., Kleber-Janke, T., & Crameri, R. (2004). Cloning allergens via phage display. *Methods, 32*(3), 212-218.

Robben, P. M., Mordue, D. G., Truscott, S. M., Takeda, K., Akira, S., & Sibley, L. D. (2004). Production of IL-12 by Macrophages Infected with *Toxoplasma gondii* Depends on the Parasite Genotype. *The Journal of Immunology, 172*(6), 3686-3694.

Roberts, T., & Frenkel, J. K. (1990). Estimating income losses and other preventable costs caused by congenital toxoplasmosis in people in the United States. *J. Am. Vet. Med. Assoc., 196*(2), 20005-24788.

Roberts, T., Murrell, K. D., & Marks, S. (1994). Economic losses caused by foodborne parasitic diseases. *Parasitology Today, 10*(11), 419-423.

Rondot, S., Koch, J., Breitling, F., & Dubel, S. (2001). A helper phage to improve single-chain antibody presentation in phage display. *Nat Biotech, 19*(1), 75-78.

Rot, A., & von Andrian, U. H. (2004). Chemokines in Innate and Adaptive Host Defense: Basic Chemokinese Grammar for Immune Cells. *Annual Review of Immunology, 22*(1), 891-928.

Rothova, A., Bosch-Driessen, L. E. H., van Loon, N. H., & Treffers, W. F. (1998). Azithromycin for ocular toxoplasmosis. *British Journal of Ophthalmology, 82*(11), 1306-1308.

Ru, B., Huang, J., Dai, P., Li, S., Xia, Z., Ding, H., et al. (2010). MimoDB: a New Repository for Mimotope Data Derived from Phage Display Technology. *Molecules, 15*(11), 8279-8288.

Ruiz, M., & Lefranc, M.-P. (2002). IMGT gene identification and Colliers de Perles of human immunoglobulins with known 3D structures. *Immunogenetics, 53*(10), 857-883.

Saba, J., Morlat, P., Raffi, F., Hazebroucq, V., Joly, V., Leport, C., et al. (1993). Pyrimethamine plus azithromycin for treatment of acute toxoplasmic encephalitis in patients with AIDS. *European Journal of Clinical Microbiology & Infectious Diseases, 12*(11), 853-856.

Sabin, A. B., & H.A., F. (1948). Dyes as microchemical indicators of a new immunity phenomenon affecting a protozoan parasite (Toxoplasma). *Science, 108*, 660-663.

Saeij, J. P. J., Boyle, J. P., Coller, S., Taylor, S., Sibley, L. D., Brooke-Powell, E. T., et al. (2006). Polymorphic Secreted Kinases Are Key Virulence Factors in Toxoplasmosis. *Science, 314*(5806), 1780-1783.

Saeij, J. P. J., Boyle, J. P., Grigg, M. E., Arrizabalaga, G., & Boothroyd, J. C. (2005). Bioluminescence Imaging of *Toxoplasma gondii* Infection in Living Mice Reveals Dramatic Differences between Strains. *Infect. Immun., 73*(2), 695-702.

Saeij, J. P. J., Coller, S., Boyle, J. P., Jerome, M. E., White, M. W., & Boothroyd, J. C. (2007). Toxoplasma co-opts host gene expression by injection of a polymorphic kinase homologue. *Nature, 445*(7125), 324-327.

Saffer, L. D., & Schwartzman, J. D. (1991). A soluble phospholipase of *Toxoplasma gondii* associated with host cell penetration. *J. Protozool., 38*, 454-460.

Sambrook, J., & Russell, D. W. (2001). *Molecular Cloning: A Laboratory Manual (3rd ed.)* (3rd ed.). New York: Cold Spring Harbor Laboratory Press.

Sayles, P. C., Gibson, G. W., & Johnson, L. L. (2000). B Cells Are Essential for Vaccination-Induced Resistance to Virulent *Toxoplasma gondii*. *Infect. Immun., 68*(3), 1026-1033.

Sblattero, D., & Bradbury, A. (2000). Exploiting recombination in single bacteria to make large phage antibody libraries. *Nat Biotech, 18*(1), 75-80.

Schier, R., McCall, A., Adams, G. P., Marshall, K. W., Merritt, H., Yim, M., et al. (1996). Isolation of Picomolar Affinity Anti-c-erbB-2 Single-chain Fv by Molecular Evolution of the Complementarity Determining Regions in the Center of the Antibody Binding Site. *Journal of Molecular Biology, 263*(4), 551-567.

Schnyder, A., & Huwyler, J. r. (2005). Drug Transport to Brain with Targeted Liposomes. *NeuroRx : the journal of the American Society for Experimental NeuroTherapeutics, 2*(1), 99-107.

Schoenberger, S. P., & Crotty, S. (2008). Immunologic Memory. In W. E. Paul (Ed.), *Fundamental Immunology* (6 ed., pp. 876-877). Philadelphia: Lippincott Williams & Wilkins.

Schreiber, R. D., & Feldman, H. A. (1980). Identification of the activator system for antibody to Toxoplasma as the classical complement pathway. *The Journal of Infectious Diseases, 141*(3), 366-369.

Schwab, J. C., Beckers, C. J., & Joiner, K. A. (1994). The parasitophorous vacuole membrane surrounding intracellular *Toxoplasma gondii* functions as a molecular sieve. *Proceedings of the National Academy of Sciences of the United States of America, 91*(2), 509-513.

Schwartzman, J. D., & Pfefferkorn, E. R. (1982). *Toxoplasma gondii*: Purine synthesis and salvage in mutant host cells and parasites. *Experimental Parasitology, 53*(1), 77-86.

Sharma, S. K., Pedley, R. B., Bhatia, J., Boxer, G. M., El-Emir, E., Qureshi, U., et al. (2005). Sustained Tumor Regression of Human Colorectal Cancer Xenografts Using a Multifunctional Mannosylated Fusion Protein in Antibody-Directed Enzyme Prodrug Therapy. *Clinical Cancer Research, 11*(2), 814-825.

Shtatland, T., Guettler, D., Kossodo, M., Pivovarov, M., & Weissleder, R. (2007). PepBank - a database of peptides based on sequence text mining and public peptide data sources. *BMC Bioinformatics, 8*(1), 280.

Shubar, H. M., Dunay, I. R., Lachenmaier, S., Dathe, M., Bushrab, F. N., Mauludin, R., et al. (2009). The role of apolipoprotein E in uptake of atovaquone into the brain in murine acute and reactivated toxoplasmosis. *Journal of Drug Targeting, 17*(4), 257-267.

Sibley, L. D., & Ajioka, J. W. (2008). Population Structure of *Toxoplasma gondii*: Clonal Expansion Driven by Infrequent Recombination and Selective Sweeps. *Annual Review of Microbiology, 62*(1), 329-351.

Sibley, L. D., & Boothroyd, J. C. (1992). Virulent strains of *Toxoplasma gondii* comprise a single clonal lineage. *Nature, 359*(6390), 82-85.

Sibley, L. D., Niesman, I. R., Asai, T., & Takeuchi, T. (1994). *Toxoplasma gondii*: Secretion of a Potent Nucleoside Triphosphate Hydrolase into the Parasitophorous Vacuole. *Experimental Parasitology, 79*(3), 301-311.

Sibley, L. D., Niesman, I. R., Parmley, S. F., & Cesbron-Delauw, M. F. (1995). Regulated secretion of multi-lamellar vesicles leads to formation of a tubulo-vesicular network in host-cell vacuoles occupied by *Toxoplasma gondii*. *J Cell Sci, 108*(4), 1669-1677.

Sidhu, S. S., Li, B., Chen, Y., Fellouse, F. A., Eigenbrot, C., & Fuh, G. (2004). Phage-displayed Antibody Libraries of Synthetic Heavy Chain Complementarity Determining Regions. *Journal of Molecular Biology, 338*(2), 299-310.

Siegel, D. L. (2001). Cell-surface selection and analysis of monoclonal antibodies from phage libraries. In C. F. I. Barbas, D. R. Burton, J. K. Scott & G. J. Silverman (Eds.), *Phage*

Display - A Laboratory Manual (pp. 23.21-23.25). New York: Cold Spring Harbor Laboratory Press.

Siegel, S. E., Lunde, M. N., Gelderman, A. H., Halterman, R. H., Brown, J. A., Levine, A. S., et al. (1971). Transmission of Toxoplasmosis by Leukocyte Transfusion. *Blood, 37*(4), 388-394.

Silverman, J. A., Qi, H., Riehl, A., Beckers, C., Nakaar, V., & Joiner, K. A. (1998). Induced Activation of the *Toxoplasma gondii* Nucleoside Triphosphate Hydrolase Leads to Depletion of Host Cell ATP Levels and Rapid Exit of Intracellular Parasites from Infected Cells. *Journal of Biological Chemistry, 273*(20), 12352-12359.

Simon, D. I., Brosius, F. C., III, & Rothstein, D. M. (1990). Sulfadiazine Crystalluria Revisited: The Treatment of Toxoplasma Encephalitis in Patients With Acquired Immunodeficiency Syndrome. *Arch Intern Med, 150*(11), 2379-2384.

Sinai, A. P., Webster, P., & Joiner, K. A. (1997). Association of host cell endoplasmic reticulum and mitochondria with the *Toxoplasma gondii* parasitophorous vacuole membrane: a high affinity interaction. *J Cell Sci, 110*(17), 2117-2128.

Sircar, A., Kim, E. T., & Gray, J. J. (2009). RosettaAntibody: antibody variable region homology modeling server. *Nucl. Acids Res., 37*(suppl_2), W474-479.

Sison, A. V., & Sever, J. L. (1999). Toxoplasmosis: Treatment and Prevention. In J. T. Queenan (Ed.), *Management of high-risk pregnancy* (4 ed., pp. 301): Wiley-Blackwell.

Sivasubramanian, A., Sircar, A., Chaudhury, S., & Gray, J. J. (2009). Toward high-resolution homology modeling of antibody Fv regions and application to antibody–antigen docking. *Proteins: Structure, Function, and Bioinformatics, 74*(2), 497-514.

Sorokulova, I. B., Olsen, E. V., Chen, I. H., Fiebor, B., Barbaree, J. M., Vodyanoy, V. J., et al. (2005). Landscape phage probes for *Salmonella typhimurium*. *Journal of Microbiological Methods, 63*(1), 55-72.

Stanford, M. R., Tomlin, E. A., Comyn, O., Holland, K., & Pavesio, C. (2005). The visual field in toxoplasmic retinochoroiditis. *British Journal of Ophthalmology, 89*(7), 812-814.

Steffens, D. L., & Williams, J. G. K. (2007). Efficient Site-Directed Saturation Mutagenesis Using Degenerate Oligonucleotides. *J Biolmol Tech., 18*(3), 147-149.

Stehlik, C., de Martin, R., Kumabashiri, I., Schmid, J. A., Binder, B. R., & Lipp, J. (1998). Nuclear Factor (NF)-κβ regulated X-chromosome-linked *iap* Gene Expression Protects Endothelial Cells from Tumor Necrosis Factor α-induced Apoptosis. *The Journal of Experimental Medicine, 188*(1), 211-216.

Stommel, E. W., Ely, K. H., Schwartzman, J. D., & Kasper, L. H. (1997). *Toxoplasma gondii*:Dithiol-Induced Ca2+Flux Causes Egress of Parasites from the Parasitophorous Vacuole. *Experimental Parasitology, 87*(2), 88-97.

Streltsov, V., & Nuttall, S. (2005). Do sharks have a new antibody lineage? *Immunology Letters, 97*(1), 159-160.

Strittmatter, C., Lang, W., Wiestler, O. D., & Kleihues, P. (1992). The changing pattern of human immunodeficiency virus-associated cerebral toxoplasmosis: a study of 46 postmortem cases. *Acta Neuropathologica, 83*(5), 475-481.

Su, C., Evans, D., Cole, R. H., Kissinger, J. C., Ajioka, J. W., & Sibley, L. D. (2003). Recent Expansion of Toxoplasma Through Enhanced Oral Transmission. *Science, 299*(5605), 414-416.

Sumyuen, M. H., Garin, Y. J. F., & Derouin, F. (1995). Early kinetics of *Toxoplasma gondii* infection in mice infected orally with cysts of an avirulent strain. *J. Parasitol., 81*(2), 327-329.

Suss-Toby, E., Zimmerberg, J., & Ward, G. E. (1996). Toxoplasma invasion: the parasitophorous vacuole is formed from host cell plasma membrane and pinches off via a fission pore. *Proceedings of the National Academy of Sciences of the United States of America, 93*(16), 8413-8418.

Suzuki, Y., Conley, F. K., & Remington, J. S. (1989). Importance of endogenous IFN-gamma for prevention of toxoplasmic encephalitis in mice. *The Journal of Immunology, 143*(6), 2045-2050.

Tan, T. G., Mui, E., Cong, H., Witola, W., Montpetit, A., Muench, S. P., et al. (2010). Identification of *T. gondii* epitopes, adjuvants, and host genetic factors that influence protection of mice and humans. *Vaccine, In Press, Uncorrected Proof*.

Tardieux, I., & Ménard, R. (2008). Migration of Apicomplexa Across Biological Barriers: The Toxoplasma and Plasmodium Rides. *Traffic, 9*(5), 627-635.

Teeling, J. L., French, R. R., Cragg, M. S., van den Brakel, J., Pluyter, M., Huang, H., et al. (2004). Characterization of new human CD20 monoclonal antibodies with potent cytolytic activity against non-Hodgkin lymphomas. *Blood, 104*(6), 1793-1800.

Tenter, A. M., Heckeroth, A. R., & Weiss, L. M. (2000). *Toxoplasma gondii*: from animals to humans. *International Journal for Parasitology, 30*(12-13), 1217-1258.

Thomas, W. D., Golomb, M., & Smith, G. P. (2010). Corruption of phage display libraries by target-unrelated clones: Diagnosis and countermeasures. *Analytical Biochemistry, 407*(2), 237-240.

Tomley, F. M., & Soldati, D. S. (2001). Mix and match modules: structure and function of microneme proteins in apicomplexan parasites. *Trends in Parasitology, 17*(2), 81-88.

Tonegawa, S. (1983). Somatic generation of antibody diversity. *Nature, 302*(5909), 575-581.

Towbin, H., Staehelin, T., & Gordon, J. (1979). Electrophoretic transfer of proteins from polyacrylamide gels to nitrocellulose sheets: procedure and some applications. *Proc. Natl. Acad. Sci., 76*(9), 4350-4354.

Tu, Z., He, G., Li, K., Chen, M. J., Chang, J., Chen, L., et al. (2005). An improved system for competent cell preparation and high efficiency plasmid transformation using different *Escherichia coli* strains. *Electronic Journal of Biotechnology 8*(1), 114-120.

Vallera, D. A., Todhunter, D., Kuroki, D. W., Shu, Y., Sicheneder, A., Panoskaltsis-Mortari, A., et al. (2005). Molecular modification of a recombinant, bivalent anti-human CD3 immunotoxin (Bic3) results in reduced *in vivo* toxicity in mice. *Leukemia research, 29*(3), 331-341.

Vaughan, T. J., Williams, A. J., Pritchard, K., Osbourn, J. K., Pope, A. R., Earnshaw, J. C., et al. (1996). Human Antibodies with Sub-nanomolar Affinities Isolated from a Large Non-immunized Phage Display Library. *Nature Biotechnology, 14*(3), 309-314.

Vidal, J. E., Colombo, F. A., Penalva de Oliveira, A. C., Focaccia, R., & Pereira-Chioccola, V. L. (2004). PCR Assay Using Cerebrospinal Fluid for Diagnosis of Cerebral Toxoplasmosis in Brazilian AIDS patients. *J. Clin. Microbiol., 42*(10), 4765-4768.

Viti, F., Tarli, L., Giovannoni, L., Zardi, L., & Neri, D. (1999). Increased Binding Affinity and Valence of Recombinant Antibody Fragments Lead to Improved Targeting of Tumoral Angiogenesis. *Cancer Research, 59*(2), 347-352.

Vodnik, M., Zager, U., Strukelj, B., & Lunder, M. (2011). Phage Display: Selecting Straws Instead of a Needle from a Haystack. *Molecules, 16*(1), 790-817.

Vugmeyster, Y., Beyer, J., Howell, K., Combs, D., Fielder, P., Yang, J., et al. (2005). Depletion of B Cells by a Humanized Anti-CD20 Antibody PRO70769 in Macaca Fascicularis. *Journal of Immunotherapy, 28*(3), 212-219.

Vutova, P., Wirth, M., Hippe, D., Gross, U., Schulze-Osthoff, K., Schmitz, I., et al. (2007). *Toxoplasma gondii* inhibits Fas/CD95-triggered cell death by inducing aberrant processing and degradation of caspase 8. *Cellular Microbiology, 9*(6), 1556-1570.

Wajanarogana, S., Prasomrothanakul, T., Udomsangpetch, R., & Tungpradabkul, S. (2006). Construction of a human functional single-chain variable fragment (scFv) antibody recognizing the malaria parasite *Plasmodium falciparum*. *Biotechnology and Applied Biochemistry, 44*(1), 55-61.

Wang, C. L., Harper, R. A., & Wabl, M. (2004). Genome-wide somatic hypermutation. *Proceedings of the National Academy of Sciences of the United States of America, 101*(19), 7352-7356.

Watters, J. M., Telleman, P., & Junghans, R. P. (1997). An optimized method for cell-based phage display panning. *Immunotechnology, 3*(1), 21-29.

Webster, J. P. (2001). Rats, cats, people and parasites: the impact of latent toxoplasmosis on behaviour. *Microbes and Infection, 3*, 1037-1045.

Wedemayer, G. J., Patten, P. A., Wang, L. H., Schultz, P. G., & Stevens, R. C. (1997). Structural Insights into the Evolution of an Antibody Combining Site. *Science, 276*(5319), 1665-1669.

Wedemayer, G. J., Wang, L. H., Patten, P. A., Schultz, P. G., & Stevens, R. C. (1997). Crystal structures of the free and liganded form of an esterolytic catalytic antibody. *Journal of Molecular Biology, 268*(2), 390-400.

Weng, W.-K., & Levy, R. (2003). Two Immunoglobulin G Fragment C Receptor Polymorphisms Independently Predict Response to Rituximab in Patients With Follicular Lymphoma. *Journal of Clinical Oncology, 21*(21), 3940-3947.

Wilcoxon, F. (1945). Individual comparisons by ranking methods. *Biometrics, 1*.

Williams, G. T. (1994). Programmed cell death: a fundamental protective response to pathogens. *Trends in Microbiology, 2*(12), 463-464.

Wilson, C. B., Remington, J. S., Stagno, S., & Reynolds, D. W. (1980). Development of Adverse Sequelae in Children Born with Subclinical Congenital Toxoplasma Infection. *Pediatrics, 66*(5), 767-774.

Wilson, M., & McAuley, J. M. (1999). Toxoplasma. In P. R. Murray (Ed.), *Manual of Clinical Microbiology* (7th ed., pp. 1374-1382). Washington D.C.: American Society for Microbiology.

Wilson, M., Remington, J. S., Clavet, C., Varney, G., Press, C., & Ware, D. (1997). Evaluation of six commercial kits for detection of human immunoglobulin M antibodies to *Toxoplasma gondii*. The FDA Toxoplasmosis Ad Hoc Working Group. *J. Clin. Microbiol., 35*(12), 3112-3115.

Wong, A., Tan, K. H., Tee, C. S., & Yeo, G. S. H. (2000). Seroprevalence of cytomegalovirus, Toxoplasma and parvovirus in pregnancy. *Singapore Medical Journal, 41*(4), 151-155.

Yang, M., Coppens, I., Wormsley, S., Baevova, P., Hoppe, H. C., & Joiner, K. A. (2004). The *Plasmodium falciparum* Vps4 homolog mediates multivesicular body formation. *J Cell Sci, 117*(17), 3831-3838.

Yang, W.-P., Green, K., Pinz-Sweeney, S., Briones, A. T., Burton, D. R., & Barbas Iii, C. F. (1995). CDR Walking Mutagenesis for the Affinity Maturation of a Potent Human Anti-HIV-1 Antibody into the Picomolar Range. *Journal of Molecular Biology, 254*(3), 392-403.

Yap, G. S., & Sher, A. (1999). Cell-mediated immunity to *Toxoplasma gondii:* initiation, regulation and effector function. *Immunobiology, 201*, 240-247.

Yavin, E., & Yavin, Z. (1974). Attachment and culture of dissociated cells from rat embryo cerebral hemispheres on polylysine-coated surface. *The Journal of Cell Biology, 62*(2), 540-546.

Yu, B., Ni, M., Li, W.-H., Lei, P., Xing, W., Xiao, D.-W., et al. (2005). Human scFv antibody fragments specific for hepatocellular carcinoma selected from a phage-display library. *World J Gastroenterol, 11*(26), 3985-3989.

Zhang, Y. W., Halonen, S. K., Ma, Y. F., Wittner, M., & Weiss, L. M. (2001). Initial Characterization of CST1, a *Toxoplasma gondii* Cyst Wall Glycoprotein. *Infect. Immun., 69*(1), 501-507.

Zhao, Y., Ferguson, D. J. P., Wilson, D. C., Howard, J. C., Sibley, L. D., & Yap, G. S. (2009). Virulent *Toxoplasma gondii* Evade Immunity-Related GTPase-Mediated Parasite Vacuole Disruption within Primed Macrophages. *The Journal of Immunology, 182*(6), 3775-3781.

Zhao, Y. O., Rohde, C., Lilue, J. T., KÃ¶nen-Waisman, S., Khaminets, A., Hunn, J. P., et al. (2009). *Toxoplasma gondii* and the Immunity-Related GTPase (IRG) resistance system in mice: a review. *MemÃ³rias do Instituto Oswaldo Cruz, 104*, 234-240.

Zheng, L., Baumann, U., & Reymond, J.-L. (2004). An efficient one-step site-directed and site-saturation mutagenesis protocol. *Nucleic Acids Research, 32*(14), e115.

Zhou, X. W., Kafsack, B. r. F. C., Cole, R. N., Beckett, P., Shen, R. F., & Carruthers, V. B. (2005). The Opportunistic Pathogen *Toxoplasma gondii* Deploys a Diverse Legion of Invasion and Survival Proteins. *Journal of Biological Chemistry, 280*(40), 34233-34244.

Zypen, E., & Piekarski, G. (1967). Endodyogeny in *Toxoplasma gondii*: A morphological analysis. *Parasitology Research, 29*(1), 15-35.